PYROLYSIS OF SUGARCANE BAGASSE

by

Thomas Johannes Hugo

Thesis submitted in partial fulfilment

of the requirements for the Degree

of

MASTER OF SCIENCE IN ENGINEERING

(CHEMICAL ENGINEERING)

in the Department of Process Engineering

at the University of Stellenbosch

Supervised by

Prof. J.H. Knoetze

Prof. J.F. Görgens

STELLENBOSCH

December 2010

Declaration

I, the undersigned, hereby declare that the work contained in this thesis is my own original work and that I have not previously in its entirety or in part submitted it at any university for a degree.

…………………………...   ……………….
Signature   Date

Abstract

The world's depleting fossil fuels and increasing greenhouse gas emissions have given rise to much research into renewable and cleaner energy. Biomass is unique in providing the only renewable source of fixed carbon. Agricultural residues such as Sugarcane Bagasse (SB) are feedstocks for 'second generation fuels' which means they do not compete with production of food crops. In South Africa approximately 6 million tons of raw SB is produced annually, most of which is combusted onsite for steam generation. In light of the current interest in bio-fuels and the poor utilization of SB as energy product in the sugar industry, alternative energy recovery processes should be investigated. This study looks into the thermochemical upgrading of SB by means of pyrolysis.

Biomass pyrolysis is defined as the thermo-chemical decomposition of organic materials in the absence of oxygen or other reactants. Slow Pyrolysis (SP), Vacuum Pyrolysis (VP), and Fast Pyrolysis (FP) are studied in this thesis. Varying amounts of char and bio-oil are produced by the different processes, which both provide advantages to the sugar industry. Char can be combusted or gasified as an energy-dense fuel, used as bio-char fertilizer, or upgraded to activated carbon. High quality bio-oil can be combusted or gasified as a liquid energy-dense fuel, can be used as a chemical feedstock, and shows potential for upgrading to transport fuel quality. FP is the most modern of the pyrolysis technologies and is focused on oil production. In order to investigate this process a 1 kg/h FP unit was designed, constructed and commissioned. The new unit was tested and compared to two different FP processes at Forschungszentrum Karlsruhe (FZK) in Germany. As a means of investigating the devolatilization behaviour of SB a Thermogravimetric Analysis (TGA) study was conducted. To investigate the quality of products that can be obtained an experimental study was done on SP, VP, and FP.

Three distinct mass loss stages were identified from TGA. The first stage, 25 to 110°C, is due to evaporation of moisture. Pyrolitic devolatilization was shown to start at 230°C. The final stage occurs at temperatures above 370°C and is associated with the cracking of heavier bonds and char formation. The optimal decomposition temperatures for hemicellulose and cellulose were identified as 290°C and 345°C, respectively. Lignin was found to decompose over the entire temperature range without a distinct peak. These results were confirmed by a previous study on TGA of bagasse.

SP and VP of bagasse were studied in the same reactor to allow for accurate comparison. Both these processes were conducted at low heating rates (20°C/min) and were therefore focused on char production.

Slow pyrolysis produced the highest char yield, and char calorific value. Vacuum pyrolysis produced the highest BET surface area chars (>300 m^2/g) and bio-oil that contained significantly less water compared to SP bio-oil. The short vapour residence time in the VP process improved the quality of liquids. The mechanism for pore formation is improved at low pressure, thereby producing higher surface area chars. A trade-off exists between the yield of char and the quality thereof.

FP at Stellenbosch University produced liquid yields up to 65 ± 3 wt% at the established optimal temperature of 500°C. The properties of the bio-oil from the newly designed unit compared well to bio-oil from the units at FZK. The char properties showed some variation for the different FP processes. At the optimal FP conditions 20 wt% extra bio-oil is produced compared to SP and VP. The FP bio-oil contained 20 wt% water and the calorific value was estimated at 18 ± 1 MJ/kg. The energy per volume of FP bio-oil was estimated to be at least 11 times more than dry SB. FP was found to be the most effective process for producing a single product with over 60% of the original biomass energy. The optimal productions of either high quality bio-oil or high surface area char were found to be application dependent.

Opsomming

As gevolg van die uitputting van fossielbrandstofreserwes, en die toenemende vrystelling van kweekhuisgasse word daar tans wêreldwyd baie navorsing op hernubare en skoner energie gedoen. Biomassa is uniek as die enigste bron van hernubare vaste koolstof. Landbouafval soos Suikerriet Bagasse (SB) is grondstowwe vir 'tweede generasie bio-brandstowwe' wat nie die mark van voedselgewasse direk affekteer nie. In Suid Afrika word jaarliks ongeveer 6 miljoen ton SB geproduseer, waarvan die meeste by die suikermeulens verbrand word om stoom te genereer. Weens die huidige belangstelling in bio-brandstowwe en ondoeltreffende benutting van SB as energieproduk in die suikerindustrie moet alternatiewe energie-onginningsprosesse ondersoek word. Hierdie studie is op die termo-chemiese verwerking van SB deur middel van pirolise gefokus.

Biomassa pirolise word gedefinieer as die termo-chemiese afbreking van organiese bio-materiaal in die afwesigheid van suurstof en ander reagense. Stadige Pirolise (SP), Vakuum Pirolise (VP), en Vinnige Pirolise word in hierdie tesis ondersoek. Die drie prosesse produseer veskillende hoeveelhede houtskool en bio-olie wat albei voordele bied vir die suikerindustrie. Houtskool kan as 'n vaste energie-digte brandstof verbrand of vergas word, as bio-houtskoolkompos gebruik word, of kan verder tot geaktiveerde koolstof geprosesseer word. Hoë kwaliteit bio-olie kan verbrand of vergas word, kan as bron vir chemikalië gebruik word, en toon potensiaal om in die toekoms opgegradeer te kan word tot vervoerbrandstof kwaliteit. Vinnige pirolise is die mees moderne pirolise tegnologie en is op bio-olie produksie gefokus. Om die laasgenoemde proses te toets is 'n 1 kg/h vinnige pirolise eenheid ontwerp, opgerig en in werking gestel. Die nuwe pirolise eenheid is getoets en vegelyk met twee verskillende vinnige pirolise eenhede by Forschungszentrum Karlsruhe (FZK) in Duitsland. Termo-Gravimetriese Analise (TGA) is gedoen om die ontvlugtigingskenmerke van SB te bestudeer. Eksperimentele werk is verrig om die kwaliteit van produkte van SP, VP, vinnige pirolise te vergelyk.

Drie duidelike massaverlies fases van TGA is geïdentifiseer. Die eerste fase (25 – 110°C) is as gevolg van die verdamping van vog. Pirolitiese ontvlugtiging het begin by 230°C. Die finale fase (> 370°C) is met die kraking van swaar verbindings en die vorming van houtskool geassosieer. Die optimale afbrekingstemperatuur vir hemisellulose en sellulose is as 290°C en 345°C, respektiewelik, geïdentifiseer. Daar is gevind dat lignien stadig oor die twede en derde fases afgebreek word sonder 'n duidelike optimale afbrekingstemperatuur. Die resultate is deur vorige navorsing op TGA van SB bevestig.

SP en VP van bagasse is in dieselfde reaktor bestudeer, om 'n akkurate vergelyking moontlik te maak. Beide prosesse was by lae verhittingstempo's (20°C/min) ondersoek, wat gevolglik op houtskoolformasie gefokus is. SP het die hoogste houtskoolopbrengs, met die hoogste verbrandingsenergie, geproduseer. VP het hootskool met die hoogste BET oppervlakarea geproduseer, en die bio-olie was weens 'n dramatiese afname in waterinhoud van beter gehalte. Die meganisme vir die vorming van 'n poreuse struktuur word deur lae atmosferiese druk verbeter. Daar bestaan 'n inverse verband tussen die kwantiteit en kwaliteit van die houtskool.

Vinnige pirolise by die Universiteit van Stellenbosch het 'n bio-olie opbrengs van 65 ± 3 massa% by 'n vooraf vasgestelde optimale temperatuur van 500°C geproduseer. Die eienskappe van bio-olie wat deur die nuwe vinnige pirolise eenheid geproduseer is het goed ooreengestem met die bio-olie afkomstig van FZK se pirolise eenhede. Die houtskool eienskappe van die drie pirolise eenhede het enkele verskille getoon. By optimale toestande vir vinnige pirolise word daar 20 massa% meer bio-olie as by SP en VP geproduseer. Vinnige pirolise bio-olie het 'n waterinhoud van 20 massa% en 'n verbrandingswarmte van 18 ± 1 MJ/kg. Daar is gevind dat ten opsigte van droë SB die energie per enheidsvolume van bio-olie ongeveer 11 keer meer is. Vinnige pirolise is die mees doeltreffende proses vir die vervaardiging van 'n produk wat meer as 60% van die oorspronklike biomassa energie bevat. Daar is gevind dat die optimale hoeveelhede van hoë kwaliteit bio-olie en hoë oppervlakarea houtskool doelafhanklik is.

Acknowledgements

Firstly I would like to thank my supervisors, Professor Knoetze and Professor Görgens, for their guidance and support over the past years.

I would like to say special thanks to Dr. Marion Carrier for her guidance and support. I am deeply indebted to her for all she has taught me over the last year.

I would like to thank my project sponsor Steve Davis from SMRI, as well as CRSES for funding for this project.

I would like to thank Dr. Stahl at Forchungszentrum Karlsruhe (FZK), who made the visit to Germany possible, as well as my friend and colleague Wale Aboyade who worked alongside me at FZK.

I would like to thank the Oppenheimer Memorial Trust for providing me with the necessary funding for the visit to FZK.

I would like to thank the workshop, especially Oom Anton, Oom Jannie, and Ulrich Büttner for their help in the construction of the fast pyrolysis unit.

I would like to thank Hanlie Botha, and the other technicians who did analyses.

I would like to thank my parents, brother, friends and loved ones for their support over the last two years.

I would like to thank my God.

Abbreviations and Nomenclature

Abbreviation	Abbreviated Word
AC	Activated Carbon
ar	Arrive (as is, original)
dwt%	Dry Weight Percentage
ESP	Electrostatic Precipitator
FBR	Fluidized Bed Reactor
FPU	Fast Pyrolysis Unit
FZK	Forschungszentrum Karlsruhe
Liquid phase or (Bio – oil)	All liquid products for pyrolysis. This includes water and oil fractions.
maf	Moisture and Ash Free
mf	Moisture Free
n.a.	Not Applicable
n.d.	Not Determined
Oil phase or (organic liquid phase)	All organics from the liquid product. (No water)
PDU	Process Demonstration Unit
Pyrolytic water	Portion of liquid phase collected in ice traps during slow and vacuum pyrolysis.
SA	Surface Area
SMRI	Sugar Milling Research Institute
Solid phase or (Char or Bio-char)	Pyrolysis char (includes ash)
SU or (US)	Stellenbosch University (University of Stellenbosch)
Sugarcane Bagasse or (Bagasse) or (SB)	The remnants from sugarcane after extraction of sugars
Tar phase	High viscosity liquid phase. Typically contains only ~3% moisture. (Only referred to in vacuum and slow pyrolysis.)
Water phase	All water from liquid product. This includes water from the biomass (moisture) and pyrolysis reaction water.
WC or (MC)	Water Content (Moisture Content)
wt% or (m%)	Weight Percentage or Mass Percentage
Yield % or (Y)	Weight option of respective product expressed as a percentage of original weight (of biomass) before pyrolysis.

Abbreviation	Name	Units
ΔT_m	Mean temperature difference	°C [or K]
A	Surface Area	m^2
Ar	Archimedes number	-
Cp	Specific heat	kJ/kg.K
E	Energy	J
f	Fluid	-
g	Gravitational acceleration	m^2/s
h	Heat transfer coefficient	W/m^2.K
H	Bed depth	m
H_{evap}	Heat of evaporation	kJ/kg
HHV	Higher heating value, (or calorific value)	MJ/kg
HHV (dry)	HHV of sample containing no water	MJ/kg
H_r	Heat of reaction	kJ/kg
ID	Inner Diameter	m
k	Thermal conductivity	W/m.K
L	Length	m
M	Mass flow rate	kg/h
n	Reaction order	-
p	Particle	-
P	Pressure	kPa [or Bar]
Q	Heat transferred per unit time	W (or kJ/h)
r	Radius	m
R	Universal gas constant	J/kg.K
Re	Reynolds number	-
RPM	Revolutions per minute	-
T	Temperature	°C [or K]
t	Time	s [or min]
u	Velocity	m/s
U_{mf}	Minimum fluidization	m/s
U_t	Terminal velocity	m/s
Y	Yield	%
α	Conversion	-
ε	Voidage	-
μ	Viscosity	Pa.s
ρ	Density	kg/m^3
τ	Residence time	s [or min]
φ	Sphericity	-

List of figures

List of tables

Table of contents

1   <u>Introduction</u>

The world's depleting fossil fuels and increasing Green House Gas (GHG) emissions have given rise to much research into renewable and cleaner energy. Biomass is unique in providing the only renewable source of fixed carbon. It is termed 'carbon neutral' because all CO_2 released form biomass combustion was previously absorbed from the air. It is recognized that biomass surpasses many other renewable energy sources, because of its abundance, high energy value and versatility. In South Africa (SA) approximately 6 million tons raw bagasse is produced annually (www.smri.org, 2009). Most large and medium sized mills can use up to 75 % of this bagasse onsite to generate heat and electricity (Zandersons *et al.*, 1999).

The projected renewable energy demand for 2013 is approximately 4% of South Africa's total energy demand. Currently almost all national electricity is provided by coal and nuclear power, 92.8 and 6.7 % respectively. Only a very small fraction is supplied by biomass, solar, wind and hydropower. Because low cost electricity plays a key role in the economic growth of this country, coal is likely to remain a very attractive energy source. However, the Department of Minerals and Energy (DME) has set a target of 10 000 GWh to be produced from renewable energy sources (mainly from biomass, wind, solar and small-scale hydro) by 2013. The bio-fuels task team aim to achieve 75% of South Africa's renewable energy needs. This strategy focuses on bio-ethanol and biodiesel.

By implementing thermo-chemical upgrading of bagasse the energy efficiency can be increased significantly, resulting in energy savings and surplus energy products (Pippo *et al.*, 2007; Garcia-Perez *et al.*, 2002). Thermo-chemical processes include combustion, pyrolysis and gasification of which the latter two are upgrading techniques. These upgrading processes are used to convert biomass into energy-dense bio-fuels namely char, bio-oil and non-condensable gasses. Different types of thermo-chemical decomposition produce different product qualities and ratios by controlling the oxygen content and process conditions. Table 1 illustrates typical weight distributions among products for different thermo-chemical processes. Fast pyrolysis is optimized for high liquid yield production; gasification maximizes gas production; vacuum pyrolysis gives a more even spread of products; slow pyrolysis and torrefaction give char as main product; and finally combustion produces heat.

Table 1: Typical product distribution from various biomass conversion techniques (Bridgwater *et al.*, 2003; Mohan *et al.*, 2006)

Process	Typical process conditions	Char wt%	Liquids wt%	Gas wt%
Fast pyrolysis	500°C, high heating rate, short vapour residence time (< 2s)	10-20	60-75	10-20
Vacuum pyrolysis	450°C, low heating rate, long - medium vapour residence time (few minutes)	20-30	35-45	25-35
Slow pyrolysis	500°C, low heating rate, long - long vapour residence time (5 min -30 min)	25-35	30-45	25-35
Torrefaction	300°C, low heating rate, long vapour residence time	70	0	30
Gasification	>800°C, high heating rate, long vapour residence time	10	5	85

Great economical advantages lie in the potential upgrading of the pyrolysis products. Liquid fuel has some advantages in transport, storage, combustion, retrofitting and flexibility in production and marketing (Bridgwater *et al.*, 1999). The alternative is char production by means of slow or vacuum pyrolysis. The char can be upgraded to activated carbon which is a high-value product, and is also used by the sugar industry to clarify raw sugar for white sugar production. This study looks into the use of pyrolysis for increasing the efficiency of bagasse utilization in the sugar industry as well as contributing to the projected renewable energy demand for South Africa in 2013.

1.1 Objectives and scope

In this project the main objective is to compare Slow Pyrolysis (SP), Vacuum Pyrolysis (VP) and Fast Pyrolysis (FP) of bagasse aimed at implementation in the sugar industry. Based on product yields and qualities from optimized experimental conditions, a qualitative comparison is possible. In order to accomplish this objective the following tasks are required:

1. The design, construction and commissioning of a Fast Pyrolysis Unit (FPU) for use in the experimental program.

2. An experimental evaluation of SP of bagasse to study the effect of heating rate and temperature on product yields and properties.

3. A comparison to a similar experimental study on VP (Carrier *et al.*, 2010) on the same pyrolysis unit.

4. Thermogravimetric Analysis (TGA) to study thermal decomposition behaviour of bagasse.

5. An experimental study on FP of bagasse to study the effect of temperature on product yields and properties on the newly constructed FPU.

6. The comparison of the newly constructed FPU with two different FPUs at Forschungszentrum Karlsruhe (FZK).

7. The final task is to produce a comparative report on SP, VP and FP to highlight the preferred pyrolysis process for production of bio-oil and bio-char.

1.2 Mind map

The mind map in Figure 1 illustrates how the different tasks fit together.

Figure 1: Mind map

3
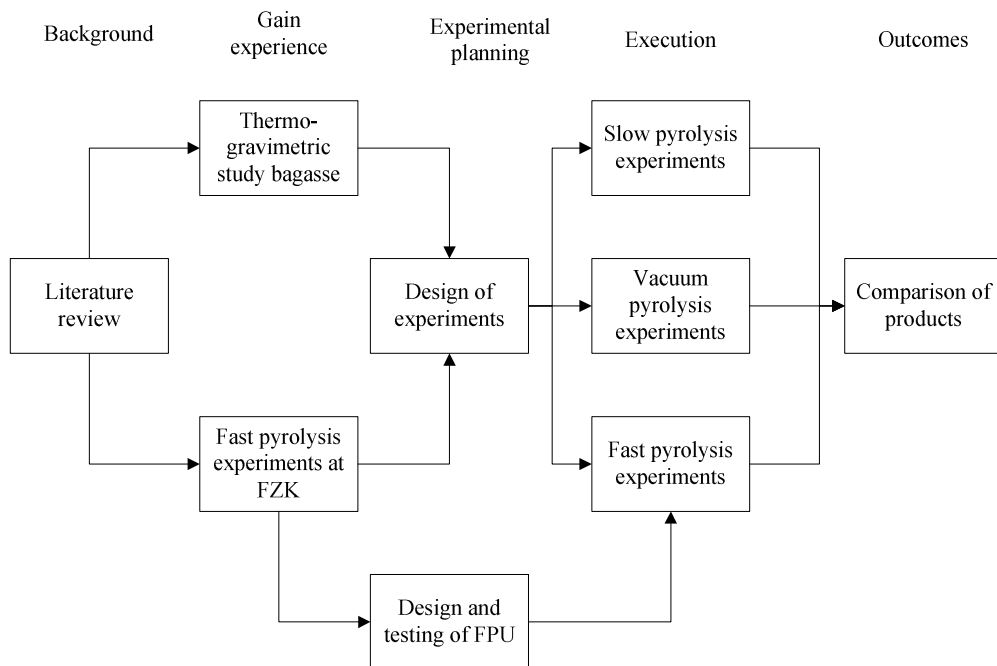
2   <u>Background and literature study</u>

2.1   Sugarcane bagasse

Sugarcane Bagasse (SB or bagasse) is the biomass that is studied in this project. Bagasse is the crushed remnants of sugarcane after syrup extraction (Devnarain *et al.*, 2002). Sugarcane is a type of grass with peripheral fibres enclosing a soft central pith (Nassar *et al.*, 1996). Sugarcane utilises solar energy by means of photosynthesis, to grow and therefore produce biomass. During photosynthesis CO_2 is extracted from the air and this CO_2 is released back into the atmosphere during combustion rendering the whole process CO_2 neutral. This energy is then released either by means of natural decay, or it can be harvested by means of controlled combustion or chemical reactions. Sugarcane is the crop that produces the highest yield of biomass over an average year. Up to 8 tons/acre of carbohydrate (sugar and bagasse) can be produced annually (Calvin, 1974). Sugarcane is a fibrous plant which causes the crushed remnants to be thin long particles that are interwoven with each other (Figure 2). Therefore bagasse has very poor flow characteristics and it tends to bunch together (Rasul *et al.*, 1999). Additional size reduction before pyrolysis will enhance the flow ability of bagasse.

Figure 2: Sugarcane bagasse

The particle density of the bagasse is particularity difficult to determine accurately because of the porosity of the particles, the voidage between the particles, and the different types of particles. Bagasse consists mainly of fibre particles, with a large length to width ratio, and small spongy dust-like particles (Rasul *et al.*, 1999). The dust-like particles have a much lower density of 220 kg/m^3, compared to the fibrous particles density of 550 kg/m^3 (Garcia-Perez *et al.*, 2002). A large variation is reported in literature on the density of bagasse. A test was done in the present study to determine the bulk density of South African bagasse (without compression); it varied between 100 - 200 kg/m^3 due to large void spaces between particles.

These differences in size, shape and density cause the different particles to segregate easily into an inhomogeneous mixture of the different particles of bagasse. Normal sampling at various depths will not produce a representative sample if the sample is segregated. To avoid sampling only certain particles a representative sample should be evenly spread on a table. Numerous samples should be taken randomly across the table each time taking precaution to collect all the biomass in a certain area. This method is repeated until a small enough representative sample is obtained (standard method applied for biomass sampling at The Department of Forestry at SU). Segregation occurs primarily as a result of size difference (Rhodes, 2005). Size reduction reduces the bulk density of bagasse, because void spaces become smaller (Rhodes, 2005).

The properties of bagasse vary with the type of sugarcane, its maturity, harvesting methods, milling methods, handling methods and sugar extraction methods. In South Africa the diffusion process is commonly used to extract sugars from cane, which may render the chemical and physical properties of bagasse different from bagasse produced in other countries (Devnarain *et al.*, 2002; Rasul *et al.*, 1999). The alternative to sugar extraction by diffusion is to squeeze and wash the cane (www.smri.org). Bagasse is a lignocellulosic compound which implies that it contains varying amounts of cellulose, hemicellulose and lignin. The study of lignocellulosic compounds is relevant to pyrolysis because decomposition these components occurs at different temperatures. Hemicellulose typically decomposes in the range of 160-360°C, while cellulose degrades at the higher temperature range of 240-390°C. The loss of lignin typically occurs at a slower rate over a much wide temperature range of 180-900°C (see detail discussion in Chapter 5). Cellulose and hemicellulose are both polymeric carbohydrate structures, termed polysaccharides. Cellulose is a polymer, consisting of linear chains of 1, 4-D-glucopyranose units. Hemicellulose a complex polysaccharide found mostly in cell walls, which is a branched structure composed almost entirely of sugars such as glucose, mannose, xylose, arabinose, methlyglucoronic and galaturonic acids. Cellulose is crystalline and strong whereas hemicellulose has an amorphous structure with little strength. The main difference between cellulose and hemicellulose is that cellulose is glucose derived and hemicellulose is derived from a variety of sugars (Mohan *et al.*, 2006). Lignins are highly branched, substituted, mononuclear aromatic polymers in the cell walls of certain biomass, especially woody species. Lignin is an amorphous cross linked resin with no distinct structure, which binds the fibrous cellulosic particles. The building blocks of lignin are believed to be a three-carbon chain attached to rings of six carbon atoms, called phenyl-propanes (Mohan *et al.*, 2006). Bagasse contains 35-50 wt% cellulose, 20 – 30 wt% hemicellulose, 20 – 27 wt% lignin, and 8 – 12 wt% extractives and ash (Garica-Perez *et al.*, 2001).

The ash content of SB is critical. Ash is the name given to all components that are not considered organic or water. It consists mostly of metal oxides. These metal oxides contaminate the products, be it chars for activated carbon or bio-oil, and therefore the ash content of the sample should ideally be as low as possible (Luo *et al.*, 2004). Ash also acts as a catalyst for unwanted reactions during pyrolysis (Bridgwater et al, 1996; Raveendran *et al.*, 1995). Bagasse has a high ash content, which is usually in the region of 3 wt% or higher (Sugar conference, 2001). In a previous study the ash composition of South African SB ranged between 1.8 - 5.4 wt% thereby illustrating how inhomogeneous samples can be (Devnarain *et al.*, 2002). Soil contamination has been reported to increase the ash content from 2.5 wt% to as high as 12 wt% (Turn, 2002). A small fraction of soil has a significant effect on the overall ash content, because it contains mostly inorganic components.

Several methods exist to remove the unwanted soil and ash from bagasse. Depending on the process, sugarcane milling may remove much of the soil from bagasse. If the soil content remains high a washing step may be included. Alternatively bagasse can be pre-treated to remove ash by means of water leaching under mildly acidic conditions (Das *et al.*, 2004). The resulting leachate was found to have potential to be used in ethanol fermentation, which could increase the economic feasibility of including this process step (Das *et al.*, 2004). The final method for reducing ash content is by discarding the smallest particle size fraction. Garcia-Perez *et al.* (2002) determined the ash content of the different size fractions of bagasse. They concluded that the ash content of the smaller particles was significantly higher. Therefore it is desirable to remove the small particles after milling. In Table 2 the ash content of the different particle size ranges is shown. By removing the finest particles, the ash content may be reduced by about a third.

Table 2: Ash content of different particle size ranges, (Garcia-Perez *et al.*, 2002)

Particle size, d (mm)	Dry bagasse (wt %)	Ash (wt %)
d > 4.75	34	1.3
0.85 < d < 4.75	44	1.6
0.45 < d < 0.85	15	2.3
0.25 < d < 0.45	4	13
d < 0.25	3	27.7

2.1.1 *Use of sugar cane agricultural residue (SCAR)*

SCAR is the remainder of the sugarcane plant that was not harvested and is composed of sugarcane leaves and cane tops and trash (roots, stems and leaves). In many countries SCAR it is burnt to facilitate easier

harvesting, or left in the field to decompose and regenerate the soil nutrients. The main drawbacks for using SCAR as energy feedstock are: collection from field, a high ash content of 6 to 10 wt%, and potential soil degradation due to high recovery of biomass (Pippo *et al.*, 2007; Beeharry *et al.*, 2000). SCAR and bagasse have similar heating values of approximately 17MJ/kg (Pippo *et al.*, 2007). A comparison of the energy value of SCAR and bagasse relative to their respective proportions is shown in Table 3.

Table 3: Bagasse equivalence of sugarcane residues (Beeharry *et al.*, 2000)

Biomass	Availability (% cane)	Moisture content (%)	Bagasse equivalence
Bagasse	30	50	1
Cane tops and leaves	31.2	68	0.62
Trash	10.2	19.3	1.61

From these results it was concluded that more that 50 % of the fibrous energy produced by the cane plant is biomass that is stored as cellulosic fibres in SCAR. Assuming effective collection of SCAR, biomass production can be boosted up to 22 dry tonnes per hectare (Beeharry *et al.*, 2000). In reality the recovery of these residues adds additional cost and complications and is therefore more expensive to use than bagasse. With ever changing economic conditions, SCAR may still become a usable energy product in the future.

2.2   Sugar industry

The South African sugarcane industry is one of the world's leading cost-competitive producers of sugar, and is ranked worldwide within the top 15 sugar exporters. Cane is predominantly produced in KwaZulu-Natal, Mpumalanga and the Eastern Cape, which are considered the most productive cultivation areas in South Africa. Approximately 320 000 ha of sugar cane is harvested each season, with an energy potential of up to 1000 GJ/ha/year (Banks *et al.*, 2006). There are currently approximately 38 200 cane growers are registered within the South African cane growers sector (www.sasa.org.za, 2010). Of these cane growers 96% are small-scale growers that produce 9 % of the total crop. In 2008 there were 14 mills located throughout the eastern part of South Africa (www.sasa.org.za, 2009). Five of these mills are owned by Illovo Sugar Ltd, four by Tongaat Hullet Sugar Ltd, two by TSB Sugar RSA Ltd, one by UCL Company Ltd and one by Ushukela Milling (Pty) Ltd. In Table 4 a summary of the total crop of sugarcane as given

by the South African Sugar Industry Directory of the 2007/2008 season is shown for the past 7 years (www.sasa.org.za, 2009). On average 22 million tons of cane is crushed annually.

It is important to draw the line between crushed sugarcane and obtainable energy. For every 1 (wet) ton of sugarcane approximately 100 kg of sugar is produced, 35 kg molasses, and 270 kg wet bagasse (Garcia-Perez *et al.*, 2002). Wet bagasse typically contains approximately 50 wt% moisture. In the 2001 season SA crushed over 21 million tons of sugarcane, resulting in approximately 6 million tons bagasse (50% moisture). According to a recent article on sugarcane energy production in SA this amount of bagasse could produce approximately 2600 GWh by direct combustion. Currently this by-product of the sugar industry is used as a fuel resource for industry (Norris *et al.*, 2007). Low efficacy boilers are typically used in the sugar industry to generate power by direct combustion of bagasse with a maximum efficiency of 26%. Pyrolysis and gasification can achieve higher energy conversion than combustion (Garcia-Perez *et al.*, 2002).

Table 4: Sugarcane production in South Africa

Season	Million tons cane crushed	Dry bagasse produced *
2001/2002	21.16	5.71
2002/2003	23.01	6.21
2003/2004	20.42	5.51
2004/2005	19.09	5.16
2005/2006	21.05	5.68
2006/2007	20.28	5.48
2007/2008	19.72	5.33
*27 wt% wet bagasse (Garcia-Perez *et al.*, 2002; Drummond *et al.*, 1996)		

2.2.1 *Uses of bagasse*

Bagasse is mainly used for onsite combustion (Asadullah *et al.*, 2007). The remainder is typically used to produce paper pulp, chemical reactants, or animal feed additives (Devnarain *et al.*, 2002). Implementing thermo-chemical processing of bagasse will extend its uses to high-density energy products (char and bio-oil) as well as activated carbon and high quality fertilizer (from char). Bagasse is a by-product from the sugar industry and is therefore a second-generation biofuel, which implies that it does not compete with food crop production. Sacrificing agricultural land for fuel production may in the future become viable if fuel prices increase significantly.

9
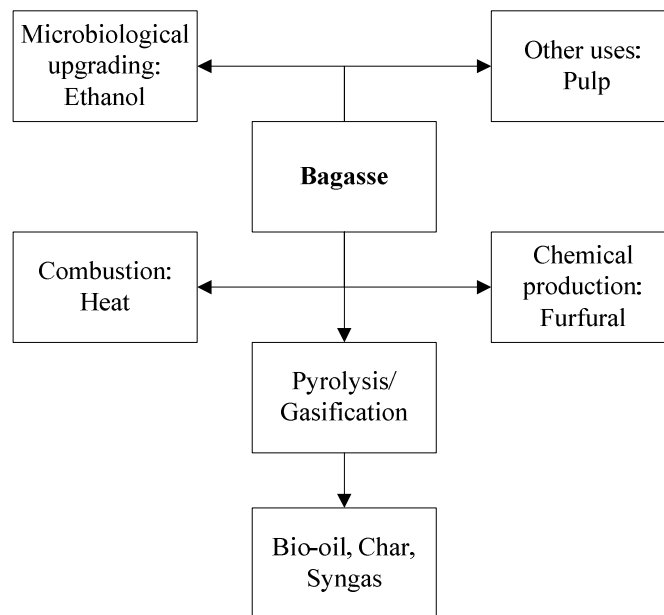
Figure 3: Applications for bagasse

When considering the implementation of further processing of bagasse it is vital to review the sizes of the respective mills in SA. As is evident from Table 5, on average approximately 1.4 million tonnes SB is crushed per season per mill. Bagasse is burnt to produce heat or electricity in most sugar mills around the world (Garcia-Perez *et al.,* 2002). When excess electricity is generated it is sold to the electricity grid. This process is called 'co-generation'. A number of sugar mills have proposed to keep generating electricity in the off season, to add value to the industry. Large quantities of bagasse will need to be stored for use in the off season. Stockpiling of bagasse makes it susceptible to degradation if stored for too long in warm humid conditions (Pippo *et al.*, 2007). Pelletisation provides a more compact method for storage of bagasse (Erlich *et al.*, 2006). Energy densification before storage can reduce storage per volume significantly. Storage, transport volume, and the degradation of energy resource will be greatly reduced by the implementation of pyrolysis as energy densification method (Pippo *et al.*, 2007).

Table 5: Cane throughput for sugarcane mills in SA (www.sasa.org.za, 2009)

Location	Sugar Mill	Million tons cane (2007-2008)
Northern Irrigated	Malelane	1.67
	Komati	2.28
	Pongola	1.31
Zululand	Umfolozi	1.03
	Felixton	1.84
	Amatikulu	1.42
North Coast	Darnall	1.08
	Gledhow (KwaDukuza)	1.18
	Maidstone	1.17
Midlands	Eston	1.41
	Noodsberg	1.45
	Union	0.67
South Coast	Sezela	2.07
	Umzimkulu	1.14
	Total	**19.72**
	Average per Mill	**1.41**

2.3 Biomass pyrolysis reactions

Pyrolysis is defined as the thermo-chemical conversion of biomass to char, bio-oil and gas, in the absence of oxygen and other reactants (Balat *et al.*, 2009; Goyal *et al.*, 2008). It always occurs before combustion and gasification where complete or partial oxidation is allowed to proceed. Pyrolysis is a complex non-equilibrium process where the biomass undergoes multistage decomposition resulting in large changes in specific volume. The reaction rate, order and product yields depend on parameters such as temperature, heating rate, pre-treatment, catalytic effects etc. (Bridgwater *et al.*, 1996 and 2002). The reaction mechanism can be approximated by combining the yields from the three lignocellulosic compounds, despite synergetic effects. Therefore the study of individual components forms the basis of the expected reaction pathways (Van de Velden *et al.*, 2010). Cellulose is the focus of much research because it is the dominant lignocellulosic compound, and therefore cellulose decomposition is best understood. The primary cellulose reaction is described by the Waterloo-mechanism, illustrated in Figure 4 (Van de Velden *et al.*, 2010).

11
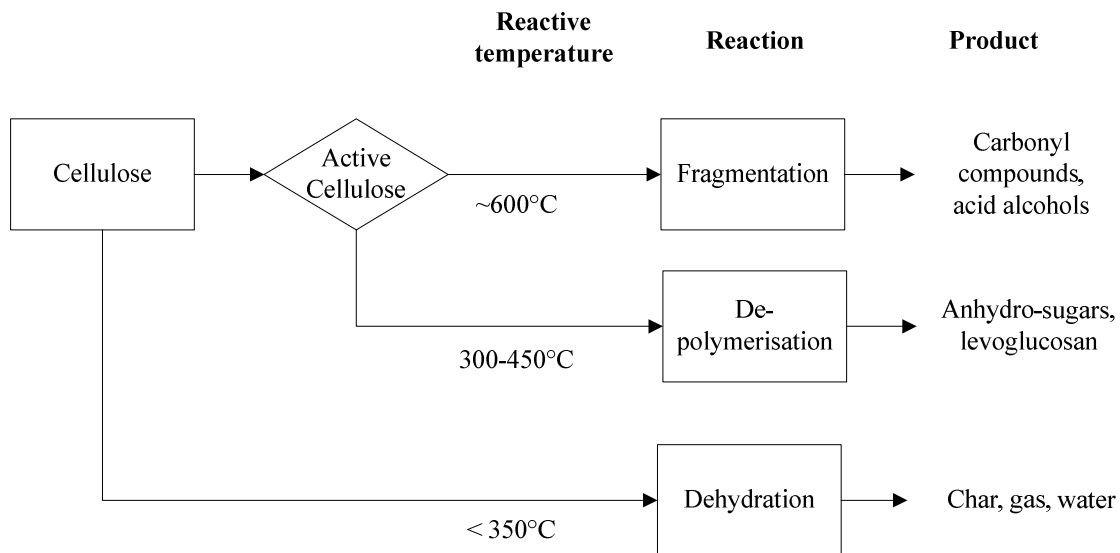
Figure 4: Primary cellulose decomposition according to Waterloo-mechanism

At low temperatures (< 350°C) dehydration is dominant which favours char, water and gas production. Depolymerisation dominates at temperatures between 300 and 450°C which produce anhydrous sugars like levoglucosan. Fragmentation of cellulose to carbonyl compounds, acids and alcohols is optimized at around 600°C. Further increases in temperature (> 650°C), or very long vapour residence times, will cause secondary reactions to occur between vapour and solid phase to form gas (Bridgwater *et al.*, 1999). The relevant secondary reaction for pyrolysis is cracking and the water-gas shift reaction: $H_2O + CO_2 \leftrightarrow H_2 + CO_2$ (Van de Velden *et al.*, 2010).

It has been suggested that the primary heat of reaction of wood pyrolysis is low, and that secondary reactions are the main cause of heat generation (Ahuja *et al.*, 1999). Because of the variety of reactions that take place during pyrolysis the reaction may be either endothermic or exothermic. For small particles with immediate removal of vapours the pyrolysis reaction is considered endothermic, whereas pyrolysis reactions in larger particles and longer vapour residence times are likely to be exothermic (Ahuja *et al.*, 1999). Pyrolysis heat requirements between 200 and 400 J/g were reported for various biomasses by Van de Velden *et al.* (2010). The current generally accepted global mechanism for lignocellulosic biomass pyrolysis is shown in Figure 5 (Van de Velden *et al.*, 2010). This is only a rough approximation because it has not been possible to establish a more detailed correlation for the biomass as a whole (Rabe, 2005).

Char 1

Char 2

Biomass

Bio-oil 1

Bio-oil 2

Gas1

Gas 2

Primary reactions   **Secondary reactions**
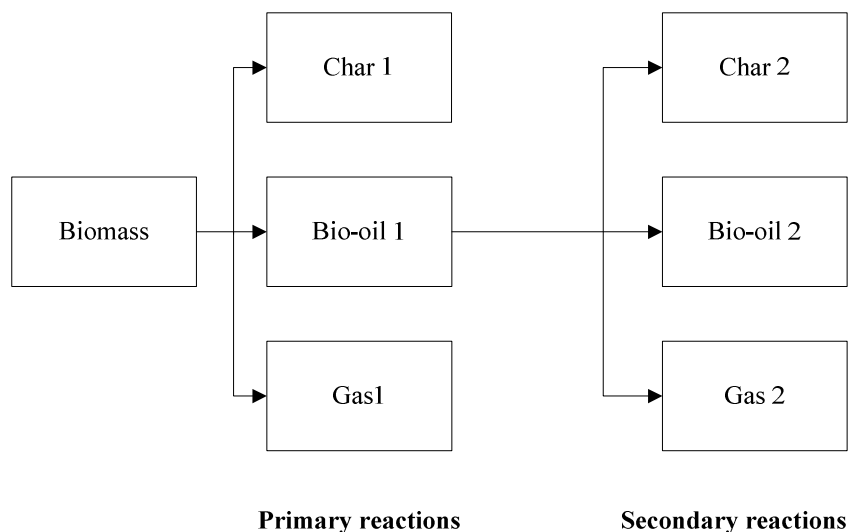
Figure 5: Global pyrolysis concept (Radlein *et al.*, 1991)

Some variations on this global mechanism have also been published. In 2001 De Jongh *et al.* proposed a slightly different mechanism where a distinction was made between vapours (long-chain compounds) and gasses (short-chain compounds). A high degree of conversion was attained during the first stage (cracking of macro molecules) during which most volatile components are released. The second stage occurs at a higher temperature, and is caused by cracking of the residual low molecular weight components to gasses and chars (Rabe, 2005). Generally all the models agree that primary reactions are ideal for bio-oil production and that secondary reactions favour char and gas production.

2.4 Influence of process conditions

This section discusses the most relevant theory on the pyrolysis process and the process conditions with special attention to design implications. Therefore the focus is on fast pyrolysis (FP) but the principles can be applied to any of the pyrolysis technologies. This theory will clarify why different pyrolysis conditions lead to different product yields and quantities.

2.4.1 *Temperature*

Temperature can be said to be the most dominant process variable with regard to pyrolysis product yields. For most types of woody biomass, the liquid yields in FP are optimized in the temperature range 500-520°C (Bridgwater *et al.*, 1999). If the reaction temperature is too low, char formation increases. At lower temperatures only certain lignocellulosic components react. Figure 6 shows a typical temperature-yield

curve for pyrolysis of wood (Bridgwater *et al.*, 1999). Similar results have been published (Gerdes *et al.*, 1999; and Asdullah *et al.*, 2007). Clearly the liquid yield is optimized around 500°C, which favours the depolymerisation reaction described in Figure 4. If the temperature is increased further, the liquid yield will decrease as a result of secondary reactions.
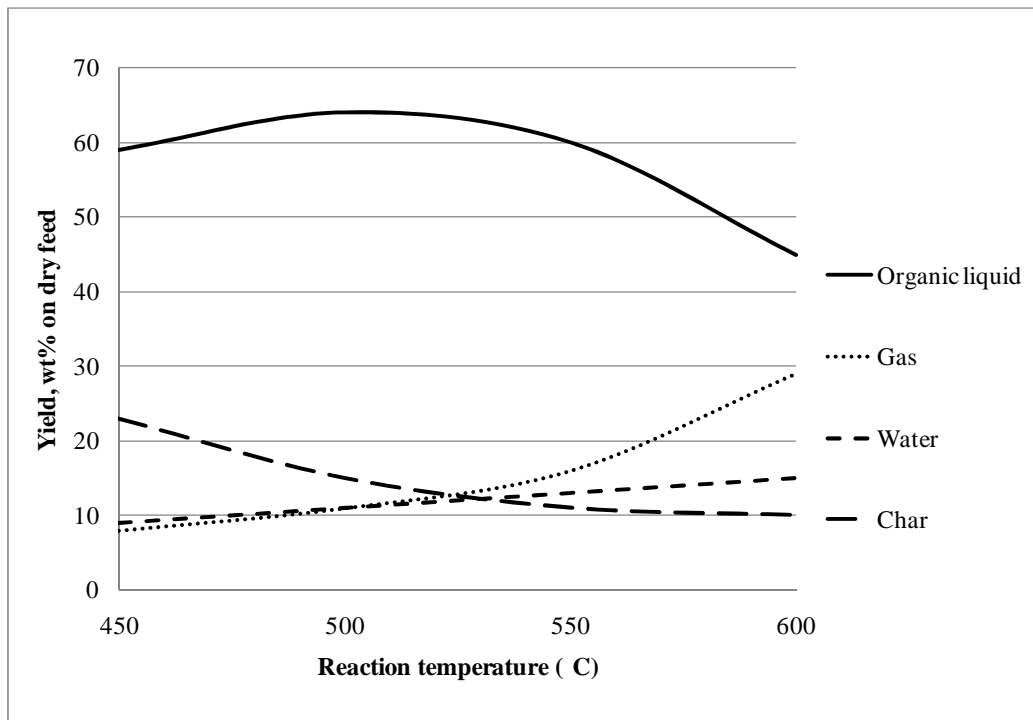
Figure 6: Typical products from FP of wood (Bridgwater *et al.*, 1999)

2.4.2   *Heating rate*

A higher heating rate produces a higher liquid product yield (Bridgewater *et al.*, 1999). This is can be seen from flash processes which are optimized for liquid production and uses high heating rates, up to 10^4 C/s (Horne *et al.*, 1996). Bahng *et al.* (2010) differentiated between fast and flash pyrolysis at their respective heating rates of 200°C/s and >1000°C/s, which is dependent on their respective particle size, <2mm and <200μm (Van de Velden *et al*., 2010). Producing powdered biomass <200μm for pyrolysis is expensive and therefore unrealistic to run at large scale.

It is difficult to control or accurately measure the heating rate of FP. Instead the heating rate is simply maximized for FP. For slow pyrolysis heating rates are much lower and are mostly operated between 10-

50 °C/min. When higher heating rates are used, the emphasis will typically shift to that of oil or vapour yield, and not char production. A slower heating rate will cause an increase in char yield, and higher temperature will reduce the yield but increase the Higher Heating Value (HHV). Heating rate had a less significant effect on the BET surface area of the chars, than hold time or temperature (Lua *et al.*, 2006).

Studies on heating rates inside FP reactors have not been reported. This is because the heating rate and flux are dependent on local condition inside a continuously fluidized-bed reactor. Heating rate effects have only been studied on batch and fixed bed scale where the heating rate is controllable. Thermogravimetric Analysis (TGA) equipment is typically used for these studies. From these test it was concluded that a higher heating rate produces an increased oil yield (Garcia-Perez *et al.*, 2002). Typical TGA experiments will study low heating rates of up to 50°C/min. However, it is not clear how experiments under controlled heating conditions with small samples can be translated to larger scale continuous reactors with high heating rates (Kersten *et al.*, 2005). Modelling devolatilization kinetics might be the most accurate method for understanding the relation.

2.4.3   *Feed-particle size*

The feed particle size is determined by the desired heat transfer rate to the particle. The thermal conductivity of biomass is very low: 0.1 W/mK along the grain and 0.05 W/mK across the grain (Bridgwater *et al.*, 1999). Therefore if the particles are too large, char formation will increase because of slow heating of the core, and secondary reactions become increasingly significant (Scott *et al.*, 1984). Particle size therefore has a direct affect on heat transfer. Scott *et al.* (1982) found that particle sizes smaller that 2 mm do not significantly affect FP product yields. Van de Velden *et al.* (2010) modelled heat transfer in small particles and found that thermal gradients only become insignificant for particles smaller than 200 μm. The generally accepted particle size for fast pyrolysis is 2 mm or smaller according to Bridgwater *et al.* (1999). The gas velocity in fluidized-bed reactors is limited to the sand blow-out velocity and maximum particle size capable of being fed through the feeder.

2.4.4   *Vapour residence time and secondary reactions*

The vapour residence time is defined as the average time a molecule spends inside the reactor, and is a function of reactor volume and sweep gas flow rate (Equation 1).

$$\tau = \frac{V[m^3]}{Q[m^3/s]}$$

Equation 1

Scott el al. (1999) measured the effect of vapour residence time on liquid yield. An increased residence time caused a rapid decrease in oil yield. It was concluded that the decrease is due to secondary cracking reactions, which reduce specific chemicals and overall liquid yield. At lower temperatures (lower than 400°C), secondary condensation occurs, which lowers the molecular weight of the liquid product. In essence the vapour residence time should be short, less than 2 seconds secondary reactions (Yaman *et al.*, 2004; Bridgwater *et al.*, 1999). It was also reported that the amount of char in the reactor had a significant effect on the rate of the secondary reaction. The composition of oil is also affected by the residence time. A mechanism was proposed by Antal *et al.* (1995) that suggests that primary tar can be rapidly converted into gasses and refractory tar (less reactive), after which the two tars form a single solution upon condensation. Ash, and char components carried over from the reactor acts as a catalyst for these secondary reactions, which is also unfavourable (Das *et al.*, 2004). A summary of the process conditions is given in Table 6.

Table 6: Summary of process conditions, effects and modelling

Parameter	Condition	Optimal condition for fast pyrolysis
Reaction temperature	500 – 520°C	Constant
Vapour residence time	< 2s	Shorter is better
Secondary cracking	Avoid	Bad for product quality and yield
Heat transfer rate	200°C/s	High as possible to increase liquid yield.
Particle size	Typically <2mm	Large particles limit heat transfer, feeding and fluidization.
Kinetic modelling	Batch wise for low hearing rates	Difficult to relate to fast pyrolysis with high heating rate and large sample sizes.

2.5   Bio-oil

2.5.1   Composition and physicochemical properties

Bio-oil is a dark brown, free-flowing organic liquid that is a mixture of highly oxygenated compounds and water, and is immiscible with other hydro-carbonaceous fuels. The immiscibility is attributed to high water content, which serves to suspend different molecules in a micro emulsion. It has a distinctive smoky

odour. Bio-oil is also known as pyrolysis oil, pyrolysis liquids, bio-crude oil, wood liquid, wood oil, or liquid smoke (Qi *et al.*, 2007; Mohan *et al.*, 2006). Because of the high oxygen and water content the heating value is significantly less than that of conventional fossil fuels. During combustion the water is evaporated which absorbs a significant portion of energy. Bio-oil is a complex mixture of different types and sizes of molecules derived from depolymerised lignocellulosic compounds. Table 7 shows the typical properties of bio-oil, compared to that of heavy fuel oil. A separate column for bio-oil from bagasse, and normal bagasse is included for comparison. It is apparent that bio-oil quality is significantly lower than that of petroleum based fuel oil. The formation of fossil fuels by anaerobic biomass degradation over geologic time is thought to produce mainly peat, lignite and coal. This is consistent with pyrolysis models for 'long residence times' and low heating rates which maximizes solid product, and minimizes liquid product (Bridgwater *et al.*, 1999).

Table 7: Comparison of physical properties of bio-oil with heavy fuel oil (Czernik *et al.*, 2004, Mohan *et al.*, 2006, Garcia-Perez *et al.*, 2002, Bridgwater *et al.*, 1999)

Physical property	**Dry Bagasse**	**Bagasse bio-oil**	**Wood bio-oil**	**Heavy fuel oil**
Water content (wt %)	0	13.8	10.2 - 35	0.1
pH	n.a.	2.7	2-3.5	
SG (20°C) (kg/L)	0.1-0.15	1.21	1.21-1.24	0.94
Elemental composition (wt %)				
C	47.5	54.6	44-63.5	85
H	5.9	6.45	5.2-7.2	11
O	40.7	38.07	32-46	1
N	0.29	0.73	0.07-0.39	0.3
Ash	5.6	0.05	0.03-0.3	0.1
Calorific Value (MJ/Kg)	18.8	22.4	15-24.3	40
Viscosity (@ 50°C; cP)	n.a.	16.4	9-137	180
Solids wt % (methanol insoluble material)	n.d.	0.38	0.17-1.14	1

The properties that have a negative impact on bio-oil relative to fuel oil will now be discussed, and suitable upgrading methods will be suggested.

2.5.1.1   Water content

Less water is considered beneficial for the energy density, transportation cost, stability and acidity (Oasmaa *et al.*, 1999). Typically 20-30 wt% water is contained in bio-oil which decreases the heating value of bio-oil by up to 25% to 17 MJ/kg, which is less than half that of fuel oil (Bridgwater *et al.*, 2002). Decreasing the water content of bio-oil is a difficult process, which leads to a viscosity increase. Below 15 wt% water the viscosity increases exponentially; for example at 4 wt% water the viscosity of the oil is 80000 cP (20°C) at which point pumping will become problematic (Westerhof *et al.*, 2007). High fluidity is essential for internal combustion in engines. Sipilae *et al.* (1998) found that viscosities were reduced by higher water content and less insoluble components. Research at the NREL showed that the increase of viscosity during storage could be reduced by adding 10-20% of an alcohol to the mixture (Dieblod *et al.*, 1999). For combustion in normal boilers, viscosity is not a big a concern.

2.5.1.2   Oxygen content

Bio-oil oxygen content is approximately 45-50 wt%, respectively distributed over most of the more than 300 components that have been identified (Mohan *et al.*, 2006). The high percentage oxygen present in the bio-oil makes it less energy dense, and is also the main cause for the immiscibility of hydrocarbons and bio-oil. Bio-oil shows a wide range of boiling points because of the many different species present therefore complicating the distillation process. Many of the unwanted characteristics of bio-oil are associated with the high oxygen content. Therefore the removal of oxygen from bio-oil could render it usable as transport fuel. Oxygen can be rejected as water (during reaction with H_2) or as CO_2. Three main routes to transport fuel are possible. The first process is hydro-treating or hydro-cracking. In this process a hydrogen producing solvent is used together with catalysts, under pressurized conditions of hydrogen or CO to remove oxygen from the oil. The removed oxygen is then collected as H_2O or CO_2. A naphtha-like product is obtained that is upgraded to diesel. This process is very expensive because of the high hydrogen requirements (Bridgwater *et al.*, 2000). The second route is catalytic cracking. Bio-oils can be catalytically decomposed to hydrocarbons with removal of oxygen. There are still some concerns with catalyst stability and life (Bridgwater *et al.*, 2000). This route is regarded as the cheaper option, however it also results in a high degree of coking (8-25%), and a reasonably low fuel quality. The final upgrading option is emulsification of bio-oil with hydrocarbons by the use of a surfactant. The optimal range of surfactant concentration was 0.5-2 wt% to achieve acceptable viscosity. Ikura *et al.*, (2003) found that by mixing 10-20 % bio-oil with diesel the viscosity and corrosiveness was greatly reduced (Qi *et al.*, 2007).

2.5.1.3 Acidity

Carboxylic acids are present in bio-oil which causes the pH to drop to the region of 2-3. This acidity makes bio-oil corrosive, and at elevated temperatures even more so (Qi *et al.*, 2007). Corrosive resistant materials of construction should be used.

2.5.1.4 Density

Bio-oil density is higher than that of conventional fuels and therefore the energy per volume is also higher. On a volume basis bio-oil has ~60% as much energy as fuel-oil, whereas on mass basis it is less than half. In terms of energy density bio-oil shows a significant improvement on dry bagasse as illustrated in Table 8.

Table 8: Volumetric energy density of dry bagasse, bio-char, bio-oil and fuel oil

Bio-fuel	HHV (MJ/kg)	Density (kg/L)	Volumetric energy density (MJ/L)	Energy equivalence relative to dry SB
Dry bagasse	18.7	0.1	1.9	1
Bio-char*	30	0.3	9	5
Bio-oil (20 wt% water)	18	1.2	21.6	12
Fossil oil	40	0.9	37.6	20

*Van de Velden *et al.*, 2010

2.5.1.5 Storage instability

Diebold *et al.* (2001) reviewed mechanisms of storage stability of FP fuels. The addition of methanol or ethanol, leads to esterification and acetalization which upgrades the fuel. The viscosity, acidity and aging rate are decreased and the heating value, volatility, and miscibility with diesel fuels are increased. This reflects on the instability of bio-oil which is exacerbated when the temperature is increased. Consequently, even when storing bio-oil at room temperature, aging causes the viscosity to increase, volatility to decrease and phase separation to occur. This is a result of processes such as polymerisation, condensation, etherification, esterification and agglomeration of oligomeric molecules (Bridgwater *et al.*, 2002).

2.5.1.6 Ash content

Some ash remains in the bio-oil which can cause corrosion and increase instability due to catalytic effects. Therefore the ash content should preferably be less than 0.1 wt% for use in engines (Qi *et al.*, 2007). Hot gas filtration can be used to reduce the ash content to less than 0.01 wt% and the alkali content to less than 10 ppm. The filtered oil performed well in tests done on a diesel engine (Shihadeh *et al.*, 2000; Bridgwater *et al.*, 2002).

2.5.1.7 Chemical composition

A broad range of chemicals is produced from the reaction of the diverse lignocellulosic structure of biomass described in chapter 2.3. Bridgwater *et al.* (2002) reported the representative chemical composition of FP liquids as shown in Table 9. Hemicellulose typically produces acetic acid and furfurals; cellulose produces levoglucosan, acetol, aldehyde and 5-hydroxymethylfurfural; lignin produces small amounts of monomer phenols but mostly oligomeric product with high molecular weight (900-2500 u). The production of specific chemicals from pyrolysis is discussed in paragraph 2.5.2.6 in more detail.

Table 9: The representative chemical composition of fast pyrolysis liquids (Bridgwater *et al.*, 2002)

Major bio-oil components	Wt %
Water	20-30
Lignin fragments	15-30
Aldehydes	10-20
Carboxylic acids	5-10
Carbohydrates	2-5
Phenols	1-4
Furfurals	2-5
Alcohols	2-5
Ketones	1-5

2.5.2 Bio-oil applications

Bio-oils can be produced from a range of biomass feedstocks and are cleaner than fossil fuels (releases 50% less nitrogen oxides). It produces a net zero CO_2 emissions and no sulfoxide emissions (Mohan *et al.*, 2006). The energy dense products are much cheaper to transport than the original biomass. Although

the lower quality of bio-oil poses some limitations on its application, there are still various processes available which can use bio-oil. Figure 7 shows different uses of pyrolysis liquids.
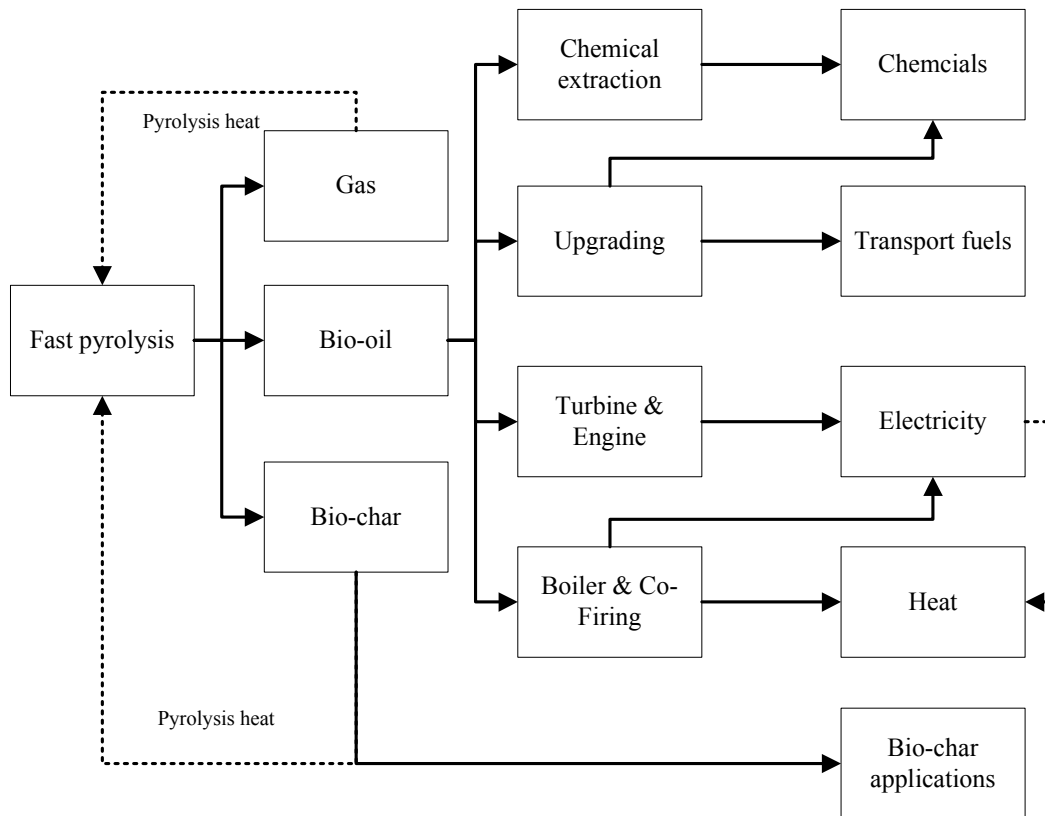
Figure 7: Applications of bio-oil (Bridgwater *et al.*, 2007)

2.5.2.1 Boiler fuel

The heating value of bio-oil is about half that of fossil fuel, and it contains a significant portion of water. Bio-oil has been successfully used as fuel at various institutions (Canmet in Canada, MIT, Neste in Finland). Among problems reported were high viscosity which was corrected by the addition of methanol and inline preheating. The boiler or furnace still required preheating with conventional fuels before bio-oil could be used (Bridgwater *et al.*, 2000). Because of the more sophisticated start-up procedure co-firing of bio-oil in coal utility boilers has also been used (Bridgwater *et al.*, 2000). Bio-oil burns cleaner than fossil fuel because it has a low sulphur and nitrogen content (Balat *et al.*, 2009).

2.5.2.2 Electricity production

Electricity production is favoured over heat production because of its easy distribution and marketing. Over recent years numerous diesel engines have been tested with bio-oil (Bridgwater *et al.*, 2002).

Positive results were reported for engine performance in terms of smooth running. The main problems that still need to be addressed are the acidic nature of bio-oil, and its tendency for soot formation and re-polymerization, which causes the viscosity to increase. The use of a bio-oil requires modifications of various parts of the engine, amongst which the most important ones are the fuel pump, the linings and the injection system. With these modifications the diesel engine can render bio-oil a quite acceptable substitute for diesel fuel in stationary engines. Successful tests have been conducted up to a 2 MWe gas turbine. There is still some uncertainty as to the stability, ash and char properties of bio-oil (Bridgwater *et al.*, 2000). Dynamotive runs a 2.5 MW gas turbine in Canada, which uses 70% of the bio-oil produced from their 130 ton/day plant (www.dynamotive.com, 2010). Electricity production in the sugar industry seems to be a suitable option but not all electricity will be used onsite. With a continuously operated turbine an infrastructure will need to be set in place to sell the remaining electricity to the grid.

2.5.2.3 Synthesis gas production

Synthesis gas is a mixture of hydrogen (H_2) and carbon monoxide (CO) that is typically produced via gasification. The syngas can then be coupled with turbines or engines to produce electricity. Alternatively the Fisher-Tropsch (FT) reaction converts syngas which was derived from coal, methane or biomass, to liquid fuels (Qi *et al.*, 2007). Syngas can be produced from bio-mass directly, or from pyrolysis products. Using pyrolysis fuel instead of biomass saves on transport costs to large gasifiers. Gasification is discussed in paragraph 2.10.2.

2.5.2.4 Steam reforming

In this process hydrogen is produced via catalytic reactions of bio-oil vapours. If approximately 80 wt% liquid is obtained from pyrolysis, 6kg of hydrogen can be produced from 100kg of pyrolyzed wood. A range of catalysts have been used by different scientists in the field (Qi *et al.*, 2007). This process requires a high capital investment.

2.5.2.5 Transport fuels

The methods for upgrading bio-oil were discussed in paragraph 2.5.1.2. These methods are all expensive, and some are still underdeveloped (Bridgwater *et al.*, 2002). Currently it seems that bio-oil is best suited for stationary combustion rather than as transport fuel. Most certainly these technologies will develop over the coming years, and may become economically feasible as the technology improves and fuel prices rise.

2.5.2.6 *Chemical extraction*

The high value of certain bio-oil components makes chemical extraction a viable alternative. The higher added value of chemicals seems to be the most interesting short term opportunity (Bridgwater *et al.*, 1999). Extraction may either be done before or after thermo-chemical processes. Typical valuable substances which can be extracted are phenols, volatile organic acids, levoglucosan, furfural, hydroxyacetaldehyde. Table 10 shows the expected yields of certain chemicals from biomass fast pyrolysis. Furfural is a high value chemical that is typically produced from hemicellulose, and is used as a reactant and selective solvent in the chemical industry (Bridgwater *et al.*, 1996). The current market price is approximately $1200-1250/t (www.prosugar.com.au, April 2010). The new furfural production plant at Proserpine sugar mill in Europe is scheduled to start operating in 2010. This technology is designed to extract up to 1.7 wt% furfural from bagasse. Levoglucosan is the single chemical that can be produced in the highest yield. Approximately 50% can be produced from cellulose at 370-410°C and 10 seconds residence time (Bridgwater *et al.*, 2002, p234.) The yields of specific components are biomass specific and the process conditions should be optimized. Component specific optimization is therefore a study in itself. This will require a thorough analysis of the lignocellulosic subcomponents, the reactions that produce the valuable chemicals, the theoretical yields that are obtainable and the appropriate market and market values of these chemicals. With this information the pyrolysis process conditions can be optimized for production of selective chemicals (Bridgwater, 1996). However the commercialization of these specialist chemicals from bio-oil will require research in low cost separation techniques and refining and is highly dependent on the market. The liquids components from pyrolysis cannot be completely vaporized, as they start to react and form a solid residue as the temperature is increased. During boiling operations some of these species start evaporating at low temperatures (100°C) and may stop boiling at about 280°C, leaving 35 -50 wt% residues. Therefore the fuel cannot be completely evaporated before combustion, (Qi *et al.*, 2007).

Table 10: Chemicals from biomass fast pyrolysis (Ballat *et al.*, 2009)

Chemical	Minimum (wt%)	Maximum (wt%)
Levoglucosan	2.9	30.5
Hydroxyacetaldehyde	2.5	17.5
Acetic acid	6.5	17
Formic Acid	1	9
Acetaldehyde	0.5	8.5
Furfuryl alcohol	0.7	5.5
1-hydrox-2-pentanone	1.5	5.3
Catechol	0.5	5
Methanol	1.2	4.5
Methyl glyoxal	0.6	4
Ethanol	0.5	3.5
Cellobiosan	0.4	3.3
1,6-anhydroglucofuranose	0.7	3.2
Furfural	1.5	3
Frutose	0.7	2.9
Glyoxal	0.6	2.8
Formaldehyde	0.4	2.4

2.5.2.7   Conclusions

Savings associated with the energy density, storage, and transport is currently the most viable advantage of producing bio-oil. The use of bio-oil is decoupled from its production, which allows it be used for energy storage. The transport of bio-oil is significantly cheaper than biomass transport. The commercialization of bio-oil has only just started and will continue to develop. It is believed that the future of bio-oil does not only lie with higher quality fuel production but also with chemical production. (Bridgwater *et al.*, 2002).

2.6 Bio-char

2.6.1 *Composition and physicochemical properties*

The properties of bio-char are diverse, and depend to a great extent on the process and the biomass used. In Table 11 the properties of bagasse and a very high quality bio-char is shown. Low ash content significantly influences the calorific value of the char and may be a high as 33 wt % for some biomasses. High ash content will reduce the HHV of the char significantly. The levels of nitrogen and sulphur are also important characteristics for predicting NO_x and SO_x emissions from combustion (Mullen *et al.*, 2010). The surface area of bio-char is an important characteristic which dictates whether or not it can be used for activate carbon production.

Table 11: Bagasse and bagasse bio-char from vacuum pyrolysis (Garcia-Perez *et al.*, 2002).

Physical property	Dry Bagasse	Bagasse bio-char
C	50	86
H	6	3
O	44	10
N	0	1
Ash	1.6	7
Calorific Value (MJ/Kg)	18.8	36
BET surface area (m^2/g)	n.d.	530

2.6.2 *Bio-char applications*

Bio-char has various industrial applications. It can be directly used as energy product or upgraded to produce activated carbon or bio-char fertilizer (Mullen *et al.*, 2010). The upgraded products have direct applications in the sugar industry and the excess can be sold as by-products.

2.6.2.1 *Combustion and gasification*

Both combustion and gasification are established technologies for char (Bridgwater *et al.*, 2002). Pyrolysis char is also suitable for briquetting. The product can then be sold as a commodity for domestic use. Normally the calorific value of bio-char is approximately 25MJ/kg which is similar to char briquettes (De Jongh., 2001).
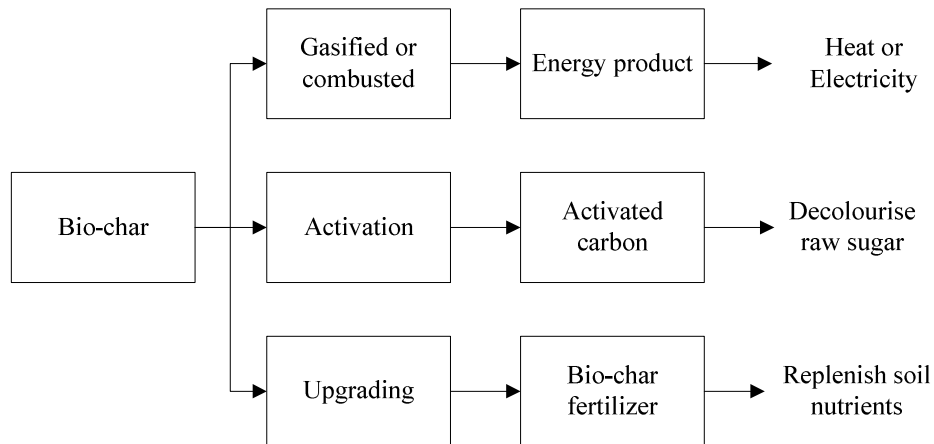
Figure 8: Bio-char applications

2.6.2.2 *Activated carbon*

Activated Carbon (AC) is a valuable adsorbent used in industries such as food processing, chemical, nuclear, and mining to purify, decolourize, detoxicate, filter, and catalyze reactions (Devnarain *et al.*, 2002). AC has a micro-porous structure, which results in high capacity surface adsorption of gasses or liquids. The adsorption capacity of AC depends mainly on its surface area, pore volume and pore size distribution characteristics. The pore sizes are defined as micro-pores (less than 2 nm), meso-pores (2-50 nm) and macro-pores (greater than 50 nm). The micro-pores contribute largely to the surface area, whereas the macro-pores act as channels to the micro-pore surfaces. Commercial AC has a surface area ranging between 800 and 1500 m^2/g. Two types of AC are commercially recognized; powdered and granulated AC. Powdered AC has an average particle size of 15-25 μ. These small sized particles are usually used in liquids to ensure that diffusion through pores are not rate limiting. Granular AC or pellets are use for gasses and liquids, depending on the application. Granular AC is usually regenerated after use, whereas powders are discarded. Granular and powder AC is produced commercially from precursor materials such as anthracite and bituminous coal, lignite, peat, wood, coconut shells, and nutshells (Pollard *et al.*, 1992). Therefore it can be said that carbonaceous agricultural by-products like bagasse are ideal for AC production. The transformation to AC can be done chemically or physically or by a combination of these two methods. The chemical method is done in one step, by adding activating agents such as $ZnCl_2$, H_3PO_4, and H_2SO_4 which are mixed into the inactivated char, after which it is washed to remove the excess chemicals. The physical method is a two step process involving pyrolysis of the raw mineral in inert atmosphere (typically slow pyrolysis) followed by activation at elevated temperatures with an oxidizing gas such as water or CO_2.

Garcia-Perez *et al.*, (2002) produced bio-char from bagasse with a surface area of 530 m^2/g, whereas Mullen *et al.*, (2010) produced bio-char from fast pyrolysis with a surface area of 0 and 3 m^2/g for corn cobs and corn stover respectively. Bagasse has a particularly suitable particle structure compared to other large scale agricultural by-products (Devnarain *et al.*, 2002; Mullen *et al.*, 2010). Figure 9 shows the surface of bagasse. It can be seen that even before carbonization the structure is already porous. This is very beneficial to high quality AC production, resulting in much research on bagasse activation over the past two decades.
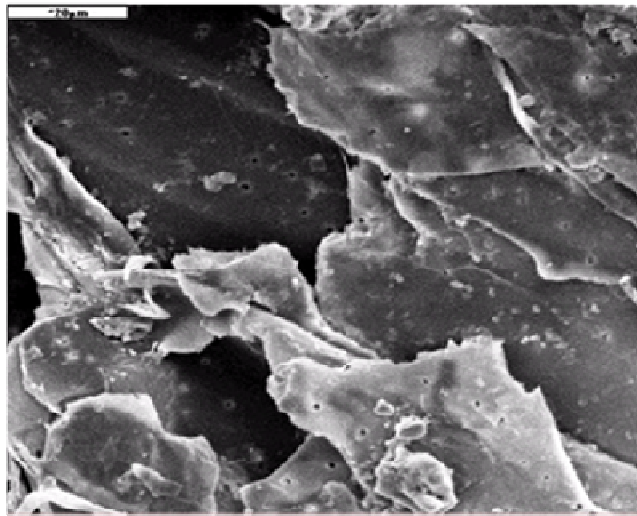
Figure 9: Scanning electron microscope reveals the surfaces of SB, showing the abundance of pores (Devnarain *et al.*, 2002) (Permission granted by SASTA to use this figure).

In the article from Devnarain *et al.*, (2002) AC from South African bagasse was investigated. The highest quality AC was produced by pyrolysis at 680°C with a hold time of 1h followed by activation with steam at 900°C. Different types of activated carbon were tested. Powdered activated carbon with high ash content (56 wt%) resulted in a significantly lower surface area. The BET surface area was 606 m^2/g compared with 995 m^2/g obtained from a sample with only 28 wt% ash. Ash therefore also has a detrimental effect on the surface area of activated carbon.

2.6.2.3   Bio-char fertilizer

An alternative to upgrading of the char is to use it as carbon fertilizer. Soil can be enriched by adding charcoal, which acts a reef for micro organisms and fungi, creating a rich micro ecosystem. Bio-char is highly absorbent and therefore increases the soil's ability to retain water, nutrients and agricultural

chemicals, and also prevents water contamination and soil erosion (Mullen *et al.*, 2010). It also contains the most of the original crop nutrients as ash, and will release them slowly. The bio-char remains in the soil for a very long time. By adding additional fertilizers to the charcoal the soil fertility will be increased dramatically. If ammonia (NH_3), carbon dioxide (CO_2), and water (H_2O) are all combined in the presence of charcoal they will form a solid, ammonium bicarbonate (NH_4HCO_3), fertilizer inside the pores of the carbon. 30% of the generated H_2 will be required to combine with all the carbon generated by the biomass. This process cleans the air by utilizing CO_2 produced from a coal plant (www.eprida.com, 2010). In many agricultural industries around the world, agricultural residues are burnt. In some cases it facilitates easier harvesting, and in other cases it is done to replenish the soil's nutrients. The remaining ash increases the soil pH and shows elevated nutrition and yields. The nutrient availability decreases only after a few seasons (Sanchez *et al.*, 1983). Lehmann *et al.*, (2003) found that charcoal applications directly increase the nutrient availability such as P and K and an increased nutrient retention for ammonium. In conclusion it can be said that bio-char from pyrolysis shows potential for use as fertilizer.

2.7 Slow pyrolysis

Slow pyrolysis, also known as conventional pyrolysis or carbonization, has been around for thousands of years where it was mostly used for charcoal production. To optimize the yield and quality of char, the following parameters are required:

- a reaction temperature in the region of 400-500°C for most biomasses;
- a slow heating rate (1-50°C/min) with large particle sizes typically < 5cm; and
- a long vapour residence time: 5 - 30 minutes char contact time to promote secondary reactions.

The vapour residence time is controlled by slowly feeding inert N_2 gas through the reactor. The longer residence time causes the vapours to continue to react and allows secondary cracking of vapours. This reduces the organic liquid yield and increases the char and gas production (Bridgwater *et al.*, 1999). The slow heating rate, and large biomass particle size causes a temperature gradient which effectively lowers the pyrolysis temperature inside the particle. Dehydration and secondary reactions therefore become the dominant reactions thereby increasing the char yield. As the char zone becomes thicker during carbonisation, the thermal conductivity decreases and the resistance to heat transfer increases. The temperature gradient appears and gradually increases and the inner zone is more difficult to heat. A typical slow pyrolysis product distribution yields 35 wt% char, 30 wt% liquid, 35 wt% gas (Table 1).

There are two industrial char production technologies, namely: kiln technologies which produce charcoal as sole product, and slow pyrolysis retorts which produce charcoal along with by-products (bio-oil and bio-gas). Carbonization in a retort allows for integrated utilization of the energy contained in the raw mineral. The by-products are usually re-used for heating. The charcoal quality is of higher grade in retort processes than kiln processes. Industrial char production by means of slow pyrolysis has a relatively short history, dating back only about 150 years (Honsbein *et al.,* 2007).

Zandersons *et al.* (1999) produced 23-28 wt% charcoal from bagasse slow pyrolysis. A two-stage process was recommended: the first stage was for drying and heating to 350°C followed by a glowing stage at 475-500°C. Form the energy balance they found that the pyrolysis volatiles would be sufficient to heat the process. The effect of different heating rates (10 and 30 °C/min) were investigated by Karaosmanoglu *et al.* (1999). It was found that higher heating rates improved liquid production. At lower heating rates more char was formed. Numerous publications of thermal degrading behaviours of bagasse have been done. The studies included inert and oxidizing conditions at different temperatures and heating rates (Katyal *et al.*, 2002). The results indicate a wide range in kinetic data due to variations in feedstock composition. Hu *et al.* (2001) investigated the effects of coal particle size on pyrolysis in a fixed bed reactor. The results indicated that increasing particle size decreases the heat transfer between particles. Similar results were reported by other researchers (Mesa-Perez *et al.*, 2005). Since bagasse particles are fine, and have a low bulk density, upgrading may be required.

Pellet production has been used to improve on the char yield in slow pyrolysis by increasing the size of the biomass particles (Erlich *et al.*, 2006). Wood pellets can also be sold as a commodity product, and are used for indoor heating. The annual production in Sweden alone is about 1 million tonnes. Cost of biomass pellet production in 2006 was about 30 Euro per ton. Pellet production holds benefits in storage, transport, moisture content and decreases heterogeneity. Erlich *et al.* (2006) reported that higher density pellets produce higher char yields, and smaller shrinkage during pyrolysis. Pellet production is therefore an expensive pretreatment but can improve pyrolysis char yields.

Much research has been published on thermogravimetric analysis of bagasse at slow pyrolysis conditions (Ouensanga and Picard, 1988; Roque-Diaz *et al.*, 1985; Varhegyi *et al.*, 1989; Caballero *et al.*, 1995: cited: Drummond *et al.*, 1996). In these studies high temperatures are investigated at low heating rates (0.5-2°C/s), and therefore it is not easily comparable to the high heating rates associated with fast pyrolysis (200 °C/s). TGA samples also typically range from 10-50 µg. In 1994 two studies were published on pyrolysis of bagasse at high temperatures, moderate heating rates and stagnant nitrogen

atmosphere. Lancas *et al.* (1994) obtained low liquid yields which suggested that secondary reactions had a significant effect. Stubington and Aiman, (1994) also reported reduced liquid yields because of secondary reactions. It was therefore clear that vapours needed to be purged to remove the volatiles from the reaction zone thereby reducing secondary reactions. Tsai *et al.* (2006) studied the pyrolysis of SB in an induction heating reactor. The volatile residence time was in the region of 38 seconds and the heating rate was 200°C/min. Liquid yields up to 50 wt% was obtained, but the quality was low due to the high water content.
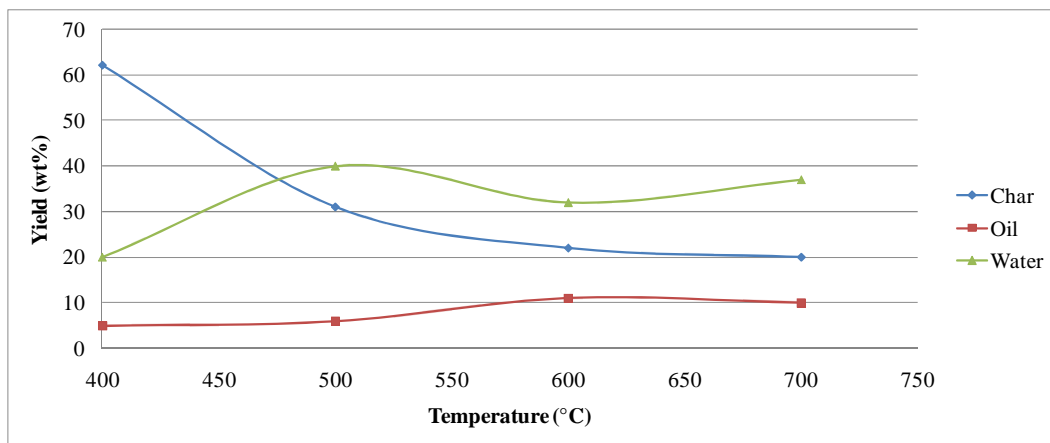
Figure 10: Pyrolysis of sugarcane bagasse by Tsai *et al.* (2006)

Bagasse was pyrolyzed in a fixed-bed reactor by Asadullah *et al.* (2007). The heating rate was around 0.9°C/s. This slow heating rate will result in a slightly increased char yield. Two condensers were used, the first at 60°C and the second at -5°C. The optimal liquid yield was 66 wt% bio-oil at 490°C. The separate yields of the two condensers are plotted in Figure 11 to illustrate the difference in quantity obtained at different temperatures.
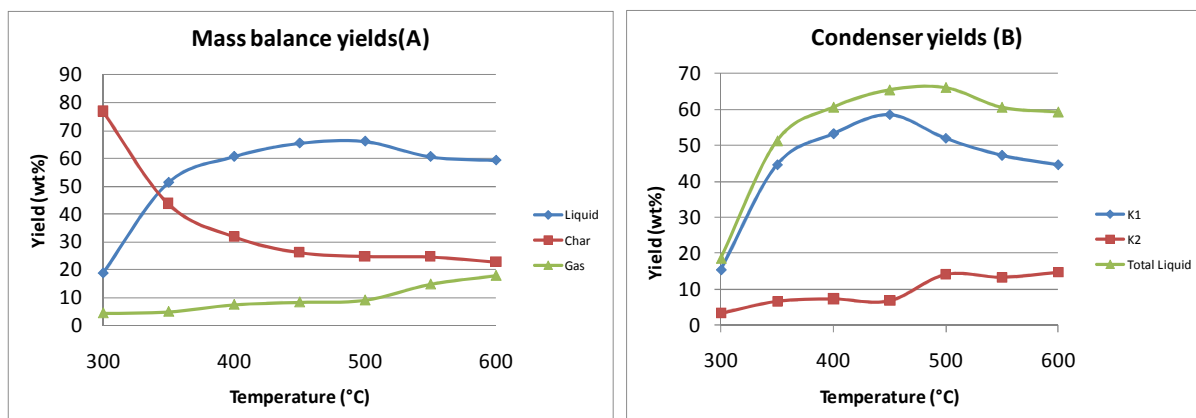
Figure 11: The results from fix bed pyrolysis; (A) shows the yields of char, liquid and gas; (B) shows yields of oil condensation at the different condensers (Asadullah *et al.* 2007).

Lab-scale slow-pyrolysis equipment normally consists of a batch reactor connected in series with condensers at various temperatures from 25°C to as low as -40°C (Figure 12). The char is collected from the reactor after the experiment.
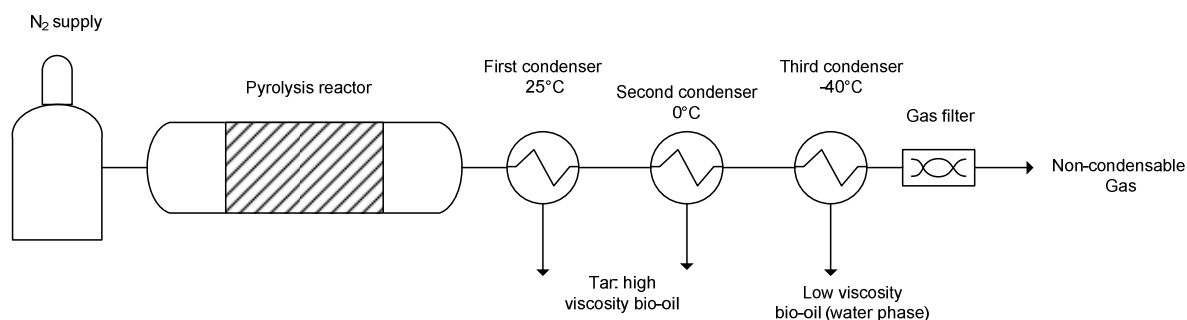
Figure 12: A simplified slow pyrolysis setup

2.8   Vacuum pyrolysis

Vacuum Pyrolysis (VP) is a more recent technology than slow pyrolysis. VP differs from slow pyrolysis mainly in that it is done under vacuum instead of using an inert gas to purge pyrolytic gas. This limits secondary reactions more effectively, which results in higher oil yields and lower gas, char and water yields. VP is usually conducted at 10-20 kPa, where conventional pyrolysis is carried out at atmospheric conditions. The temperature range is similar to conventional pyrolysis, and typically lies somewhere between 350 and 520°C (Rabe, 2005). Because of the lower pressure biomass fragments tend to evaporate

31

more easily. This removes them from the reaction zone, and results in a significantly reduced residence time. Therefore the bio-oil obtained is of superior quality compared to slow pyrolysis.

The earliest work on VP dates back to 1914 (De Jongh, 2001). Most of the pioneering experimental work was conducted by Professor Roy, with his earliest publications dating back to 1983. In 1990 a performance study on a 30kg/h vacuum pyrolysis unit was published (Roy *et al.*, 1990). This plant was operated at 9.3 kPa (abs). Economic analysis showed profitability only when by-products could be sold as high value chemicals. Some of the findings of Roy's experimental work are listed below:

- heat transfer calculations showed that radiation was the primary mode of heat transfer between the reactor and the particle bed;
- heat transfer could be increased by agitating the reactor bed, and thereby reducing the surface area required; and
- the optimum reactor pressure was determined to be 15kPa.

In 1997 Roy *et al.* developed a horizontal moving and stirred bed reactor. In 1998, the first industrial scale vacuum pyrolysis reactor (3.5 t/h) was constructed (Rabe *et al.*, 2005). Zandersons *et al.* (1999) used a fixed bed reactor to pyrolyse bagasse briquettes. Up to 28 wt% charcoal was obtained. More recently Garcia-Perez, (2002) did a study on SB vacuum pyrolysis to provide background data in the field. The smallest particles (<450 μm) were removed because they exhibit a very high ash content. 34.4 wt% bio-oil and 19.4 wt% char was obtained from this unit. Compared to the pilot-plant setup it produced 5 wt% less char but 4 wt% more bio-oil. Both solid and liquid fuel can be obtained from vacuum pyrolysis in more even proportions whereas slow and fast pyrolysis focuses on char and bio-oil production respectively. Both solid and liquid fuels can be utilized at industrial sugarcane mills for combustion, and both products can be upgraded. High quality bio-oil is obtained from VP making it ideal as feedstock for commodity chemical production. Apart from the increase in quality of bio-oil, char surface area is also significantly enhanced by the low pressure atmosphere (Lua *et al.*, 2005). These effects are discussed in more detail in chapter 4.

The equipment typically used to study vacuum pyrolysis is mostly similar to that of slow pyrolysis. The only major difference is the addition of the vacuum pump and removal of the nitrogen cylinder as illustrated in Figure 13.
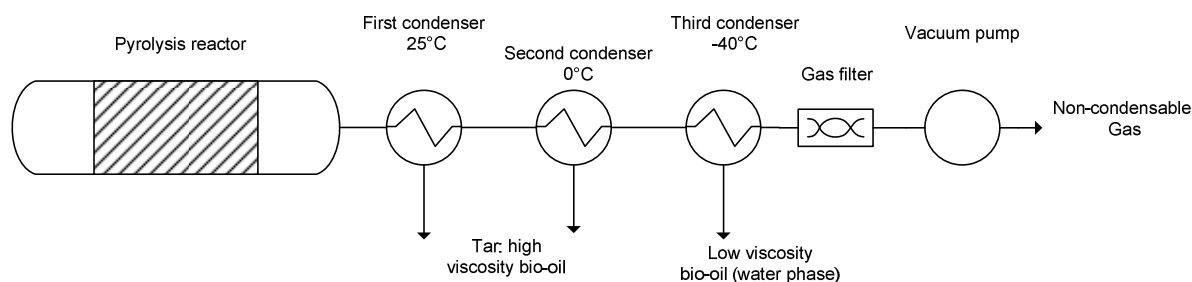
Figure 13: A simplified vacuum pyrolysis setup

2.9 Fast Pyrolysis (FP)

As the name suggests, the 'fast-pyrolysis' reaction occurs rapidly, in a few seconds or less. Therefore this process is dependent not only on the chemical reaction rate, but also on heat and mass transfer as well as phase transition. This is achieved by avoiding moderate temperatures (<400°C) and long residence times (> 2 s). As discussed in chapter 2.3 char production is favoured at lower temperatures and secondary reactions are minimized by removing the vapours from the reaction zone. To avoid fractionation of the oil product rapid cooling of vapours is essential. Therefore the biomass heating is done 'fast', the removal of vapours is done 'fast', and cooling is done 'fast' to obtain the maximum amount of bio-oil. The essential features of a FP process are summarized in Table 12 (Bridgwater *et al.*, 1999).

Table 12: The essential features of a fast pyrolysis process

Fast pyrolysis parameter	Comment
Very high heating and heat transfer rates	Small particles are usually required (< 2mm)
Controlled pyrolysis reaction temperature	500 – 520°C for most biomasses is optimal
Short hot vapour residence times	Less than two seconds is preferable
Rapid cooling	Avoids fractionation of oil and secondary reactions

2.9.1 *Review of literature on fast pyrolysis*

Pioneering work on fluidized bed reactors was done by Scott *et al.* (1982) with their earliest publication in 1982. Their experimental design involved variations in feedstock, temperature, vapour residence time, and particle size. Additional publications on this topic were published by Agblevor *et al.*, (1994), Horne and Williams (1996), Bridgwater *et al.*, 1999; Lou *et al.*, (2003), Kersten *et al.*, (2005), etc. These publications formed the foundation for theory on pyrolysis process conditions discussed in chapter 2.4. In

the 1990s the first pilot plants were constructed in Spain, Italy, the UK, Canada, Finland, and the Netherlands (Kersten *et al.*, 2005; Bridgwater, 1999b). The main technology providers are listed Table 13 (Lange *et al.*, 2007).

Table 13: Main fast pyrolysis technology providers

Technology provider/ trademark	Country	Scale (kg/h)	Reactor type
Dynamotive Biotherm™	Canada	400 and 4000	Fluidized bed reactor
Ensyn RTP™	Canada	1000	Circulating fluidized bed reactor
BTG	Netherlands	250	Rotating cone reactor
Pyrovac/ pyrolcycling™	Canada	50 and 3500	Vacuum reactor

Many different types of woody biomass have been used for experimental studies on FP. Most literature focuses on wood from the forestry industry. The literature on fast pyrolysis of bagasse is reasonably limited. The most extensive work on sugarcane bagasse pyrolysis was done by Garcia-Perez *et al.* (2002) who published various articles on vacuum pyrolysis of bagasse. The bio-oil obtained from this research proved to be high quality oils. Low moisture content, viscosity and acidity as well as high calorific values we obtained, compared to other bio-oils. The amount of liquid product obtained is not only dependent on how effective the reaction was, but also on how effective cooling and condensation is done.

Pyrolysis of bagasse was done in a wire mesh reactor by Drummond *et al.* (1996) at over the temperature range 400-700°C, and heating rates up to 1000°C/s. Figure 14 shows the results from pyrolysis of 7 mg of dried bagasse. The samples were heated at 1°C/s or 1000°C/s and then held for 30 seconds at the set temperature and then cooled at 200°C/s. The maximum liquid yield was found to be 55 wt% at 500°C and 1000°C/s. The results showed very low char yields in the region of 5 wt% even though the ash and fixed carbon content was estimated at 1.6 and 11.9 dry wt% respectively. The low char value suggests that some char entrainment into the oil phase might have occurred or that the experimental error might be significant due to the small sample size.
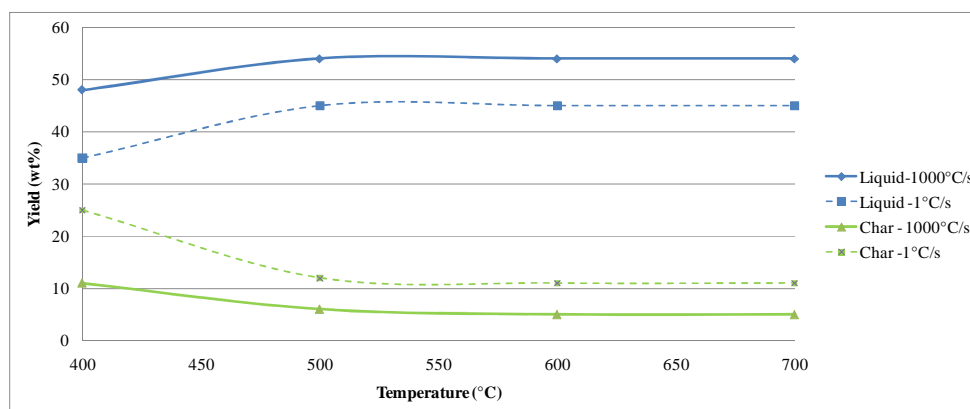
Figure 14: Fast pyrolysis of sugarcane bagasse by Drummond and Drummond, (1996)

These previous publications on pyrolysis of SB indicate variability within results, due differences in reactors, procedures, condensation systems, etc. (Table 14). Most of these previous studies only did pyrolysis on small samples in order to achieve a controllable heating rate. These studies show that fast pyrolysis of bagasse can produce a liquid yield of at least 55 wt% and that values as high as 66 wt% have been reported.

Table 14: Typical results for bagasse and wood pyrolysis

	Bagasse pyrolysis			Wood pyrolysis
Reference	Dummond and Drummond (1996)	Tsai *et al.*, (2006)	Asadullah *et al.*, (2007)	Bridgwater *et al.*, (1999)
Optimal temperature (°C)	500	500	490	500
Heating rate (°C/s)	1000	3.33	0.85	>200
Sample size (g)	0.007	10	200	n.d.
Vapour residence time (s)	0.005	38	0.5 -60	<2
Liquid yield (wt%)	54.6	50	66	65-70
Char yield (wt%)	8	20	25	15

2.9.2 _Technology and process characteristics_

Biomass FP has been extensively reviewed by a number of scientists (Bridgwater _et al._, 1999; Goyal _et al._, 2008; Mohan _et al._, 2005; S. Kersten _et al._, 2005). These reviews typically discuss the parameters important for reactor design, the challenges involved, some comparisons of different feedstocks, and evaluation of product quality. A number of literature articles also deal more directly with the design aspects of FP units, of which the most extensive design review was done by Gerdes _et al._ (2002). The sub-processes of fast pyrolysis are illustrated in Figure 15.
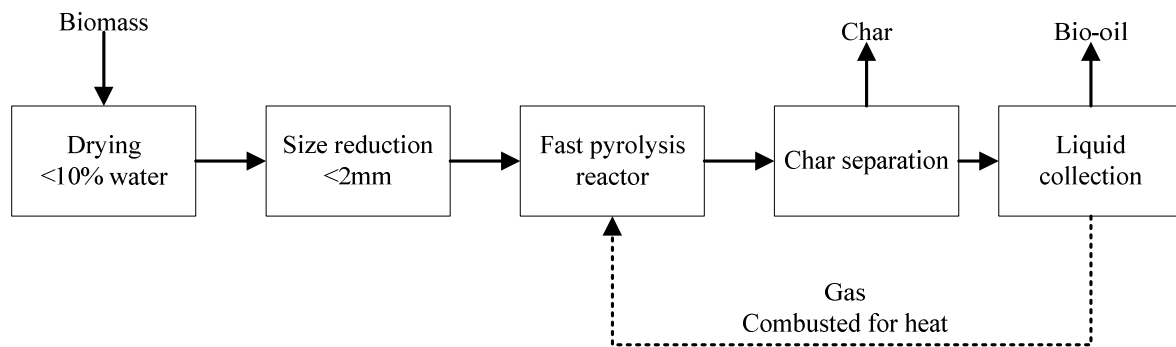
Figure 15: Sub processes of fast pyrolysis (Bridgwater, 2002)

2.9.2.1 _Feed water content_

Drying to about 10 wt% is usually required before pyrolysis. The pyrolysis reaction generates additional water resulting in a bio-oil that contains 15-35 wt% water (Westerhof _et al._, 2007). Generally less water in bio-oil is beneficial for energy density, stability and acidity (Oasmaa _et al._, 1999). The effect of water on bio-oil is discussed in paragraph 2.5.1.1. Bagasse contains about 50 wt% moisture as received and can typically be air dried to 10 wt% moisture before pyrolysis. The effect of water content was studied by Westerhof _et al._ (2007) who found that by increasing the moisture content of the feedstock the char and gas yields increased, the produced water decreased and the organic yield remained constant. It was found the increase of water content limited the heat transfer through the particle as a result of evaporation. Stubington _et al._ (1993) reported that a moist atmosphere (damp N_2 used as fluidizing gas) caused an increase in secondary reactions and gas yield. Excess water has a negative effect on fast pyrolysis conditions.

2.9.2.2 _Particle size reduction_

For most reactor types the particle size is strongly linked to the heat-transfer rate inside the particle. These effects are discussed in detail in paragraph 2.4.3. The generally accepted fast-pyrolysis particle size is less

than 2mm to ensure effective heat transfer to the particles in fluidized-bed type reactors (Bridgwater *et al.*, 1999). Size reduction adds additional processing cost. From an economic perspective additional size reduction should be justified by an adequate increase in bio-oil yield. Reactors that employ an ablative heating mechanism can utilize larger particles (paragraph 2.9.3).

2.9.2.3 Char removal

Rapid and effective separation of char particles is required, because char acts as a vapour cracking catalyst, therefore increasing secondary reactions. Two cyclones are usually used, the first for the bulk removal of solids and the second for removal of residual fines. Unavoidably some char fines will entrain downstream from the cyclones into the oil thereby exacerbating the instability of the oil (Bridgwater *et al.*, 2002). Different filtration methods have produced high quality char-free oils at the expense of 10-20 wt% of the oil yield due to further cracking of vapours (Bridgwater *et al.*, 2002). A different approach is to accept the char in the oil because it increases the HHV. FP products can be used to produce char-oil slurries which are then used in entrained flow gasifiers (Henrich, 2007; Lange, 2007).

2.9.2.4 Liquid collection

The product that exits the hot reaction zone comprises vapours, aerosols, gasses from the biomass as well as the carrier gas or fluidizing gas. These vapours require rapid cooling to stop secondary reactions. Slow cooling fractionates the oil by preferential collection of highly viscous lignin derived components, which may block the equipment (Bridgwater *et al.*, 1999). Rapid quenching is achieved by direct contact heat exchange, instead of indirect heat exchange (like shell and tube heat exchangers), resulting in a single phase bio-oil. The use of an immiscible hydrocarbon solvent as cooling liquid is widely practiced in lab scale setups. Dynamotive uses bio-oil from previous runs for cooling (www.dynamotive.com, 2009). The temperature at which the gas exits the condensation system affects the properties and yield of the oil. Lower temperatures will condense more moisture and volatile organic vapour which acts as solvents in bio-oil thereby decreasing the viscosity and tendency to phase separate (Bridgwater *et al.*, 2002). Higher temperatures (~90°C) will condense very little water and will produce a high viscosity, high calorific value and less stable bio-oil. Extreme cooling to sub zero temperatures is common practice in most lab scale pyrolysis units. However, since most of the oil is collected at higher temperatures, sub zero cooling is not done for large scale units. The remaining aerosol, that exits the condenser, requires coalescence which is commonly achieved by electrostatic precipitation which is discussed in more detail in chapter 3.7 (Bedmutha *et al.*, 2009).

2.9.3   *Fast-pyrolysis reactors*

Various reactor types have been used in order to optimize the parameters shown in Table 12. Pyrolysis has received considerable creativity and innovation to optimize these parameters. A thorough review of pyrolysis reactor configurations was published by Bridgwater and Peacocke, (1999) and Henrich *et al.* (2007). The fundamental difference between the types of FP reactors is the mechanism for heat transfer (Table 15). Gas-solid heating is mostly convective heat transfer and solid-solid heating is mostly conductive heat transfer (Bridgwater *et al.*, 1999).

Table 15: Heating mechanisms for FP reactors

Heating mechanism	Reactor type
Gas heating (N_2)	Gas fluidized bed reactors
Sand heating	Mechanically fluidized rotating cone and twin screw reactors
Direct contact heating	Ablative reactors (no fluidizing)

2.9.3.1   *Gas Fluidized Bed Reactors*

Biomass particles are fed to a cylindrical reactor, where incoming N_2 gas fluidizes and heats the particles. A high gas flow rate ensures rapid heating and short vapour residence times. The linear flow rate inside the reactor is dependent on particle size and reactor height, and is typically in the region of 0.3 m/s (Yanik *et al.*, 2007). Fluidized bed reactors are simple, and the technology is well understood. The reactors are easy to construct and operate, they are reliable and have consistent performance, and produce high liquid yields of 65 to 75 wt% (Bridgwater *et al.*, 1999). Small biomass particles (<2 mm) are required to achieve high heating rates. A secondary material, usually inert sand, is used to improve fluidization and heat transfer (Bridgwater, 2002). The main disadvantage of the reactors is the energy that is wasted to heat and cool the large amount of N_2 gas. Circulating Fluidized Bed Reactors (CFBR) are very similar to fluidized bed reactors, except that the char residence time is almost the same as with as for vapours and gas (Bridgwater, 2002).
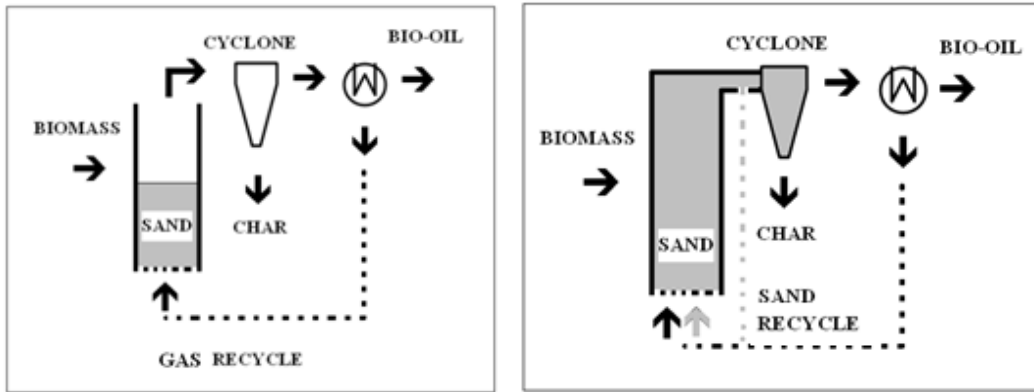
Figure 16: (Left): Fluidized bed reactor; (Right): Circulating fluidized bed reactor (Henrich *et al.*, 2007).

2.9.3.2   Mechanically fluidized reactors

Instead of using gas, biomass can be fluidized by mechanical agitation or mixing. The twin screw reactor operates by transporting biomass with large amounts of hot sand. This method wastes less energy on heating and cooling of a fluidizing gas. The hot sand particles can be recycled and do not require cooling after a cycle in the reactor. The challenge posed by this method is the recycling of the sand. At Foschungszentrum Karlsruhe (FZK) extensive work is being conducted with on twin-screw reactors, also referred to as Lurgi-Ruhrgas mixer reactors (Henrich *et al.*, 2007). The rotating-cone reactor transports sand and biomass by centrifugal forces (instead of mechanical screws), where after the hot sand is also recycled to the reactor. The mixer reactor and rotating-cone reactor is shown in Figure 17. Mechanically fluidized bed reactors also require small particles for efficient heat transfer.
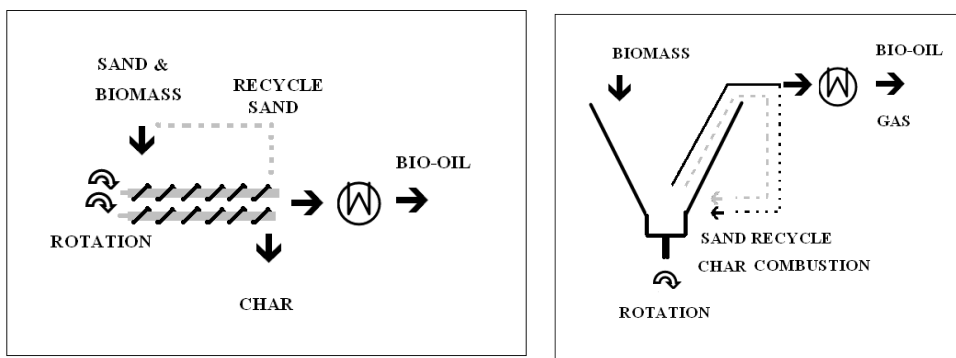
Figure 17: Left: Auger reactor (LR mixer reactor); Right: Rotating cone reactor (Henrich *et al.*, 2007).

.

2.9.3.3   Direct contact reactors

Ablative pyrolysis is different from the previous mentioned concepts. Instead of transferring heat by hot gas or sand, the biomass is pressed against the hot reactor wall, which causes it to "melt" as illustrated in Figure 18 (Bridgwater, 2002; Henrich, 2007). As the biomass is mechanically moved away, the residual oil film lubricates successive biomass particles and rapidly evaporates. The vapours are collected similarly to the other processes. One of the major advantages of ablative pyrolysis reactors is that much larger particles may be used than with fluidized bed reactors. Char is continuously abraded off the particles exposing fresh biomass for conversion. Therefore the reaction rate is not limited by heat transfer through particles, so large particles may be used. This will save money with feed preparation.
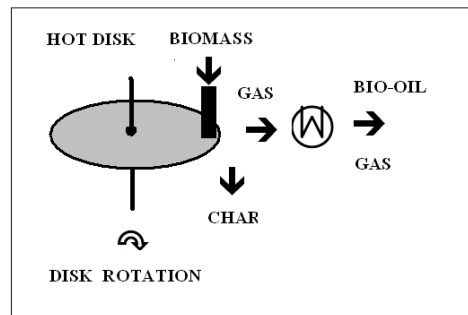
Figure 18: Ablative reactor (Henrich *et al.*, 2007).

2.9.3.4   An overview of fast-pyrolysis reactor characteristics for bio-oil production

Table 16 shows a summary of some of the key features of the different FP reactors. The undesirable characteristics are shown in black and desirable characteristics shown in white cells, and gray indicates moderate characteristics. The level of complexity is a good estimation of relative capital cost (Honsbein *et al.*, 2007). Similarly the gas and feed requirements gives a relative estimate of operating costs.

Table 16: Comparison of some of the key features of fast pyrolysis systems (Demo plants have a large throughput (200-2000 kg/h); Pilot plants (20-200 kg/h); Lab (1-20kg/h); (Honsbein *et al.*, 2007)) (LR-reactor is similar to rotating cone reactor)

Reactor type	Status	Bio-oil wt %	Level of complexity	Inert gas requirement	Feed size	Specific size
Fluidized bed	demo	75	medium	high	small	medium
Circulating fluidized bed	pilot	75	high	high	medium	large
Rotating cone	pilot	65	high	low	small	small
Ablative	lab	75	high	low	large	small
Vacuum	demo	60	high	low	large	large

2.9.4 *Description of a fluidized-bed pyrolysis plant*

Fluidized-bed technology is well known and construction is relatively simple. Therefore a fluidized-bed reactor is the most suitable reactor type for the first FP lab-scale unit at Stellenbosch University (SU). Figure 19 shows an example of a fluidized-bed FP plant. Biomass feedstock is fed continuously into the reactor. At the bottom of the reactor preheated recycled N_2 gas enters to fluidize the incoming biomass particles. The biomass reacts, which causes the particles to shrink and be transported with the volatiles. Larger particles may remain inside the reactor. The gas particle mixture then enters a series of two cyclones to separate the entrained small char particles. The clean gas then enters a direct contact quench column, to achieve rapid cooling. A light hydrocarbon (isopar blend), which is immiscible with the pyrolysis liquids, is used for cooling. The condensed product then collects at the bottom of the collection vessel, and the isopar is recycled. The uncondensed gasses enter an electrostatic precipitator, which collects entrained aerosols. Finally a dry ice condenser is used to collect any higher boiling point components. A gas meter records the amount of gas passing by, after which it is burned to supply process heat.
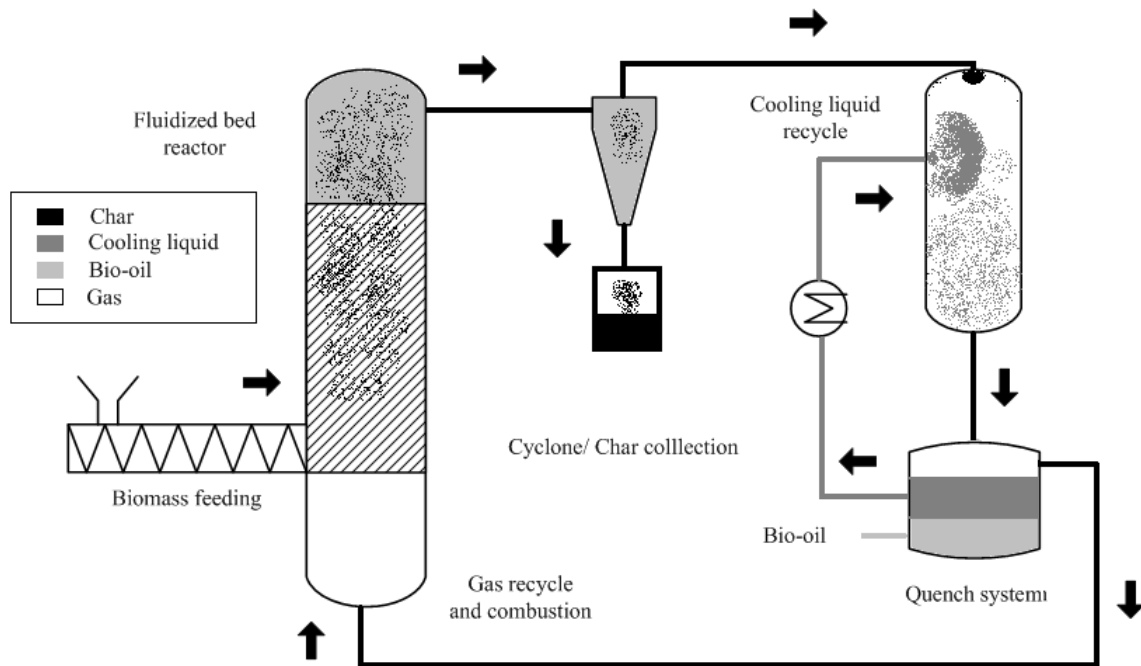
Figure 19: Simple representation of a fluidized bed fast pyrolysis setup (www.dynamotive.com, 2009)

2.10 Other thermo-chemical processes

Pyrolysis combustion and gasification are all thermo-chemical processes. The different processes and their main products are shown in Figure 20.
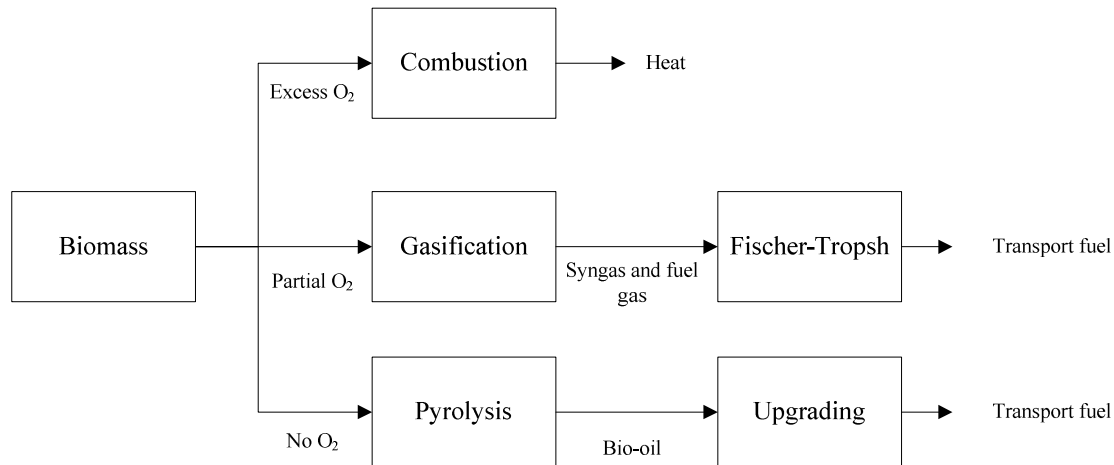
Figure 20: Thermo-chemical processes

2.10.1 *Combustion applications*

Solid biomass combustion is an established technology that has been used widely for many years. Industrially there are numerous methods for generating electricity from heat produced by combustion. These applications include: steam turbines, reciprocating steam engines, Stirling engines, indirect fired gas turbines, and direct fired gas turbines. A recent review showed that the steam turbine is the only established technology (Bridgwater *et al.* 2007). The other methods have efficiency advantages but are not commercially available (Bridgwater *et al.*, 2000). Low efficiency combustion systems are typically used at sugarcane mills. Biomass combustion may require drying to <50 wt% water, and size reduction (Goyal *et al.*, 2008).

2.10.2 *Gasification*

Biomass is converted into a combustible non-condensable gas mixture by partial oxidation of biomass at high temperature (800-1300°C). The gas consists mostly of carbon monoxide (CO), Carbon dioxide (CO_2), hydrogen (H_2) and methane (CH_4). This mixture is called the producer gas. Producer gasses can be used to run internal combustion engines (both compression and spark ignition), and can be used as substitute for furnace oil in direct heat applications (Goyal *et al.*, 2008). Apart from direct power production these gasses may also be used to produce methanol or syngas (also see 2.5.2), in an

economically viable way. The formation of these species can be explained by the following main chemical reactions that take place during gas production:

Combustion reactions:

$$C + \tfrac{1}{2}O_2 \Leftrightarrow CO \qquad \Delta H = -111 \text{ MJ/kmol}$$
$$CO + \tfrac{1}{2}O_2 \Leftrightarrow CO_2 \qquad \Delta H = -283 \text{ MJ/kmol}$$
$$H_2 + \tfrac{1}{2}O_2 \Leftrightarrow H_2O \qquad \Delta H = -242 \text{ MJ/kmol}$$
$$C + O_2 \Leftrightarrow CO_2 \qquad \Delta H = -394 \text{ MJ/kmol}$$
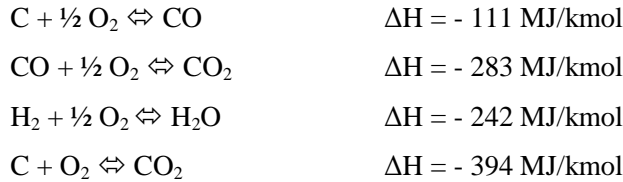
The Boudouard-reaction:

$$C + CO_2 \Leftrightarrow 2CO \qquad \Delta H = +172 \text{ MJ/kmol}$$

Water gas reactions:

$$C + H_2O \Leftrightarrow CO + H_2 \qquad \Delta H = +131 \text{ MJ/kmol}$$
$$CO + H_2O \Leftrightarrow CO_2 + H_2 \qquad \Delta H = -41 \text{ MJ/kmol}$$
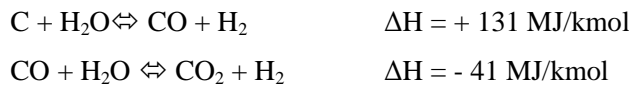
Methane forming reactions:

$$C + 2H_2 \Leftrightarrow CH_4 \qquad \Delta H = -75 \text{ MJ/kmol}$$
$$CO + 3H_2 \Leftrightarrow CH_4 + H_2O \qquad \Delta H = -206 \text{ MJ/kmol}$$
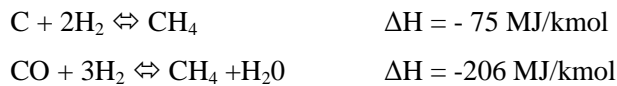
The reaction enthalpy (ΔH) is shown at 0°C and 1bar (abs) as obtained from Ullmann's Encyclopaedia (2002) (Lange, 2007).

2.10.3 *Torrefaction*

Torrefaction is a slightly less aggressive approach to biomass upgrading than pyrolysis. This is an alternative means of thermo-chemical conversion of biomass. It is conducted in an inert atmosphere similar to conventional pyrolysis. However the temperature is lower and ranges between 200 and 300°C. This technology is less sophisticated and can be seen as something in-between combusting dried biomass and pyrolysis products. The torrefied biomass is a solid, char like substance. The advantages of torrefied biomass over dry biomass are listed below (CGPL, 2006 and Pach *et al.*, 2002):

- Lower moisture content. This results in a higher heating value and increased energy density of the biomass.
- The particles are brittle and therefore size reduction is achieved more easily.
- The particles are hydrophilic. Whereas dried biomass regains moisture torrefied biomass does not gain humidity in storage, and is therefore more stable and resistant to fungal attack.

43

- Combustion: Reduced smoke formation during burning. The weight is reduced to approximately 70 wt%. 80-90% of the original energy content is retained in the torrefied biomass.

Torrefied biomass has applications in the following industries: as raw mineral for pellet production; as reducer for smelters in the steel industry; for the manufacturing of charcoal or activated carbon; as feedstock for gasification, and can be used as co-firing feed for boilers. Pioneering work in torrefaction was reported in the 1930 in France, although no publications of this work could be obtained. In the 1980's a 14 Kton/year plant was commissioned in France for briquette production. Burgois and Doat published torrefaction work which resulted in the construction of a continuous torrefaction plant in 1987 where the product was used as a reducing agent for the production of silicon metals (CGPL, 2006). Pach *et al.* (2002) published results regarding torrefaction of birch, pine and sugarcane bagasse on lab scale. It was found that the type of biomass influenced the product distribution significantly. The wood (birch and pine) favoured solid production and therefore less liquid and gaseous products than bagasse. Finer particles tended to produce more liquid. Bergman *et al.* (2005) published literature on electricity savings with regards to size reduction and pellet production. In 2006, at the Indian Institute of Science, a project was completed on the torrefaction of bamboo. A 1 ton/hr pilot plant was constructed. The optimal torrefaction temperature was found to be around 250°C. Moisture absorption of the product was about 6 wt%, approximately half of raw bamboo (CGPL, 2006). From the literature it can be said that torrefaction is a suitable alternative to conventional pyrolysis, depending on the application of pyrolysis char.

2.11 Thermogravimetric analysis

Thermogravimetric analysis (TGA) is the most common technique for investigating the devolatilization behaviour of biomass. TGA involves heating a sample mass at specific heating rate and measuring the change in mass as a function of temperature and time. A number of researchers have used this method to investigate the thermo-chemical characteristics of bagasse (Garcia-Perez *et al.*, 2001; Stubington *et al.*, 1993; Erlich *et al.*, 2005; Darmstadt *et al.*, 2001; Varhegyi *et al.*, 1989). Derivative Thermogravimetry (DTG) is usually also applied to the TGA data, to determine the rate of weight loss as a function of temperature. Small samples are used (10-20 mg) to eliminate temperature gradients within the samples. Typically only low heating rates (1 - 50°C/min) are studied in normal TGA equipment and therefore the conditions are similar to slow pyrolysis. The data obtained from TGA and DTG can be used to obtain kinetic parameters and model the devolatilization behaviour of biomass. Because of the complex nature of

biomass single component modelling is not adequate. For modelling purposes biomass can be subdivided into lignocellulosic components as shown in Figure 21. This is discussed in more detail in chapter 5. The comparison of fast pyrolysis and TGA is challenging due to the significant differences in heating rate and sample sizes.

```
                          ┌─────────────┐
                          │   Biomass   │
                          └──────┬──────┘
          ┌──────────────┬───────┴───────┬──────────────┐
          ▼              ▼               ▼              ▼
  ┌──────────────┐ ┌──────────┐  ┌──────────┐ ┌──────────────┐
  │Hemi-cellulose│ │Cellulose │  │  Lignin  │ │  Extractives │
  └──────────────┘ └──────────┘  └──────────┘ └──────────────┘
```
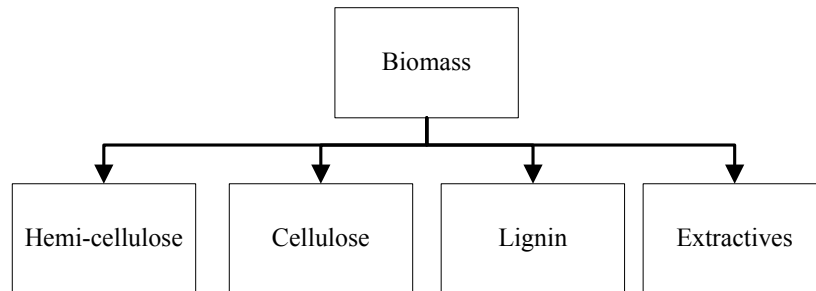
Figure 21: Biomass subcomponents

2.12 Implementation of FP in the sugar industry

Pippo *et al.*, (2007) evaluated the disposal practices of SB in the agro industries in terms of cost and energy balance. The advantages FP implementation in sugar industry is listed below:

- Conversion of bagasse and SCAR to bio-oil could be a solution to the problem of energy storage. This will create a stock which can be used locally as the need arises.
- A sugarcane mill factory has an appropriate energy infrastructure to assimilate technologies like FP.
- The infrastructure for transportation and distribution of conventional fossil liquid fuels can also be used for bio-oil.
- Bio-oil can be transported to remote, isolated towns and used for domestic tasks.
- Bio-oil stores 11 times more energy in the same unit volume of bagasse.
- Storable bio-oil provides an alternative to the total conversion of sugarcane biomass into electricity. Alternative applications now also become possible.
- On the basis of the pyrolysis infrastructure it is possible to introduce gasification technology without a large additional investment.

The disadvantages can be summarized as follows:

- The conversion process is endothermic.
- Bio-oil is not a stable fuel.

- Bio-oil upgrading is very expensive.
- There are no bio-oil standard properties or a specific bio-oil market.

Pippo *et al.* (2007) also conducted an economic assessment on this topic. In conclusion it was said that the implementation of any modern system for energy recovery from sugarcane biomass residue in developing countries could only be feasible under condition of government subsidies. The South African government is subsidizing renewable energy electricity (www.nersa.org.za, 2010). The increasing bio-oil price could provide incentive for private capital joint-venture projects to accelerate development in this industry. In 2006 it was speculated that 50\$/bbl could provide enough incentive. The current oil price is 83\$/bbl and the predicted price one year from now is 96\$/bbl (www.oil-price.net, April 2010). Therefore the implementation of FP at the sugar industry has growing potential that is economically dependent on the current increasing oil price.

2.13 Conclusions and problem statement

The utilization of bagasse as energy product in the sugar industry is not optimized with respect to current upgrading technologies. Volumetric energy densification by means of thermo-chemical processing is a suitable upgrading technology. Biomass pyrolysis produces storable and upgradable energy-dense products in the form of char and bio-oil, and is therefore deemed 'most suitable' for the sugar industry. The different pyrolysis processes produce varying amounts of char and bio-oil. Both products are useable in the sugar industry and present certain advantages. Char can be combusted or gasified as a solid energy-dense fuel, used as bio-char, or upgraded to activated carbon. High quality bio-oil can be combusted or gasified as a liquid energy-dense fuel, can be used as a chemical feedstock, and shows potential for upgrading to transport fuel quality. Experimental work on slow, vacuum and fast pyrolysis is required in order to investigate the quality of products that can be obtained from sugarcane bagasse.

Therefore the main research problem for this thesis is: "Which of the pyrolysis processes, slow, vacuum and fast pyrolysis are best suited for bio-oil and bio-char production from sugarcane bagasse and present a suitable alternative to direct combustion in the sugar industry?"

3   Design of a fast pyrolysis reactor

3.1   Introduction

This chapter discusses the design of a Fast-Pyrolysis Unit (FPU) for Stellenbosch University (SU). To shape a foundation for the design, a comparative review was completed on similar reactors used in previous pyrolysis related research. Standard design methods as well as, scale-up and practical experience contributed to the final design. In some cases the designs were modified in order to make use of readily obtainable material, or to save construction time and money. The objective is to design and construct a fluidized bed FPU capable of operating at a biomass flow rate of 1-2 kg/h.

3.2   Review: Fast Pyrolysis Units (FPUs)

A detailed discussion on the Fast-Pyrolysis (FP) theory is given in chapters (2.3 and 2.4). A fluidized-bed reactor was chosen for the new FPU because of its relative simple construction and operation. Previous fluidized bed FPUs are reviewed in this section. A motivation will be given for the most appropriate choice of components for the new FPU. The most extensive FP design review was given by C. Gerdes *et al.*, (2002). Table 17 shows the important design parameters for 6 different fluidized-bed FPUs.

Table 17: Comparison of fluidized-bed FPUs.

Specification	Yanik *et al.*, 2007	Westerhof *et al.*, 2007	Horne *et al.*, 1996	Lou *et al.*, 2004	Gerdes *et al.*, 2002	Rocha *et al.*, 2002
Feed rate (kg/h)	0.1	1	0.23	3	5	100
Height (mm)	33	420	500	700-1200	550	5000
Internal diameter (mm)	40	100	75	80	140	412
Waal thickness (mm)					5	
Heating (kW)				6	7.7	
Gas type	N_2	N_2	N_2	N_2	N_2	
Linear flow rate (m/s)	0.3	0.17				
Volumetric flow rate (Nm^3/h)	0.66			4.5	10	
Vapour residence time (s)	2	1	2.5			
Sand bed volume (L)	0.05		0.35			
Material of construction		SS 316			SS 1.4841	
Maximum temperature (°C)	500	480-500	400-550	700	1200	450-500
Bio-oil yield (wt%)	50			56	65	
Experiment duration (h)	1	2		2		
Particle size (mm)	2	2				

3.3   Mass and energy balance

The pyrolysis-process mass balance is shown in Figure 22. During pyrolysis biomass undergoes a process that yields gas, liquid and solid products. The product fractions were estimated from literature to be 0.65, 0.2 and 0.15 for oil, char and gas respectively. Nitrogen is inert and is not produced by the pyrolysis reaction. Therefore inlet and outlet mass flow rates of nitrogen are equal.
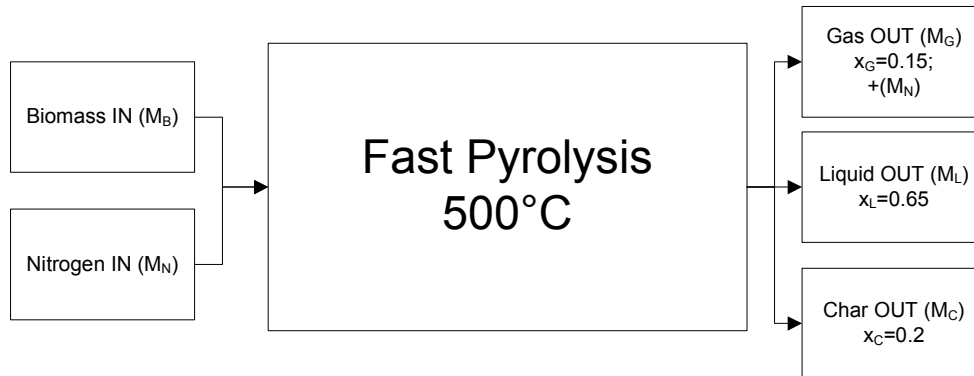
Figure 22: Mass balance: (Mass flow rate shown)

$M_B + M_N = M_N + M_G + M_L + M_C$

and (N_2 IN = N_2 OUT)

$M_B = M_G + M_L + M_C$

Equation 2

3.3.1   *Flow rates into the process*

The reactor is designed with a biomass flow rate of 1.5 kg/h (0.42 g/s). The nitrogen (N_2) flow rate inside the reactor is determined by fluidization characteristics. The N_2 gas velocity required for 2mm particles inside a FP fluidized-bed reactor is in the region of 0.3m/s (Yanik *et al.* 2007). Assuming a maximum linear velocity inside the reactor of 0.6 m/s, the mass flow rate N_2 is 4.35 kg/h. The maximum N_2 mass flow rate will be taken as 5 kg/h to increase the robustness of the design. For practical operation the N_2 flow rate should be in the region of 2 – 3 kg/h.

3.3.2   *Process description and design mass balance*

In Table 18 the mass balance used for design purposes is shown. The process flow diagram is shown in

Figure 23. N_2 enters at 5 kg/h and biomass at 1.5 kg/h. The main N_2 stream is heated in heater (Q03) and the remaining 10% of the N_2 is fed to the feeder (F02) to avoid hot reactor gases from entering the feeding system. In the reactor (R04) biomass is converted into gas and char of which 95 wt% is separated by the cyclones (C05 and C06). The remaining 5 wt% of the char is carried off into the liquid collection system (T07, D08 and EP09). Bio-oil is collected from stream (S10) and gas exits at stream (S11).

Table 18: Design mass balance for pyrolysis plant

Mass flow rates (kg/h)											
Stream (S)	S01	S02	S03	S04	S05	S06	S07	S08	S09	S10	S13
N_2	5.00	4.50	0.50	0.50	5.00	0.00	5.00	0.00	5.00	0.00	5.00
Biomass	0.00	0.00	0.00	1.50	0.00	0.00	0.00	0.00	0.00	0.00	0.00
Gas	0.00	0.00	0.00	0.00	1.20	0.00	1.20	0.00	0.23	0.00	0.23
Char	0.00	0.00	0.00	0.00	0.30	0.21	0.09	0.08	0.02	0.02	0.00
Bio-oil	0.00	0.00	0.00	0.00	0.00	0.00	0.00	0.00	0.98	0.98	0.00
TOTAL	**5.00**	**4.50**	**0.50**	**2.00**	**6.50**	**0.21**	**6.29**	**0.08**	**6.22**	**0.99**	**5.23**
Process conditions											
Temperature (°C)	25	25	25	50	500	500	500	500	450	10	15
Pressure (bar)	3.00	1.20	1.20	1.15	1.15	1.15	1.10	1.10	1.05	1.00	1.00
Gas density N_2 (kg/m^3)	3.44	1.37	1.37	1.21	0.51	0.51	0.49	0.49	0.50	1.21	1.18
Volumetric flow rate N_2 (m^3/h)	1.5	3.3	0.4	0.4	9.8	0.0	10.3	0.0	10.1	0.0	4.2
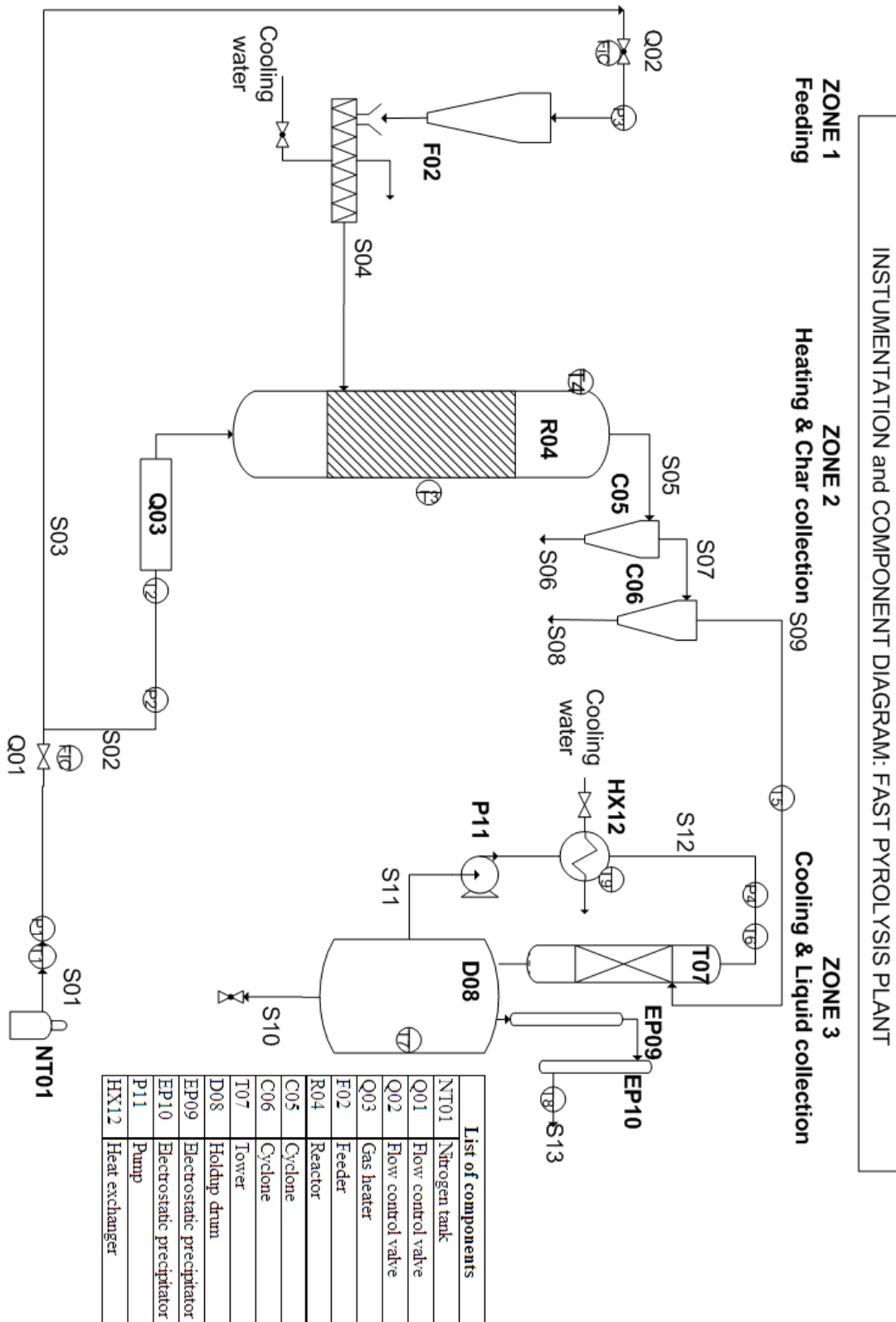
Figure 23: Instrument and component diagram for the FPU_1

3.3.3   *Energy balance*

The energy balance of the system can be viewed as the separate combination of N_2 gas and biomass and pyrolysis products. N_2 gas does not undergo phase change or reaction and it therefore requires heating and cooling to the design temperatures. Biomass requires heating, and then undergoes a reaction resulting in phase change. The pyrolysis product requires cooling and condensation.
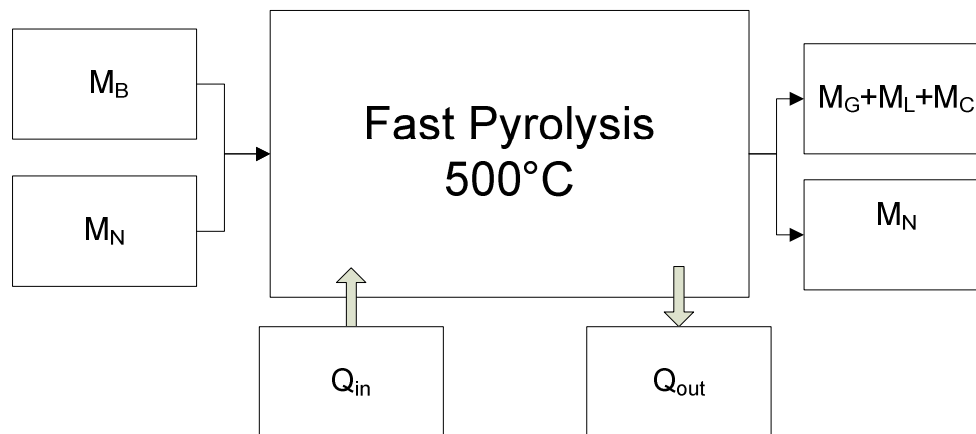
Figure 24: Energy balance

$$E_{out} = E_{in} + E_{generated} - E_{consumed} - E_{accumulated} + E_{losses}$$

<div align="right">Equation 3</div>

At steady state the accumulation of energy is zero. A well insulated reactor will only have minor heat losses to the environment. Generally the fast pyrolysis reaction is considered slightly endothermic with values between 200 and 400 J/g (Van de Velden *et al.*, 2010) (also see paragraph 2.3). Therefore at a biomass flow rate of 0.4 g/s approximately 150 J/s could be required. During pyrolysis energy is required in the form of heat, to create the reactive conditions. Equation 4 was used to calculate the heating and cooling requirements shown in Table 19 and Table 20. The references for thermodynamic properties are given in paragraph 11.2.1 in the appendix.

$$Q_{in} = \Delta E = \Delta E_{heating} + \Delta E_{evap} + \Delta E_{rxn}$$

$$= \sum M_i \int_{25}^{500} C p dT + \sum M_i \Delta H_{evap} + \sum M_i \Delta H_{rxn}$$

$$= M_{Biomass} C p_{ave} \Delta T + M_{Nitrogen} C p_{ave} \Delta T + M_{water} \Delta H_{evap} + (M_{biomass} - M_{water}) \Delta H_{rxn}$$

Equation 4

Table 19: Heating requirements

Species	M (kg/h)	Cp (ave) (kJ/kg.K)	ΔH (ave) kJ/kg	ΔT (K)	Q (kJ/h)	Q (kW)
Biomass heating	1.50	1.20	n.a.	475	855	0.24
Dry biomass reaction (90 wt%)	1.35	n.a.	150	n.a.	203	0.06
Water phase change (10 wt%)	0.15	n.a.	2300	n.a.	345	0.10
Nitrogen heating	5.00	1.10	n.a.	475	2613	0.73
Total						1.12

The design heating capacity for the reactor is 3kW to account for losses. Cooling calculations were done similarly, except that no reaction takes place (Table 20). The design cooling capacity is also 3 kW.

Table 20: Cooling requirements

Species	M (kg/h)	Cp (ave) (kJ/kg.K)	ΔH (ave) kJ/kg	ΔT (K)	Q (kJ/h)	Q (kW)
Bio-oil cooling	0.98	2.20	n.a.	490	1051	0.29
Water phase change (25%)	0.24	n.a.	2300	n.a.	561	0.16
Oil phase change (75%)	0.73	n.a.	1150	n.a.	841	0.23
Pyrolytic gas cooling	0.23	1.5	n.a.	490	221	0.05
Nitrogen cooling	5.00	1.10	n.a.	490	2695	0.75
Total						1.48

3.4 Fast pyrolysis Fluidized Bed Reactor (FBR)

Fluidization is defined as an operation by which a bed of solids acquires fluid-like properties by passing a fluid through it. When a fluid is passed upward through a bed of particles the pressure loss in the fluid will increase due to frictional resistance. At the point where the upward drag force equals the weight of the particles, the bed becomes fluidized (Figure 25). A further increase causes instabilities and bubbling will start to occur. A further increase will cause slugging (large bubbles) and thereafter transport the sand out of the vessel (Rhodes, 2005). Controlled bubbling fluidization is ideal for the pyrolysis reactor, since

the sand should remain inside the reactor. The sand in the reactor will improve fluidization and heat transfer of biomass (Cui *et al.* 2007). The bubbling bed will promote mixing, expand the bed, and the breaking of bubbles will burst sand into the freeboard.
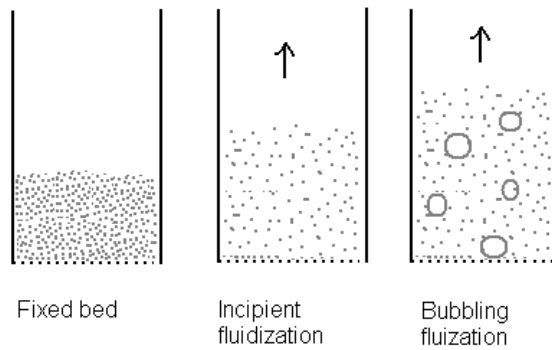
Figure 25: Fluidization of sand

Sand particles will be fluidized inside the reactor. Typical particle size range is in the region of 400 – 600 μm (Yanik *et al.* 2007). The sand particles are assumed to have a sphericity of 1. The sphericity of a particle is defined as the ratio of the surface area of a sphere (with the same volume as the given particle) to the surface area of the particle. Biomass particles are not spherical and therefore the sphericity (φ) needed to be calculated. The particles were simulated as cylindrical rods with a sphericty of 0.55 (calculation in paragraph 11.2.3). x_{sv} is the diameter of a sphere having the same surface to volume ratio as the particle in question (Equation 5).

$$x_{sv} = \varphi x_p$$

Equation 5

To calculate the pressure drop though a bed of particles Equation 6 is used (Rhodes, 2005). Where 'ρ_p' is particle density (kg/m^3); 'ρ_f' is fluid density (kg/m^3), 'H' is the bed depth (m); M is bed mass (kg); 'ε' voidage; 'A' is the cross-sectional area (m^2) of the vessel; and g is gravitational acceleration (9.81 m^2/s).

53

$$\frac{Mg}{A}\left[1-\frac{\rho_f}{\rho_p}\right] = \Delta P = H(1-\varepsilon)(\rho_p - \rho_f)g$$

<div align="right">Equation 6</div>

The fluid velocity at which the particles become fluidized is 'U_{mf}' and is also referred to as the velocity at incipient fluidization. U_{mf} increases with particle size and density. Inside the fast pyrolysis FBR both sand and biomass particles should be fluidized. The flow rate should be slightly above U_{mf} for sand. As biomass particles enter they should become fluidized and small particles will be carried off. The larger particles will react and thus decrease in size and density and will eventually also entrain in the gas. Some larger particles may remain in the sand bed. The equations used to calculate U_{mf} for the sand and biomass are shown below. The Reynolds number at minimum fluidization is 'Re_{mf}', and 'μ' is the kinematic viscosity of the fluid. The dimensionless Archimedes number (Ar) can be calculated as follows:

$$150Re_{mf}\left(\frac{1-\varepsilon}{\varepsilon^3}\right)+1.75\frac{\left(Re^2_{mf}\right)}{\varepsilon^3} = Ar = \frac{\rho_f(\rho_p-\rho_f)gx_{sv}^3}{\mu^2}$$

<div align="right">Equation 7</div>

$$Re_{mf} = \frac{\rho_f U_{mf} x_{sv}}{\mu}$$

<div align="right">Equation 8</div>

By solving the left and right hand side of Equation 7 simultaneously, Re_{mf} can be found which will then be used to calculate U_{mf}. The appropriate particle size range for sand particles was found to be in the region of 400 – 600 μm, similar values were reported by (Yanik *et al.*, 2007).

A force balance on the particles is required to calculate at what velocity the particles will be transported out of the reactor. The Stokes equation (Equation 9) is the result of this force balance on a single particle falling under gravity. U_t is the terminal velocity (m/s) of the particle. Stokes law can be assumed to apply to the bed of particles, only if the particle interaction and voidage effects are accounted for. Therefore the altered Stokes equation is shown in Equation 10 to calculate the corrected particle velocity (U_p).

$$U_t = \frac{x^2(\rho_p-\rho_f)g}{18\mu}$$

<div align="right">Equation 9</div>

$$U_p = U_t . \varepsilon^n$$

<div align="right">Equation 10</div>

The values of n are calculated by making use of the Kahn and Richardson (1989) equation as recommended by Rhodes (2005).

$$\frac{4.8 - n}{n - 2.4} = 0.043 Ar^{0.57} \left(1 - 2.4 \left(\frac{x_{sv}}{D_{tube}} \right)^{0.27} \right)$$

<div align="right">Equation 11</div>

Where, Ar is the Archimedes number, and x_{sv} the corrected particle size (m), and D_{tube} the vessel diameter (m). A typical voidage of 0.45 was used for the calculation.

The calculations are listed in paragraph 11.2.4 in the appendix. Properties and assumptions are listed in Table 60. The minimum fluidization and transport velocities are calculated in Table 61 and Table 62 respectively. When comparing all the results from the fluidized bed calculations (Table 21) the range of linear velocities inside the reactor can be identified for the different particles. As shown for 2 mm biomass particles slightly higher velocities were used in previous research (Yanik *et al.*, 2007). In practice the velocities may be slightly higher and are dependent on biomass density.

<div align="center">Table 21: Gas velocities in the fluidized bed</div>

	Particles	Minimum fluidization occurs	Vertical forces on particle is in equilibrium	Typical velocities in FBRs for 2 mm particles	
	x_p (mm)	U_{mf} (m/s)	U_p (m/s)	U (m/s)	Reference
Biomass	3.0	0.16	0.40	0.25 - 0.3	Yanik *et al.*, 2007
	2.0	0.07	0.16	0.3 - 0.4	Lou *et al.*, 2004
	1.0	0.02	0.03		
Sand	0.6	0.28	0.95		
	0.5	0.20	0.59		
	0.4	0.13	0.33		

3.4.1 *Biomass reaction mechanism*

The shrinking core model describes the physical changes during the reaction inside the reactor (Fogler, 2006). This model predicts that as the biomass reacts the particles become smaller and smaller. During pyrolysis a combination of size and density reduction will occur simultaneously. As they decrease they become small or light enough to entrain in the gas stream.

3.4.2 *Fluidizing Gas*

Nitrogen (N_2) is generally used as inert fluidizing medium because it is the cheapest option available. For larger pyrolysis units N_2 should be recycled into the system to save operational costs. Gerdes *et al.*, (2002) recycled N_2, and flared off a bleed stream. The scaled down gas flow rate from Lou *et al.* (2004) suggests a consumption of 2-4 m^3/h N_2 for SU-FPU. With approximately $8m^3$ of useable N_2 in a gas cylinder only about 1hour of continuous operation is possible. This will allow enough N_2 to purge the reactor during heating (before a run) and cooling (after a run) at a low flow rate.

Nitrogen is continuously fed through the reactor, and undergoes a temperature change as it is heated. This temperature change causes a density decrease which results in a higher volumetric gas flow rate (Equation 12). FP is normally done at atmospheric pressure and is optimized at 500°C for most biomasses (Gerdes *et al.*, 2002). However, the pressure inside the reactor may be slightly above the atmospheric pressure because of the pressure drop over downstream equipment. Table 22 shows density values at 1 bar and 1.2 bar to illustrate the effect of pressure.

$$PV = nRT$$

Equation 12

Where: 'P' is pressure (kPa); 'V' is Volume (m^3); 'n' is mol (Kmol); 'R' is kJ/kmol.K and 'T' is temperature (K), (Cengel, 2003).

Table 22: Design values for nitrogen gas density

Density (1.2 bar) [kg/m3]	Density (1 bar) [kg/m3]	Temperature (°C)
1.37	1.15	25
0.53	0.44	500

3.4.3 *Reactor size and material of construction*

The sizes of the FPUs reviewed in Table 17 ranged from 0.1 to 100 kg/h. The reactor size and feed rate, used in the study by Lou *et al.* (2004), is the closest match to the FPU at SU. The ideal construction material for a FP reactor is SS 1.4841 because of its high-temperature resistance. However SS 316 has been previously used, and proven to work. Material SS 316 is readily obtainable in South Africa, whereas SS 1.4841 is not. The materials cost for the reactor would be 5 times more if the high-temperature steel were to be used. Literature suggests a reactor ID of 0.07 - 0.08 m with a fluidizing gas flow rate of 2 - 4 m^3/h. The reactor wall thickness of at least 5 mm will be used similar to Gerdes *et al.* (2002). The size of the reactor was found not to be critical because flow rates and particle sizes can be altered to some extent to achieve the desired fluidization. A FBR diameter of 75 mm is known to cope with a biomass feed rate of 2kg/h, (Lou *et al.* 2004). A larger L/D ratio for reactor dimensions will allow higher gas flow rates to be tested (before sand is bubbled out of the reactor). This will improve the heat transfer inside the FBR because of more vigorous mixing. The rector volume necessary to achieve a vapour residence time under 2 seconds, determined the height of the reactor. To keep large particles and sand from being blown out of the reactor at high gas flow rates the top section of the reactor has a diameter of 90mm (Gerdes *et al.*, 2002). Refer to Figure 49 size enlargement effects and paragraph 11.2.12 for component drawings (Figure 53).

3.5 Feeding system

The feeding system consists of a hopper, with an attached feeder. The biomass is fed continuously into the reactor, which is slightly overpressure. The objectives for the design of the feeder are to:

1. achieve a constant flow rate of biomass;
2. investigate the control options;
3. overcome challenges involved with overpressure inside the reactor; and
4. prevent reactions from occurring inside the feeding system.

The most common feeder type used is a screw feeder, and most lab scale plants use this type of feeding system (Gerdes *et al.* 2002; Yanik et al 2007). A screw, connected to an electrical motor, turns inside a pipe and forces the biomass to flow. The advantages are (Gerdes *et al.*, 2002; Yanik *et al.*, 2007):

1. it can be used for many types of biomass;

2. it feeds at a constant volumetric flow rate (therefore if biomass density is constant then it will also give a constant mass flow rate); and

3. the design is simple, and can easily be modified.

A second type of feeder that can be considered is an air operated piston feeder. This type of feeder will cause pulsating flow which is not ideal. The construction will be more challenging, and this design is not favoured by most researchers. Problems may occur with different types of biomass. However, by using a piston operated feeder the problems with reactor overpressure are eliminated. Based on practical experience, simple construction and low system pressures a screw feeder was designed for use at the FPU.

3.5.1 Reactor overpressure

A slight overpressure (0.1 bar) may be present inside the reactor. Consequently heated gasses will escape at the feed inlet if appropriate precautions are not taken. A system should be implemented to ensure that this does not occur. During operation of the screw feeder the tube will be filled with biomass, which leaves a significant air gap inside the feeding tube where hot gasses from the reactor will be able to flow. The feeding system will be sealed and a slight overpressure (with N_2 gas) will be applied.

3.5.2 Volumetric or Gravimetric control

A constant feed rate into the reactor is ideal for pyrolysis. The feeder might not be able to feed constantly because of a variation in feedstock density, hopper level, or clogging. Implementation of gravimetric control can account for density variation. If the controller senses a decrease in mass flow rate, the screw speed will be increased to hold the system at its set point. The entire feeding system will be placed on a platform scale or load cell. Therefore the feeding system requires a flexible connection. This system will also be subject to unforeseen interactions, like bumping against the feeding section which may upset the control system. An attempt was made to implement gravimetric control on the PDU (at FZK); but was found to operate less accurate than volumetric feeding due to interactions (personal communication: Dr Ralf Stahl). The alternative is volumetric control which can be applied accurately if constant biomass density can be achieved. At FZK a volumetric feeder was used at the lab scale fast pyrolysis reactor discussed by Yanik *et al.* (2007). Owing to the challenges with gravimetric control, a volumetric feeding was implemented at the FPU at SU. Feeder calibration is required for each type of biomass to determine the exact mass flow rate (Yanik *et al.*, 2007).

3.5.3 *Overheating of the feeding section*

The reactor temperature will be maintained at approximately 500 °C, because it is the known optimal temperature for biomass pyrolysis (Bridgwater *et al.*, 1999). This high temperature will cause heating of the feeding pipe. If the feeding section is not kept cool enough fouling and char deposits may form. Therefore a water-cooled heating jacket was designed to reduce the temperature around the feeding pipe. This will keep the feeding section temperature low enough to ensure that no reactions occur outside the reactor.

A 200 mm long double pipe heat exchanger was constructed at the tip of the feeding unit. The energy balance is shown in paragraph 11.2.6 of the appendix.

3.5.4 *Sizing*

The feeder design included a hopper, attached to a screw feeder. The top of the hopper will have a biomass loading cap for easy loading of the biomass. The screw pipe system requires some design. Because of the variability of different biomasses, the design must be robust enough to handle different biomasses. A hollow core screw, with a pitch equal to the diameter, will be used because practical experience has shown that this is best for fibrous particles such as bagasse. The sizing for this design is listed in Table 63, and illustrated in Figure 58, (paragraph 11.2.5).

Table 23: Calculation for flow rate at 50% filling of screw

Dimensions (mm)		Percentage filling	Pitch volume (L)	RPM	Volumetric feed rated (L/h)
Pipe ID	37	50%	0.037	10	10.97
Screw OD	34			20	21.93
Void	1.5			30	32.90
				40	43.87

A flow rate of 10-20 L/h will be required for different biomasses. Therefore this feeder is capable of achieving the desired flow rate. These calculations suggest that smaller pipe sizes can be used (Table 23) but were mainly selected on availability. The larger pipe size will reduce the bridging effect inside the hopper. The hopper is sized based on the approximate bulk density of the material. The hopper walls leading to the screw all have steep inclines to reduce the effect of bridging. If bridging persists a tapping device may be installed. The drawing of the feeder is shown in paragraph 11.2.12, Figure 58.

3.6 Direct contact cooling tower

According to Bridgewater *et al.* (1999) efficient liquid collection is one of the major challenges with pyrolysis. This is because the pyrolysis vapours are not true vapours but rather, a combination of true vapours, micron-sized droplets and polar molecules bonded with water molecules. The cooling rate affects the liquid collection. Slow cooling leads to collection of more lignin derived compounds, which causes the viscosity to increase, and fractionates the product which could cause blocking (Gerdes *et al.*, 2002). Slow condensation also allows more time for secondary reactions to continue (Gerdes *et al.*, 2002). Rapid cooling is therefore desired for fast pyrolysis where a single phase bio-oil is desired.

3.6.1 *Type of heat exchanger*

Direct contact heat-exchangers provide rapid quench-cooling and are preferred for fast pyrolysis (Gerdes *et al.*, 2007; Bridgwater *et al.*, 1999). A cooling liquid, that is immiscible with bio-oil, is sprayed onto the hot pyrolytic gasses. Indirect heat-exchangers, such as conventional shell and tube or double pipe heat exchangers usually do not give sufficient heat transfer coefficients (Coulson and Richardson, 2005). Pyrolysis is considered a dirty process and therefore cleaning of high surface area plate heat-exchangers will be very difficult. A direct contact heat exchanger was designed for the FPU at SU.

3.6.2 *Cooling liquid*

It is vital that contact of a foreign liquid with bio-oil should render the bio-oil unchanged after condensing and separation. Furthermore the cooling liquid should be inert, immiscible with bio-oil and safe under the specified operating condition. Light hydrocarbons are used for this purpose (Gerdes *et al.*, 2002; Bridgwater *et al.*, 1999). Hydrocarbons are combustible and therefore a mixture with a high boiling point and flash temperature is used ensure safe operating conditions. According to Prof. Bridgwater isopar blends are most suitable for this application (personal communication). Isopar is the brand name given to a range of iso-paraffinic hydrocarbon liquids with narrow boiling point ranges. The product information was obtained from ExxonMobil and is shown in Table 65 in paragraph 11.2.7 in the appendix.

Some fast pyrolysis technology providers use bio-oil from a previous runs for direct contact cooling of pyrolysis vapours (www.dynamotive.com, 2009). This is unfortunately not an option for experimental setups because large quantities of coolant are required and fresh bio-oil will be contaminated by the previous bio-oil mix. Water can also be used as coolant it but will mix with bio-oil and therefore jeopardize the mass balance accuracy. The FP setup used in the study from Henrich *et al.*, (2007) (and Lange *et al.*, 2007) uses water for direct contact cooling in the second condenser.

3.6.3   *Energy balance and sizing*

The amount of energy that need to be removed from hot pyrolysis gasses as they enter the condensation system was determined in paragraph 0 to be 1.48kW. The design cooling capacity is 3kW.

Hot pyrolysis gasses are contacted with the cooling liquid which is sprayed into a fine mist to increase the cooling surface area. The heat will be removed from the incoming gas stream by evaporation of cooling liquid and direct heat-exchange between molecules. The flow rate of cooling liquid inside the tower depends on the amount of evaporative cooling that is done. Different configurations of isopar cooling to provide over 3 kW of cooling is shown in Table 24. The variables are % evaporation of coolant, the change in temperature of coolant, and the mass flow rate of coolant. This gives an estimate of the flow rate required to achieve the desired cooling capacity. It is evident that evaporative cooling is dominant due to the small coolant temperature difference.

The minimum design flow is 1 L/min (45 kg/h). An air operated, diaphragm pump is used to transport the coolant through the system with maximum coolant flow rate and pressure, 12 L/min and 5 bar respectively. This system is more than sufficient to provide the necessary cooling.

Table 24: Different configurations of isopar cooling to provide over 2 kW of cooling

Variables			Isopar properties		Calculation		
Evaporation %	ΔT	m kg/h	H_{evap} kJ/kg	Cp kJ/kg°C	$Q = mCp\Delta T$ kJ/h	H_{evap} kJ/h	Q_{total} kW
10	10	50	1942	2.01	1007	9711	2.98
50	10	11	1942	2.01	221	10682	3.03
100	10	5.5	1942	2.01	111	10682	3.00
100	20	5.5	1942	2.01	221	10682	3.03

A nozzle will be used to spray the coolant into the tower. The sizes of the droplets will determine the heat exchange surface area inside the tower. Two nozzle types were tested for the tower spray system. The nozzle characteristics are listed in the appendix, paragraph 11.2.8, Table 66. The PJ model gives a very fine mist which will result is a high heat transfer surface area. However, this type of nozzle can clog easily if any solids enter the liquids stream. The TF model provides fine atomization, and is operated at higher flow rates, and does not clog easily. At the specified flow rate the PJ model gives approximately twice the heat transfer area of the TF model. Three nozzle connectors were installed on the tower; one at the top and two below the gas inlet.

When a rapid approach to thermal equilibrium is achieved the sizing of the tower is not critical and can be based on experience with similar processes. Direct contact heat exchangers give very high heat transfer coefficients typically in the range of 100 - 2000 W/m^2°C (Coulson and Richardson, 2005). A conservative estimate was made to calculate the time required to achieve the desired heat exchange of 3kW. The calculation of the surface area produced by each type of nozzle is shown in paragraph 11.2.8, Table 66 in the appendix. The heat exchange area will decrease as the droplets coalesce. Equation 13 is used to calculate the required heat transfer. The calculation for the mean temperature difference (ΔT_m) is given in paragraph 11.2.9. From Table 25 it can be seen that in all cases the predicted gas residence time is well under 1 second, to achieve the desired amount of cooling. The heat transfer coefficient was taken as 1000 and 100 W/m^2°C to compare the effect that this may have on the design (Test A and B). The efficiency is due to the large surface area and high mean temperature. The effect of a change in mean temperature difference is shown in test B and C.

$$Q = A \times \Delta T_m \times U$$

<div align="right">Equation 13</div>

Where 'Q' is the heat transfer rate (W), 'A' is the heat transfer surface area (m^2) , 'ΔT_m' is the mean temperature difference (°C) and 'U' is the overall heat transfer coefficient (W/m^2°C).

Table 25: Calculation of time required to achieve heat exchange inside the cooling tower.

Test	Nozzle type	Area m^2	ΔT °C	U W/m^2°C	Q kJ/s	Time required (s) to transfer 3 kW of heat
	TF	1	104	1000	104	0.03
A	PJ	2	104	1000	208	0.01
	TF	1	104	100	10	0.29
B	PJ	2	104	100	21	0.14
	TF	1	52	100	5	0.58
C	PJ	2	52	100	10	0.29

The cooling tower is overdesigned because it does not add too much to the expenses involved with the design. The volume of the tower is calculated based on a residence of 10 seconds at an outlet gas flow rate of 3.5 N.m^3/h. The cooling tower volume will be in the region of 10 L. A large L/D ratio will be used because this is normally the case for cooling towers (Coulson and Richardson, 2005). This will allow the

tower to be constructed from standard pipe sizes instead of manufacturing a drum. Hot gasses will rise to the top and cold gasses to the bottom. The tower was constructed from (D =100mm) SS316 tube and the different sections were connected with clamp and ferrule assemblies, with chemically resistant teflon seals. Sections were required to allow access to the nozzles. The bio-gas inlet pipe has a downward slope to ensure that no liquid coolant enters the hot zone. The gas is forced down the tower into the liquid collection vessel. See section 11.2.12 for detailed drawing.

3.6.4   *Liquid collection vessel*

The liquid collection vessel is sized to provide 25 L of buffer volume with approximately 5 L of freeboard space. A square drum was constructed from SS 316. The bottom plate is skewed so that all bio-oil can accumulate on one side of the vessel for easy draining. Bio-oil is immiscible with isopar and collects at the bottom because of its high density (1.2 g/ml), and isopar collects at the top (0.75 g/ml). Two valves were installed on the front side; one at the bottom to drain the bio-oil and one slightly above the bio-oil level to draw off the isopar for recycling to the tower (see section 11.2.12 for detailed drawing).

3.6.5   *Cooling unit*

Cooling is supplied to the new FPU by means of a water cooled water chiller. The chiller was supplied by Diaken, model number 'EWWP104KAW1N', has a nominal cooling capacity of 13 kW, and uses 3.6 kW of power. The basic specifications of the chiller unit are listed in Table 70 in paragraph 11.2.11. This unit is more than capable of providing the calculated 3 kW of cooling. This is the smallest chiller that was commercially available at the time of construction. The chiller cannot be directly connected to the coolant holdup vessel, because the required minimum cooling volume (62L) of the chiller is significantly higher than the volume of the liquid collection vessel (25L). Apart from this, fouling problems are prone to occur if a cooling pipe is located inside the liquid collection vessel. Therefore a water bath is chilled and the coolant (isopar) for the condenser tower will be circulated inside the cold water bath by means of a copper coil system. The operation temperature of the unit is dependent on the type of cooled liquid that is used.

3.7   Electrostatic Precipitators (ESPs)

ESPs are typically used in industry to remove particles from gas streams (Parker, 2003). In the case of pyrolysis it is used to recover small micron sized bio-oil droplets from the gas stream (Yanik *et al.* 2007;

Bridgwater *et al.* 2002; Gerdes *et al.* 2001). The simplest form of an ESP is a round pipe with a weighed wire that is suspended in the centre, and is commonly used for pyrolysis. The wire (discharge electrode) is energized with a High Voltage (HV) which creates a high electrical field (corona) around the discharge electrode. The corona ionizes gas molecules as they enter the ESP. This causes the formation of positive and negative ions (depending on + or – charge applied to discharge electrode) (Parker, 2003). Assuming a positive corona, the positive gas ions are immediately captured by the neutral electrode (inner pipe wall). The negative ions and electrons are forced by the electric field to migrate into the inter-electrode space. As the gas particles pass through the inter-electrode space they become charged, either by collision with ions/electrons or by induction (only the smallest particles). The charged particles are then forced by the electric field towards the collecting electrode (inner pipe wall) (Parker, 2003).

The corona characteristics are affected by the presence of electropositive or electronegative gasses which easily absorb or reject negative ions. In a pyrolysis setup liquid droplets will be collected, and will then flow to the bottom of the condenser drum. The electrical resistivity is of importance. Reverse ionization may occur if the resistivity is greater than 10^{12} Ωcm, which will reduce the efficiency considerably because of the large charge buildup at the collection electrode (Parker, 2003). Bedmutha *et al.* (2009) found that impurities in the nitrogen carrier gas greatly affected the voltage-current characteristics, but it was showed to vary significantly less when a mist was introduced to the gas. Parker (2003) states that negatively energized ESPs are normally used for industrial gas cleaning operations because the corona initiation voltage is lower and the breakdown voltage is higher. However, nitrogen and hydrogen do not form negative ions by electron attachment. Therefore positive corona is used for FP gas-cleaning (Bedmutha *et al.*, 2009).

ESPs can be operated at temperatures of up to 850ºC. The temperature does not significantly affect the separation efficiency of the device (Parker, 2003). The operating temperature mostly affects the material of construction for this unit. ESPs are usually operated at ambient conditions.

3.7.1 *Sizing*

The linear gas flow rate for industrial dry precipitators is typically about 15 m/s and is reduced to 1.5 m/s through the precipitator, (Parker, 2003). However, a linear velocity of 0.3 m/s is suggested by Bebmutha *et al.* (2009) for use in pyrolysis applications. Specific sizing can be done if the mean droplet size is known, from which the drift velocity can be calculated at a given voltage (Bebmutha *et al.* 2009). At FZK a single stage ESP was used (Yanik *et al.*, 2007), but it was shown by Bedmutha *et al.* (2009) that a two

stage ESP performs better. A two stage ESP consists of an ionizing section followed by a collection section, whereas ionizing and collection occurs simultaneously in a single stage ESP. In Figure 26 the difference is illustrated.

A simple weighed wire design was implemented based on the ESP used by Yanik *et al.* (2007). The ESP was separated from the bio-oil collection vessel by an electrical insulator. The sizing was based on a similar residence time. The present design employed a slightly shorter residence time because the ESP used by Yanik *et al.* (2007) was found to be overdesigned during testing. A linear velocity close to the recommended velocity of 0.3 m/s was used (Bebmutha *et al.* 2009). Figure 26A illustrates the first design.

Table 26: Comparison of size and linear velocity of different ESPs

	FZK	Bedmutha *et al.*, 2009	US
ID (m)	0.04	0.06	0.06
L (m)	0.50	0.45	0.50
U (m/s)	0.16	0.30	0.25
Residence time (s)	3.0	1.5	2.0
kV	10	16	15

The conductive nature of the bio-oil posed problems for the design of the ESP. The oil was found to collect on the sides of the tube and would run down onto the electrode weight and create a short circuit thereby significantly reducing the efficiency of the unit. The discharge electrode was eventually redesigned similar to the design of Bedmutha *et al.* (2009) (a two stage ESP). Because of the updraft gas flow in the first ESP the effective length of the collection electrode is shorter, only 0.3 m. Consequently not all vapours collect at one ESP, and a second unit was required. The modified design is shown in Figure 26B.
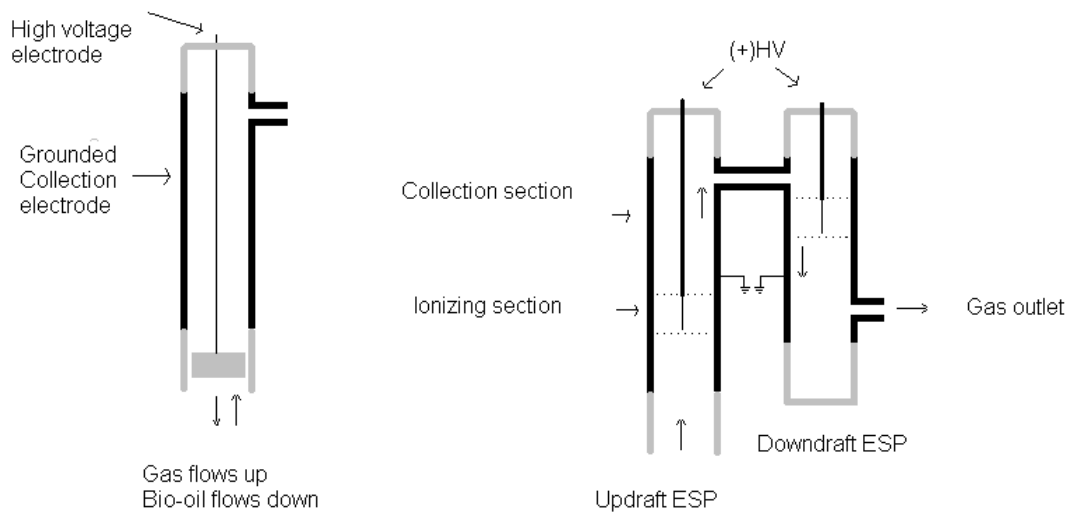
Figure 26: (A): Drawing of the original (single stage) electrostatic precipitator. (B) Modified design: Two two-stage ESPs; one updraft, and one downdraft gas flow. Black indicates conductive materials and gray indicates electrical insulation (Glass or Teflon). Detailed drawings are shown in Figure 56 in the appendix.

3.8   Additional equipment

3.8.1   *Oven*

Large pyrolysis plants often use fuel gas burners to provide heat to the reactor. This allows for the combustion of incondensable pyrolytic gasses, resulting in a cleaner and more energy efficient system. Gas heaters are typically not used for small FPU because it will increase capital costs and hazards associated with the unit. Two practical heating systems were investigated. Heating elements can be directly mounted onto the reactor (Lou *et al.*, 2004; Gerdes *et al.*, 2002) or an oven approach (Westerhof *et al.*, 2007; Yanik *et al.*, 2007) can be employed. Local suppliers could not meet the specifications for the first option. The oven approach was therefore implemented. The advantages with heating inside an oven included accessibility of all components and easy operation. Due to the size of this oven a lifting system was installed.

The pyrolysis oven draws 6.6kW which is more than double the design value of 3kW. The increased electrical power will decrease the time required to heat the oven. A two piece round cylindrical oven was constructed by a local kiln manufacturing company. Under normal conditions (small reactor size) only the top and bottom sections of the oven are used. A fibreglass partition was installed in the bottom section of

the oven, because this section will need to be warmer than the top section to heat cold nitrogen. The dimensions of the oven are given in Figure 54 in the appendix, (paragraph 11.2.12). An onboard control system uses Proportional-Integral-Derivative (PID) control, to maintain process set points.
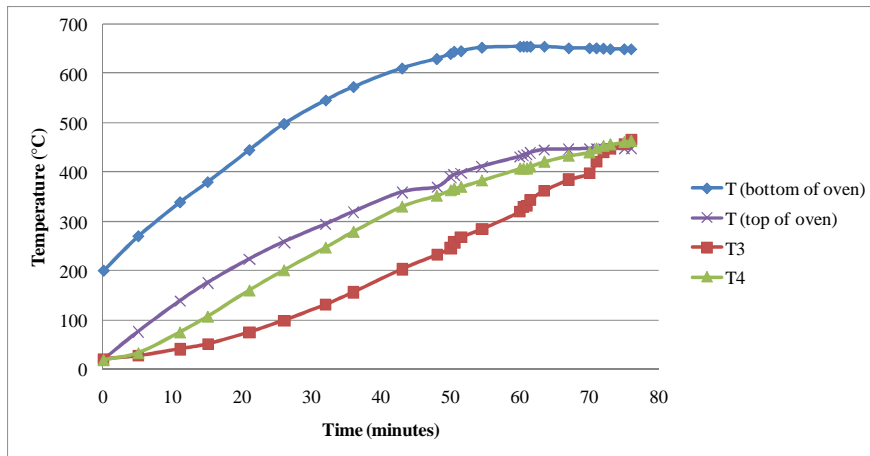
Figure 27: Shows the temperatures inside the oven and reactor during heating of the oven. T_3 is in the middle, and T_4 is at the top of the reactor.

The oven was calibrated in order to achieve a small temperature difference in the reactor (Figure 27). The commissioning of the oven is discussed in paragraph 11.2.18. A temperature difference of 10°C was allowed inside the reactor. No additional preheating of the gas was required. For each different reactor temperature set point the oven will require calibration. In Figure 27 the oven and reactor temperatures during heating are shown. The top two curves show the oven temperature that reaches equilibrium. After about 70 minutes the variation of temperature inside the reactor (T_3 and T_4) approaches zero. T_3 should be slightly hotter that T_4 to heat the incoming biomass and provide energy for the endothermic pyrolysis reaction. The oven calibration for different reactor temperatures is shown in Table 27.

Table 27: Reactor temperature (°C) at different oven set points

Reactor temperature (°C)	428 ± 4.5	495 ± 4.5	526 ± 2.2
Set point for top of oven	420	470	510
Set point for bottom of oven	570	670	710
Oven temperature difference	150	200	200

3.8.2 *Piping*

The generalized equation for optimum stainless steel pipe sizing, from Coulson and Richardson (2005), was applied for the design (Equation 14). The objective was to choose a single tube size for all hot gasses. For the gas flow a 16 mm SS316 tube was chosen slightly larger than the recommended value to accommodate fouling. Fouling problems often occur in the pipe section between the reactor and cooling tower. For cooling liquid circulation and nitrogen supply a 10 mm tube is used. The availability of pipes and fittings, and pump specifications also posed some limitations on the choice of pipe sizes. The calculations are shown in Table 71 in Paragraph 11.2.16.

$$D_{optimum} = 260G^{0.52}\rho^{-0.37}$$

Equation 14

Where G = mass flow rate (kg/s) and ρ = density (kg/m^3).

3.8.3 *Cyclones*

The single cyclone system did not achieve a high degree of separation at FZK (Yanik *et al.*, 2007). Similar problems were reported by Gerdes *et al.* (2002). Therefore two cyclones will be used in series to increase the separation efficiently. Problems with very small particles may still persist. The standard procedure for the design of a high efficiency cyclone was followed from Coulson and Richardson (2005). The typical characteristics include; an efficiency of 85%, a typical inlet gas flow velocity of 10 - 20 m/s, and a pressure drop of 0.1 kPa. The standard cyclone sizing dimensions are illustrated in Figure 28 (A). Using this design and typical flow rates inside a cyclone, the characteristic diameter was calculated (Table 72, in paragraph 11.2.17). The design was altered slightly to allow the use of standard Material Of Construction (MOC). The final dimensions are shown in Figure 28 (B).
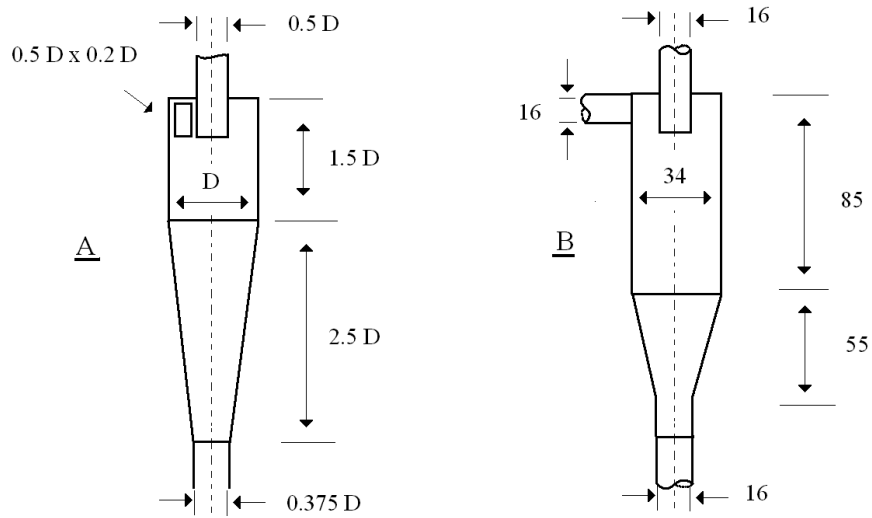
Figure 28: (A) Standard cyclone dimensions (Coulson and Richardson, 2005); (B) Final dimensions of cyclone (mm)

3.8.4 *Control and instrumentation*

The control system is used by the operator to monitor the process and ensure safe operating conditions, and record data. No PID (Proportional Integral Derivate) control loops are required for the system. Components such as the oven and chiller have onboard PID control to maintain these units at their specified set points. To monitor the process temperature and pressure various sensors were installed at the FPU (see Figure 23). The process conditions and set points can be altered from the touch screen. Every 30 seconds a data point is logged onto a flash disk. The sensors and control instrumentation for the FPU is listed in Table 74 (paragraph 11.2.19 & 11.2.15).

3.9 Safety

To ensure safe operation of the equipment unfamiliar operators should be trained by a person that is familiar with the equipment. An operation manual is given in paragraph 11.2.21. A risk assessment is given in paragraph 11.2.22. The two most severe risks that were identified are associated with the flammability of the coolant, and hot surfaces on the equipment.

3.10 Summary

In Table 28 a summary is given of components that were chosen for new FPU. The full component specifications are given in paragraph 11.2.11. The component and instrumentation diagram is shown in Figure 23. Photographs of the main components are shown in Figure 59 and Figure 60.

Table 28: Component summery

Unit	Type
Reactor	Gas fluidized bed reactor (75 mm diameter)
Fluidizing gas	N_2 with a mass flow controller
Heating	Oven
Feeding	Pressurized screw feeder
Solid collection	2 Cyclones in series
Cooling	Direct contact cooling tower
Aerosol collection	2 Electrostatic precipitator in series
Control	Data logging for process instrumentation

4 <u>Comparison of slow and vacuum pyrolysis of sugarcane bagasse</u>

Prelude to chapter 4

This chapter forms part of the experimental work on pyrolysis of sugarcane bagasse. The joint article entitled, *"Comparison of slow and vacuum pyrolysis of sugar cane bagasse"* was written by T.J. Hugo and Dr. M. Carrier and was supervised by Prof J.H. Knoetze and Prof J.F. Görgens from Stellenbosch University. All experimental and analytical work relating to slow pyrolysis was done by T.J. Hugo and similarly, the experimental work relating to vacuum pyrolysis was done by Dr Carrier. In all cases identical protocols were followed. From the first submission of the article some minor corrections were required. The article has recently been re-submitted, with correction to *The Journal of Analytical and Applied Pyrolysis*".

Marion Carrier, Thomas Hugo, Johann Görgens, Hansie Knoetze*

Department of Process Engineering, University of Stellenbosch, Private Bag X1 Matieland, 7602, South Africa

*Corresponding author: Prof. Hansie Knoetze, Tel: 021 808 4488 Fax: 021 808 2059 Email: jhk@sun.ac.za

4.1 Abstract:

Experimental results for slow and vacuum pyrolysis of sugar cane bagasse, in the same reactor allowing the comparison of these two processes, are reported. The experimental results showed that vacuum pyrolysis leads to a higher BET specific surface area whereas slow pyrolysis seemed to favour the HHV of charcoal. Detailed yields of products are presented and the influence of temperature and heating rate were studied using a design of experiments and an ANOVA analysis. From the results the optimum experimental conditions to maximise the yields of char and bio-oil products, as well as their heating value and specific surface area characteristics, were established. The optimal yields of bio-oil for vacuum pyrolysis were obtained at 400-500 °C and a heating rate of 15-24 °C min^{-1}, and for char the corresponding values are 340-350 °C and 18-24 °C min^{-1}. Slow pyrolysis produced the highest char yield. The optimal ranges of temperature and heating rate differ from that of vacuum pyrolysis mainly due to the short residence time of the vapours in the case of vacuum pyrolysis. Optimum conditions for bio-oil and char yields did not correspond with conditions to optimize the BET surface and HHV for chars, and to minimize the water content of the products.

4.2   Introduction

Thermo-chemical processes such as pyrolysis and gasification have recently become a topic of interest for conversion of biomass into clean energy and valuable products. The choice of the process depends on the desired product. Fast pyrolysis leads to a high yield of bio-oil while vacuum and slow pyrolysis offer a good compromise for the production of char and bio-oil, providing high yields and with superior quality of the char products [1]. Bio-oil potentially represents a valuable liquid fuel for boilers, while its chemical composition suggests that it is a challenging matrix for isolation of chemicals, as well as nutritional and pharmaceutical products. The char represents a good feedstock both for boiler fuel and the production of activated carbon. Comparative studies have been carried out between the different types of pyrolysis: slow, fast and vacuum [2-9]. They differ in terms of chemistry, overall yields and quality of products. A precise comparison is possible if the pyrolytic treatment is carried out in the same reactor. Nevertheless, some authors compared the trend of pyrolysis products from various reactors and they justified the deviations in absolute values by differences in the reactor configurations and conditions [5-9]. The design of the reactor can induce major differences in the results which do not come from the pyrolytic process and the comparison could be difficult to evaluate. This study proposes to convert through vacuum and slow pyrolysis biomass in the same reactor.

It is recognized that biomass surpasses many other renewable energy sources, because of its abundance, high energy values and versatility. Since bagasse is the most abundant crop waste in the world [10], it may be used as an energy product without directly compromising production of food and thus affecting food prices.

The influence of process parameters such as temperature, pressure, heating rate and residence time has been extensively studied [11-15]. When temperature increases under normal pyrolysis conditions the char yield decreases and the release of volatile matter increases. With regards to the char quality, an increase in temperature will increase the ash and fixed carbon content. Consequently, there is a decrease in volatile matter in the char with an increase in pyrolysis temperatures. Therefore, higher temperatures yield chars of greater quality, although the char yield diminishes [11]. The optimal yield for bio-oil is reached at an intermediate temperature. At higher temperatures more compounds are degraded, leading to the formation of non-condensable gases and a decrease in bio-oil yields [12]. Concerning the pressure, it is widely accepted in scientific literature that higher pyrolysis pressures will increase the number of re-condensation reactions, which leads to more of the vapours becoming trapped on the char, thereby

72

increasing the water content in bio-oils while reducing their quality. The presence of water in bio-oil lowers the energy density and the flame temperature of the oils; it may lead to ignition difficulties, and may cause pre-evaporation of the oil resulting in injection difficulties during preheating [12]. The heating rate in pyrolysis substantially influences product yields, with higher heating rates leading to higher liquid product yields [13]. The mass transfer restrictions that apply to the volatile contents of biomass can be improved by slowing down the pyrolysis reactions. A longer residence time favours secondary reactions such as thermal cracking, repolymerization, and recondensation, thereby minimizing liquid yield. However, employing a higher heating rate removes these limitations on the yield of bio-oil. As a result, the oil yield increases substantially under fast pyrolysis conditions [14]. Moreover, the heating rate also has an effect on the BET surface area of the char produced in the pyrolysis process. A low heating rate of 5 °C min^{-1} was not effective to remove volatile matter from char during the pyrolysis of pistachio-nut shells. For a low heating rate of 5-10 °C min^{-1} the subsequent activation of char resulted in an insufficient pore structure for the production of activated carbon. However, for higher pyrolysis heating rates of 20 °C min^{-1} and above, the devolatilization reactions were sufficiently intense, resulting in a highly developed porous structure. This porous structure will lead to the development of mesomacropore structures during the subsequent activation, as the CO_2 molecules can diffuse into the pores more easily [15]. Consequently, the BET surface area and micropore volume increase for pyrolysis heating rates greater than 10 °C min^{-1}, resulting in char that is more suitable for activated carbon production. Finally, increasing the pyrolysis residence time will increase the fixed carbon content of the char, because of an increase in the fraction of volatile matter released from the char during pyrolysis [15].

This study presents the different experimental conditions applied in statistically-designed experiments conducted in vacuum and slow pyrolysis of sugar cane bagasse. The objectives of these subsequent experiments were: firstly, to determine the reproducibility of the results concerning char and bio-oil yields, and secondly, to determine the optimal experimental conditions, in particular temperature and heating rate, to maximise the yields of char and bio-oil, together with the calorific value of these products. The BET surface area of chars produced under the selected experimental conditions was also determined to estimate their value as feedstock for the production of activated carbon.

4.3   Methods and materials

4.3.1   *Sugarcane bagasse*

The sugar cane bagasse was provided by the Sugar Milling Research Institute in Durban. The bagasse was stored indoors while the experiments were conducted. The bagasse was dried for three days in ambient

atmosphere. Before pyrolysis, the material was milled in a Retsch ZM200 mill and sieved through a JEL (J. Engelsmann) sieve machine for 10 min.

4.3.2 *Vacuum and slow pyrolysis*

The reactor consists of a 1 m long, 60 mm OD quartz tube, heated by six well insulated, computer controlled heating elements. The heated chamber is connected to a condensation train and a vacuum pump. The pipes leading from the reactor to the condensation train are maintained at 160 °C to limit condensation before the traps (Figure 29). The vacuum pump or the nitrogen flow, respectively used in vacuum and slow pyrolysis, removed the organic vapours and gas products from the reactor through the condensation train according to different residence times (Table 29). The condensable gases were then condensed in the traps and recovered as liquid, which were later weighed and analyzed. The condensation train in the final set-up consisted of five condensers; for vacuum pyrolysis, the first was held at room temperature, the second and third at -10°C and the last two at -78°C (dry ice temperature) whereas all the condensers were held at -10 ℃ in slow pyrolysis. A control program was designed to control the heating rate (9.1-21.0 ℃ min^{-1}), pyrolysis time (fixed to 1 h) and final pyrolysis temperature (350-530 ℃ and 260-570 ℃ for vacuum and slow pyrolysis respectively). Once the reaction finished, the set-up was allowed to cool under vacuum or atmospheric pressure until the sample temperature was below 120 °C. The sample holder was then removed and weighed, after which the residue (charcoal) was removed and stored for analysis. A typical run would take between 2 and 3 hours, after which the reactor was allowed to cool for ± 2 h depending on the pyrolysis temperature employed. Table 29 presents the different experimental conditions used for the experiments conducted in the batch runs.

Table 29: Experimental conditions for the vacuum and slow pyrolysis of the sugarcane bagasse.

Process	Temperature (°C)	Heating rate (°C min^{-1})	Hold time (min)	Residence time of gases	Pressure (kPa abs)	Flow rate of N$_2$ (L min^{-1})	Mass of bagasse (g)
Vacuum	350-530	9-23	60	2 s	8	-	40
Slow	260-570	5-29	60	2.8 min	101	1	40

The main difference between vacuum and slow pyrolysis lies with the method of removing vapours from the reaction zone. In vacuum pyrolysis, vacuum is used instead of a purge gas as with slow pyrolysis. Because of the lower pressure biomass fragments tend to evaporate more easily. This removes them from the reaction zone, and results in a significantly reduced residence time, 2-3 s for vacuum pyrolysis against 165-170 s for slow pyrolysis. The last difference depends on the temperature of the two last condensers.

This should play a role on the amount of condensates trapped in each condenser and the possible effect of condenser temperatures will be discussed in paragraph 4.4.2.1.
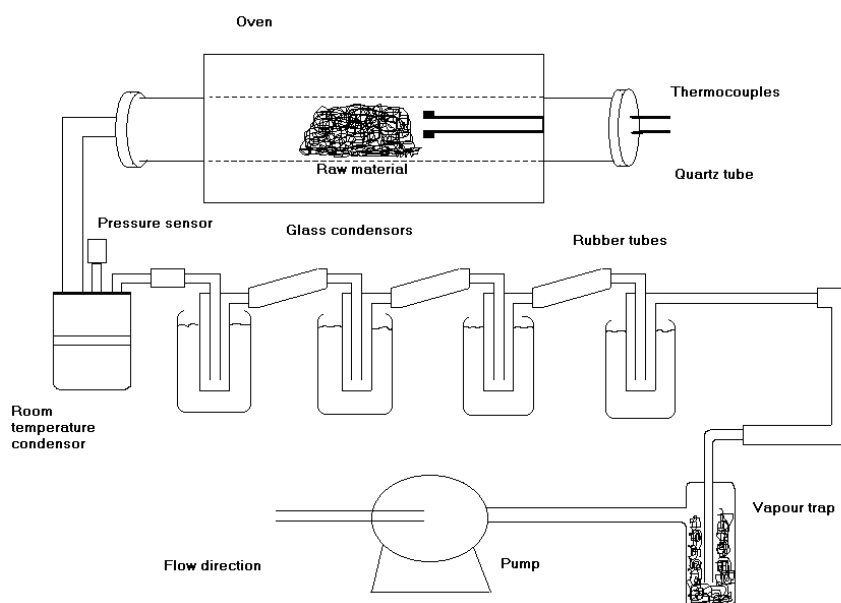

Figure 29: Experimental set-up

4.3.3   *Analyses*

The moisture content was determined by drying 1-2 g of bagasse at 105 °C to constant weight. Ash analysis was done on the samples by heating the samples in air to 575 ± 25°C and weighing the residue after a cooling period at room temperature in a dessicator. A Metrohm KF Titrino and a standardized Karl-Fischer reagent were used to determine the water content in the liquid phase. The elemental analysis was carried out on a Eurovector EA Elemental analyzer. The energy values of the charcoal and oil were determined using a Galenkamp bomb calorimeter. A Ni/Cr wire was used with 1 g of sample and benzoic acid as primary standard. The surface area of the charcoal was determined using the multipoint Brunauer, Emmett and Teller (BET) analysis on a Micrometrics ASAP 2010 system. Once degassed on a VacPrep 061 system at 300 °C, the sample was introduced in the N_2 adsorption equipment.

4.3.4   *Design of experiments*

The design of experiments (DOE) statistical tool was used in the planning of the experiments to optimise process parameters. The influence of the process parameters on the yield and quality of pyrolysis products was studied experimentally with a central composite design. This method is suitable for studying the influence of the experimental variables, and also the influence of their interactions on the

75

product distribution. In this study two operational variables were studied and then 10 experiments are required with the following ranges: Temperature, T (350-500 °C for vacuum pyrolysis and 300-550 °C for slow pyrolysis) and Heating Rate HR (10-20 °C min^{-1} for vacuum pyrolysis and 5-30 °C min^{-1} for slow pyrolysis). The response variables studied in the experimental design were: Ychar (wt.%), Ybio-oil (wt.%), Ypyrolytic water (wt.%) respectively represent the ratio between the weight of solids collected in the reactor, the weight of tarry phase collected from the first condenser at room temperature and the weight of pyrolytic water phase from the four remaining condensers at the end of the experiment and the weight of (dry) bagasse introduced into the system. The response, Ygas, was not considered in this study because of the large deviation due to the presence of losses.

Additionally, three response variables that define the characteristics of the solid char and the bio-oil products were measured. These were the carbon content of the char, the specific surface area (BET) of the char, and the Higher Heating Value (HHV) for the char and liquid products.

Experimental data were used for statistical modelling and an analysis of variance (ANOVA) to determine the optimal values of pyrolysis temperature and heating rate to maximise the yields of char and bio-oil. The influence of the operational variables on the response variables was investigated individually using ANOVA analysis. A 90% confidence level was used for the response variables, resulting in a significance level (α) of 0.1. A p-value lower than 0.1 for a term of the ANOVA table would therefore indicate statistical significance.

4.4 Results and Discussion

4.4.1 *Initial characterization*

4.4.1.1 *Repartition of particle size*

The air-dried samples were screened to give fractions presented in Table 30. Fractions with particle diameters in the range of 425-850 µm were selected for the different groups of experiments. This range is interesting because it limits the influence of particle size on the rate of the process [11]. Therefore the number of parameters which have an influence on yields is limited to the temperature and the heating rate. In addition, the removal of small particles limits the influence of the ash content [15].

Table 30: Distribution of particle sizes for 1 kg of original sugarcane bagasse.

Particle size (µm)	< 180	180-425	425-850	850-1700	1700-2800	> 2800
Original bagasse (%)	6.0 ± 0.3	17.8 ± 0.3	22.5 ± 0.3	16.4 ± 0.3	12.1 ± 0.3	23.5 ± 0.3

4.4.1.2   Chemical and physical characterizations

Table 31 shows the main characteristics of the bagasse used. The bagasse received in the laboratory contained 15.41 ± 0.04 % of moisture. The moisture content was lowered to 13.45 ± 0.03 % after milling. Elemental analysis is close to general elemental composition of bagasse. However, the ash content is quite high, 3.12 wt.% because of the particle size selection (425-850 µm). Indeed, Garcia et al. [15] worked with a bagasse fraction about 0.85-4.75 mm which contained 1.6 wt.% of ash and then showed that the ash content of the smallest particles was much higher. The ash is the name given to all components that are not considered organic or water and consists mostly of metal oxides. These metals could lead to different results concerning yields of products and contaminate products. The initial heating value is equal to 18.5 MJ kg^{-1}.

Table 31: Main characteristics of the milled sugarcane bagasse (* obtained by subtraction)

Water content (%)	Ash content (dry,wt.%)	C	H	N	O + S *	HHV (MJ kg^{-1})
				(dry, wt.%)		
15.41 ± 0.04	3.12 ± 0.02	50.2	5.6	1.1	40.0	18.5

4.4.1.3   Initial experimental results: Repeatability

Table 32 presents the average product yields obtained in replicate experiments for the selected range of pyrolysis temperatures. The standard deviations and maximum variation for each pyrolysis product provided in Table 32 incorporate both the random experimental error and differences in temperature between experiments, and therefore represent an overestimation of the random variation between samples. The standard deviations in the results in Table 32 could also be partly attributed to the random method applied to selection of samples for vacuum pyrolysis. No formal sub-sampling method was applied.

Several trends were observed in these initial experiments that were of relevance for obtaining reproducible vacuum pyrolysis results. A low initial mass loading of bagasse led to high standard deviations in char yields, from 7.7 % to 21.2 %, as well as variations in the water content for these experimental conditions. Increasing the mass loading to 30g did not reduce the experimental deviations sufficiently, while repeatable results in char yields and water content could be obtained with a feedstock loading of 40 g. A relatively small change of 0.7 ºC min^{-1} in the heating rate had a substantial effect on

bio-oil yield, from 8.7 % to 13.3 %, while the char yield varied between 19.0 % and 19.7 % under these conditions (data not shown). Accurate control of the heating rate was therefore essential for repeatable experimental results. Additional experimental errors that may affect the char yield from the process include not placing the sample correctly within the hot zone, resulting in temperature gradients and incomplete reactions, leaking of air into the reactor, and changes in the feedstock character between runs due to the lack of sub-sampling, aging and moisture content. Experimental errors that may influence the bio-oil yields are an air leakage into the reactor (resulting in water condensation reactions) and incorrect cleaning. These possible experimental errors were addressed in subsequent statistically designed experiments. The accuracy of the oil yield was further improved by heating the pipes connecting the hot zone of the reactor to the vacuum traps to over 160 °C, to avoid condensation. The final set of statistically designed experiments was performed under the conditions of an initial mass loading of 40 g and particle sizes of 425-850 μm. Based on these improvements in the experimental procedures and the results obtained in Table 32, the repeatability of vacuum pyrolysis experiments was considered to be sufficient to allow the use of statistically designed experiments to optimise operational values for temperature and heating rate.

Table 32: Vacuum pyrolysis of the SB at 8 kPa abs and variable temperatures (400, 450 and 500°C).

		Average	Standard deviation	Max deviation	No. of pairs	Heating rate ($°C\ min^{-1}$)	Temperature ($°C$)
1	Char, %	23.0	3.8	7.6	3	19.6-21.9	464-485
	Water, %	22.9	4.2	8.4	3		
	Oil, %	14.3	3.1	6.1	3		
2	Char, %	18.5	2.0	3.8	3	11.3-13.0	436-460
	Water, %	22.9	3.9	7.8	3		
	Oil, %	9.9	3.5	5.5	3		
3	Char, %	16.2	3.2	6.1	3	7.1-10.7	491-502
	Water, %	19	4.9	9.5	3		
	Oil, %	8.1	1.9	3.8	3		

4.4.2   Vacuum and slow pyrolysis

Because vacuum pyrolysis and slow pyrolysis were carried out in the same reactor, the following results point out the effects of nitrogen purge and vacuum.

4.4.2.1   Yields of products

Using a slow heating rate, 4.9-28.9 ºC min^{-1}, vacuum and slow pyrolysis lead to comparable yields for both charcoal and liquid above a temperature of 400 ºC.

Above 400 ºC, the average production of oil is more important during the vacuum pyrolysis reaching 23.6 ± 4.3 wt.% against 18.7 ± 5.0 wt.% in slow pyrolysis and this opposite trend is observed for the water production 19.1 ± 2.3 wt.% and 24.6 ± 3.5 wt.% for vacuum and slow pyrolysis respectively. The total average production of liquid is substantially higher for slow pyrolysis at 43.3 ± 8.5 % against 36 ± 6.6 % in vacuum pyrolysis. This difference cannot be due to the use of a dry ice to trap gases from vacuum pyrolysis of bagasse because the opposite trend would have been observed. Dry ice traps were found make a very small contribution to the overall liquid condensation and were therefore excluded in the slow pyrolysis experiments. This observation can be attributed to the residence time, which is longer for slow pyrolysis (2.8 min) than for vacuum (2-3 s). This longer residence time increases the contact period between gases and char leading to a higher production of water because of the presence of numerous secondary reactions.

On average above 400 ºC, the yield of charcoal from slow pyrolysis is higher than that from vacuum pyrolysis, 29.4 ± 0.3 wt. % and 18.8 ± 0.3 wt.% respectively. The low charcoal yield of the vacuum pyrolysis process can be explained by the low pyrolysis pressure. As already mentioned, during pyrolysis the gas atmosphere in the reactor consists of organic vapours formed from decomposing feedstock material. During biomass pyrolysis, the evolving macromolecule vapours contain a high concentration of oxygen functional groups, which can easily undergo condensation reactions. These condensation reactions when they occur ultimately lead to solid products that increase the charcoal yield. Under vacuum conditions the vapours are quickly removed by the vacuum pump from the reactor. Thus, during vacuum pyrolysis condensation reactions are limited and the charcoal yield is reduced relative to atmospheric pyrolysis. Table 33 summarizes previous works dealing with slow and vacuum pyrolysis on sugar cane bagasse. The main difference with the literature lies in the production of oil in vacuum conditions.

Table 33: Yields of products from slow and vacuum pyrolysis studies (* with losses).

Process and conditions	Ychar	Yoil	Ypyrolytic water	Ytotal liquid	Ytar	Ygas	Ref
Vacuum: 500 ℃/12 kPa/12 ℃ min^{-1}	19.4	43.2	18.8	62.0		17.6	[16]
This study 501℃/8 kPa/12 ℃ min^{-1}	16	23.3	19.7	43.0			
Slow: 850 ℃/10 ℃ min^{-1}	22			48	5	25	[17]
Slow: 430 ℃	23	26	30.7 *	56.7*		20.3	[18]
This study 420℃/21.3 ℃ min^{-1}	32.6	19.4	23.6	43.0			

4.4.2.2   Influence of temperature and heating rate on the charcoal yield and characterization

Figure 30 present the effects of temperature and heating rate on the char yield from slow and vacuum pyrolysis, as predicted by the model fitted to the experimental data. The highest yield of char according to the model was obtained at a heating rate of 18-22 ℃ min^{-1} and for a temperature above 350 ℃ in the case of vacuum pyrolysis and for a heating rate range of 2-16 ℃ min^{-1} and for a temperature above 240 ℃ for slow pyrolysis. The yield of char decreased from 26 % to 16 % with an increase in the temperature for vacuum pyrolysis and from 79 % to 23 % for slow pyrolysis. As the pyrolysis temperature is increased for each heating rate, the yield of char decreased with a corresponding increase in the volatiles (gas and liquid) yield as reported before for vacuum and slow pyrolysis conditions [12, 19-32]. Below 310 ℃, mass loss is low and significant degradation occurs between 300 and 500 ℃. The high yield of char at low temperature indicates that the material has only been partially pyrolysed. Indeed, a previous kinetic study on the determination of thermochemical characteristics of bagasse using thermogravimetry analysis indicated that at 261 ° C for heating rates between 10-20 ℃ min^{-1} only 8-11 wt.% of bagasse weight were lost during slow pyrolysis.

At the lower temperature range, 340-400 ℃, the high rate of weight loss, 0.12 % ℃$^{-1}$ is primarily due to the large initial amount of volatiles that can be easily released with increasing temperature as well as the loss of water moisture to a lesser extent. Further increasing pyrolysis temperature progressively, from 400 to 540 ℃, decreases the char yield but at a slower rate, 0.04 % ℃$^{-1}$.
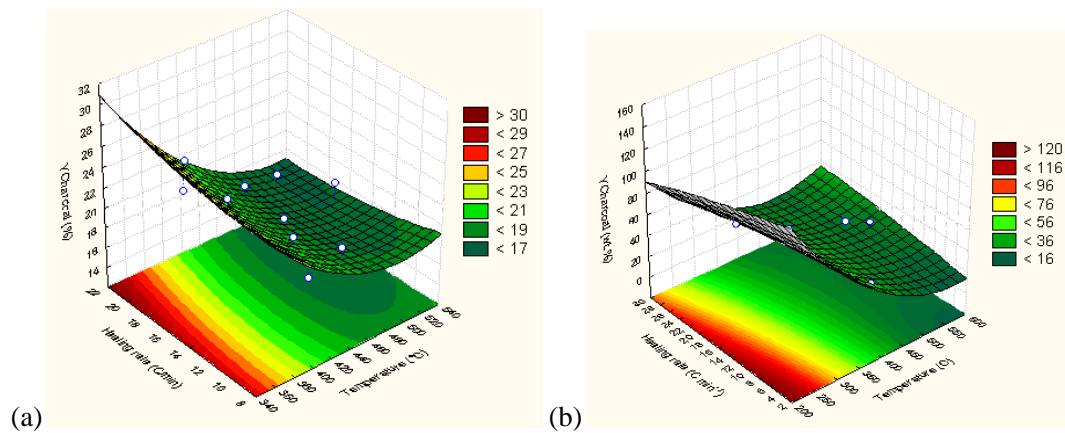
(a)

(b)

Figure 30: Evolution of charcoal yields according to the temperature and the heating rate: (a) vacuum pyrolysis and (b) slow pyrolysis.

ANOVA analysis of the experimental data for char yield indicated that the char yield was only affected by the pyrolysis temperature, and not by the heating rate in the case of vacuum pyrolysis, whereas charcoal yield from slow pyrolysis is controlled by both parameters. This observation indicates that the heating rate can increase the number of secondary reactions only if the residence time is long enough and this can also increase the charcoal yield.

Usually, high temperature and longer residence time favour the production of gas and decrease the charcoal yield [26, 28, 29]. In both cases, the same tendency can be seen, namely, the decrease of charcoal yield at high temperature. The BET, ash content and high heating values (HHV) of the chars are presented in Table 34 and Table 35.

Table 34: Ash, BET and HHV of charcoals from vacuum pyrolysis of sugarcane bagasse (8 kPa abs)

Sample	%Ash	HHV (MJ kg^{-1})	BET (m^2 g^{-1})
Initial bagasse	3.1	17.386	
1- (407,9.1)	15.7		257 ± 7
2- (501,12.0)	16.4		418 ± 11
3- (412,20.7)	16.5		49 ± 2
4- (517,21)	17.3	22.9	296 ± 8
5- (458,15.4)			315 ± 9
6- (394,15.1)	17.2	21.3	8.4 ± 0.2
7- (527,16.4)			291 ± 8
8- (457,10.2)		21.3	221 ± 10
9- (458,19.1)	19.4		307 ± 8
10- (483,19.2)		24.9	396 ± 10
11- (364,16.5)	20.2		56 ± 2
12- (407,10.4)	17.5	23.4	-
13- (474,16.5)	16.2	22.8	333 ± 8

The average HHV of the char was 21.1 MJ kg^{-1} and 23.6 MJ kg^{-1} for vacuum and slow pyrolysis respectively. The highest calorific values for char were obtained between 420-480 °C for a range of heating rates between 14-20 °C min^{-1} in vacuum conditions whereas slow pyrolysis reached the optimum at above 500 °C and below 8 °C min^{-1}. Under these conditions bagasse treated pyrolytically results in an increased HHV relative to the original biomass (Table 34 and Table 35).

The calorific values of char from vacuum pyrolysis obtained in the present study were lower than previous reports, ranging from 27 MJ kg^{-1} [33] to 36 MJ kg^{-1} [34]. In the present study, the HHV is slightly lower due to the high ash content of the char relative to that of the bagasse feedstock [35]. The HHVs for charcoal from slow pyrolysis are higher than the ones from vacuum pyrolysis for temperatures above 394 ºC. Another explanation other than the ash content, for the HHV difference can be the following. Biomass pyrolysis is a complex combination of reactions leading to different products classified as primary, secondary and tertiary. Experimental parameters and particularly the residence time control their concentration. The longer the residence time is, the higher the number of secondary and tertiary reactions. These secondary and tertiary products are characterized by phenolics and olefins and methyl derivatives of aromatics [40]. Among these products, naphthalene (29.5 MJ kg^{-1}) and toluene

(42.9 MJ kg^{-1}) [41] are known for their high HHV. The presence of such products still adsorbed on the char could increase the HHV value. According to Ahuja et al., the presence of secondary reactions leads to carbon enrichment of the final residue [42]. In addition, it can be seen that the highest HHV of char from vacuum pyrolysis is obtained in the temperature range of 390-470 ºC, where the degradation of cellulose and lignin take place [27] yielding combustible gases and condensable liquid tar. The highest HHV for slow pyrolysis are obtained at a higher range of temperature above 450 ºC. This observation confirms the important role of pressure on the quality of products.

A second characteristic, the BET surface area, was determined to evaluate the quality of charcoal for potential activated carbon production. The BET surface area of chars was the highest at high pyrolysis temperatures (Table 34 and Table 35). The high specific surface area of chars (300-400 m^2 g^{-1}) makes these materials valuable feedstocks for the production of activated carbons. The highest specific surface areas for vacuum pyrolysis, 396-418 m^2 g^{-1}, were obtained in a temperature range of 460-540 °C for a heating rate range of 8-24 °C min^{-1} (Figure 31a). The trends observed for slow pyrolysis are shown in Figure 31b where, the highest BET surface area (333 m^2 g^{-1}) is obtained for a temperature above 550 ºC and a heating rate above 20 ºC min^{-1}. For some samples taken at low pyrolysis temperatures, the BET analysis was impossible due to the high content of volatile organics.

Table 35: Ash, BET and HHV of charcoals from slow pyrolysis of sugarcane bagasse under 1 mL min^{-1} of nitrogen

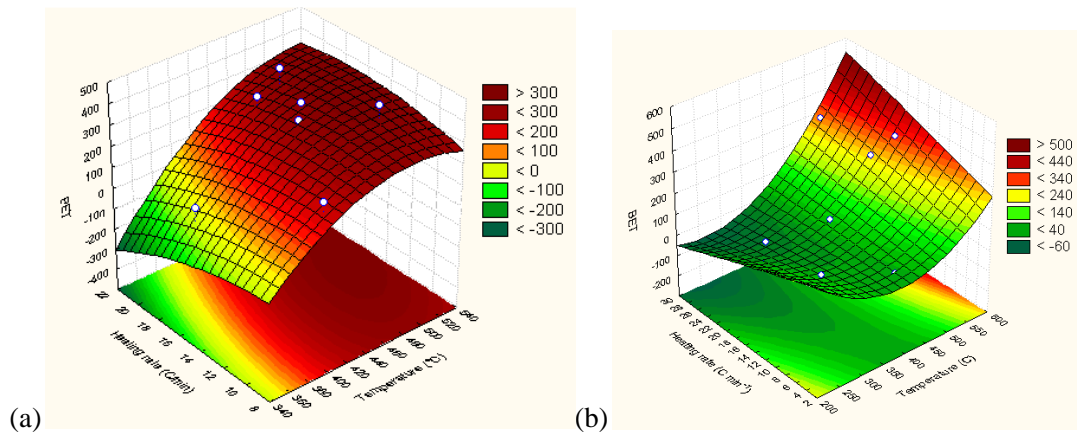| Sample	%Ash	HHV (MJ kg^{-1})	BET (m^2 g^{-1})
Initial bagasse	3.1	17.386	
1- (261,17.7)		18.92	
2- (411,4.9)	21.1	26.00	30.8 ± 0.7
3- (525,28.9)	20.4	23.12	295 ± 8
4- (530,19.3)		25.07	251 ± 6
5- (310,21.5)		19.92	3.0 ± 0.1
6- (420,21.3)	13.0	25.82	29 ± 1
7- (570,17.8)	15.7	27.67	333 ± 9
8- (304,10.0)	7.4	19.76	40 ± 1
9- (412,17.7)	10.0	24.82	43 ± 1
10- (415,17.7)	9.8	25.20	72 ± 2

Figure 31: Evolution of BET surface areas of charcoals according to the temperature and the heating rate: (a) vacuum pyrolysis and (b) slow pyrolysis.
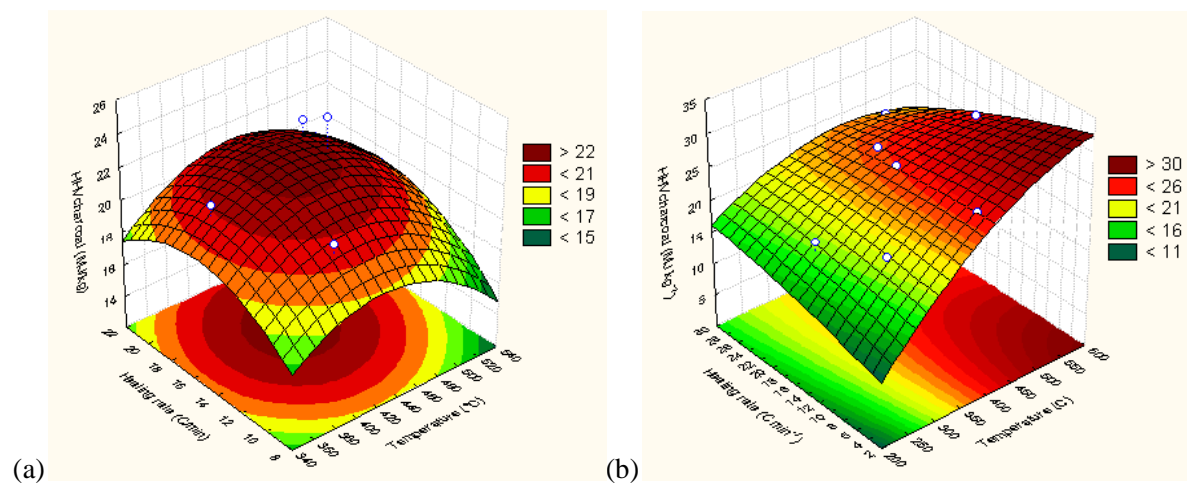

Figure 32: Evolution of HHV of charcoals according to the temperature and the heating rate: (a) vacuum pyrolysis and (b) slow pyrolysis.

Literature suggests that conventional pyrolysis (10-30 °C min^{-1}, 600 °C) leads to BET surface areas of 320-335 m^2 g^{-1} [36-37], while the specific surface area of chars from vacuum pyrolysis can reach higher values, up to 529 m^2 g^{-1} [34]. The high surface area found for the char samples from vacuum pyrolysis suggests that the pores remain open during this process. Increasing the pyrolysis temperature, from 340 to 540 °C for vacuum pyrolysis and from 200 to 550 °C for slow pyrolysis, increases the evolution of volatiles from the bagasse, resulting in increased pore development in the chars and then an increase in BET surface area. The highest BET surface area from vacuum pyrolysis can be explained by the presence

of vacuum. Vacuum intensifies the devolatilization due to a higher reaction rate [38] and causes both a decrease of partial pressure of products and residence time.

According to the ANOVA analysis, temperature had a significant effect on BET surface area, while the heating rate had no effect (data not shown). Nevertheless in previous studies a significant influence of heating rate on the BET surface area and micropore volume of activated carbon from pistachio-nut shells during vacuum pyrolysis treatment was demonstrated [15]. An optimal heating rate of 10 °C min^{-1} was observed, which was sufficiently effective to remove volatile matter and to conserve a microstructure leading to high BET surface areas [15]. According to a study in vacuum conditions [39], the basic microstructure is already formed at 500 °C, although some of these pores are blocked by the pyrolysis products, unless high-temperature treatments are used.

4.4.2.3 Influence of temperature and heating rate on the liquid yield and characterization

Bio-oils were considered as a mixture of pyrolytic water and tarry phases. Vacuum pyrolysis produced a total liquid phase containing 30.7 wt.% and 62.5 wt.% on average water and tar respectively. An opposite trend is observed for the slow pyrolysis, where 71.4 % and 28.6 % were obtained respectively. This tendency can be explained by the difference of the temperature for the different condensers. The tarry bio-oil from vacuum pyrolysis contained the lowest amount of water (4.2 wt.%). The larger amount of water found in the liquid phase from slow pyrolysis is due to the presence of numerous reactions producing water. This water makes the measurement of HHV impossible.

The quality of bio-oils can be improved by reducing the water content. For example, Garcia et al. [15] mixed the condensed liquids collected in the traps, and subsequently evaporated the lightest compounds and a portion of the water from the bio-oil, by incubation for 30 min at 45°C in a rotary evaporator.

4.4.2.4 Influence of temperature and heating rate on the water yield

Figure 33 show the evolution of water yield versus temperature and heating rate. The water content is critical for the quality of bio-oils, as it has a significant effect on the HHV. The highest liquid phase water content was obtained for the temperature range of 380-460 °C and for a heating rate of 22-24 °C min^{-1}. A decrease in water content at temperatures above 480 °C can be seen (Figure 33).
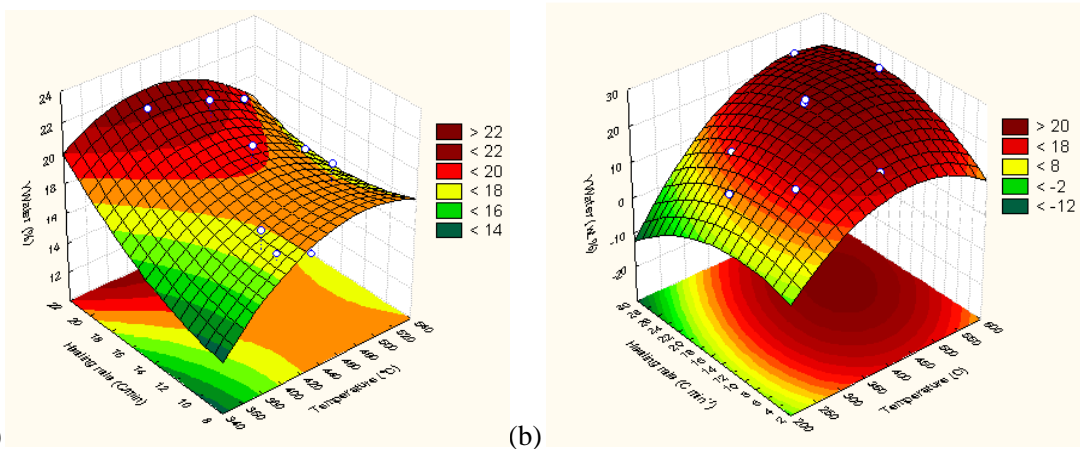
Figure 33: Evolution of water yields according to the temperature and the heating rate: (a) vacuum pyrolysis and (b) slow pyrolysis.

The ANOVA analysis identified a significant effect of the heating rate on the water yield (data not shown). As indicated in previous studies, a slow heating rate and a long residence time favour secondary reactions such as thermal cracking, re-polymerization, and re-condensation, thereby minimising the liquid yield. As a result, the liquid and water yields from biomass increased with higher pyrolysis heating rates.

4.4.2.5   *Influence of temperature and heating rate on bio-oil yield and characteristics*

The yield of tarry bio-oil presented in Figure 34 was optimized in the temperature range of 400-500 ℃ with a heating rate of 15-24 ℃ min[-1] for vacuum pyrolysis and between 425-550 ℃ with a heating rate of 16-24 ℃ min[-1] for slow pyrolysis (Figure 34). The graph trends for bio-oil yield from vacuum pyrolysis and slow pyrolysis are similar.
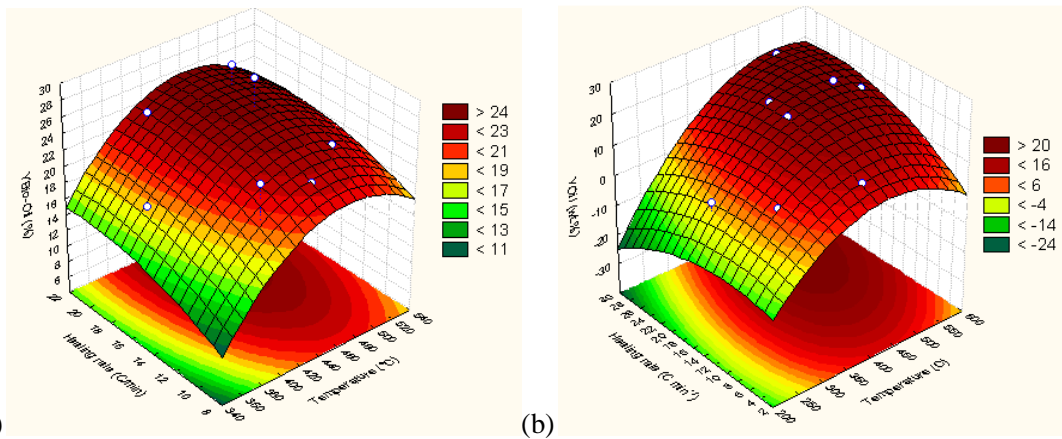
Figure 34: Evolution of oil yields according to the temperature and the heating rate: (a) vacuum pyrolysis and (b) slow pyrolysis.

The ANOVA analysis indicated that only the temperature had a statistically significant effect on the bio-oil yield in slow pyrolysis (data not shown). It is known that the heating rate has an important role on product yields and higher rates lead to higher liquid product yields [42]. The range of heating rates investigated was those applicable to slow and vacuum pyrolysis while the higher oil yields are usually obtained with the high heating rates associated with fast pyrolysis. However, fast pyrolysis fell outside the scope of this study.

4.4.2.6   Influence of the temperature and the heating rate on the HHV of bio-oil from vacuum pyrolysis

The highest calorific value for bio-oil was 23.5 MJ kg^{-1} (Table 34) which is lower than the HHV of petroleum fuels used typically in gas turbines (approximately 40 MJ kg^{-1}). Nevertheless, the highest bio-oil observed in the present study compares very well with values reported in literature, ranging from 5.12 MJ kg^{-1} [33] to 22.4 MJ kg^{-1} [34]. According to Figure 35, the highest bio-oil calorific values were obtained at 520-540 °C, independently of the heating rate. This observation was confirmed by the ANOVA analysis, which indicated a significant effect of the temperature on the heating value (data not shown).
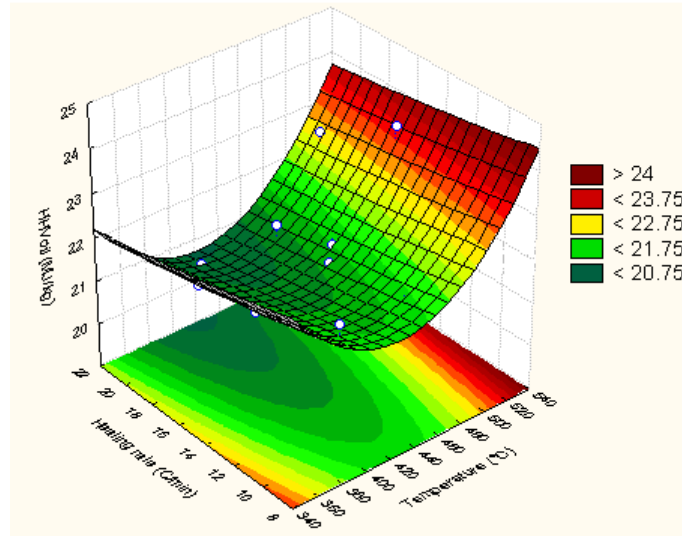
Figure 35: Evolution of higher heating values according to the temperature and the heating rate for vacuum pyrolysis.

4.4.3 *Determination of the value of independent parameters: temperature and heating rate.*

The equipment shows a significant overshoot when controlling temperature and heating rate. Therefore the set points for the independent variables could not be used directly, and were recalculated for the heating rate. Reactor temperature could either be taken as the highest temperature or the average of the recorded values during the pyrolysis time. Table 36 shows the different ranges of temperature and heating rate for optimal results, Ycharcoal, Ywater, Ybio-oil, BET and HHV charcoal, obtained according to the temperature considered.

Table 36: Ranges of temperature (T) in ºC and heating rate (HR) in ºC min^{-1} to obtain the optimal yields, BET and HHV of charcoals.

	Slow pyrolysis		Vacuum pyrolysis	
	Max. Temp.	Average Temp.	Max. Temp.	Average Temp.
Ycharcoal	T: <260	T: <250	T: 500->540	T: 490-520
	HR: <25	HR: <24	HR: 16->2	HR: 17-21
Ywater	T: 420-560	T: 410-540	T: 350-475	T: 340-480
	HR: 12-25	HR: 13-25	HR: >22	HR: >20
Ybio-oil	T: 430-580	T: 420-560	T: 430-500	T: 420-490
	HR: 14-29	HR: 14-29	HR: 15-24	HR: 15-23
BET	T: >540	T: >550	T: >480	T: >470
	HR: >11	HR: >12	HR: 12-21	HR: 12-21
HHV charcoal	T: >430	T: >440	T: 400-475	T: 390-465
	HR: <11	HR: <10	HR: 14-20	HR: 14-20

It can be seen that to obtain the optimal values of yields, BET and HHV, the temperature and heating rate have shifted following the maximum temperature or the average temperature chosen. The ranges of temperature and heating rate are smaller considering the temperature for slow and vacuum pyrolysis. Therefore it is important to know how the temperature is defined, i.e. highest temperature reached or average temperature. It was decided to use the maximum temperature values to take into account all byproducts which could be generated at such a temperature.

4.5   Conclusions

The reproducibility of experimental results was primarily dependent on accurate determination of water and gas yields. The standard deviations in char and bio-oil yields, due to experimental error and/or feedstock variations, ± 1.5-5.8 %, were within an acceptable range for statistical analysis.

The vacuum pyrolysis of sugarcane bagasse leads to yields for pyrolytic water, tar and char, being produced in similar quantities. Optimal conditions for temperature and heating rate to optimize the yields of bio-oil and char are presented in Table 37. Slow pyrolysis produced the highest char yield. The optimal ranges of temperature and heating rate differ from those for vacuum pyrolysis, mainly caused by the short residence time involved in the case of vacuum pyrolysis.

Optimum conditions for bio-oil and char yields did not correspond with conditions to optimize the BET surface and HHV for chars, and to minimize the water content of products (Table 36). Bio-oil production was maximized around a heating rate of 15 °C min^{-1} for both processes. The optimum temperature differs, namely 500 and 450 °C for vacuum and slow pyrolysis, respectively.

Conditions for maximising the char yield (> 30 wt.%), required a temperature of 350 °C which did not correspond with the conditions for a high BET surface area (> 300 m^2 g^{-1}), which required a temperature of 460 °C in the case of vacuum pyrolysis. The same trend was observed for slow pyrolysis where the optimal BET surface area was obtained at higher temperature.

Table 37: Optimum experimental conditions for yields and product properties.

Process	Optimum conditions	YTar (wt.%)	HHV (MJ kg^{-1})	YCharcoal (wt.%)	BET (m^2 g^{-1})	HHV (MJ kg^{-1})	YWater (wt.%)
Vacuum pyrolysis	Range of temperature (°C)	400-500	520-540	340-350	460-540	420-480	380-460
	Range of heating rate (°C min^{-1})	15-24	8-22	18-24	8-24	14-20	22-24
Slow pyrolysis	Range of temperature (°C)	450-600	-	200-250	> 550	450-600	425-550
	Range of heating rate (°C min^{-1})	14-28	-	2-24	> 20	2-12	10-22

As indicated by the ANOVA analysis, the influence of heating rate on the BET, HHV, Yoil and water content was not significant in both processes.

The main difference between the two processes in terms of residence time had an influence on the quality of products characterized by HHV and BET. The slow pyrolysis conditions favoured HHV of charcoal whereas vacuum pyrolysis improved the BET surface area of charcoal and led to bio-oil with high HHV. Indeed, the quality of bio-oil from the slow pyrolysis of sugarcane bagasse was decreased by the presence of a high quantity of water.

The HHV and BET results show that it is important to take the ultimate application of the char into account when choosing a process and deciding on the optimum conditions as the optimum conditions for fuel grade char differ from the optimum conditions for high surface area.

4.6   Acknowledgements

5 Non-isothermal kinetic analysis of the devolatilization of corn cobs and sugarcane bagasse in an inert atmosphere

Prelude to chapter 5

This chapter studies the reactivity of bagasse lignocellulosic subcomponents. The joint article entitled *"Non-isothermal kinetic analysis of the devolatilization behaviour of agricultural wastes: corn cob and sugarcane bagasse"* was co-authored by A. Aboyade and T. J. Hugo and was supervised by Dr. M. Carrier, Prof J.H. Knoetze, Prof J. F. Görgens from Stellenbosch University and Dr. R. Stalh from Forschungszentrum Karlsruhe. All experimental and analytical work relating to Sugarcane Bagasse was done by T.J. Hugo and similarly, the experimental work relating to Corn Cobs was done by A. Aboyade. Work relating to the kinetic modelling of both biomasses was done by A. Aboyade. The article was presented by T.J. Hugo at the SACEC conference held in September 2009.

Akinwale O. Aboyade[a,b], Thomas J. Hugo[a], Marion Carrier[a], Edson L. Meyer[b], Ralph Stahl[c], Hansie Knoetze[a], Johann F. Görgens[a,*]

[a]Department of Process Engineering, Stellenbosch University, Stellenbosch, South Africa

[b] Fort Hare Institute of Technology, University of Fort Hare, Alice, South Africa

[c] Institute of Technical Chemistry-Division of Chemical and Physical Processing, Forschungszentrum Karlsruhe, Germany

5.1 Abstract

Corn cobs and sugarcane bagasse are two of the most important agricultural residues in South Africa in terms of current availability and potential for use as a bioenergy resource. Optimization of the thermochemical conversion of these feedstocks requires characterisation of devolatilization behaviours and kinetics. The thermal decomposition of both materials in an inert atmosphere was studied by non-isothermal thermogravimetric analysis (TGA) and suggested three distinct mass loss stages: first a moisture loss step (25-110 °C), then a devolatilization stage from 200 °C for corn cobs and 230 °C for sugarcane bagasse and finally the cracking of heavier components at 340 °C for corn cobs and at 370 °C for sugarcane bagasse. Friedman's isoconversional method was applied using the AKTS Thermokinetics software to estimate the dependence of the apparent activation energy of the samples and their pseudo-

[*] Corresponding author. Tel.: +27 21 808 3503; fax: +27 21 808 2059.
E-mail address: jgorgens@sun.ac.za (J. Görgens).

components on the extent of conversion. Global apparent activation energies were not constant in this respect suggesting that both materials are complex energetic materials as is their pseudo-components. The similarity in devolatilization behaviour and kinetics of sugar cane bagasse and corn cobs suggested that, aside from possible heat transfer and other transport phenomena effects, there should be no kinetic limitations to the co-processing of these materials in thermochemical processes such as combustion, pyrolysis and gasification.

Keywords: Biomass, Devolatilization, Pyrolysis, Thermogravimetric Analysis (TGA), Non-isothermal, Kinetic Analysis, Corncobs, Sugarcane bagasse.

5.2   Introduction

In the last few decades there has been global attention on biomass as a renewable energy source. In addition to its perceived environmental benefits, biomass conversion to energy products also has the potential to reduce dependence on petroleum imports and to improve the security of energy supply in less developed countries. In South Africa, agricultural residues have been identified as one of the potential sources for renewable energy in the medium to long term future [1]. Residues are excellent as feedstock for energy conversion because they are in most cases already collected and are available at low cost. Furthermore, unlike energy crops, energy production from agricultural by-products does not compete for agricultural land.

Thermochemical processing such as gasification and pyrolysis have emerged as a promising route for the efficient conversion of crop residues and other lignocellulosic biomass into modern energy products [2,3]. Gasification and pyrolysis convert carbonaceous fuel to syngas and pyrolysis oil respectively, both of which can then be further converted to fuels and/or useful chemicals through processes such as Fischer-Tropsch Synthesis [2]. The modelling of thermochemical conversion allows optimisation of the yields of gas, oil and/char products, but requires characterisation of devolatilization parameters such as the reaction kinetics of the particular feedstock [4].

Devolatilization is a key step in thermochemical conversion and describes the process where volatile matter consisting of gas and condensates are released as the solid fuel is heated, usually under an inert atmosphere [5]. The release of volatiles is due to the scission of chemical bonds in the natural polymers that comprise lignocellulosic biomass, primarily cellulose, hemicelluloses and lignin [6,7]. Devolatilization is a complex process consisting of numerous competing and parallel reactions over a wide temperature range. Non-isothermal thermogravimetric analysis (TGA) is frequently employed in investigating the kinetics of devolatilization. It involves heating a sample mass at specific heating rate and following its change in mass as a function of temperature and/or time [8]. The sample mass and particle

94

size must be small enough to reduce the effect of mass and transport phenomena. Non-isothermal procedure involves fewer inaccuracies than isothermal experiments [9-11]. Various procedures for evaluating kinetic parameters from such data have been developed, and the vast majority of them can be classified as either 'model-free' or 'model-fitting'. The question of which of these approaches is better is still the subject of some controversy [12-14]. Up till now, the model-fitting approach has found wider application in biomass thermochemical conversion studies, although it is widely recognised that the method suffers from two main deficiencies, particularly in cases where data from only a single heating rate is applied: i) it can often yield to different values of the kinetic parameters describing the same thermogravimetric curve, leading to an ambiguity in terms of interpretation of the results; ii) it generally tends to yield one set of kinetic parameters for the whole range of conversion, therefore not taking into account the complexity of mechanisms involved during pyrolysis of plant biomasses. In contrast, a study dealing with the thermal behaviour of energetic materials clearly showed that the decomposition of most solid state processes do not follow a single mechanism and as such determined kinetic parameters varies with the reaction extent [15]. An evaluation of progress in kinetic analysis research by the ICTAC Kinetic Project [12,16-19] and a mathematically demonstration carried out by Budrugeac [20] concluded that the isoconversional analysis based on non isothermal data was successful in correctly describing the multi-step kinetics, showing for instance, the dependence of the parameters on conversion, using data from multiple heating rates.

Many researchers have used one or the other of these approaches in the kinetic study of the pyrolysis of sugarcane bagasse [21-27]. Studies on the thermochemical kinetics of corn cobs are much fewer [9,28,29]. It can be seen from Table 38 that results from the same biomass can vary in a large range, which is a reflection of lack of conformity in the methods of kinetic parameter determination employed till date. Much of these results was obtained using data from a single thermoanalytical curve, and according to the ICTAC project [19], this kind of analysis should no longer be accepted for publishing. The table shows only Garcia-Perez et al [21] used the isoconversional approach showing the dependence of activation energy on conversion. They did not however extent the application of the technique to the calculation of the parameters of the lignocellulosic components (cellulose, hemicellulose and lignin) that makes up the biomass. This work aims at obtaining information on the devotalization behaviour and kinetics of corn cobs and sugarcane bagasse - two of the most important agricultural residue in South Africa [30,31]. In keeping with the above comments, the differential isoconversional (Friedman's) method has been employed to obtain the variation of kinetic parameters over the entire range of conversion for the samples and their lignocellulosic pseudo-components.

Table 38: Kinetic parameters for the pyrolysis of sugarcane bagasse and corncobs previously reported in literature

Biomass	Reference	Method	Heating rate ($°C\ min^{-1}$)	Temp (°C)	Activation Energy, E ($kJ\ mol^{-1}$)	Pre-exponential factor, A (s^{-1})	Reaction order, n
SB	Garcia-Perez et al [21]	Friedman's method (0.05<α<0.75)	10, 20, 40, 60		150-175 175-205 205-170		1
SB	Munir et al [22]	nth order single reaction model	10	216-445 214-424	58 71		0.5 0.5
SB	Nassar et al [23]	Single first order	5	225-350 380-560	87.90 46.68		
SB	Ahmaruzzaman et al [24]	Coats and Redfern	1-100	<400 400-500 >500	30.08 40.07 225.81	44.68 min^{-1}	1.5 4 4
SB	Aiman and Stubington [25]	Single first order Freeman and Carrol Cheng and Fong	5, 10, 20, 50	173-422	70.3-87.5 75.3-133.5 93.2	$0.67\text{-}29.6*10^{4}$	
SB	Roque-Diaz et al [26]		10	20-110 110-170 170-250 250-310 310-380	35 21 14 64 188		0.9 0.1 1.0 0.4 1
CC	Zabaniotou et al. [9]	Single first order	20	190-280 355-400	75 64.66	$1.86*10^{6}$ $1.08*10^{4}$	
CC	Cao et al. [28]	Single first order	5 10 30	213-290 290-358 225-303 303-368 233-321 321-385	135.3 67.6 135 85.3 119.6 176	$1.05*10^{12}$ $6.3*10^{7}$ $1.09*10^{12}$ $5.28*10^{6}$ $8.9*10^{10}$ $3.5*10^{15}$	3 2 3 1 3.2 0.34

5.3 Material and Methods

5.3.1 *Samples*

Dried corn cobs (CC) were collected from a farm in the Free State province in South Africa, soon after grain harvesting in 2008. Sugar-cane bagasse (SB) used in this work was provided by the South African

Sugar Milling Research Institute (SMRI). First, dried samples of both materials were chopped to a size < 1mm; afterwards representative fractions were milled using a cryogenic grinder and sieved with a fraction of 125 to 350µm retained for the experimental runs. The physical and chemical characteristics of the samples are compared to literature in Table 39.

Table 39: Physical and chemical characteristics of corncobs (CC) and sugarcane bagasse (SB)

	CC	SB	CC	CC	SB	SB
	Present study	Present study	Ioannidou et al. [29]	Sonobe et al. [32]	Drummond and Drummond [33]	Munir et al. [22]
HHV(MJ/kg)	17.2	17.5				17.7
Proximate Analysis (wt% dry basis)						
Moisture	6.5	6.8	7.6			
Volatiles	80.2	76.9	84.3	82.2	86.5	81.5
Fixed Carbon [*]	16.7	17.8	7.63	16.9	11.9	13.3
Ash	3.1	5.3	8.06	0.9	1.6	5.2
Ultimate analysis (wt% dry and ash free basis)						
C	49.0	50.3	43.8	45.5	46.3	46.2
H	6.0	6.3	6.2	6.2	6.3	6.3
O [*]	44.7	43.1	50	37.9	47.2	45.7
N	0.3	0.3		1.3	0.2	1.8
S	0.08	0.07		0.0		

[*] Calculated by difference

5.3.2 *Experimental Method*

The high heating value (HHV) of the samples was measured using a plain jacket calorimeter (Parr Instruments, USA, Model 1341). Ultimate analysis was done using a Vario EL elemental analyzer (Elementar Analysensysteme, Hanau, Germany). A Netzsch STA 409 balance was used for thermogravimetric analysis. Low sample masses and particle sizes (approximately 20-50 mg, and <350 µm) were used in order to reduce the occurrence of secondary vapour-solid interactions, and the effects of mass and intra-particle heat transfer [34]. For each experimental run, samples were held at room temperature for 15 minutes, heated to 105°C and held again for 30 minutes. At this stage, the sample mass would have stabilized at a constant dried weight and was then heated to 700°C at the following

heating rates; 10 °C min^{-1}, 20 °C min^{-1}, 30 °C min^{-1}, 40 °C min^{-1}, and 50 °C min^{-1}. The nitrogen flow during pyrolysis was set to be 55ml min^{-1} (protective gas into the balance) plus 15ml min^{-1}directly into the oven chamber. For combustion of the formed char the temperature was maintained at 700 °C for a further 30 minutes and the nitrogen flow into the balance was kept constant at 55 ml min^{-1} and 15 ml min^{-1}of oxygen were fed into the oven (instead of 15 ml min^{-1} nitrogen). Variation of the sample residual mass with respect to time and temperature change (TG data), and its derivative with respect to time (DTG data), were continuously collected using the Netzsch Proteus software. Two runs were conducted for each heating rate to confirm the reproducibility of the results.

5.3.3   *Kinetic analysis*

The kinetic analysis of biomass thermal decomposition is usually based on the rate equation (Equation 15) [8,16]:

$$\frac{d\alpha}{dt} = A\exp\left[\frac{-E}{RT}\right]f(\alpha)$$

Equation 15

Where α is the reacted fraction of the sample or conversion, A and E are the Arrhenius parameters - pre-exponential factor and activation energy respectively, and $f(\alpha)$ is the reaction model. There are two main approaches for the mathematical determination of these three parameters, commonly referred to the kinetic triplets, from non-isothermal TG data, i.e. model-fitting and model-free or isoconversional methods. The model-fitting approach is based on the initial assumption of a function for $f(\alpha)$ from a selection of available and well known models [35-37] and the fitting of the chosen model to experimental data in order to obtain the Arrhenius parameters. The classical application of the model-fitting approach is to manipulate the differential or integral form of the rate equation until a straight line plot can be obtained. The reaction model that gives the straightest line is selected and E and A are then obtained from the values of slope and intercept. Examples of this method are those by Coats and Redfern [38], Freeman and Carrol [39], and Duvvuri et al [40]. The common criticism of the model fitting approach is that the values of the Arrhenius parameters obtained are often ambiguous. The ambiguity lies in the basis of the approach which is the adoption of a reaction model - α. The parameters thus calculated are inevitably tied to the specific reaction model assumed. The situation frequently arises where different reaction models

98

are able to satisfactorily fit the data whereas the corresponding values of *E* and *A* are decisively different [36,41,42].

In contrast to the model-fitting methods, the isoconversional approach does not require the choosing of a reaction model and is thus 'model-free'. It allows the estimation of *E* as a function of conversion, α independent of the reaction model, $f(\alpha)$. The key concept behind this approach is that the reaction rate for a constant extent of conversion depends only on the temperature [36]. The isoconversional approach employs data from multiple heating rates as this is the only practical way to obtain data on the variation of the reaction rate at a particular extent of conversion. The most common application of the isoconversional analysis was developed by Friedman [43] and is used in this work. The method involves computing the logarithms of the Arrhenius rate equation to get:

$$\ln\left(\frac{d\alpha}{dt}\right) = \ln\left(\beta\frac{d\alpha}{dt}\right) = \ln[A \bullet f(\alpha)] - \frac{E}{RT}$$

<div align="right">Equation 16</div>

A plot of $\ln\left(\frac{d\alpha}{dt}\right)_i$ against $1/T_i$ at the same degree of conversion from data taken at various heating rates will result in a series of lines, each with slope equal to –*E/R* corresponding to each value of conversion, α, at different heating rates β. Thus the dependence of *E* on α is obtained. Value for *A* are similarly obtained from the intercept.

The decomposition of biomass is too complex to be realistically described using the single component model in Equation 15, so a multi-component model is also sometimes employed. The material studied is assumed to be composed of pseudo-components, where a pseudo-component refers to a group of reactive species that exhibit similar reactivity e.g. cellulose, hemicellulose, and lignin [44]. Under this scenario Equation 15 becomes;

$$\frac{d\alpha}{dt} = \sum \gamma_i A_i \exp\left[\frac{-E_i}{RT}\right] f(\alpha_i)$$

<div align="right">Equation 17</div>

where γ_i is the contribution of pseudocomponent *i* to the total mass loss.

Normally, multi-component analysis of biomass devolatilization kinetics conducted via the model fitting approach [10,27,45]. This is the first time to our knowledge where the isoconversional approach has been used. All kinetic analysis in this work was done using the AKTS-Thermokinetics software. Up to 16 000 data points per curve were used in the analysis. Data smoothing of the raw TGA data was done according to Savitzky and Golay [46].

5.4   Results and Discussion:

5.4.1   *Analysis of thermo-analytical curves*

Characteristics of thermoanalytical data with regards to weight loss (TG) and derivative weight loss (DTG) for CC and SB biomass at different heating rates were compared (Figure 36). Weight loss curves are presented for the temperature range 100-700°C, the loss of mass at lower than 100°C can be attributed to the demoisturization of the samples (6.5-11. 8 wt.% and 5.0-7.1 wt.% respectively for CC and SB between 100-200℃). In general, three distinct weight loss stages could be identified, in agreement with previous findings [47-49]. Following moisture loss, a temperature range with negligible weight loss (<1.5% for CC, and <1% SB between 100-200°C) was observed for both materials, which was followed by the start of the second stage of weight loss, i.e. devolatilization, at 200°C for CC and at 230°C for SB. The insignificant weight loss in this section prior to the start of devolatilization has been attributed to the removal of bound moisture and the start of polysaccharide hydrolysis [47,50]. Much of the devolatilization occurred in second stage of weight loss, a result of the thermal breaking of weak bonds in the polymeric structure of the constituent components of the biomass and the formation of stronger, more stable bonds to take their place [26]. Lignocellulosic biomasses such as CC and SB are known to comprise hemicelluloses, cellulose and lignin as the major components [41,51,52] and the devolatilization stage has been shown to correspond mainly to the degradation of these components [53]. Hemicelluloses typically decompose in the range of 160-360 °C, while cellulose degrades at the higher temperature range of 240-390 °C [27]. The loss of lignin typically occurs at a slower rate over a much wide temperature range of 180-900 °C [34,54,55]. On the DTG curves the temperatures at which maximum rate of weight loss occurred are described by the position of the peaks in the curve. The DTG curve of SB during the devolatilization stage shows two distinct peaks (which is represented by a noticeable change in slope of the TG curve). Based on the temperature range at which cellulose, hemicelluloses and lignin have been previously observed to decompose [34,51,54], the DTG peaks of SB can be assigned as follows: The first DTG peak, with maxima at 295-321 °C, is probably due to the decomposition of hemicelluloses and the second is due to cellulose, 350-376 °C (Table 40). Lignin decomposes throughout the whole temperature

range and cannot be assigned a distinct peak [56,57]. The DTG peaks are much closer to each other for CC than for SB with the maximum of hemicelluloses and cellulose peaks occurring at a lower temperature, 283-323 °C and 318-339 °C respectively. Antal and Varhegyi [58] ascribed the cause of the merged DTG peaks to the catalytic behaviour of mineral matter present in biomass. This may explain why SB with an ash content of 5.3% exhibits a more distinct peak compared to CC which has 3.1% ash content.

The third stage sees a much lower rate of weight loss (12% for CC and 10% for SB) than the second stage (58% for CC and 60% for SB). According to Roque-Diaz et al. [26], for SB, this stage of biomass decomposition corresponds to the end of cellulose decomposition, and the degradation of heavier volatiles, the cracking of C-C bonds and the formation of char. The decomposition of lignin has also been reported to continue into this stage [59]. Figure 36 and Table 40 show that the third stage starts at 330°C for CC and 376°C for SB.

Table 40: Devolatilization parameters for CC and SB at different heating rates

Sample	Heating rate ($°C\ min^{-1}$)	T_h (°C)	T_c (°C)	T_f (°C)	$\%R_s$ (at 680 °C)
CC					
	10	283	318	330	20.3
	20	305	330	365	20.8
	30	308	337	375	20.0
	40	312	339	387	19.5
	50	323	323	410	22.3
SB					
	10	295	350	376	24.1
	20	307	362	391	19.5
	30	312	370	400	18.7
	40	320	374	412	21.6
	50	321	376	417	19.5

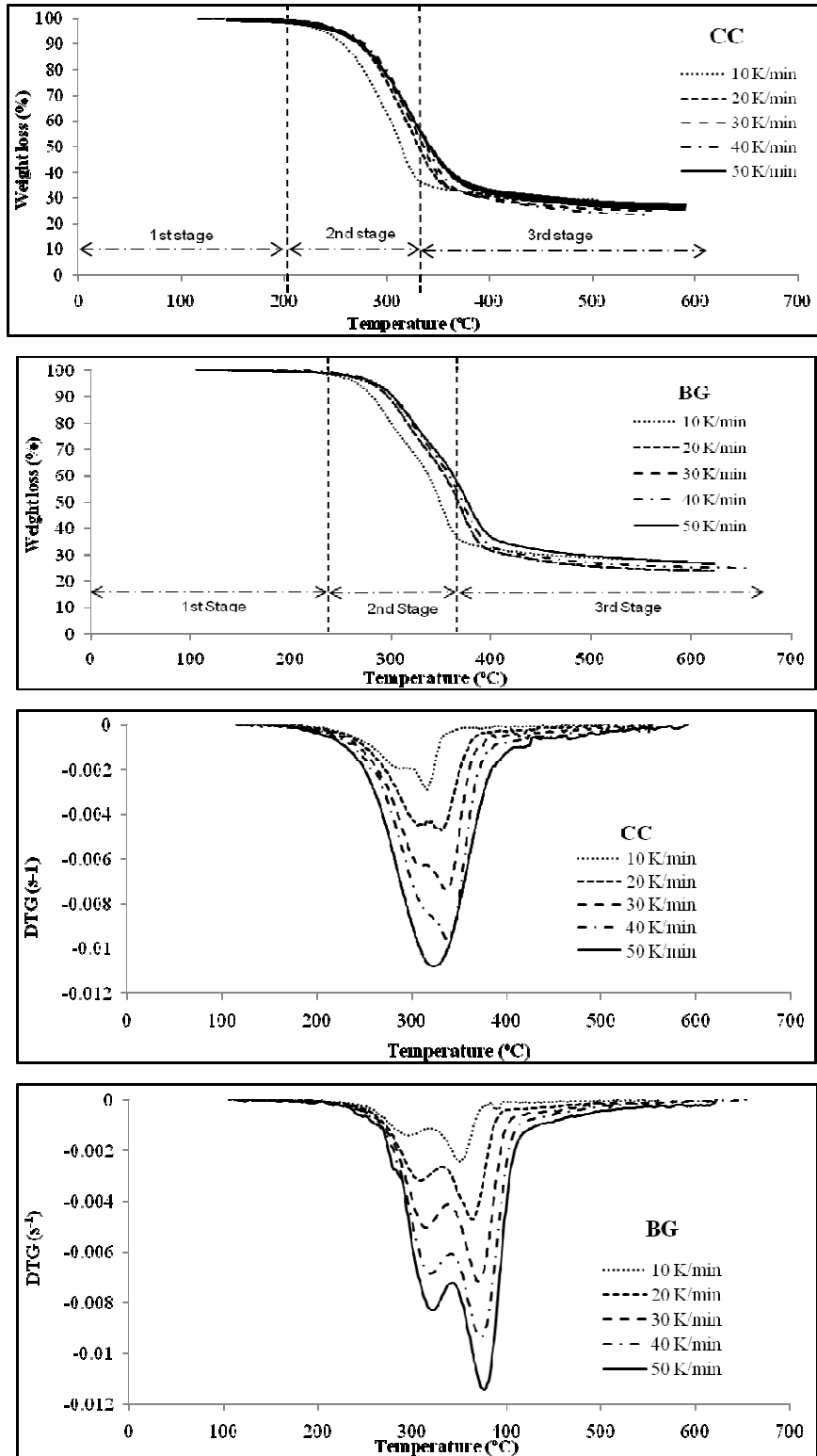T_f; the final temperature of cellulose degradation

Figure 36: TG and DTG curves of CC and SB at various heating rates

5.4.2 *Influence of heating rate on devolatilization parameters*

The effect of heating rate on the thermoanalytical curves can also be observed in Figure 36 and Table 40. Both the TG and DTG curves tended to shift towards higher temperatures with increasing heating rates. The DTG peaks also shifted to higher temperatures at increasing heating rates, from 295 °C to 321 °C and from 350 °C to 376 °C for the maximum weight loss of SB's hemicelluloses and cellulose, respectively (see also Table 40). For CC, the peaks in the DTG curve are so close that they tended to overlap, especially at higher heating rates. According to Haykiri-Acma et al. [60] and Di Blasi [4] the overlapping of DTG peaks was probably due to sufficiently low heating rates allowing enough time for each individual component in the biomass to decompose at its own typical peak temperature, while at high heating rates decomposition is almost simultaneous and as such adjacent peaks are united to form broader and higher peaks. Conversely to the trend in DTG peaks observed here, Biagini et al. [7] reported a greater distance between peaks at higher heating rates in their study of rice husk, cacao shell and olive cake.

As seen from Table 40, the point at which maximum rate of devolatilization occurs varied from 283 °C at 10 °C min^{-1} to 339 °C at 50 °C min^{-1} for CC, and from 295 °C at 10°C min^{-1} to 376 °C at 50 °C min^{-1} for SB. This trend of a systemic shift of maximum decomposition rate has been reported previously [7,55,61]. Figure 37 shows the effect of heating rate on the temperature at which specific extents of conversion are reached. For both materials the temperature at which a certain extent of conversion was achieved increased with the rise in heating rate, even though the time taken to reach that temperature was successively less. For instance, while 80% conversion could be achieved for CC at about 325°C using a heating rate of 10°C min^{-1}, the same extent of conversion could only be reached at a temperature of 361°C at a heating rate of 50 °C min^{-1}.
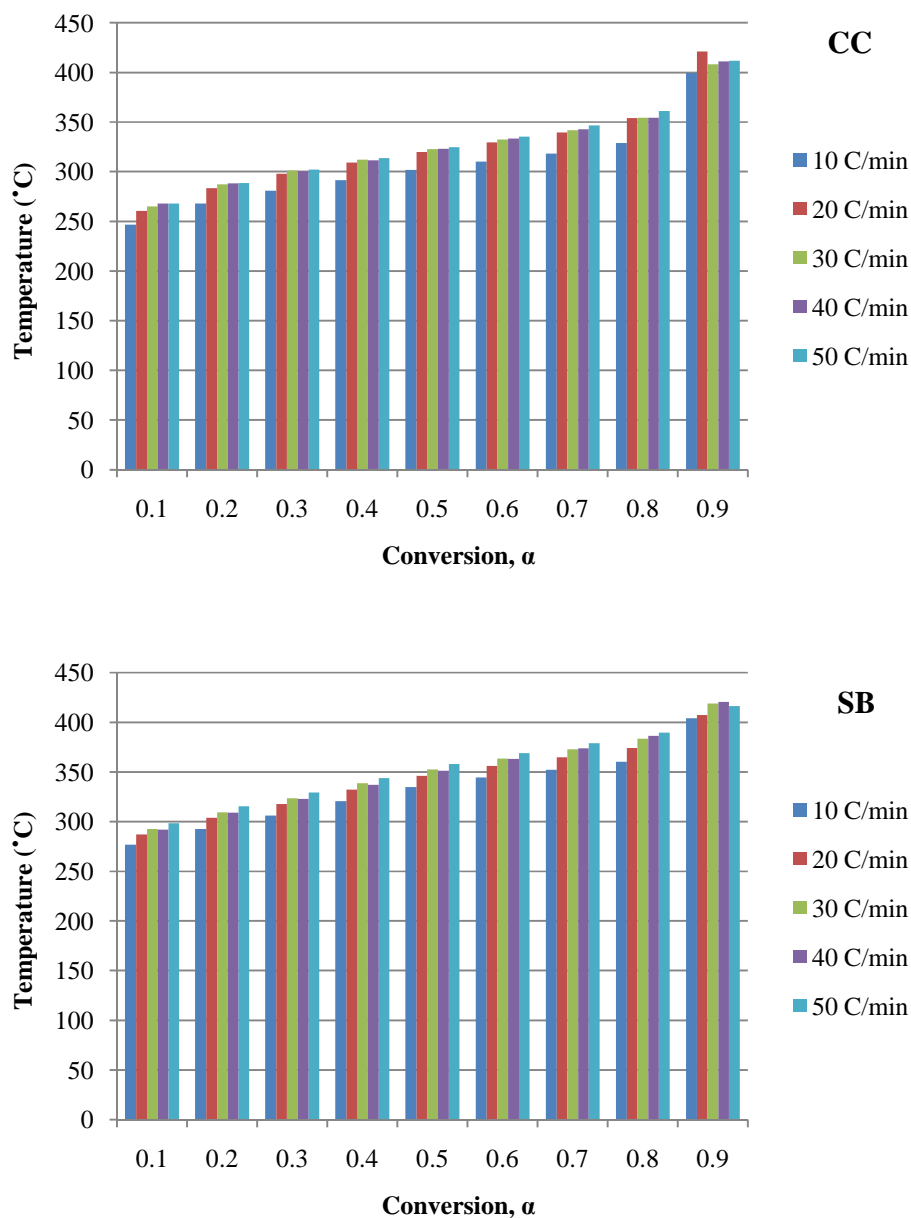
Figure 37: Influence of heating rate on extent of conversion temperature for CC and SB

5.4.3   *Kinetic analysis*

The pyrolysis of organic matter is a complex process and parameters obtained from the thermo-analytical curves have only limited use in describing the reactions involved. A detailed kinetic evaluation is

therefore often necessary to determine reaction rate parameters [29]. Kinetic evaluation in this study focused on the devolatilization zone i.e. stage 2 of Figure 36.

5.4.3.1 Single component kinetics

Values for the apparent global activation energy E were calculated for both materials from the slope of the isoconversional lines in the Friedman's plot for the conversion range of 0.1-0.9 (Figure 38). E varied with the extent of conversion for both materials. This has previously been interpreted as evidence of the existence of a multi-step reaction mechanism [14,16]. E, as determined here, is not the actual activation energy of any particular single reaction step, but is rather an aggregate value reflecting the contributions of the individual reaction steps to the overall reaction rate. These contributions, for a complex process as biomass devolatilization, will vary with respect to temperature and extent of reaction [14], hence the observed variation of E and $ln(A*f(\alpha))$ with conversion shown in Figure 39. The vertical lines delimit the conversion range for which the correlation coefficient is below 0.8 highlighting the calculation limitations arising from experimental data variations towards the end of pyrolytic conversion [5].

The trend of E dependence on α was quite similar for both CC and SB, nevertheless SB is less reactive than CC requiring generally higher activation energies; 225 kJ/mol for SB against 170 kJ/mol for CC at 0.5 conversion for example. At the start of devolatilization (α<0.20), the apparent activation energy for both materials increased from 50 kJ mol^{-1} to 170 kJ mol^{-1} and 210 kJ mol^{-1} for CC and SB respectively. E remained relatively constant in the range 0.20<α<0.58 for CC and 0.20<α<0.50 for SB. Biagini et al [5] also noticed a similar plateau in their study of rice husks, olive cake and cacao shells. At higher extents of conversions, apparent activation energy decreased continuously reaching 80 and 50 kJ mol^{-1} for SB and CC respectively. Higher E values were apparently due to the decomposition of the less reactive components in the biomass, the lowest E indicates that chemical reactions that take place during devolatilization are less energetically costly. In general, the pyrolysis of SB requires more energy indicating the presence of different bond natures then different lignocellulosic structures. This also explains why higher temperatures were required to achieve similar conversion levels for SB than for CC, as earlier observed.

 The range of overall E values obtained here for SB agreed well those that arrived at by Garcia-Perez et al. [21] using the same isoconversional method, i.e. 150-200 kJ mol^{-1} in the conversion range, 0.05-0.75. There is much fewer literature available to compare CC results with, although Cao et al. [28] and Zabaniotou et al. [9] obtained 68-176 kJ mol^{-1} and 65-75 kJ mol^{-1} respectively, using a single first order reaction model (Table 38).
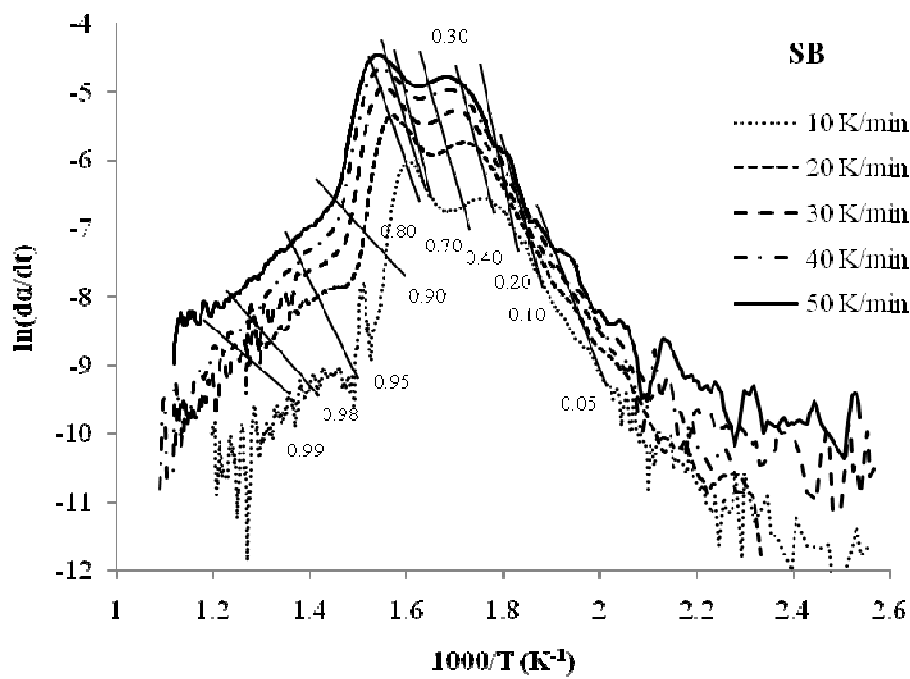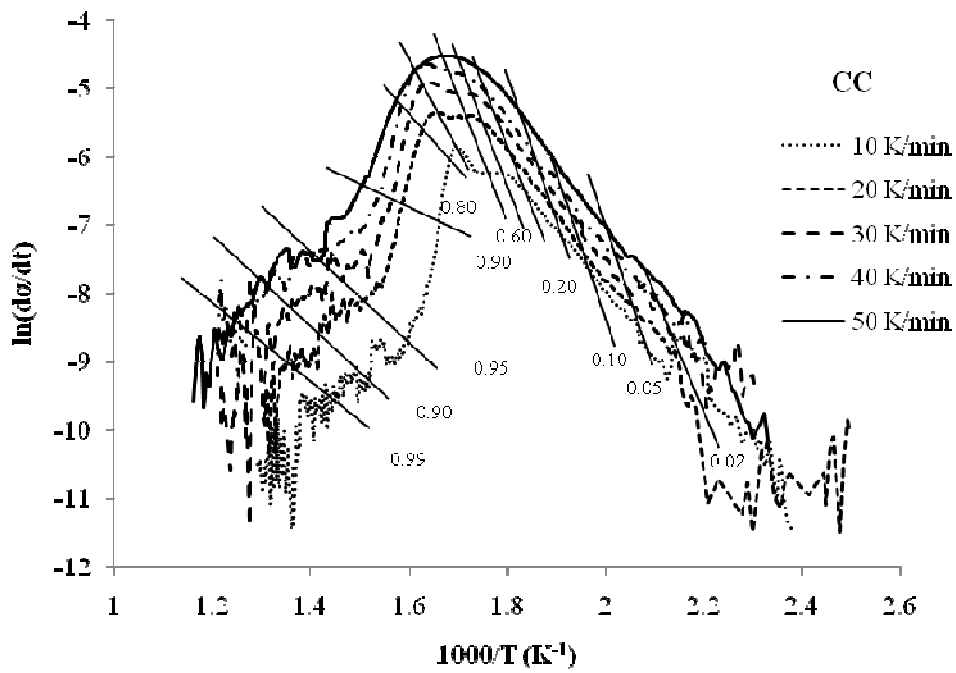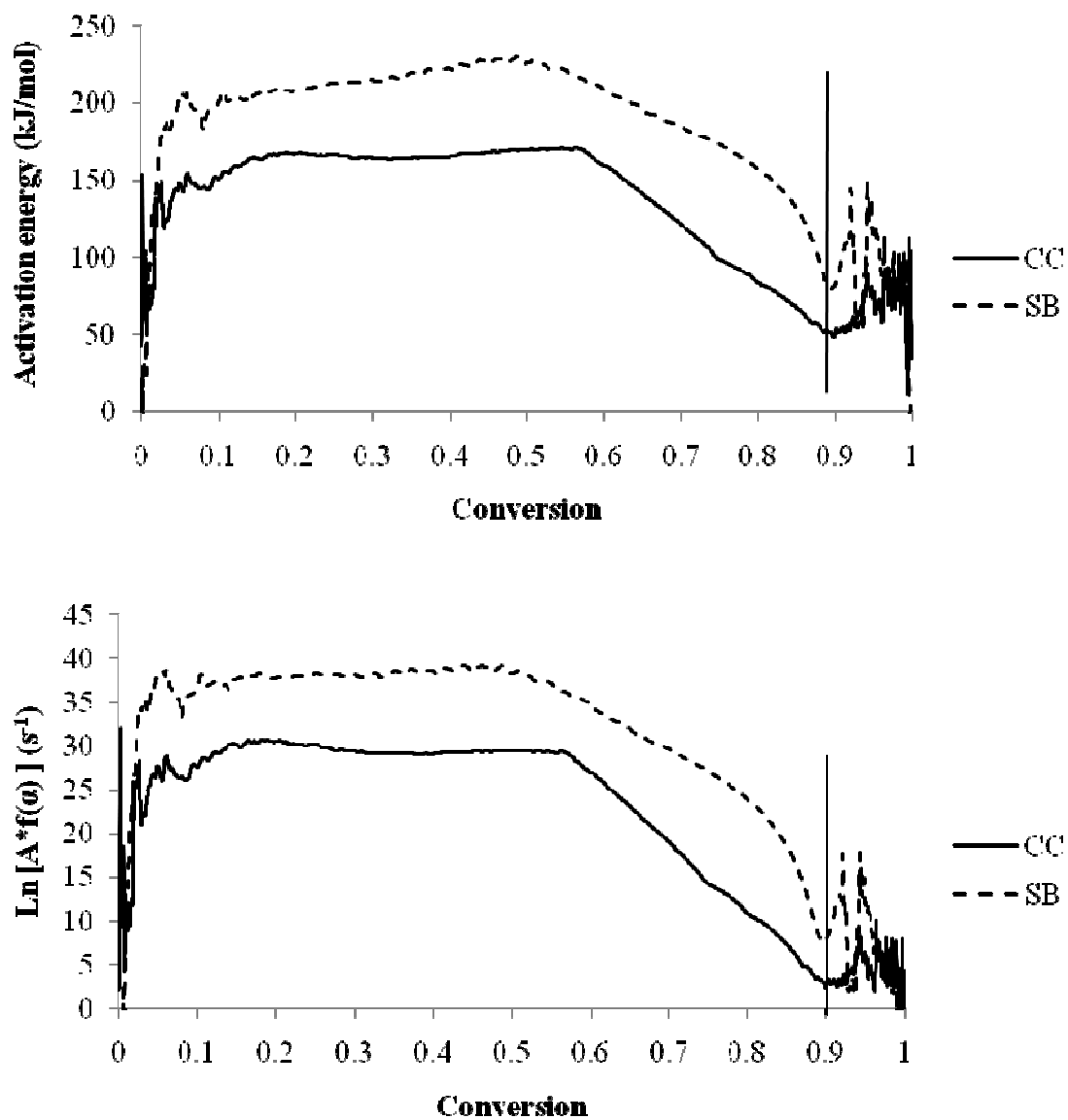
Figure 38: Friedman's plots for CC and SB

Figure 39: Apparent activation energy and pre-exponential factor dependence on conversion for CC and SB

5.4.3.2   Multi-component kinetic parameters determination

The *E* values computed above using Friedman's method were for the overall decomposition assuming a multi-step process and represents aggregate values reflecting the contributions of the individual reaction steps to the global reaction rate [36]. For analysis of the individual reacting fractions in the biomass (multi-component analysis), each DTG curve was deconvoluted using the AKTS-Thermokinetics software. Figure 40 shows the deconvolution of the DTG curves at 20C/min. The peaks shown correspond to hemicelluloses, α-cellulose and lignin for both CC and SB. From the peak parameters, the same isoconversional method has been applied to determine kinetic parameters relating to the conversion of each pseudo-component. The figure shows that cellulose had a larger overall peak area and decomposed over a wider range (270-390°C) in SB than in CC (300-360°C). The shape and position of peaks assigned to hemicellulose for both samples are more similar. Overall, the differences in the behaviour of the pseudo-components for both samples can be said to account for the difference observed in the overall devolatilization behaviour of samples, particularly with regard to more distinct double peaks observed in the DTG curve for SB.

The contributions of the pseudo-components hemicelluloses (H), cellulose (C) and lignin (L) are 58 wt.%, 23 wt.% and 18.1 wt.% for CC and 28 wt.%, 45 wt.% and 28 wt.% for SB respectively. These values correspond to the SB's lignocellulosic composition reported in literature, 30.4 wt.% (H), 40.7wt.% (C) and 18.8 wt.% (L) [62], and differ slightly from the CC's values, 40.5 wt.% (H), 34.3 wt.% (C) and 18.8 wt.% (L) [63]. This latter observation could be explained by the presence of extractives whose devolatilization occurs generally in the same range of temperature as hemicellulose.

The trend of activation energy and pre-exponential factor against the conversion are presented in Figure 41. As was previously the case, the vertical line indicates the values for which the quality of the model fitting to the original data is superior to 0.8. The CC's data led to the lowest correlation coefficient, this result could reportedly be improved with acetone and water washes which remove extractives and mineral matter respectively [58]. The simulation of the thermal behaviour of hemicelluloses, cellulose and lignin showed that the decomposition of these materials did not follow a single mechanism because the determined activation energies and pre-exponential factors varied during the course of the devolatilization. This observation indicates that hemicelluloses, cellulose and lignin are, like the biomass from which they are derived, complex materials.

In general, the pyrolytic degradation of SB's pseudo-components required more energy than CC's (Figure 41). The value of activation energy for each pseudo-component in a given biomass differs significantly from the others which means that hemicelluloses, cellulose and lignin are a unique material, as have been observed by other authors [64-66]. Previous studies which determine the global kinetic parameters to each individual pseudo-component are only available for SB (Table 41). Disagreements can be observed

regarding the activation energy required for hemicelluloses' devolatilization which values are in general higher for a range of conversion between 0.1-0.8 (Figure 41). Some studies showed the existence of a linear relationship between the activation energies and bond orders in the molecule of each reactant [67,68]. A quick calculation of the energy required to break the chemical bonds of representative structures for each pseudo-components has been established in Table 43. The glucose and xylan structures have been used to represent the cellulose and hemicelluloses respectively while the coniferyl, sinapyl and coumaryl structures have been selected to represent the lignin. Lignin required more energy to be degraded which is in disagreement with the reported activation energy values presented here. This highlights the existence of strong cellulose-hemicelluloses bonds in CC and SB biomasses as demonstrated in a wood pyrolysis study [69].

Table 41: Values of kinetic parameters from previous works dealing with SB Pyrolysis

Component	Activation energy (kJ/mol)	Pre-exponential factor	Reference
Hemicelluloses	105	9.204	[21]
	105-111		[70]
Cellulose	235	19.489	[21]
	195-213		[70]
Lignin	26	1	[21]

Table 42: Determination of average bond energy for pseudo-components of plant biomasses

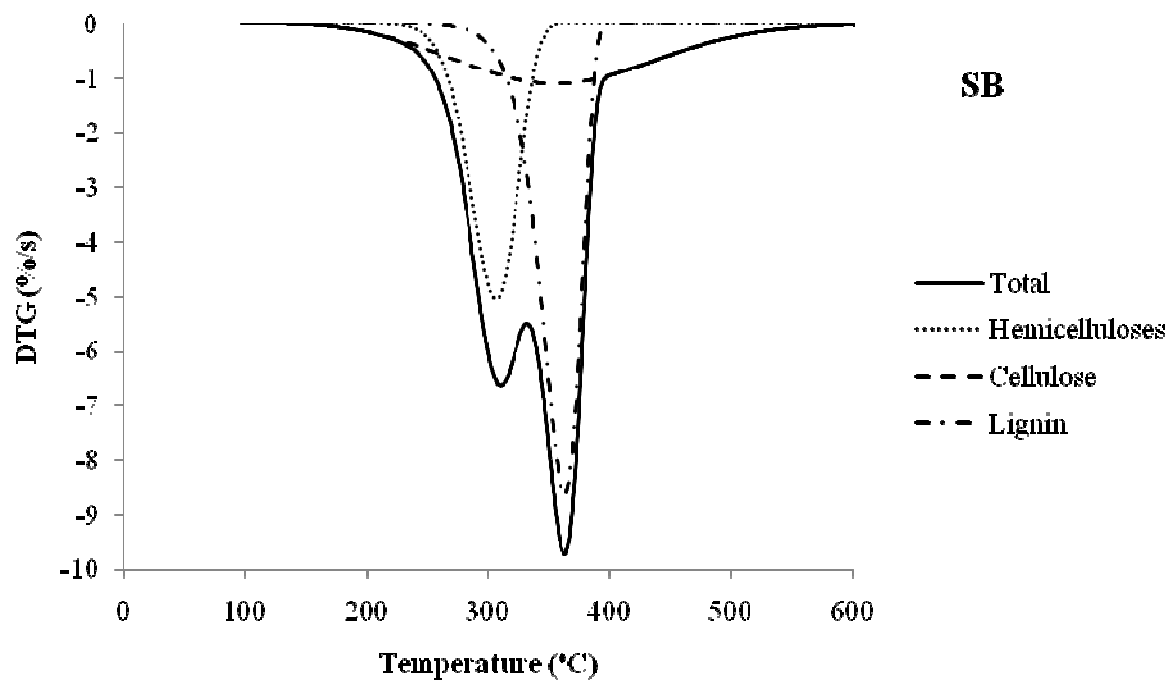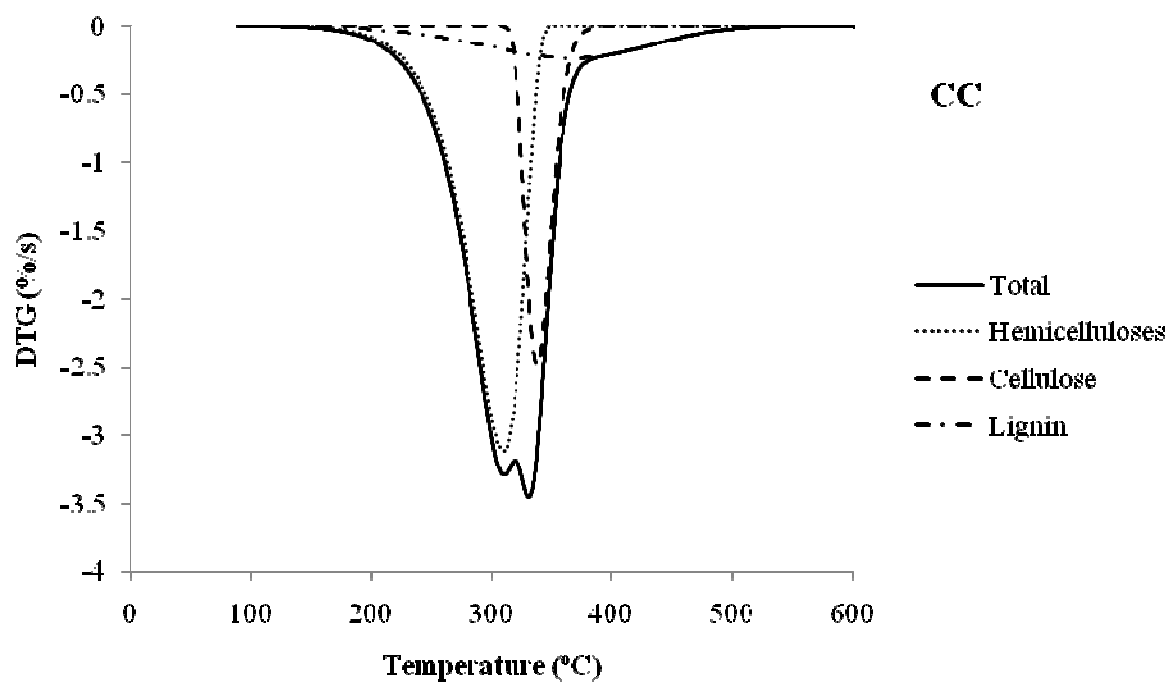| Nature of bond	Hemicelluloses Type of bond (%)	Cellulose Type of bond (%)	Lignin Type of bond (%)	Standard bond energy (kJ/mol)
H-O	7.6	13.0	8.0	111
H-C	33.0	34.8	40.0	99
O-C	30.5	26.1	16.0	85.8
O=C	2.5			179
C-C	22.9	26.1	15.0	83
C=C	3.5		16.0	146
Total energy (kJ/mol)	95.9	92.3	98.0	

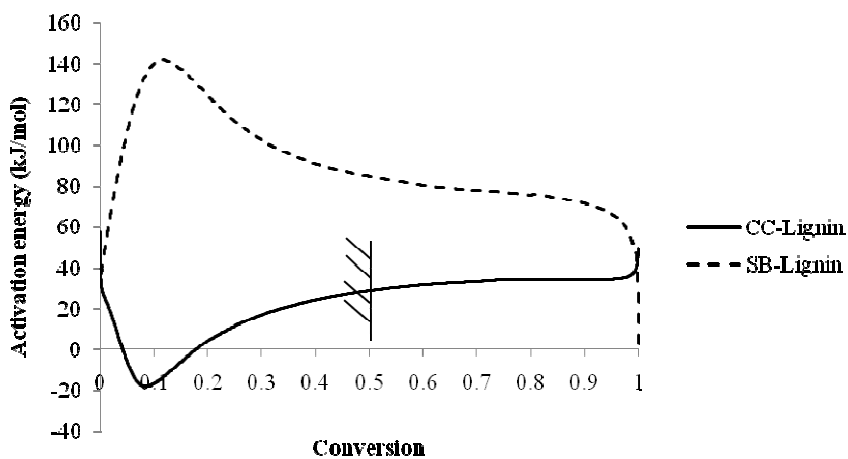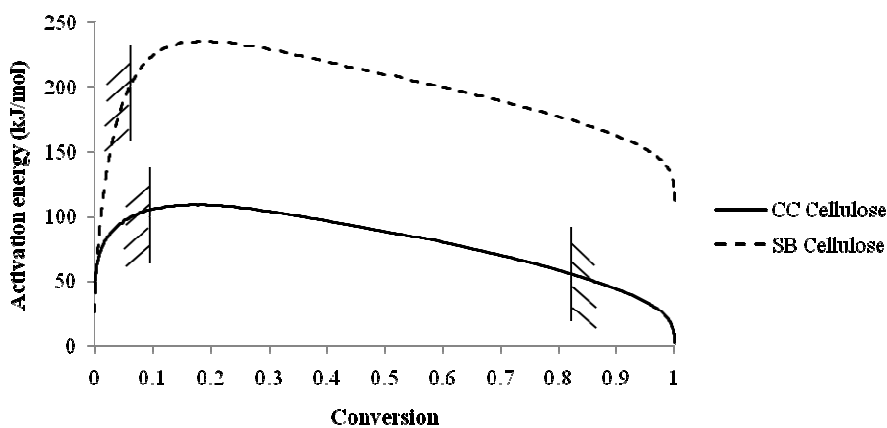Figure 40: Deconvoluted DTG curves from thermogravimetric analysis of CC and SB at 20 C/min
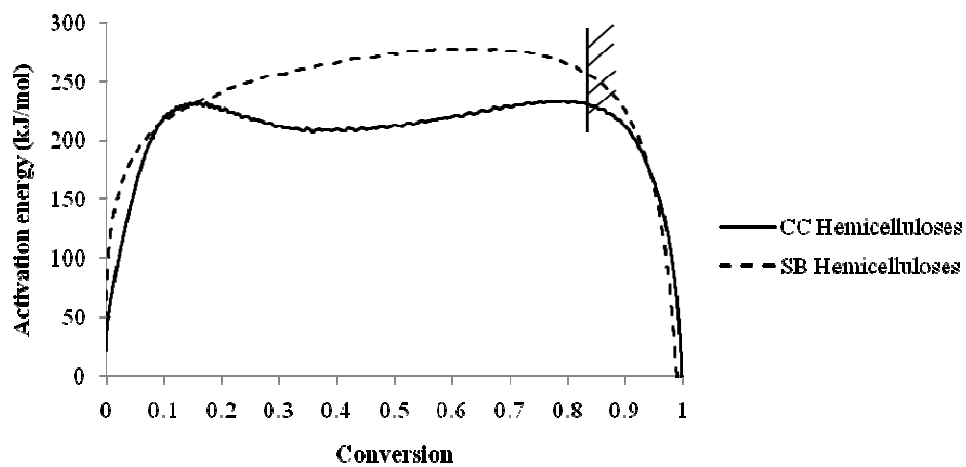
Figure 41: Deconvolution computation of DTG curves from thermogravimetric analysis of CC and SB at 20°C/min.

5.5 Conclusions

The thermal decomposition of CC and SB in an inert atmosphere was studied by non-isothermal thermogravimetric analysis and suggested three distinct mass loss stages: a first moisture loss (25-110 °C), a devolatilization stage from 200 °C for corn cobs and 230 °C for sugarcane bagasse and finally the cracking of heavier components at 340 °C for corn cobs and at 370 °C for sugarcane bagasse. Friedman's isoconversional method was applied using the AKTS Thermokinetics software to estimate the dependence of the apparent activation energy' of the samples and their pseudo-components on the extent of conversion. Global apparent activation energies were not constant in this respect suggesting that both materials are complex energetic materials as is their pseudo-components. The similarity in devolatilization behaviour and kinetics of sugar cane bagasse and corn cobs suggested that, aside from possible heat transfer and other transport phenomena effects, there should be no kinetic limitations to the co-processing of these materials in thermochemical processes such as combustion, pyrolysis and gasification.

5.6 Acknowledgments

6 Comparison of different types of fast pyrolysis of sugarcane bagasse

6.1 Introduction

This chapter focuses on the comparison of results from different Fast Pyrolysis (FP) systems developed at Stellenbosch University (SU) and Forchungszentrum Karlsruhe (FZK). Three different reactors were used to convert Sugarcane Bagasse (SB) mainly into bio-oils. The first objective was to perform experimental runs at SU on a Fast Pyrolysis Unit (FPU) to test the equipment, to achieve repeatability of results, and to investigate the effect of temperature on the product yields. The second objective was to compare the results from SU with the results from different FP plants located at FZK in terms of products yields and quality. A discussion on previous research dealing with FP of bagasse is included in paragraph 2.9. These studies reported liquid yields in the range of 55 wt% to as high as 66 wt% from pyrolysis of bagasse (Drummond and Drummond, 1996; Tsai *et al.*, 2006; Asadullah *et al.* 2007).

6.2 Materials and methods

6.2.1 Description of equipment and procedures

In this study two reactors at Forschungzentrum Karlsruhe (FZK) are compared to the newly designed FP reactor at Stellenbosch University. For the purpose of this chapter the units are referred to by their 'kg/h' biomass feed rate. Both units $FPU_{0.1}$ and FPU_{10} are located at FZK in Germany and were described by Yanik *et al.* (2007) and Henrich *et al.* (2007) respectively. FPU_1 is the new fast pyrolysis unit at Stellenbosch University (SU). Table 43 summarises the main characteristics of each FPU.

Tests at FZK were only done at the known optimal temperature for most lignocellulosic biomasses of 500°C to produce high liquid yields. Previous studies also showed that the optimum for bagasse is 500°C (Drummond *et al.*, 1996). Bio-oil yields are not sensitive to small changes in temperature (near the optimum) and may change only 4 wt% with a temperature deviation of 50°C from the optimal temperature (Bridgwater *et al.*, 1999).

Table 43: Different pyrolysis units that were used in this study

Unit	$FPU_{0.1}$	FPU_1	FPU_{10}
Description (Ref)	Lab scale unit at FZK (Yanik *et al.*, 2007)	Lab scale unit at SU	Development unit at FZK (Henrich *et al.*, 2007)
Size	**0.1 kg/h**	**1 kg/h**	**10 kg/h**
Temperatures	500°C	428-526°C	500°C
Vapour residence time	1-2 s	1.6 s	1 s
Reactor	Fluidized bed	Fluidized bed	Screw reactor
Solid collection	Single cyclone	Dual cyclone	Single cyclone
Char entrainment into bio-oil	Some visible particles	No visible particles	char collected with bio-oil
Liquid collection	3 Condensers and 1 dry ice condenser	Single direct contact condenser	3 Condensers
Analysis	None	Char and liquid	Char, liquid, and gas
Biomass preparation	Milling (2mm)	Milling (2mm) and Sieving (>250μm)	Milling (4mm)

6.2.1.1   Description of $FPU_{0.1}$: FZK lab scale unit

A lab scale continuously fluidized bed reactor (ID: 40 mm, L: 300 mm) was used for the experiments. A screw-feeder continuously feeds at 100 g/h into the reactor which is partially filled with silica sand (400-600 μm) to a depth of 37 mm. The feed hopper is stirred to avert bridge formation, and the feed rate is volumetrically calibrated before each run. Nitrogen gas is divided into two streams, the main stream for fluidizing (0.25 - 0.3 m/s at operating temperatures), and the resulting 10% into the pressurized feeding hopper. The reactor residence time is in the region of 1-2 s. The reactor is allowed to heat and reach steady state, under continuous nitrogen flow. Before the start of an experiment the gas flow rate is checked to account for deviations that occur over time. Volatiles and char exit the reactor and enter the cyclone where most of the char collects at the bottom of the cyclone. Thereafter the volatiles enter a counter current double pipe heat exchanger which is maintained at 14ºC by a chilling unit. The pipe section from the reactor to the heat exchanger is also heated to prevent pre-condensation. In this first heat exchanger liquids along with some chars accumulate. Hereafter the vapours pass through two ice baths (0°C) to collect more condensable liquids. Two Electrostatic Precipitators (ESPs) were used to collect micro droplets of the heavier compounds from the vapour. The vapour finally passes through a methanol-dry ice trap (-40°C) which condenses some high volatile components. The remaining gas exits the system after passing through a gas meter which measures the cumulative volume of gas. All components are weighed before and after each run to determine the total weight of the non-gas species. The condensation

system causes fractionation of liquid product, and therefore this process produces a tar and a pyrolytic water phase.
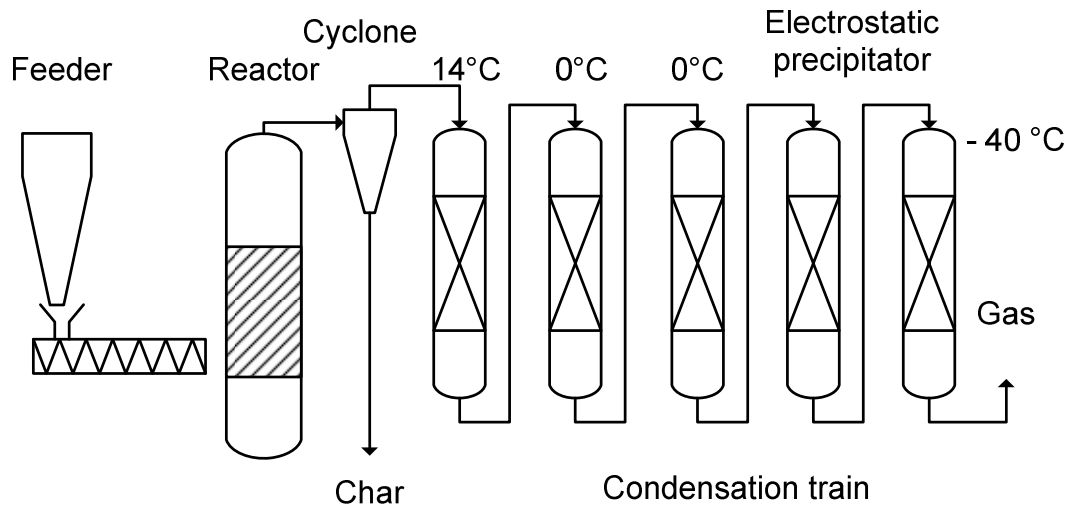

Figure 42: Schematic diagram of $FPU_{0.1}$ (Yanik *et al.*, 2007)

6.2.1.2   Description of FPU_1: Stellenbosch University Fast Pyrolysis Unit

The components of FPU_1 were discussed in chapter 3. For each run the oven is heated over a period of approximately 90 min at which time a pseudo steady state is reached. When the temperature difference inside the reactor is within 10°C biomass is fed into the process. The monitoring system records all data from the electronic sensors. After each run a mass balance is done to determine the liquid and solid yields, the gas yield is calculated from the difference. The process produces one single phase bio-oil. Most of the bio-oil is directly collected from the bottom of liquid collection vessel. All small components are weighed before and after cleaning. The acetone oil form washing of the larger units is collected to determine the oil weight after evaporation.

6.2.1.3   Description of FPU_{10}: FZK Process Demonstration Unit

Pyrolysis with twin screw (LR) reactors is a well understood technology at FZK (Henrich *et al.*, 2007). One of the most important advantages of this method is that biomass is mechanically fluidized and does not require heating of cold fluidizing gas. The reactor (1.5 m long) is normally operated at 10 kg/h (biomass). The central part is a hot sand loop with bucket elevator, operated at 500°C, and is used to mechanically fluidize and heat the biomass. Figure 43 shows the simplified flow diagram. Nitrogen is

used to purge oxygen from the reactor, and neon is used as a tracer compound to determine the amount of gas. Sand is indirectly reheated in the sand heater and then mixed with the dry biomass particles in the twin screw reactor. A fast stream of gaseous, vaporised and solid pyrolysis products leaves the reactor. The char is immediately removed from the hot zone after pyrolysis. The char container is outside the heated zone, unlike the fluidized bed reactors used in this study. The first condenser is a shell and tube heat exchanger, with a mechanical wall scraper to remove oil deposits from the inner walls of the condenser. This condenser can be operated within a range of temperatures (typically 20-40°C). The oil is directly mixed with char from the cyclone, to produce an oil wet char which will be used to produce the slurry. Chemical extraction is therefore required to determine the final solid and liquid fractions. A second condenser uses water as cooling liquid to condense more oil from the gas. An electrostatic precipitator removes the remaining aerosols from the gas, where after the gas is analysed by with an online Gas Chromatograph (GC). Only the collection containers are weighed to close the mass balance, therefore some products unavoidably remain in the system.
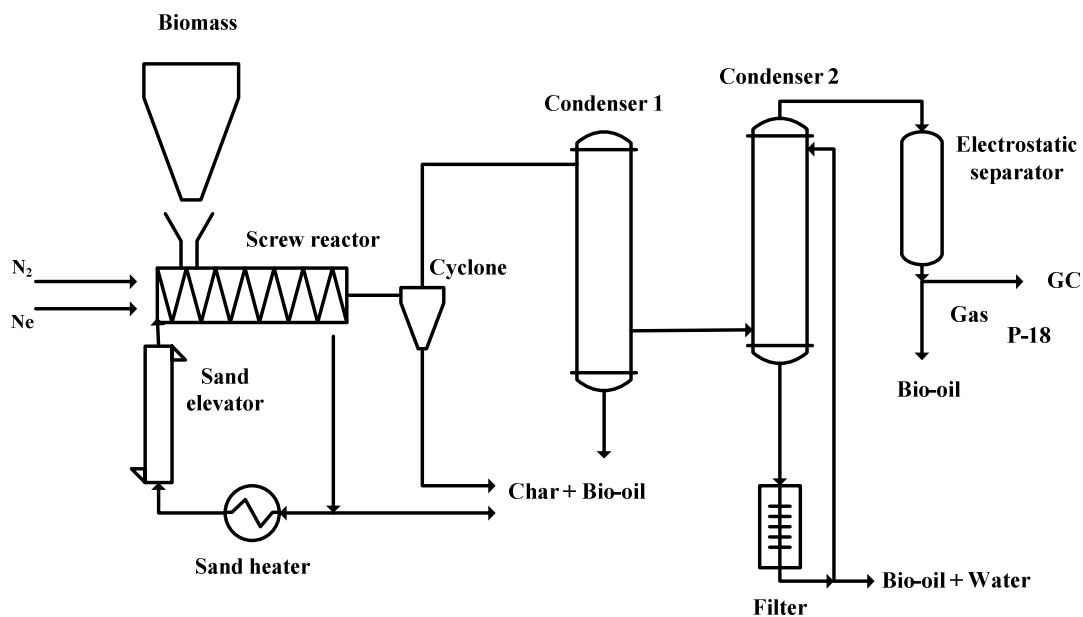

Figure 43: Schematic diagram of FPU_{10} (Henrich *et al.*, 2007)

6.2.2 *Bagasse*

Two different batches of bagasse were used for FP experiments. All bagasse was supplied by the SMRI from KwaZulu-Natal in South Africa. Table 44 shows the characteristics of bagasse. At SU the biomass

was passed through a shredder mill followed by rotor mill (Retsch ZM 200) with sieve size 2mm. Particles smaller than 250 µm were discarded, because of entrainment problems that occurred. Consequently the ash content of 'US bagasse' is significantly lower than 'FZK bagasse'. Size reduction at FZK was done with a Fritch (Pulverisette 25) cutting mill with sieve sizes 4mm, 2mm and 1mm. The prepared biomass was stored in closed containers.

Table 44: The proximate analysis, ultimate analysis and HHV of bagasse.

Particle size (mm)		
Milled	4	2
Sieved	NA	> 0.25
Proximate analysis (dry wt%)		
Volatiles (without moisture)	82.50	81.78
Fixed carbon	11.90	13.17
Ash	5.60	2.87
Ultimate analysis (dry wt%)		
C	47.5	
H	5.9	
O	40.7	
N	0.29	
S	0.07	
Calorific value (MJ/kg)		
HHV	18.79	

An analysis on the ash composition of bagasse showed that the major inorganic compounds were Si, Al, and Fe, which contributed 38.2, 2.5, and 2.5 wt% to the ash, respectively.

6.2.3 *Analyses*

Water content (WC) and ash content analyses were carried out in triplicate at 102°C for 24h (ASTM E871) and at 575°C for 4h (ASTM D1102), respectively. A Metrohm KF Titrino with standard Karl-Fisher reagent was used to determine the WC of the oil phase (in duplicate). Elemental analysis for C, S, N was done on the oils at a neighbouring institute. The char was analysed for C, S, N, H at SU by a Eurovector EA elemental analyser (in duplicate). The Surface Area (SA) of chars was determined (in

duplicate) using a multipoint Brunauer, Emmett and Teller (BET) analysis on Micrometrics ASAP 2010 system.

The HHV of bio-oils was measured with an IKA C200 calorimeter. To calculate the HHV from the elemental and ash analysis, the correlation from Channiwala *et al.* (2002) was used (Equation 18). The weight fraction is denoted by 'x' and subscripts are the elemental and ash composition of the organic compound.

$$HHV[MJ/kg] = 0.3491x_C + 1.1783x_H + 0.1005x_S - 0.1034x_O - 0.0151x_N - 0.0211x_{ash}$$
Equation 18

The products from FPU_{10} were analysed by the analytical facility at FZK. The analyses included: solid content of the slurry product by means of methanol extraction; continuous Gas Chromatography (GC) analysis on pyrolysis gas; Water Content (WC) on oils by means of Karl Fisher titration; elemental analysis of bio-oil, and char.

6.2.4   Data analysis

In order to establish and comment on experimental repeatability of the FPU_1, the standard deviation was calculated from 3 runs at similar conditions. The measurement error was also calculated and combined with the experimental error to produce a final error value.

Multiple samples are taken during an experiment at FPU_{10}. Three to four samples were taken from the oil and char containers and the gas was analysed 8–10 times during each experiment.

A single factor ANOVA test was done on data from FPU_{10} (two data points) and FPU_1 (three data points) at 500°C to establish if there is a difference in their product yields and qualities. The results showed that the bio-oil products were mostly similar and that the char products were different (Table 79 in appendix).

6.3   Results from FPU_1

6.3.1   Repeatability
The first objective is to establish system repeatability and address any operational problems with the unit. The results from the first four runs are displayed in Table 45. These runs may still be viewed as

commissioning because some modifications were done during some of the experiments. The amount of bagasse fed to the reactor ranged from 90-200 g. Small sample sizes were used because of problems with size reduction. The biomass was dried 2.8-6.3 wt% moisture.

Table 45: Pyrolysis yields for R1–R4 on FPU_1 (*obtained by subtraction)

Temperature (°C)	520 ± 3	520 ± 2	508 ± 6	497 ± 6
Run number	R 1	R 2	R 3	R 4
Y_{char} (wt%)	11	11	11	11
Y_{liquid} (wt%)	34	53	35	55
Y_{oil} (wt%)	25	40	25	47
Y_{gas} (wt%)*	55	37	54	35

The best runs were runs 2 and 4 which produced 53 wt% and 55 wt% of bio-oil and 11 wt% char for both, respectively. The bio-oil yields are lower than typical values of 60 wt% reported in literature for lignocellulosic biomasses (Mohan *et al.*, 2006). Larger sample sizes (300 g) were used for experiments R5-R9 to improve repeatability. The product yields are presented in Table 46. Similar deviations were reported in literature by Westerhof *et al.* (2007) who reported 1.7 wt% on the liquid yield, and Yanik *et al.* (2007) who reported up 3.1 wt% on the liquid yield.

Table 46: Pyrolysis yields for R5 – R9 on FPU_1 (*by subtraction)

Temperature (°C)	428 ± 5	495 ± 2				526 ± 3
Run number	R 7	R 5	R 6	R 9	Average	R 8
Y_{char} (wt%)	11 ± 1	10 ± 1	10 ± 1	8 ± 1	9 ± 1	11 ± 1
Y_{liquid} (wt%)	59 ± 3	63 ± 3	65 ± 3	68 ± 3	65 ± 3	59 ± 3
Y_{oil} (wt%)	51 ± 3	55 ± 3	57 ± 3	59 ± 3	57 ± 3	51 ± 3
Y_{gas} (wt%)*	29 ± 4	26 ± 4	26 ± 4	24 ± 4	25 ± 4	29 ± 4

6.3.2 *Process conditions*

Before the interpretation of results, it seems necessary to clarify the possible effect of operating conditions such as the residence time, the cooling temperature, and the nitrogen and isopar flow rates on pyrolysis product yields. These process conditions are summarized in Table 47.

Table 47: Process conditions for runs R5 – R9 on FPU$_1$

	R5,6&9	R 7	R 8
Reactor temperature (°C)	495 ± 2	428 ± 5	526 ± 3
Cooling temperature (°C)	12.2 ± 0.4	11.7 ± 0.9	10.4 ± 0.6
N$_2$ flow rate (m^3/h)	2.5 ± 0.0	2.5 ± 0.1	2.5 ± 0.1
Coolant flow rate (L/min)	3 ± 0.3	3± 0.6	2 ± 1
Vapour residence time (s)	1.6	1.6	1.6

The average vapour residence time was 1.6 seconds and the biomass feed rate 0.9 kg/h. The residence time is shorter than two seconds which is typically the bench mark for FP. From previous literature it seems that a variation of vapour residence time in the reactor is acceptable between 1 and 2 seconds at 480-500°C without significantly affecting the product yields (Westerhof *et al.*, 2007; Scott *et al.*, 1999; Yanik *et al.*, 2007). The residence time variation is small compared to the tested ranges and will not significantly affect the product yields. Some variability is noted with the isopar flow rate because the pump is air operated with a manual valve and therefore it is difficult to duplicate the flow rate exactly each time. This slight variability should not have a significant effect on the cooling since the flow rate is much higher than the heat transfer limiting value. The operated flow rates will translate to 90-130 kg/h where the design flow rate was 20 kg/h. At the higher flow rates the cooling temperature is also slightly lower because the residence time of the cooling liquid in the chiller bath is longer. A comparison of the thermodynamic energy shows that the cooling capacities of the different flow rates are very similar because of the slight temperature differences. The cooling capacity ranges from 0.23-0.25 kW (non evaporative cooling) at an isopar flow rate of 3-2 L/min at the respective temperatures (12 and10°C).

6.3.3 *Temperature*

The variation of product yield with temperature is illustrated in Figure 44. Based calculated error of FPU$_1$ and the yields that were obtained at higher and lower temperatures it can be said that the optimum liquid yield for bagasse was 65 ± 3 wt% at 495°C. These yields compared well to previous research on wood

pyrolysis (Bridgwater *et al.*, 1999), and are higher than most values reported for bagasse (Drummond and Drummond, 1996; Tsai *et al.*, 2006) (see Table 14, paragraph 2.9.1).

The char yield did not vary significantly over the temperature range investigated. The slight decrease in char yield at 500°C may be as result of the variation of WC of the feedstock (appendix Table 77). Westerhof *et al.* (2007) found that heat transfer limitations due to the evaporation of moisture causes the pyrolysis temperature to be lower, therefore favouring char production. A wide range of char yields are reported in literature (Drummond and Drummond, 1996; Tsai *et al.*, 2006; Asadullah *et al.* 2007). At lower heating rates (< 3.3°C/s) high char yields were obtained (up to 25%), and lower char yields were obtained for higher heating rates. The gas yield was obtained by subtraction and is therefore an estimate. Values from 25-30 wt% were reported. Yanik *et al.* (2007) reported a gas yield of 39 wt% for straw which is elementally similar to bagasse.

Figure 44: Product yields from FPU_1 of SB at different temperatures. (*Gas yields obtained by subtraction)
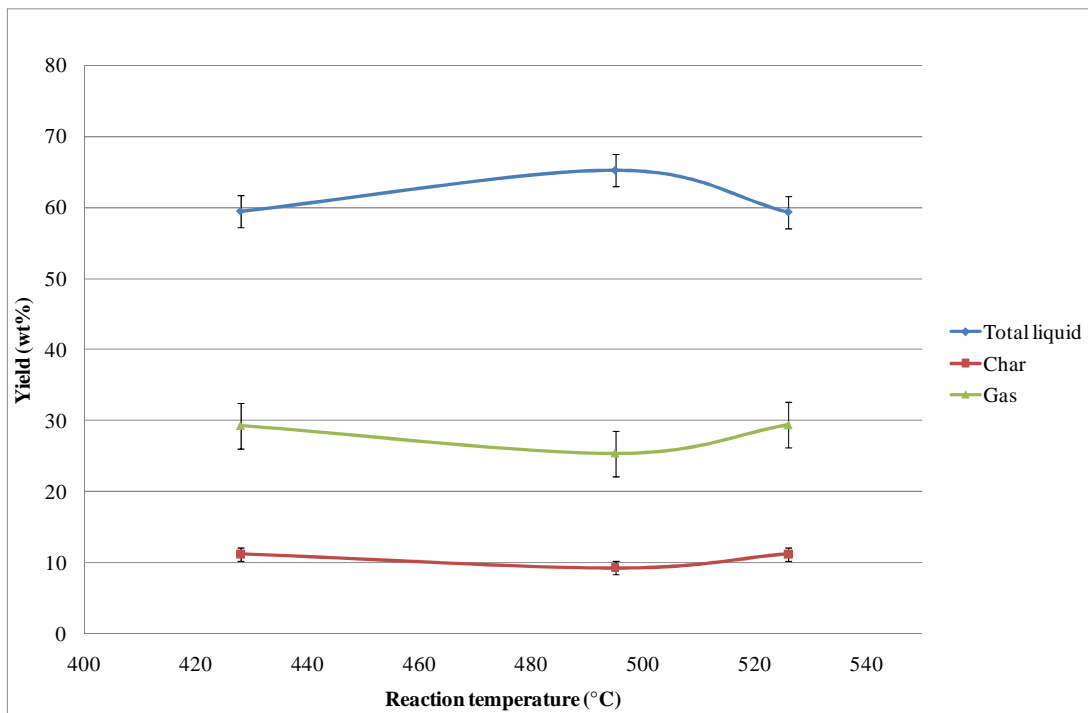
6.4   Results from FPU$_{0.1}$

Three runs were conducted at 500°C with 100 g of bagasse (9 wt% water). About 50 wt% of the original biomass is condensed in the first condenser and electrostatic precipitator. Additional cooling at zero and sub-zero temperatures increased the liquid recovery by 20 wt%. The average liquid yield for the first 3 experiments was 71 ± 2 wt% (Table 48). A small amount of visible char entrained into the liquid product.

Table 48: The mass balance from experiments on FPU$_{0.1}$ (*calculated by difference).

Temperature (°C)	500			
Run number	1	2	3	Average
Y_{char} (wt%)	14 ± 2	11 ± 2	12 ± 2	12 ± 2
Y_{liquid} (wt%)	69 ± 2	73 ± 2	71 ± 2	71 ± 2
Y_{gas} (wt%)*	16.8 ± 0.8	15.9 ± 0.8	17.4 ± 0.8	16.7 ± 0.8

6.5   Results from FPU$_{10}$

Two experiments were conducted at 500°C with bagasse on the twin screw reactor (FPU$_{10}$). The temperature of the first condenser was 20°C and 40°C for runs FZK 05 and 06 respectively. This only effects the distribution of oil collection within the system. In both experiments 30-40 kg of bagasse was pyrolyzed over 4 hours. The results from the mass balance are presented in Table 49. The mass balance closure could be calculated, because the gas yield was measured and not obtained by subtraction as with the other FPU units. Run 05 showed a large mass balance deficit of 8 wt%, compared to 3 wt% in run 06. Approximately 9 wt% less liquid was accounted for in run 05 than run 06. Therefore run 06 produced, and most accurate liquid yield of 68 wt%. The solids product showed good repeatability. The lower liquid yield in run 05 is therefore mainly caused by loss of liquid product within the process. The gas yields are similar to previous publications (Bridgwater *et al.*, 1999).

Table 49: Shows the mass balance from the FPU_{10}

Temperature (°C)	500		
Run number	05	06	Average
Y_{char} (wt%)	17	17	17
Y_{liquid} (wt%)	59	68	64 ± 6
Y_{oil} (wt%)	49	55	52 ± 5
Y_{gas} (wt%)	16	12	14 ± 3
Mass balance closure (%)	92	97	95 ± 4

6.6   Comparison the different FPUs and their products

6.6.1   *Product yields*

The average product yields at 500°C of the different FPUs are shown in Table 50. FPU_1, and $FPU_{0.1}$ produced less char than FPU_{10}. These two reactors are both fluidized bed reactors, which are susceptible to char entrainment into the liquid phase. In these reactors the char remains in the hot zone for the duration of the experiment (1h), and is therefore kept for longer periods at reactive conditions. Previous studies on the thermogravimetric behaviour of bagasse showed that lignin decomposes over a wide temperature range up to 900°C (Garcia-Perez *et al.*, 2000). Lua *et al.* (2005) showed that an increased hold time at 400°C increases the fixed carbon content of char. At the pyrolysis conditions (500°C) some un-reacted lignin compounds are still present, and may slowly continue to react, resulting in a decreased char yield. The predicted char residue (fixed carbon and ash) is 14.6 wt% and 16.3 wt% for the sieved and original bagasse used in the study, respectively (on wet basis, from Table 44). Since sieved bagasse was used at FPU_1 slightly lower char yields are expected.

Table 50: Comparison of yields from different FPUs (*gas obtained by subtraction).

Temperature (°C)	500		
Run number	$FPU_{0.1}$	FPU_1	FPU_{10}
Y_{char} (wt%)	12 ± 2	9 ± 1	17 ± 2
Y_{liquid} (wt%)	71 ± 2	65 ± 3	64 ± 6
Y_{oil} (wt%)	n.d.	57 ± 3	52 ± 5
Y_{gas} (wt%)*	17 ± 0.8	25 ± 4	19 ± 3

All three FPUs produced a dark brown liquid of low viscosity for the main liquid phase, which is consistent with previous studies (Horne *et al.*, 1996). Cryogenic condensers from $FPU_{0.1}$ produced a yellow coloured product, with very low viscosity. The condensers allow the additional collection of volatile compounds which may have increased the liquid yield from $FPU_{0.1}$. In light of the low temperature cooling and the char entrainment, the yields from $FPU_{0.1}$ compares well to the yields obtained from the other units.

The average bio-oil yield from FPU_{10} showed a large deviation due to some product loss from the first run. The gas yields from $FPU_{0.1}$ and FPU_1 were obtained by subtracting the char and oil yields from the biomass weight. Therefore these values include the loss of product within the process. Somewhat more gas was produced from FPU_1 than the other two units.

6.6.2 *Bio-oil analysis*

A summary of the bio-oil analysis is given in Table 51. The analysis of bagasse is included for comparison. The bio-oil from FPU_1 and FPU_{10} contained similar amounts of water. The ash content of the bio-oil from FPU_1 shows significantly less (0.12 ± 0.03 wt%) ash contamination compared to the FPU_{10} experiments (5.0 ± 0.2 wt%). The removal of fines from bagasse for FPU_1 experiments reduced the amount of available ash, and thereby contributed to the lower bio-oil ash content. A large fraction of the ash remains in the bio-oil from the FPU_{10} experiments which may be a secondary effect from the char-oil separation. The use of methanol as solvent may extract some ash from the chars which then remains in the bio-oil. Previous studies also showed a great variation of ash content with bagasse (Devnarain *et al.*, 2002). Because the fines were removed from bagasse for tests done on FPU_1, the ash % was greatly reduced.

To calculate the bio-oil HHV the hydrogen content was estimated for FPU_1 since it could not be measured. The result from the analysis of FPU_{10} (6.4 wt% H_2) was used for these calculations. Because this introduces uncertainty, the results will only be used to comment on trends in the data and estimate the HHV. To validate calculation method the HHVs were also measured. The calculated and measured HHV are shown to compare well for runs conducted at 500°C, but deviate for runs at lower and higher temperatures (R7 and R8). This suggests that the assumption for hydrogen content is only valid if the reaction temperatures are the same. The carbon content (45 wt%) and HHV (18 MJ/kg) from bio-oil produced at FPU_1 and FPU_{10} gave similar results at 500°C (Table 51). The values obtained for carbon content from runs R7 and R8 are very high which affects the calculated HHV, but was not noted with the

measured HHV. This could point to inaccuracy of the carbon measurements for runs R7 and R8. The HHVs are slightly higher (18 MJ/kg) than typical literature values of 17 MJ/kg reported by Bridgwater *et al.* (1999). Horne *et al.* (1996) reported a lower average carbon composition for bagasse of 38.6 wt% with a uniform trend, whereas a range of values (45 - 54 wt%) were reported from this study.

By performing a mass balance on the water, the pyrolytic (reaction) water can be calculated as the difference. A small amount of water will remain in the exit gas, but this amount is more or less constant for all runs. The pyrolytic water (appendix: Figure 64) curve follows an opposite trend to that of the total liquid yield (Figure 44). The oil yield was maximized and the water yield was minimized at 500°C.

Table 51: Water content (WC), ash content, elemental composition and HHV of bio-oil from FPU_1 and FPU_{10}.

Unit	Runs (Temp)	Yield (wt%)	H_2O wt%	Ash wt%	C wt%	H^1 wt%	O^2 wt%	N wt%	S wt%	HHV^3 (MJ/kg)	HHV^4 (MJ/kg)
SB	n.a.	n.a.	0	5.6	47.5	5.9	40.7	0.3	0.07	19.2	18.8
FPU_1	R7 (428°C)	59 ± 3	21.8 ±0.9	0.08 ±0.07	50 ± 2	n.d.	43 ± 2	0.3 ±0.1	0.03 ±0.01	21 ± 1	17.9 ± 0.1
	R5,6,9 (495°C)	65 ± 3	20.3 ±0.9	0.08 ±0.07	45 ± 2	n.d.	48 ± 2	0.5 ±0.1	0.06 ±0.01	18 ± 1	18.1 ± 0.1
	R8 (526°C)	59 ± 3	21.2 ±0.9	0.00 +0.07	54 ± 2	n.d.	39 ± 2	0.5 ±0.1	0.12 ±0.01	22 ± 1	17 ± 0.1
$FPU_{0.1}$	3 X (500°C)	71 ± 2				n.d.					
FPU_{10}	2 X (500°C)	67	19 ± 3	5 ± 0.2	44 ± 2	6.4 ± 0.1	45.2	n.d.	n.d.	17.3 ± 0.5	17.9

1: Averaged from FZK results and applied to SU results
2: Calculated by difference
3: Calculated
4: Measured

6.6.3 *Char analysis*

The results from the char analysis show ash compositions of 24 and 22 wt% from FPU_{10} and FPU_1 respectively. This comparison should be seen in light of how much ash entered the system and how much exited in the bio-oil. The unsieved bagasse used for FPU_{10} contained 3 wt% more ash (Table 44) than sieved bagasse and the bio-oil contained a high ash content of 5 wt %.

The chars from FPU_1 contained on average 10 wt% more carbon, than the chars from FPU_{10} (Table 52). The chars from FPU_1 also have lower hydrogen content. This can be attributed to the longer residence time of char at pyrolytic conditions: 2 hour at FPU_1 compared to a few minutes FPU_{10} (Lua *et al.*, 2005). Ash also acts as a catalyst which could favour carbonization and reduce the hydrogen content. The average char HHV from FPU_1 is 24.68 MJ/kg at 500°C, which is higher than the char from FPU_{10}. This can be attributed to the higher carbon content. A comparison of the different runs at different temperatures on FPU_1 suggests that carbon wt% is optimized at 500°C.

The BET surface area of the char product from FPU_1 ranged from 233-282 m^2/g. The char from experiments on the $FPU_{0.1}$ had a surface area of 187 m^2/g. The char residence time in these two similar reactors is the same (2h), but bagasse contained less ash for FPU_1 experiments. Devnarain *et al.* (2002) reported that the ash content of chars caused a decrease in SA after activation, which could explain the differences in surface area. Das *et al.* (2004) confirmed these findings with values of 98 to 243 m^2/g for different de-ashing treatments on bagasse. In paragraph 2.6.2.2 it was shown that bagasse has a particularly suitable particle structure compared to other large scale agricultural by-products. Therefore bagasse produces a superior char and the removal of bagasse fines increases the BET surface area.

Table 52: AC, elemental composition, BET surface area and HHV for the different chars obtained from FPU_1 and FPU_{10}.

Unit	Runs (Temp)	Yield (wt%)	Ash wt%	C wt%	H[1] wt%	O+S wt%	N wt%	HHV[2] (MJ/kg)	BET SA (m^2/g)
SB	n.a.	11.9	5.6	47.5	5.9	40.7	0.3	19.2	n.d.
FPU_1	1 X (428°C)	11 ± 1	14.1 ± 0.4	66 ±6	1.37 ± 0.01	18.3	0.55 ± 0.06	22 ± 2	n.d.
	3 X (495°C)	9 ± 1	22 ± 2	69 ±3	1.6 ± 0.1	6.6	1.3 ± 0.3	25 ± 2	255
	1 X (526°C)	11 ± 1	20 ± 2	65 ± 3	1.3 ± 0.2	12.9	1.2 ± 0.2	22 ± 2	282
$FPU_{0.1}$	2 X (500°C)	12 ± 2	n.d.						187
FPU_{10}	3 X (500°C)	17	24.8 ±0.5	53 ± 2	3.4 ± 0.2	18.6	0.51 ± 0.06	20.0 ±0.6	n.d.

1: Calculated by difference

2: Calculated

126

6.6.4 *Gas analysis*

The dominant species in the exit gas were CO_2 and CO and small amounts of H_2 and CH_4 were present. The formation of these species can be explained by the chemical reaction discussed in section 2.10.2. Figure 45 shows the variation of the concentration of the gas species. The curves present a reasonable variation on a near linear trend. In Table 53 elemental composition is shown for the gas. The HHVs were calculated from known heating values for the gas components. The heating values are very much dependent on the effectiveness of liquid collection and biomass type as shown by Raveendran *et al.* (1996).

Table 53: The chemical and elemental composition of the incondensable gas from FPU_{10}

Run	Units	Run 5	Run6
H_2	g/kg	0.39	0.31
CO	g/kg	60.20	48.44
CH_4	g/kg	5.18	3.94
CO_2	g/kg	97.35	72.77
C_2H_4	g/kg	1.00	0.84
C_2H_6	g/kg	0.99	0.70
C_3H_8	g/kg	1.72	1.30
C_4's	g/kg	2.06	2.53
C_5+	g/kg	5.67	5.15
C	wt%	37.7 ± 0.5	38.5 ± 0.3
H	wt%	2 ± 0.2	2.2 ± 0.0
O	wt%	60.3 ± 0.7	59 ± 0.4
HHV (MJ/kg)	wt%	8.9 ± 1.7	9.56 ± 0.6

Literature on sophisticated GC analysis of various types of biomass pyrolysis is scares. Therefore these results are compared to Mullen *et al.* (2010), who studied FP of corn cobs and corn stover in a fluidized-bed reactor at 500°C. Similar proportions of gas species were obtained as shown in Table 54. The large difference in HHVs is explained by the fact Mullen did not measure for hydrocarbons $>C_2$ that have very high energy content. Even at low concentrations these hydrocarbons significantly contribute to the HHV of the gas.

Table 54: Comparison of gas composition to literature (based on at least two runs)

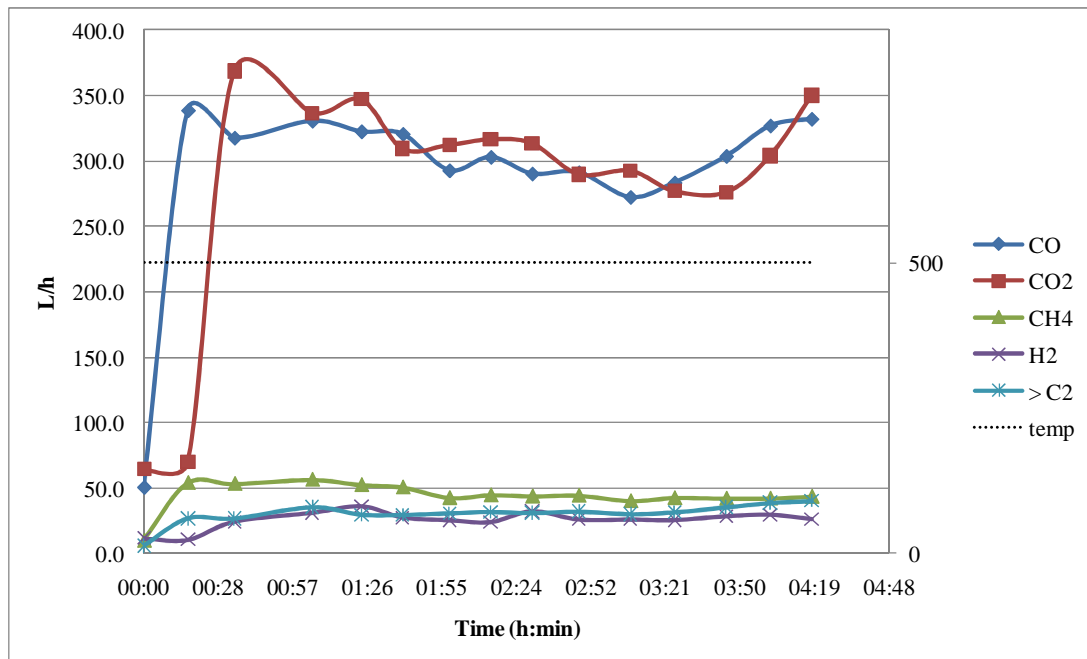| Gas compound	FZK$_{10}$	Mullen *et al.*, 2010	
	Sugarcane bagasse	Corn cobs	Corn stover
CO$_{2\ Vol\%}$	42.1	51.5	40.3
CO $_{Vol\%}$	43.0	40.9	51.6
CH$_{4\ Vol\%}$	6.3	6.3	6
H$_{2\ Vol\%}$	3.9	1.3	2
>C$_{2\ Vol\%}$	4.7		
HHV (MJ/kg)	9.23	4.9	6
Gas yield (wt%)	14	20.3	21.9

Figure 45: The variation of gas components volumetric flow rate for FPU$_{10}$ run 05 at 500°C

6.6.5 *Product energy distribution*

When performing pyrolysis on a certain feedstock it is interesting to look into how the original energy is distributed among the products. The energy value of dry bagasse was 18.96 MJ/kg which is consistent with results from Asadullah *et al.* (2007) who reported 19.1 MJ/kg. Table 55 gives a summary of the energy distribution among product from FP at 500°C (complete version: Table 80). The average energy content for the bio-oil is similar for both FPU_1 and FPU_{10}, (64 and 60 respectively). By combining the products into a single slurry mixture the energy content of a single product can be increased to between 70 and 80% of the original biomass energy. Lange (2007) obtained 79% of biomass energy for slurry production from straw pyrolysis on FPU_{10}.

Table 55: A summary of the energy balance from pyrolysis 500°C

Product	FPU_{10}			FPU_1		
	Yield wt%	Carbon wt%	Energy %	Yield wt%	Carbon wt%	Energy %
Bio-oil	68	64	60	65	62	64
Bio-char	17	26	18	9	13	12
Gas	24	12	7	n.d.	n.d.	n.d.

7 Preferred pyrolysis process for bio-oil and bio-char production from bagasse

7.1 Introduction

To establish which pyrolysis process is the most favourable for the sugar industry, Slow Pyrolysis (SP), Vacuum Pyrolysis (VP), and Fast Pyrolysis (FP) processes need to be compared in a suitable manner. Since economic comparison is not included in the scope of this work, the focus of the comparison will be the products. It is therefore necessary delineate the individual products from each of the pyrolysis processes, in terms of energy and product properties. Therefore depending on the type and application of the products, different processes are favoured.

7.2 Review of slow and vacuum pyrolysis data

The results from chapter 4 (Carrier *et al.*, 2010) on VP and SP are briefly reviewed to display the data similarly to the FP work. Instead of commenting on the separate yields of tar and pyrolytic water phase only a total liquid yield is discussed. Data from the newly constructed fast pyrolysis unit (FPU_1) will be used for this chapter, and is simply referred to as 'FP'.

7.2.1 *Slow pyrolysis (SP)*

Conventional SP has been used for many years, whereas today modern techniques like VP and FP present many advantages. The primary objective of the work on SP was to produce a qualitative comparison to the work done on VP. The experimental conditions were kept identical as far as possible. Both VP and SP were done in the same reactor, which has not been reported before. The statistical optimisation of experimental conditions was focussed on pyrolysis temperature and heating rate as the primary factors that determine the yield and quality of products. Temperature (250 - 570°C) and heating rate (2-29°C/min) was varied, and the results were analysed for product yields, with specific emphasis on char properties HHV and BET surface area. The effects of temperature and heating rate on yields and characteristics were studied using an ANOVA analysis. Temperature was found to be the most significant process variable. At the optimal temperature of 500 ± 25°C and the highest heating rate, the organic liquid yield was 17.8 ± 0.6 wt% and water in liquid phase 26.8 ± 0.5 wt%. The total liquid product (45 ± 2 wt%) is of substandard quality because it contains 60 wt% water on average. The char yield was naturally a maximum at the lowest temperature (200°C) and slowest heating rate (2-5°C/min) producing 75 – 80 wt% char. These conditions simulate torrefaction, and therefore the product has a low calorific

value and surface area. The HHV and surface area of chars at moderate heating rate and high temperature, were optimized at 28 MJ/kg at (570°C; 18°C/min) and 333 m^2/g at (550°C; 15°C/min) respectively. At these high temperatures the char yield was 25 ± 3 wt%. In conclusion it can be said that a trade-off exists between the yield of char and the quality thereof. Therefore the most favourable property of the char will dictate which route will present the most advantages, be it energy content and surface area (low yields), or simply the aging stability (high yields). From an energy perspective it does not make sense to produce liquids via SP.

7.2.2 *Vacuum pyrolysis (VP)*

VP offers a good compromise over SP, by exploiting the advantages of low pressures inside the reaction zone (Carrier *et al.*, 2010). The experimental conditions and objectives were similar to that of the SP study. The liquid phase yields were optimized at 460 ± 20°C and at a heating rate range of 20 ± 4 °C/min which produced 31 ± 3 wt% liquid organics and 15 ± 2 wt% water. The combined liquid product ($45 \pm 3\%$) therefore contains approximately 32 wt% water which is a significant improvement on slow pyrolysis liquids. The charcoal yield decreases with temperature and was found to stabilize at temperatures greater than 480°C, yielding 16 wt% char. The HHV (23 ± 2 MJ/kg) of the chars remained constant over the temperature range 400-500°C. The optimal SA of the chars was 396-418 m^2/g, at 460-540°C and a heating rate of 8-24°C/min. It can be concluded that temperature is the dominant process variable for VP. The quality of the liquid product was upgraded because the vacuum removes vapours from the reaction zone, which reduces the secondary reactions that produce water. Because more organics end up in the liquid phase, the calorific value of chars is somewhat less than for SP. It can be concluded that the mechanism for pore formation is improved at low pressure, thereby producing higher surface area chars.

7.3 Preferred conditions for bio-oil production

The optimization of bio-oil production is relatively straight forward from an energy perspective. The desired product should have a high yield and HHV. The water content should be as low as possible, but is typically constrained by an unwanted exponential viscosity increase below 15 wt%. Owing to these characteristics, FP produces the highest quality and yield of bio-oil, which was not rivalled by the other types of pyrolysis processes investigated. Therefore the question rather becomes, "Which type of FP process should be used for bio-oil production from sugarcane bagasse?" Since similar yields can be

obtained from both the screw reactor and FBR, the advantages of a certain reactor type will most probably lie with the quality of solid product.

Table 56: Optimal conditions for bio-oil yield.

Unit	Conditions	Dry HHV (MJ/kg)	Liquid yield (%)	Moisture content (%)	Relative energy (%)
SB	Dry (0% moisture)	18.8	n.a.	0%	100
SP	500 ± 25 °C and 25 ± 4 °C/min	n.d.	45 ± 2	60	n.d.
VP	460 ± 20 °C and 20 ± 4 °C/min	21.7 ± 0.5	47 ± 2	32	37
FP*	495 ± 10 °C	18 ± 1	65 ± 3	20	67

*Wet HHV shown

High value or high yield chemicals can be extracted from bio-oil as an alternative to the energy product. Chemical extraction as an application for bio-oil is discussed in paragraph 2.5.2.6. Since catalytic effects from natural or added catalysts determines to a great extent which chemicals are produced, pyrolysis can be optimized to produce certain high yielding chemicals (Bridgwater, 1996). The economic feasibility of adding a distillation step for collecting valuable chemicals is dependent on the market price and the yields of these chemicals. The remainder of the bio-oil product after chemical extraction will probably be used for energy production. Therefore the energy quality of the bio-oil cannot be disregarded, suggesting that FP will probably remain the most economical option unless it can be proven that vacuum pyrolysis can produce significantly higher yields of valuable compounds. Future studies should look into chemical production from different pyrolysis processes. The infrastructure for commercial use of bio-oil is still at the early stages of development. Therefore the development of an energy market for bio-oil first needs to be established before attempting extra processing for chemical extraction. It is believed that the future of bio-oil does not only lie with higher quality fuel production but also with the use of bio-oil as chemical feedstock (Bridgwater *et al.*, 2002).

7.4   Preferred conditions for bio-char production

Char quality and yield are not optimized simultaneously. At higher process temperatures the yield decreases and the quality increases. In this study it was found that bagasse can be treated at 250°C to produce up to 80% char product and effectively increase the energy density from 17.5 to 18.9 MJ/kg. The product is brittle, hydrophilic, and contains 80-90% of the original energy, and is resistant to fungal attack. Because this is a mild energy treatment, processing costs will be minimal. The main drawback from torrefaction of bagasse is that the biomass volume is not significantly decreased, and therefore storage and transportation still remains expensive. At optimal heating values the highest yield of char was 28 wt%. Honsbein *et al.* (2007) obtained hardwood yields which ranged from 35 – 40 wt%. Larger particle sizes were used (5cmX5cmX15cm) which favours slow pyrolysis because core heating occurs slower. The particle thickness results in a longer char-vapour contact time which increases the probability for secondary reactions (Katyal *et al.*, 2003). Since bagasse particles are already fine they present more advantages for fast pyrolysis.

The alternative is to produce high quality chars at lower yields. The specific quality-property of the char, (HHV or surface area), is dependent on the application of the product. Table 57 shows the conditions for optimizing the HHV, SA, and the char yield at these conditions. When a high HHV is favoured, slow pyrolysis produces the highest quality chars. During slow pyrolysis the HHV and SA are optimized simultaneously at very similar process conditions, whereas with vacuum pyrolysis the conditions differ slightly more.

The characteristically high surface area of bagasse also renders it useful as a non-energy product (paragraph 2.6.2). This study has proven that VP produces the highest BET SA chars (chapter 4). These chars are the best option for decolourizing raw sugar. Because bagasse produces high SA chars compared to other agricultural residues, this should be the favoured option for the use of solid pyrolysis products.

Table 57: Shows the conditions at which the highest quality chars were obtained

Unit	Condition	HHV (MJ/kg)	BET SA (m^2/g)	Char yield (%)	Relative energy (%)
SB	Dry (0% moisture)	18.8			100
SP	530 - 570°C and 18°C/min	25 ± 3		25 ± 3	33
	530 - 570°C and 15°C/min		293 ± 41		
VP	420-480°C and 17°C/min	24 ± 2		17 ± 2	22
	460-540°C and 17°C/min		347 ± 65		
FP	430 - 530°C	24 ± 2	249 ± 24	10 ± 2	13

7.5 Effect of pyrolysis temperature on product yields

In this section different graphs are used to illustrate the data from different pyrolysis processes more clearly. Figure 46 and Figure 65 (appendix) shows the variation of yield for liquid and char respectively. The three curves were statistically tested to prove that they are from different distributions (paragraph 11.4.1).

The optimal heating rate for liquid production, as shown in Table 56, was 22°C/min for vacuum and slow pyrolysis, whereas FP heating rates may be as high as 200°C/s (Bahng *et al.*, 2009). The high heating rate resulted in a liquid yield increase of approximately 20 wt%. Putun *et al.* (2007) compared to FP at 50°C/s with SP at 0.12°C/s and reported a 10 wt% increase in liquid yield. The liquid yield for VP was found to be optimized at 40-50°C less than for SP and FP. The trend noted from the pyrolysis curve suggests that a higher heating rate shifts the curve up (higher yield) and lower pressures shifts the curve to a lower temperature. A stepwise increase in final char yield (see appendix Figure 65), from FP to VP to SP, corresponds well to the opposite trend observed in liquid organic yield (decrease from FP to VP to SP).
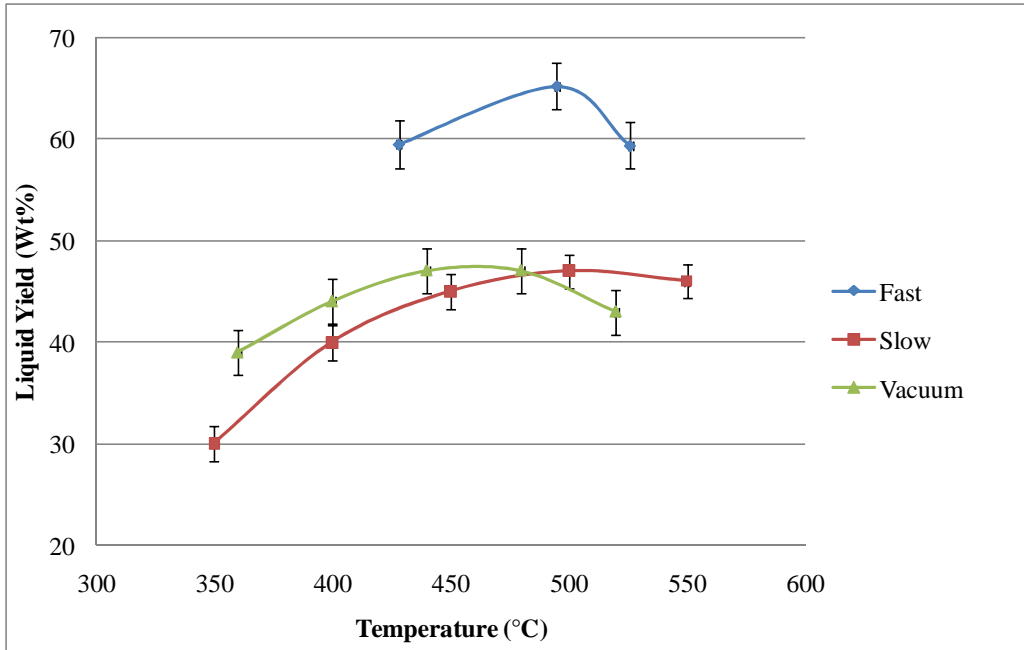
Figure 46: Liquid product yield from slow, vacuum, and fast pyrolysis.

The product yields of the three pyrolysis systems at their respective optimal liquid producing conditions are shown in (Figure 47). The gas yield is similar for SP and FP but is slightly higher for VP. The lower system pressure causes species to be slightly more volatile. The bottom two sections of each bar graph show the valuable organic product, from liquid and char. The actual useful energy product is the bottom two sections minus the energy for water vaporization.

Figure 47: Product yield distributions for FP, SP, and VP (gas yield by difference)
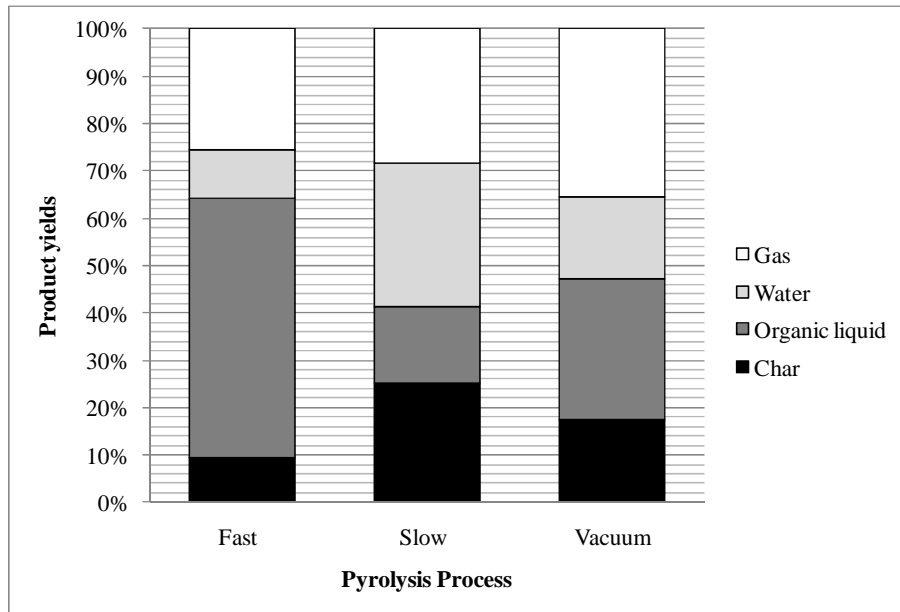
8   <u>Conclusions</u>

Based on the inefficient utilization of bagasse with respect to current technologies, pyrolysis was identified as a potential upgrading technology for the sugar industry. The objective of this study was to investigate the advantages and drawbacks from Slow Pyrolysis (SP), Vacuum Pyrolysis (VP), and Fast Pyrolysis (FP). A summary of the finding of this study is given below. Based on these findings conclusions were drawn.

The first task was the design and construction of a 1.5 kg/h FP unit. During commissioning some modifications were done.

1. The unit functioned without operational problems during testing and gave reproducible results.
2. Direct contact heat exchange performed well. A single phase bio-oil instead of fractionated product was obtained.
3. Electrostatic separators functioned well.
4. The yields of products obtained compared well with previous literature (Bridgwater *et al.*, 1999)
5. The yields of products obtained from bagasse fast pyrolysis in the newly constructed unit compared well to other reactors tested at FZK.

The next task was the evaluation, of SP and comparison to VP of bagasse. An article was co-authored with Dr. M. Carrier entitled: "Comparison of slow and vacuum pyrolysis of sugarcane bagasse".

1. The maximum amount of bio-oil was produced at a heating rate of 15 °C min^{-1} for both processes. The optimum temperatures were 500 and 450 °C for VP and SP, respectively. VP produced a superior quality bio-oil with lower water content that SP.
2. A trade-off existed with regards to the char yield and char properties.
3. The highest BET surface area for the char (> 300 m^2 g^{-1}) was produced by VP at 460 °C. The same trend was observed for SP where the optimal BET surface area was obtained at a higher temperature.
4. SP produced char with the highest HHV (28 MJ/kg) at a temperature range of 450-600°C. The energy value is higher than commercially available 'Charca Brikets' (24.8 MJ/kg) (De Jongh, 2001).
5. An ANOVA analysis proved that temperature was the dominant variable. The influence of heating rate on the BET, HHV$_{oil}$, Y$_{oil}$ and water content was not significant in both processes. The

main difference between the processes is residence time which had a significant influence on the quality of products.

6. With regards to this study the optimal process is dependent on the application of the product.

TGA was studied as a means of investigating the devolatilization behaviour of bagasse. An article was co-authored with A. Aboyade entitled: 'Non-isothermal kinetic analysis of the devolatilization behaviour of corn cobs and sugarcane bagasse".

1. The thermal decomposition of bagasse was studied and three distinct mass loss stages were identified. The first stage (25 - 110°C) is moisture evaporation. In the second stage at 230°C devolalitzation occurs. The final stage occurs at temperatures above 370°C and is associated with the cracking of heavier bonds and char formation.
2. The devolatilization stage is the most important with regard to pyrolysis.
3. The optimal decomposition temperatures for hemicellulose and cellulose were identified as 290°C and 345°C, respectively. Lignin was found to decompose over the entire temperature range without a distinct peak.
4. An increased heating rate resulted in a narrower devolatilization temperature range and increased the optimal decomposition temperatures for lignocellulosic decomposition. Bagasse is expected to follow this similar trend during FP at significantly higher heating rates.
5. Friedman's isoconvertional method predicted a constant activation energy of 200 kJ/mol for bagasse in the pyrolytic conversion range 20 – 80%. A multi-component model was fitted to the data and compared well to chemical analysis data from literature.

From fast pyrolysis of bagasse on different reactors the following conclusions were drawn:

1. Bio-oil production from bagasse was optimized at 500°C for FP.
2. The newly designed FP_1 gave reproducible liquid yields of 65 ± 3 wt% at the established optimal temperature and compared well to results from the other two FP units. The FP bio-oil had a water content of 20 wt% and the HHV was estimated to be 18 ± 1 MJ/kg.
3. Bagasse fines presented problems in terms of entrainment into liquids, especially with fluidized bed reactors. Screw reactors do not have such high gas flow rates, and are therefore more suited for bagasse.
4. The removal of fines from bagasse produced higher quality bio-oils.

5. The char quality decreases if chars are not removed from the hot pyrolysis zone and the main pyrolysis reaction.

FP, VP, and SP were compared to identify the preferred process for the production of bio-oil and char. The following conclusions were drawn:

1. The productions of either high quality bio-oil or high surface area char were found to be application dependent.

2. The char yield was optimized at 28 wt% by slow pyrolysis with the highest HHV (28 MJ/kg) at a temperature range of 450-600°C. The energy value is higher than commercially available 'Charca Brikets' (24.8 MJ/kg)

3. Under FP conditions 20 wt% extra bio-oil was produced compared to SP and VP.

4. The energy distribution on average for liquid, char and gas from FP was 60 ± 4 wt%, 18.4 ± 0.3 wt%, and 7 ± 1 wt% respectively. FP was found to be the most effective process for producing a single product with over 60% of the original biomass energy. The energy per volume of FP bio-oil was estimated to be 11 times more than dry bagasse.

5. Bagasse particles are already reasonably fine, compared to other slow pyrolysis feeds, and therefore present more advantages to fast pyrolysis.

6. The highest BET surface area of the char product from FP_1 was 280 m^2/g and had an average HHV of 24 ± 2 MJ/kg. The surface area of the chars suggests that the chars are suitable for further activation. VP of bagasse produces the highest BET surface area char of up to 410 m^2/g.

9 <u>Recommendations and future work</u>

9.1 TGA

It is recommended that TGA is studied at higher heating rates. With this data it may be possible to draw conclusions between FP data and the corresponding TGA data. Using this data, together with kinetic analysis and modelling may improve reactor design in the future.

The coupling of Mass Spectrometry (MS) or Fourier Transform Infrared spectroscopy (FTIR) to TGA equipment will allow continuous product identification. It will be interesting to study specific chemical products can be obtained at different process conditions. Catalyst effects may also be studied with this equipment.

9.2 Fast pyrolysis unit

Some modifications could provide for easier operation of the unit and upgrade the unit's capabilities.

- The FPU should be adapted to analyse and measure the amount of incondensable gas that exit the cooling system. This can be achieved by using a cumulative gas flow meter, or by including a trace compound (e.g. Ne) and continuously analyzing the gas.
- The rope heaters used to heat the section of pipe between the oven and cooling tower should be upgraded. This can be done by either redesigning the type of heater, or using shorter rope heaters.
- If the gas cylinder level is below about 1 third it cannot be used for an experiment. The installation of a dual-gas cylinder system for nitrogen supply will be ideal, since no nitrogen will be wasted.
- The limiting factor for the amount of biomass that can be pyrolyzed in a single run is the reactor volume. Previous designs used reactor overflow containers. Alternatively the particle size and gas flow rate may be altered to ensure minimal accumulation of char in the reactor.
- The implementation of a cryogenic condenser.
- An appropriate cutting mill for preparing the biomass to the correct particle size.
- Since electrostatic separators can function at high temperatures it may be interesting to design a electrostatic separator for char separation inside the oven. This technology has not been reported before.

9.3 Bagasse pyrolysis

FP was found to be optimal for liquid production and contained the most energy in a single product. VP produced high surface area chars. Because both of these processes produce important products for the sugar industry it would be ideal to combine their effects into one process. Therefore a vacuum fast pyrolysis reactor would be ideal, since it would be able to produce high liquid yields as well as high surface area chars depending on the reaction conditions. Fluidized-bed rectors cannot be used for this purpose. A mechanically fluidized bed reactor will be required.

9.4 Ash

The effect of ash and other catalysts on specific chemicals from bagasse should be investigated. The effect of the different pyrolysis processes on specific chemicals yields should also be studied. Economically viable ash removal techniques should be tested. Discarding the smallest particle size fraction from bagasse lowered the ash content of bagasse by approximately 50%. By studying the additional ash removal techniques similar to the study from (Das *et al.* 2004) the quality of bagasse may be significantly increased. Integrating this work with TGA results may also produce interesting results.

9.5 Sugarcane agricultural residues

This study did not investigate the possibility of using cane tops and leaves as pyrolysis feedstock. From previous literature it seems that there are significant added benefits from using these products. However they also require additional processing because of high ash content, soil contamination, water content and the need to be collected from the plantation. Therefore it is recommended to implement the pyrolysis of bagasse before considering lower quality feedstock.

10 References

References for chapter 4 and 5 are given in original article format.

10.1 References for chapter 2

1. Ahuja, P.; Humar, S. and Singh, P.C. (1996) "A Model for primary and Heterogeneous Secondary Reactions of Wood Pyrolysis". *Chem. Eng. Technol*. 19: 272-282
2. Antal, M.J. jnr.; Varhegyi, G. (1995) "Cellulose pyrolysis kinetics: the current state of knowledge". *Ind. Eng. Chem*. 34: 703-717
3. Asadullah M.; Rahman, M. A.; Ali, M.; Rahman, M.S.; Motin, M.A. (2007) "Production of bio-oil from fixed bed pyrolysis of bagasse".*Fuel* 86: 2514–2520
4. Bahng, M.; Mukarake, C.; Ribichaud, D.J.; Nimlos, M.R. (2009) "Current technologies for analysis of biomass thermochemical processing: A review". *Analyitca Chimica Acta* 651: 117-138
5. Balat, M.; Balat, M.; Kirtay, E.; Balat, H. (2009) "Main routes for the thermo-conversion of biomass into fuels and chemicals. Part 1: Pyrolysis systems." *Energy conversion Management* 50: 3147-3157
6. Banks, D.; Schaffler, J. (2006) "The potential contribution of renewable energy in South Africa". www.earthlife.org.za, 2008
7. Bedmutha R.J.; Ferrante L.; Briens C.; Berruti F.; and Inculet I. (2009) "Single and two stage electrostatic demisters for biomass pyrolysis application". *Che. Eng. And Processing* 48: 1112-1120
8. Beeharry, R. P. (2002) "Strategies for augmenting sugarcane biomass availability for power production in Mauritius". *Biomass and Bioenergy* 20: 421–429
9. Bergman, P. C. A; Kiel, J. H. A (2005) "Torrefaction of biomass upgrading". Published at 14th European *Biomass Conference & Exhibition*
10. Bridgewater, A.V. (1996) "Production of high grade fuels and chemicals from catalytic pyrolysis of biomass"; *Catalysis Today* 29: 285-295
11. Bridgwater, A.V.; Meier, D.; Radlein, D. (1999) "An overview of fast pyrolysis of biomass." *Organic Geochemistry* 30: 1479 – 1493
12. Bridgwater, A.V. (1999, b) "Principles and practice of biomass fast pyrolysis process for liquids". *Journal of Analytical and Applied Pyrolysis* 51: 3-22
13. Brigdwater A.V.; Peacocke, G.V.C. (2000) 'Fast pyrolysis process for biomass". *Renewable and Sustainable Energy Reviews* 4: 1-73
14. Bridgwater, A.V.; Toft, A.J.; Brammer, J.G. (2002) "A techno-economic comparison of power production by biomass fast pyrolysis with gasification and combustion". *Renewable and Sustainable Energy Reviews* 6: 181–248
15. Bridgwater, A.V. (2003) "Renewable fuels and chemicals by thermal processing of biomass". *Chemical Engineering Journal* 91: 87–102
16. Bridgwater A.V. (2007) "IEA - Biomass pyrolysis." *IEA – Bioenergy*, Task 34
17. Calvin, M. (1974) "Solar energy by Photosynthesis". *Science* 184: 375-381
18. CGPL (Combustion, Gasification, and Propulsion Laboratory), (2006) "Project completion report on torrefaction of bamboo". http://cgpl.iisc.ernet.in, 2008
19. Czernik, S.; Bridgwater, A. V. (2004) "Overview of Applications of Biomass Fast Pyrolysis Oil". *Energy & Fuels* 18: 590-598
20. Darmstadt, H.; Garcia-Perez., M.; Chaala, A.; Cao, N.; Roy C. (2000) "Co-pyrolysis under vacuum of sugar cane bagasse and petroleum residue: Properties of the char and activated char products". *Carbon* 39: 815 – 825
21. Das, P.; Ganesh, A.; Wangikar, P. (2004) "Influence of pre-treatment for deashing of sugarcane bagasse on pyrolysis products". *Biomass and Bio-energy* 27: 445–457
22. De Jongh, W. A. (2001) "Possible applications for vacuum pyrolysis in the processing of waste materials". M.Sc. Thesis, Department of process Engineering, Stellenbosch, South Africa

23. Devnarain, P.; Arnold, D.; Davis, S. (2002) "Production of activated carbon from South African sugarcane bagasse". *Proc S Afr. Sug. Technol. Ass.* 76: 477 - 489

24. Dieblod J.P. (1999) "A review of the chemical and physical mechanisms of the storage stability of fast pyrolysis bio-oils." http://www.p2pays.org/ref/19/18946.pdf , May 2010

25. Dummmond, A.F.; Drommond, I.W. (1996) "Pyrolysis of Sugar Cane Bagasse in as Wire-Mesh Reactor" *Ind. Eng. Chem. Res.* 1263-1268

26. Erlich, C.; Bjornbom, E.; Bolado, D.; Giner, M.; Fransson, T. H. (2006) "Pyrolysis and gasification of pellets from sugar cane bagasse and wood". *Fuel* 85: 1535–1540

27. Garcia-Perez, M.; Chaala, A.; Wang, Y.; Roy, C. (2000) "Co-pyrolysis of sugar cane bagasse with petroleum residue. Part one thermogravimetric analysis". *Fuel* 80: 1245 -1259

28. Garcia-Perez, M.; Chaala, A.; Wang, Y.; Roy, C. (2002) "Co-pyrolysis of sugar cane bagasse with petroleum residue. Part 2: product yield and properties". *Journal of analytical and applied pyrolysis* 65: 111- 135

29. Garcia-Perez, M.; Chaala, A.; Roy, C.; (2002); "Vacuum pyrolysis of sugarcane bagasse". *Fuel* 81: 893-907

30. Gerdes, C.; Simon, C.; Ollesch, T.; Meier, D.; Kaminsky, W. (2002) 'Design, construction and operation of a fast pyrolysis plant for biomass'. *Engineering life science* 2: 167-174

31. Goyal. H.B.; Seal. D.; Saxena, R.C.; (2008); "Bio-fuels from thermo-chemical conversion of renewable resources: A review". *Renewable and Sustainable Energy Reviews* 12: 504–517

32. Henrich, E. (2007) "The status of the FZK concept of biomass gasification". Summer School, University of Warsaw: hppt/www.baumgroup.de/Renew/download/5 - Henrich - paper.pdf

33. Honsbein, D. (2007) "Feasibility of pyrolysis oil production in Namibia". Report based on PhD thesis, Ashton University

34. Horne, P.A.; Williams, P.T. (1996) " Influence of temperature on the products from flash pyrolysis of biomass" *Fuel* 75, 1051-1059

35. Hu, G.; Fan, H.; Lui, Y (2001) "Experimental studies on pyrolysis of Datong coal with solid heat carrier in a fixed bed". *Fuel Processing Technology* 69 (3): 221-228

36. Ikura, M.; Stanciulescu, M.; and Hogan, E. (2003) 'Emulsification of pyrolysis derived bio-oil in diesel fuel'. *Biomass and Bioenergy* 24: 221 – 232

37. Karaosmanoglu, F.; Tetik, E.; Gollu, E. (1999) "Bio-fuel production using slow pyrolysis of the straw and stalk of the rapeseed plant". *Fuel Processing Technology* 59: 1-12

38. Katyal. S.; Thambimuthu, K.; Valix, M. (2002) "Carbonisation of bagasse in a fixed bed reactor: Influence of process variables on char yield and characteristics". *Renewable Energy* 28: 713–725

39. Kersten, S.; Wang, X.; Prins, W.; Swaaji W. (2005) 'Biomass Pyrolysis in a fluidized bed reactor. Part1: Literature review and model simulations' *Ind. Eng. Chem. Res.* 44: 8773-8785

40. Lange, S. (2007) "Systemanalytische untersuch zur Schellpirolyse"; Doctorial thesis at Karlsruhe University, Germany.

41. Lehmann, J. (2002) "Slash and char: A feasible alternative for soil fertility management in the central Amazon?" *17'th World congress of soil science*, Bangkok, Thailand, Parper no. 449: 1-12

42. Lua, A.C.; Yang, T. (2005) "Characteristics of activated carbon prepared from pistachio-nut shell by zinc chloride activation under nitrogen and vacuum conditions" *Journal of Colloid and Interface Science* 290: 505-513

43. Luo, Z.; Wang, S.; Liao, Y.; Zhou, J.; Gu, Y.; Cen, K. (2004) "Research on biomass fast pyrolysis for liquid fuel". *Biomass and Bioenergy* 26: 455 – 462

44. Mesa-Perez, J.M.; Cortez., A.; Rocha, J.D.; Brossard-Perez, L.E.; Olivares-Gomez, E. (2005) "Unidimensional heat transfer analysis of elephant grass and sugar cane bagasse slow pyrolysis in a fixed bed reactor". *Fuel Processing Technology* 86: 565– 575

45. Mohan, D.; Pittman, C.U.; Steele, P.H.(2006) "Pyrolysis of Wood/Biomass for Bio-oil: A Critical review". *Energy & Fuels* 20: 848-889

46. Nassar, M.M.; Ashour, E.A.; Wahid, S.S. (1996) "Thermal characteristics of bagasse", *Journal of applied polymer science* 61: 885-890

47. Norris, G. (2007) "Biomass waste to electricity: KwaZulu-Natal". *USB Leaders' lab*, 8 -11

48. Oasmaa, A.; Czernik, S. (1999) " Fuel oil quality of biomass pyrolysis oils – state of the art for the end users" *Energy fuels* 13, 914-921

49. Pach M.; Zanzi R.; Björnbom, E. (2002) "Torrefied Biomass a Substitute for Wood and Charcoal". *6th Asia-Pacific International Symposium on Combustion and Energy Utilization*; www.techtp.com

50. Pippo, A. W.; Garzone P.; Conrnacchia G. (2007) "Agro-industry sugarcane residues disposal: The trends of their conversion into energy carriers in Cuba" *Waste Management* 27: 869–885

51. Pollard, S.J.T.; Fowler, G.D.; Sollars, C.G.; Perry, R. (1992) "Low const adsorbands for waste and water treatment: a review." *Science Total Enviroment* 116: 31-52

52. Qi, Z.; Jie, C.; Tiejun, W.; Ying, X. (2007) "Review of biomass pyrolysis oil properties and upgrading research". *Energy Conversion and Management* 48: 87–92

53. Rabe, R. C.; Knoetze J. H. (2005) "A model for vacuum pyrolysis of bagasse" Msc Thesis, Stellenbosch

54. Rasul, M. G.; Rudoph, V. Carsky M. (1999) "Physical properties of bagasse". *Fuel* 78: 905-910

55. Raveendran, K.; Ganesh A.; Khilar, K.C. (1995) "Influence of mineral matter on biomass pyrolysis characteristics". *Fuel* 74: 1812–1822.

56. Reina, J.; Velo, E.; Puigjaner, L. (1998) " Kinetic study of the pyrolysis of waste wood" *Industrial and Engineering Chemitry research* 37: 4290-4295

57. Rhodes, M. (2005) 'An Introduction to particle technology'*Wiley*

58. Roy, C, De Caumia, B., Plante, P. (1990) "The role of extractives during vacuum pyrolysis of wood". *Journal of applied Polymer Science* 41: 337 – 348

59. Scott, D.; Priskorz, J. (1984) "Continuous flash pyrolysis of biomass". *Canadian Journal of Chemical Eng*. 62: 404.

60. Scott, D.; Priskorz, J. (1982) " Flash pyrolysis of Aspen-Polar wood". *Canadian Journal of Chemical Eng*. 60: 666.

61. Scott, D.S.; Majerski, P.; Piskorz, J.; Radlein, D. (1999) "A second look at fast pyrolysis of biomass: the RTI process" *J. of anal. and appl. Pyrolysis* 51: 23-37

62. Shihadeh, A.; Hochgreb, S. (2000) "Diesel engine combustion of biomass pyrolysis oils" Energy fuels 14: 260-274

63. Sipile, K.; Kuoppala, E.; Fagernas, L.; Oasmaa, A. (1998) "Characterization of biomass-based flash pyrolysis oils" *Biomass and Bio-energy* 14 (2): 103 -113

64. Stubington, J.F.; Aiman, S. (1994) " Pyrolysis kinetics of bagasse at high heating rates" *Energy and Fuels* 8: 194-203

65. Stubington, J.F.; Aiman, S. (1993) " Pyrolysis kinetics of bagasse at low heating rates" *Biomass and Bio-energy* 5: 113-120

66. Sugar Conference (2001) "Fast pyrolysis of bagasse to produce bio-oil fuel for power generation" http://www.biooil.ru/docs/2001SugarConferencePaper.pdf

67. Tsai, W.T.; Lee, M.K.; Chang, Y.M. (2006) "Fast pyrolysis of rice straw, sugarcane bagasse and coconut shell in an induction-heating reactor". *Journal of Analytical and Applied Pyrolysis* 76: 230–237

68. Turn S. Q. (2002) "Analysis of Hawaii Biomass Energy Resources for Distributed Energy Applications". http://hawaii.gov/dbedt/info/energy/publications/biomass-der.pdf

69. Van de Velden, M.; Baeyens, J.; Brems, A.; Janssens, B.; Dewil, Raf. (2010) "Fundamentals, Kinetics and endothermicity of biomass pyrolysis reaction" *Renewable energy* 35: 232-242

70. Varhegyi G.; Antal, M.J.; Szekely, T.; and Szabo, P. (1989) "Kinetics of the thermal decomposition of cellulose, hemicellulose, and sugarcane bagasse," *Energy & Fuels* 3: 329-335.

71. Westerhof, R.; Kuipers, N.; Kersten, S.; Swaaij, W. (2007) "Controlling the water content of biomass fast pyrolysis oil" *Ind. Eng. Chem. Res. 46*: 9238-9247

72. www.dynamotive.com, (May 2010)

73. www.eprida.com, (May 2010)

74. www.oil-price.net, (May 2010)

75. www.prosugar.com.au, (April 2010)

76. www.sasa.org.za , (November 2009), South African Sugar Industry Directory, 2007-2008.

77. www.smri.org, (October 2009)

78. Yaman, S. (2004) "Pyrolysis of biomass to produce fuels and chemical feedstocks". *Energy Conversion and Management* 45: 651–671

79. Yanik, J., Konmayer C., Saglam, M., Yuksel M., (2007) "Fast pyrolysis of agricultural wastes: Characterization of pyrolysis products" *Fuels processing tech*. 88: 942 – 947

80. Zandersons, J.; Gravitis, J.; Kokorevics, A.; Zhurinsh, A.; Bikovens, O.; Tardenaka, A.; and Spice, B.(1999) "Studies of the Brazilian sugarcane bagasse carbonisation process and products properties" *Biomass and Bioenergy* 17: 209 – 219

10.2   References for chapter 3

1. Asadullah, M.; Rahman, M. A.; Ali, M.; Rahman, M.S,; Motin, M.A.; and Sultan, M. (2007) "Production of bio-oil from fixed bed pyrolysis of bagasse". *Fuel* 86: 5214 -2520

2. Bedmutha R.J.; Ferrante L.; Briens C.; Berruti F.; and Inculet I. (2009) "Single and two stage electrostatic demisters for biomass pyrolysis application". *Che. Eng. And Processing* 48: 1112-1120

3. Bridgwater, A.V.; Meier, D.; and Radlein, D.; (1999); "An overview of fast pyrolysis of biomass." [*Org. Geochemistry* 30: 1479-1493

4. Coulson and Richardson's chemical engineering, 4th edition, (2005), *Elsevier*.

5. Cui, H.P.; Grace, J.R. (2007) "Fluidization of biomass particles: A review of experimental multiflow aspects" *Chem Eng Sci* 62: 45-55

6. Gerdes, C.; Simon, C.; Ollesch, T.; Meier, D.; Kaminsky, W. (2002) 'Design, construction and operation of a fast pyrolysis plant for biomass'. *Engineering life science* 2: 167-174

7. Horne, P.A.; Williams, P.T. (1996) " Influence of temperature on the products from flash pyrolysis of biomass" *Fuel* 75: 1051-1059

8. Luo, Z.;Wang, S.;Liao, Y.; Zhou, J.; Gu, Y.; and Cen, K. (2004) "Research on biomass fast pyrolysis for liquid fuel" *Biomass and Bioenergy* 26: 455-462

9. Parker, K. (2003) 'Electrical operation of electrostatic precipitators'. *The Institution of Engineering and Technology*

10. Personal communication (2009): Bridgwater, A.V.; Aston University, Chemical Engineering and Applied Chemistry Department

11. Personal communication (2008): Stahl. R; FZK department ITC-CPV

12. Radlein, D.; Piskorz, J.; Scott, D.S. (1991) "Fast pyrolysis of natural polysaccharides as a potential industrial process" *J. Anal. App. Pyrolysis* 19: 41-63

13. Rath, J.; Wolfinger, M.G.; Steiner, G.; Kramer,G.; Barontini, F.; Cazzani, V. (2003) "Heat of wood pyrolysis" *Fuel* 82: 81-91

14. Rhodes, M. (2005) 'An Introduction to particle technology', *Wiley*

15. Rocha, J.; Gomez, E.; Mesa Perez, J.; Cortez, L.; Seye, O.; and Brossard Gonzalez, L. (2002) "The demonstration fast pyrolysis plant to biomass conversion in brazil" *WREC*

16. Westerhof, R.; Kuipers, N.; Kersten, S.; Swaaij, W. (2007) "Controlling the water content of biomass fast pyrolysis oil" *Ind. Eng. Chem. Res*. 46: 9238-9247

17. www.engineeringtoolbox.com, (March 2010)

18. www.exxonmobil.com, (May 2010)

19. Yanik, J.; Konmayer C.; Saglam, M.; Yuksel M. (2007) "Fast pyrolysis of agricultural wastes: Characterization of pyrolysis products" *Fuels processing tech*. 88: 942 – 947

20. Fogler, H.S. (2006) "Elements of chemical reaction engineering" *Prentice-hall International, Inc.*

21. Cengel, Y.A. (2003) "Heat transfer a practical approach" Second edition, *McGraw-Hill*

22. Azev, V.S.; Gerasimova, G.N.; Luneva. V.V. (1985) "Formulation of stable mixtures of diesel fuels with methanol", *Chemistry and technology of fuels and oils*, 21: 560-563

10.3   References for chapter 4

1.   A.V. Bridgewater; *Chem. Eng. J*. 91 (2003) 87.
2.   A.E. Putun, E. Onal, B.B. Uzun, N. Ozbay, *Industrial Crops and Products* 26 (2007) 307.
3.   O. Onay, O. M. Kockar, *Biomass and Bioenergy* 26 (2004) 289.
4.   O. Onay , O. M. Kockar, *Renewable Energy* 28 (2003) 2417.
5.   O. Ioannidou, A. Zabaniotou, E.V. Antonakou, K.M. Papazisi, A.A. Lappas, C. Athanassiou, *Renewable and Sustainable Energy Reviews* 13 (2009) 750.
6.   J.-G. Li, Y.-T. Fang, Y.-Q. Zhang, C.-Y. Li, Y. Wang, *Ranliao Huaxue Xuebao* 36 (3) (2008) 273.
7.   M. Dall'Ora, P. A. Jensen, A. D. Jensen, *Energy & Fuels* 22 (2008) 2955.
8.   A. Zabaniotoua, O. Ioannidoua, E. Antonakoub, A. Lappasb, *International Journal of hydrogen energy* 33 (2008) 2433.
9.   H. Koca, O. M. Kockar, *Energy Sources*, Part A, 29 (2007) 1457.
10. J.M. Encinar, F.J. Beltrán, A. Bernalte, A. Ramiro, J.F. González, *Biomass and Bioenergy* 11 (1996) 397.
11. A. Demirbas, *Fuel Processing Technology* 88 (2007) 591-597.
12. A.V. Bridgwater, Peacocke G.V.C. *Renewable Sustainable Energy Rev*. 4 (2000) 1.
13. O.M. Kockar, O. Onay, A.E. Putun, E. Putun, *Energy Sources* 22 (2000) 913.
14. A. C. Lua, T. Yang, *Journal of Colloid and Interface Science* 276 (2004) 364.
15. M. Garcia-Perez M., A. Chaala, C. Roy, *Journal of Analytical and Applied Pyrolysis* 65 (2002) 111.
16. D. Mwasiswebe, Unpublished Thesis on the 'Production of activated carbon from south African sugarcane bagasse', University of KwaZulu-Natal, Durban (2005).
17. J. Zandersons, J. Gravitis, A. Kokorevics, A. Zhurinsh, O. Bikovens, A. Tardenaka, B. Spinc, *Biomass and Bioenergy* 17 (1999) 209.
18. J.M. Encinar, J. F. Gonzalez, J. Gonzalez, *Fuel Processing Technology* 68 (2000) 209.
19. M.F. Laresgoiti, B.M. Caballero, I. de Març, A. Torres, M.A. Cabrero, M.J. Chomon, *Journal of Analytical and Applied Pyrolysis* 71 (2004) 917.
20. V. Minkova, M. Razvigorova, E. Bjornbom, R. Zanzi, T. Budinova, N. Petrov, *Fuel Processing Technology* 70 (2001) 53.
21. N. Ozbay, A.E. Putun, B.B. Uzun, E. Putun, *Renewable Energy* 24 (2001) 615.
22. R.F. Probstein, R.E. Hicks, Synthetic Fuels. *McGraw-Hill Book Company*: New York 1982
23. R. Zanzi, K. Sjostrom, E. Bjornbom, *Biomass and Bioenergy* 23 (2002) 357.
24. A.E. Putun, A. Ozcan, H.F. Gercel, E. Putun *Fuel* 80 (2001) 1371.
25. O. Onay, O.M. Kockar, *Biomass Bioenergy* 26 (2004) 289.
26. A. E. Putun, N. Ozbay, E. A. Varol, B.B. Uzun, F. Ates, *Int. J. Energy Res*. 31 (2007) 506.
27. H.B. Goyal, D. Seal, R.C. Saxena, *Renewable and Sustainable Energy Reviews* 12 (2008) 504.
28. S. Katyal, K. Thambimuthu, M. Valix, *Renewable Energy* 28 (2003) 713.
29. A. C. Lua, T. Yang, *Journal of Colloid and Interface Science* 276 (2004) 364.
30. G.Q. Lu, J.C.F. Low, C.Y. Liu, A.C. Lua, *Fuel* 74 (1995) 344.
31.   K. Gergova, S. Eser, *Carbon* 34 (1996) 879.
32. W.T. Tsai, M.K. Lee, Y.M. Chang, *J. Anal. Appl. Pyrolysis* 76 (2006) 230.
33. H. Darmstadt, M. Garcia-Perez, A. Chaala, N.-Z. Cao, C. Roy, *Carbon* 39 (2001) 815.
34. N.H. Hassan, S.A. Saad, K.N. Ismail, S.A. Ong, N. Ibrahim, R. Santiago, International Conference on Environmental Research and Technology (ICERT 2008).
35. S.A. Channiwala, P.P. Parikh, *Fuel* 81 (2002) 1051-1063.

36. P.B. Devnarain, D.R. Arnold, S.B. Davis, Proc. S. *Afr. Sugar Technol. Ass*. 2002.

37. G.Q. Lu, D.D. Do, *Fuel Process Technol*. 28 (1991) 35.

38. R.C. Bansal, J.B. Donnet, F. Stoeckli, *Active Carbon, Marcel Dekker Inc*, New York, 1988, pp 1-27 (Chapter 1).

39. R. J. Evans, C. C. Elam, M. Looker, M. Nimlos, Prepr. *Symp. Am. Chem. Soc. Div. Fuel Chem*. 44 (1999) 256.

40. E. A. Avallone, T. Baumeister, A. Sadegh, L. S. Marks, Marks' standard handbook for mechanical engineers.

41. P. Ahuja P., S. Kumar S., P. C. Singh, *Chem. Eng. Technol*. 19 (1996) 272.

42. A.V. Bridgwater, G.V.C. Peacocke, *Renewable and Sustainable Energy Reviews* 4 (2000) 1.

10.4 References for chapter 5

1. Department of Minerals and Energy, White Paper on the Renewable Energy Policy of the Republic of South Africa, Department of Minerals and Energy, 2003.

2. A. Faaij, Modern Biomass Conversion Technologies, (n.d.).

3. R. Sims, R. Schock, A. Adebulugbe, I. Fenhann, W. Konstantinaviciute, W. Moomaw, et al., Energy supply. In Climate Change 2007: Mitigation. Contribution of Working Group III to the Fourth Assessment Report of the Intergovernmental Panel on Climate Change [B. Metz, O.R. Davidson, P.R. Bosch, R. Dave, L.A. Meyer (eds)],, (2007).

4. C. Di Blasi, Modeling chemical and physical processes of wood and biomass pyrolysis, Progress in Energy and Combustion Science. 34 (2008) 47-90.

5. E. Biagini, A. Fantei, L. Tognotti, Effect of the heating rate on the devolatilization of biomass residues, Thermochimica Acta. 472 (2008) 55-63.

6. C. Di Blasi, Modeling chemical and physical processes of wood and biomass pyrolysis, Progress in Energy and Combustion Science. 34 (2008) 47-90.

7. E. Biagini, A. Fantei, L. Tognotti, Effect of the heating rate on the devolatilization of biomass residues, Thermochimica Acta. 472 (2008) 55-63.

8. M.E. Brown, Introduction to thermal analysis: techniques and applications, Kluwer Academic Publishers, 2001.

9. A. Zabaniotou, O. Ioannidou, E. Antonakou, A.A. Lappas, Experimental study of pyrolysis for potential energy, hydrogen and carbon material production from lignocellulosic biomass, International Journal of Hydrogen Energy. 33 (2008) 2433-2444.

10. G. Varhegyi, Aims and methods in non-isothermal reaction kinetics, Journal of Analytical and Applied Pyrolysis. 79 (2007) 278-288.

11. J.O. Jaber, S.D. Probert, Non-isothermal thermogravimetry and decomposition kinetics of two Jordanian oil shales under different processing conditions, Fuel Processing Technology. 63 (2000) 57–70.

12. A.K. Burnham, Computational aspects of kinetic analysis Part D: The ICTAC kinetics project–multi-thermal-history model-fitting methods and their relation to isoconversional methods, Thermochimica Acta. 355 (2000) 165–170.

13. S. Vyazovkin, A unified approach to kinetic processing of nonisothermal data, International Journal of Chemical Kinetics. 28 (1996) 95-101.

14. S. Vyazovkin, Model-free kinetics, Journal of Thermal Analysis and Calorimetry. 83 (2006) 45-51.

15. B. Roduit, L. Xia, P. Folly, B. Berger, J. Mathieu, A. Sarbach, et al., The simulation of the thermal behavior of energetic materials based on DSC and HFC signals, Journal of Thermal Analysis and Calorimetry. 93 (2008) 143–152.

16. A. Kemmler, M.E. Brown, M. Maciejewski, S. Vyazovkin, R. Nomen, J. Sempere, et al., Computational aspects of kinetic analysis Part A: The ICTAC kinetics project-data, methods and results, Thermochimica

Acta. 355 (2000) 125-143.

17. M. Maciejewski, Computational aspects of kinetic analysis Part B: The ICTAC Kinetics Project–the decomposition kinetics of calcium carbonate revisited, or some tips on survival in the kinetic minefield, Thermochimica Acta. 355 (2000) 145–154.

18. S. Vyazovkin, Computational aspects of kinetic analysis Part C: The ICTAC Kinetics Project–the light at the end of the tunnel?, Thermochimica Acta. 355 (2000) 155–163.

19. B. Roduit, Computational aspects of kinetic analysis Part E: The ICTAC Kinetics Project–numerical techniques and kinetics of solid state processes, Thermochimica Acta. 355 (2000) 171–180.

20. P. Budrugeac, Differential non-linear isoconversional procedure for evaluating the activation energy of non-isothermal reactions, Journal of Thermal Analysis and Calorimetry. 68 (2002) 131–139.

21. M. Garci`a-Pèrez, A. Chaala, J. Yang, C. Roy, Co-pyrolysis of sugarcane bagasse with petroleum residue. Part I: thermogravimetric analysis, Fuel. 80 (2001) 1245-1258.

22. S. Munir, S. Daood, W. Nimmo, A. Cunliffe, B. Gibbs, Thermal analysis and devolatilization kinetics of cotton stalk, sugar cane bagasse and shea meal under nitrogen and air atmospheres, Bioresource Technology. 100 (2009) 1413-1418.

23. M.M. Nassar, E.A. Ashour, S.S. Wahid, Thermal characteristics of bagasse, Journal of Applied Polymer Science. 61 (1996) 890-885.

24. M. Ahmaruzzaman, D.K. Sharma, Non-isothermal kinetic studies on co-processing of vacuum residue, plastics, coal and petrocrop, Journal Of Analytical And Applied Pyrolysis. 73 (2005) 263-275.

25. S. Aiman, J. Stubington, The pyrolysis kinetics of bagasse at low heating rates, Biomass and Bioenergy. 5 (1993) 113-120.

26. P. Roque-Diaz, C. University, L. Villas, C.V. Zh. Shemet, V.A. Lavrenko, V.A. Khristich, Studies on thermal decomposition and combustion mechanism of bagasse under non-isothermal conditions, Thermochimica Acta. 93 (1985) 349-352.

27. G. Varhegyi, M.J. Antal, T. Szekely, P. Szabo, Kinetics of the thermal decomposition of cellulose, hemicellulose, and sugarcane bagasse, Energy & Fuels. 3 (1989) 329-335.

28. Q. Cao, K. Xie, W. Bao, S. Shen, Pyrolytic behaviour of waste corn cob, Bioresource Technology. 94 (2004) 83-89.

29. O. Ioannidou, A. Zabaniotou, E.V. Antonakou, K.M. Papazisi, A.A. Lappas, C. Athanassiou, Investigating the potential for energy, fuel, materials and chemicals production from corn residues(cobs and stalks) by non-catalytic and catalytic pyrolysis in two reactor configurations, Renewable and Sustainable Energy Reviews. 13 (2009) 750-762.

30. Department of Minerals and Energy, White Paper on the Renewable Energy Policy of the Republic of South Africa, Department of Minerals and Energy, 2003.

31. L. Lynd, H. Von Blottnitz, B. Tait, J. de Boer, I. Pretorius, K. Rumbold, et al., Converting plant biomass to fuels and commodity chemicals in South Africa : a third chapter?, South African Journal of Science. 99 (2003) 499-507.

32. T. Sonobe, N. Worasuwannarak, S. Pipatmanomai, Synergies in co-pyrolysis of Thai lignite and corncob, Fuel Processing Technology. 89 (2008) 1371-1378.

33. A.F. Drummond, I.W. Drummond, Pyrolysis of Sugar Cane Bagasse in a Wire-Mesh Reactor, Industrial and Engineering Chemistry Research. 35 (1996) 1263-1268.

34. M.J. Antal, G. Varhegyi, Cellulose pyrolysis kinetics: the current state of knowledge, Industrial and Engineering Chemistry Research. 34 (1995) 703-717.

35. M.E. Brown, Introduction to thermal analysis: techniques and applications, Kluwer Academic Publishers, 2001.

36. S. Vyazovkin, Model-free kinetics, Journal of Thermal Analysis and Calorimetry. 83 (2006) 45-51.

37. J.Guo,A.C.Lua, Kinetic study on pyrolysis of extracted oil palmfiber; isothermal and non-isothermal conditions, Journal of Thermal Analysis and Calorimetry. 59 (2000) 763-774.

38. A.W. Coats, J.P. Redfern, Kinetic parameters from thermogravimetric data. II., Journal of Polymer Science

Part B: Polymer Letters. 3 (1965) 917-920.

39. E.S. Freeman, B. Carroll, The application of thermoanalytical techniques to reaction kinetics: the thermogravimetric evaluation of the kinetics of the decomposition of calcium oxalate monohydrate, J. Phys. Chem. 62 (1958) 394-397.

40. M.S. Duvvuri, S.P. Muhlenkamp, K.Z. Iqbal, J.R. Welker, Pyrolysis of natural fuels, Journal of Fire & Flammability. 6 (1975) 468-477.

41. B. Ramajo-Escalera, A. Espina, J.R. García, J.H. Sosa-Arnao, S.A. Nebra, Model-free kinetics applied to sugarcane bagasse combustion, Thermochimica Acta. 448 (2006) 111-116.

42. S. Vyazovkin, A unified approach to kinetic processing of nonisothermal data, International Journal of Chemical Kinetics. 28 (1996) 95-101.

43. H.L. Friedman, Kinetics of thermal degradation of char-forming plastics from thermogravimetry. Application to a phenolic plastic, in: Wiley Subscription Services, Inc., A Wiley Company New York, 1964.

44. G. Varhegyi, Aims and methods in non-isothermal reaction kinetics, Journal of Analytical and Applied Pyrolysis. 79 (2007) 278-288.

45. J.A. Caballero, J.A. Conesa, Mathematical considerations for nonisothermal kinetics in thermal decomposition, Journal of Analytical and Applied Pyrolysis. 73 (2005) 85-100.

46. A. Savitzky, M. Golay, Smoothing and simplified least squares procedures, Analytical Chemistry. 36 (1964) 1627-1639.

47. P. Roque-Diaz, C. University, L. Villas, C.V. Zh. Shemet, V.A. Lavrenko, V.A. Khristich, Studies on thermal decomposition and combustion mechanism of bagasse under non-isothermal conditions, Thermochimica Acta. 93 (1985) 349-352.

48. A. Kumar, L. Wang, Y.A. Dzenis, D.D. Jones, M.A. Hanna, Thermogravimetric characterization of corn stover as gasification and pyrolysis feedstock, Biomass and Bioenergy. 32 (2008) 460-467.

49. O. Ioannidou, A. Zabaniotou, E.V. Antonakou, K.M. Papazisi, A.A. Lappas, C. Athanassiou, Investigating the potential for energy, fuel, materials and chemicals production from corn residues(cobs and stalks) by non-catalytic and catalytic pyrolysis in two reactor configurations, Renewable and Sustainable Energy Reviews. 13 (2009) 750-762.

50. K.G. Mansaray, A.E. Ghaly, Determination of kinetic parameters of rice husks in oxygen using thermogravimetric analysis, Biomass and Bioenergy. 17 (1999) 19-31.

51. E. Biagini, F. Barontini, L. Tognotti, Devolatilization of Biomass Fuels and Biomass Components Studied by TG/FTIR Technique, Industrial & Engineering Chemistry Research. 45 (2006) 4486-4493.

52. T. Sonobe, N. Worasuwannarak, S. Pipatmanomai, Synergies in co-pyrolysis of Thai lignite and corncob, Fuel Processing Technology. 89 (2008) 1371-1378.

53. E. Biagini, F. Barontini, L. Tognotti, Devolatilization of Biomass Fuels and Biomass Components Studied by TG/FTIR Technique, Industrial & Engineering Chemistry Research. 45 (2006) 4486-4493.

54. G. Varhegyi, M.J. Antal, T. Szekely, P. Szabo, Kinetics of the thermal decomposition of cellulose, hemicellulose, and sugarcane bagasse, Energy & Fuels. 3 (1989) 329-335.

55. P. Luangkiattikhun, C. Tangsathitkulchai, M. Tangsathitkulchai, Non-isothermal thermogravimetric analysis of oil-palm solid wastes, Bioresource Technology. 99 (2008) 986-997.

56. J.A. Caballero, J.A. Conesa, R. Font, A. Marcilla, Pyrolysis kinetics of almond shells and olive stones considering their organic fractions, Journal of Analytical and Applied Pyrolysis. 42 (1997) 159-175.

57. M.J. Antal, G. Varhegyi, Cellulose Pyrolysis Kinetics: The Current State of Knowledge, Industrial and Engineering Chemistry Research. 34 (1995) 703-717.

58. M.J. Antal, G. Varhegyi, Cellulose pyrolysis kinetics: the current state of knowledge, Industrial and Engineering Chemistry Research. 34 (1995) 703-717.

59. A. Kumar, L. Wang, Y.A. Dzenis, D.D. Jones, M.A. Hanna, Thermogravimetric characterization of corn stover as gasification and pyrolysis feedstock, Biomass and Bioenergy. 32 (2008) 460-467.

60. H. Haykiri-Acma, S. Yaman, Slow-Pyrolysis and -Oxidation of Different Biomass Fuel Samples, Journal of Environmental Science and Health, Part A: Toxic/Hazardous Substances and Environmental Engineering. 41

(2006) 1909.

61. M. Garci`a-Pèrez, A. Chaala, J. Yang, C. Roy, Co-pyrolysis of sugarcane bagasse with petroleum residue. Part I: thermogravimetric analysis, Fuel. 80 (2001) 1245-1258.

62. G.L. Guo, D.C. Hsu, W.H. Chen, W.H. Chen, W.S. Hwang, Characterization of enzymatic saccharification for acid-pretreated lignocellulosic materials with different lignin composition, Enzyme and Microbial Technology. 45 (2009) 80–87.

63. G. Garrote, E. Falqué, H. Domínguez, J.C. Parajó, Autohydrolysis of agricultural residues: Study of reaction byproducts, Bioresource Technology. 98 (2007) 1951-1957.

64. F. Shafizadeh, Introduction to pyrolysis of biomass, 1982.

65. W. de Jong, Nitrogen compounds in pressurised fluidised bed gasification of biomass and fossil fuels, PhD, Technische Universiteit Delft, 2005.

66. G.R. Ponder, G.N. Richards, Thermal synthesis and pyrolysis of a xylan, Carbohydrate Research. 218 (1991) 143-155.

67. Z. Gao, I. Amasaki, T. Kaneko, M. Nakada, Calculation of activation energy from fraction of bonds broken for thermal degradation of polyethylene, Polymer Degradation and Stability. 81 (2003) 125–130.

68. F. Jianfen, X. Heming, Theoretical study on pyrolysis and sensitivity of energetic compounds.(2) Nitro derivatives of benzene, Journal of Molecular Structure: THEOCHEM. 365 (1996) 225–229.

69. T. Hosoya, H. Kawamoto, S. Saka, Cellulose-hemicellulose and cellulose-lignin interactions in wood pyrolysis at gasification temperature, Journal of Analytical and Applied Pyrolysis. 80 (2007) 118–125.

70. G. Varhegyi, M.J. Antal, E. Jakab, P. Szabó, Kinetic modeling of biomass pyrolysis, Journal of Analytical and Applied Pyrolysis. 42 (1997) 73-87.

10.5 References for chapter 6

1. Asadullah M.; Rahman, M. A.; Ali, M.; Rahman, M.S.; Motin, M.A. (2007) "Production of bio-oil from fixed bed pyrolysis of bagasse". *Fuel* 86: 2514–2520

2. Bridgwater, A.V. (1996) "Production of high grade fuels and chemicals fro, catalytic pyrolysis of biomass", *Catalysis today*: 285-295

3. Bridgwater, A.V.; Meier, D.; Radlein, D. (1999) "An overview of fast pyrolysis of biomass." *Organic Geochemistry* 30: 1479 – 1493

4. Carrier, M.; Hugo, T.J.; Knoetze, J.H.; Gorgens, J.F. (2010) "Comparison of slow and vacuum pyrolysis of sugarcane bagasse" Submitted: *Journal of analytical and applied pyrolysis*

5. Channiwala, S.A.; Parikh, P.P. (2002) 'A unified correlation for estimating HHV of solid, liquid and gaseous fuels'. *Fuel* 81: 1051-1063

6. Das, P.; Ganesh, A.; Wangikar, P. (2004) "Influence of pre-treatment for deashing of sugarcane bagasse on pyrolysis products". *Biomass and Bio-energy* 27: 445–457

7. Dummmond, A.F.; Drommond, I.W. (1996) "Pyrolysis of Sugar Cane Bagasse in as Wire-Mesh Reactor" *Ind. Eng. Chem. Res*. 1263-1268

8. Gerdes, C.; Simon, C.; Ollesch, T.; Meier, D.; Kaminsky, W. (2002) 'Design, construction and operation of a fast pyrolysis plant for biomass'. *Engineering life science* 2: 167-174

9. Goyal. H.B.; Seal. D.; Saxena, R.C. (2008) "Bio-fuels from thermo-chemical conversion of renewable resources: A review". *Renewable and Sustainable Energy Reviews* 12: 504–517

10. Horne, P.A.; Williams, P.T. (1996) " Influence of temperature on the products from flash pyrolysis of biomass" *Fuel* 75: 1051-1059

11. Jia, O.; Lua, A. C. (2008) "Effects of pyrolysis conditions on the physical characteristics of oil-palm-shell activated carbons used in aqueous phase phenol adsorption" *J. Anal. Appl. Pyrolysis* 83: 175-179

12. Lange, S. (2007) "Systemanalytische untersuch zur Schellpirolyse"; Doctorial thesis at Karlsruhe University

13. Lua, A.C.; Yang, T. (2005) "Characteristics of activated carbon prepared from pistachio-nut shell by zinc chloride activation under nitrogen and vacuum conditions" *Journal of Colloid and Interface Science* 290: 505-513

14. Luo, Z.; Wang, S.; Liao, Y.; Zhou, J.; Gu, Y.; Cen, K. (2004) "Research on biomass fast pyrolysis for liquid fuel". *Biomass and Bioenergy* 26: 455 – 462

15. Mohan, D.; Pittman, C.U.; Steele, P.H. (2006) "Pyrolysis of Wood/Biomass for Bio-oil: A Critical review". *Energy & Fuels* 20: 848-889

16. Mullen, C.A.; Boateng, A.A.; Goldberg, N.M.; Lima, I.M.; Laird, D.A.; Hicks, K.B. (2010) "Bio-oil and bio-char production from corn cobs and stover by fast pyrolysis" *Biomass and Bio-energy* 34: 67-74

17. Raveendran, K.; Ganesh A.; Khilar, K.C. (1995) "Influence of mineral matter on biomass pyrolysis characteristics". *Fuel* 74: 1812–1822.

18. Scott, D.S.; Majerski, P.; Piskorz, J.; Radlein, D. (1999) "A second look at fast pyrolysis of biomass: the RTI process" *J. of anal. and appl. Pyrolysis* 51: 23-37

19. Tsai, W.T.; Lee, M.K.; Chang, Y.M. (2006) "Fast pyrolysis of rice straw, sugarcane bagasse and coconut shell in an induction-heating reactor". *Journal of Analytical and Applied Pyrolysis* 76: 230–237

20. Ullmann; (2002), "Gas production: Ullmann's Encyclopaedia of industrial chemistry" *Wiley*-VCH-verlag

21. Westerhof, R.; Kuipers, N.; Kersten, S.; Swaaij, W. (2007) "Controlling the water content of biomass fast pyrolysis oil" *Ind. Eng. Chem. Res*. 46: 9238-9247

22. Yanik, J.; Konmayer C.; Saglam, M.; and Yuksel M. (2007) "Fast pyrolysis of agricultural wastes: Characterization of pyrolysis products" *Fuels processing tech*. 88: 942 – 947

10.6 References for chapter 7

1. Carrier, M.; Hugo, T.J.; Knoetze, J.H.; Gorgens, J.F. (2010) "Comparison of slow and vacuum pyrolysis of sugarcane bagasse" Submitted: *Journal of analytical and applied pyrolysis*

2. Bridgewater, A.V. (1996) "Production of high grade fuels and chemicals from catalytic pyrolysis of biomass"; *Catalysis Today* 29: 285-295

3. Bridgwater, A.V.; Toft, A.J.; Brammer, J.G. (2002) "A techno-economic comparison of power production by biomass fast pyrolysis with gasification and combustion". *Renewable and Sustainable Energy Reviews* 6: 181–248

4. Honsbein, D. (2007) "Feasibility of pyrolysis oil production in Namibia". Report based on PhD thesis, Ashton University

5. Katyal. S.; Thambimuthu, K.; Valix, M. (2002) "Carbonisation of bagasse in a fixed bed reactor: Influence of process variables on char yield and characteristics". *Renewable Energy* 28: 713–725

6. Bahng, M.; Mukarake, C.; Ribichaud, D.J.; Nimlos, M.R. (2009) "Current technologies for analysis of biomass thermochemical processing: A review". *Analyitca Chimica Acta* 651: 117-138

7. Putun, A.E.; Onal, E.; Uzun, B.B.; Ozbay, N. (2007) *Industrial Crops and Products* 26: 307.

10.7 Bibliography

1. Fogler, H.S. (2006) "Elements of chemical reaction engineering" *Prentice-hall International, Inc.*

2. Cengel, Y.A. (2003) "Heat transfer a practical approach" Second edition, *McGraw-Hill*

3. Rhodes, M. (2005) 'An Introduction to particle technology', *Wiley*

4. Parker, K. (2003) 'Electrical operation of electrostatic precipitators'. *The Institution of Engineering and Technology*

5. Coulson and Richardson's chemical engineering, 4th edition, (2005), *Elsevier*.

11 Appendix

11.1 Practical experience at FZK

During the last term of 2008 a scientific visit to FZK was undertaken. The hosting department, Institute for Technical Chemistry Division of Chemical-Physical Processing (ITC-CPV), specializes in the field of FP. The work done forms part of this master's project on the pyrolysis of bagasse. The benefits of the scientific visit were:

- learning from their experience in the design of lab scale pyrolysis plants ;
- conducting experimental work on their fluidized bed FP setup;
- conducting experimental work on their twin screw FP reactor;
- learning from scientists whom have extensive experience in the field of pyrolysis; and
- establishing ties between SA and Germany which may also allow for future exchanges between the SU and FZK.

Experimental work was done on a lab-scale FP unit (100g/h), as well as a FP Process Demonstration Unit (PDU) (10 kg/h). The small scale unit is the unit discussed in chapter 3.2 from Yanik *et al.* (2007). The operation of this equipment reveals specific challenges with FP with regards to biomass and equipment type. This insight into the design will significantly enhance the quality of construction and operation of a lab scale FPU at SU. Sugarcane bagasse (SB) was characterized for elemental composition; water content; ash content; energy value; and particle size distribution all of which is vital for experimental comparison. A significant amount of time and effort was saved by doing these experiments at an institute with fully functional equipment and enough resources. The thermal decomposition of SB was studied with the thermogravimetric equipment at FZK. The results of the thermal decomposition of bagasse will be published in a joint article, with A. Aboyade (Chapter 5). This article addresses the kinetics of the devolatilization behaviour of SB and corn cobs. By undertaking this scientific visit to FZK important international ties were established. A three year biofuel research exchange program between FZK and SU has been set up.

11.2 Appendix for chapter 3

This appendix is used clarify certain calculations, commissioning tests, general operational procedures and reasoning related to the design and operation of the fast pyrolysis unit. Appendix 11.2 should be read in conjunction with chapter 3.

11.2.1 *Thermodynamic properties for the energy balance*

The enthalpy of evaporation and specific heat capacity for water and nitrogen were obtained from Cengel (2003) and. The specific heat capacity of biomass vary 1.1 - 1.2 kJ/kg.K at 500°C (Van de Velden *et al.*, 2010). Bio-oil was assumed similar to diesel because no specific thermodynamic properties could be obtained (Azev et al, 1985). Bio-gas consists of approximately 90 vol% CO and CO_2 (Mullen *et al.*, 2010). The bio-gas specific heat capacity was estimated from CO and CO_2 be close to 1 kJ/kg.K (www.engineeringtoolbox.com, 2009). To account for variation and increase the robustness of the design the value was slightly increased to 1.5 kJ/kg.K. Average Cp values were used over the temperature range 25 – 500°C.

11.2.2 *Calculation of gas density*

Table 58 lists the constants for the calculation of the gas density by using the ideal gas law (Equation 12). Figure 48 shows the effect of temperature on the gas density.

Table 58: Constants for gas density calculation

Calculating gas density		
Pressure	1.2	bar
Gas constant [R]	8.314	kJ/kmol.K
Molar mass N_2	28.0134	kg/kmol
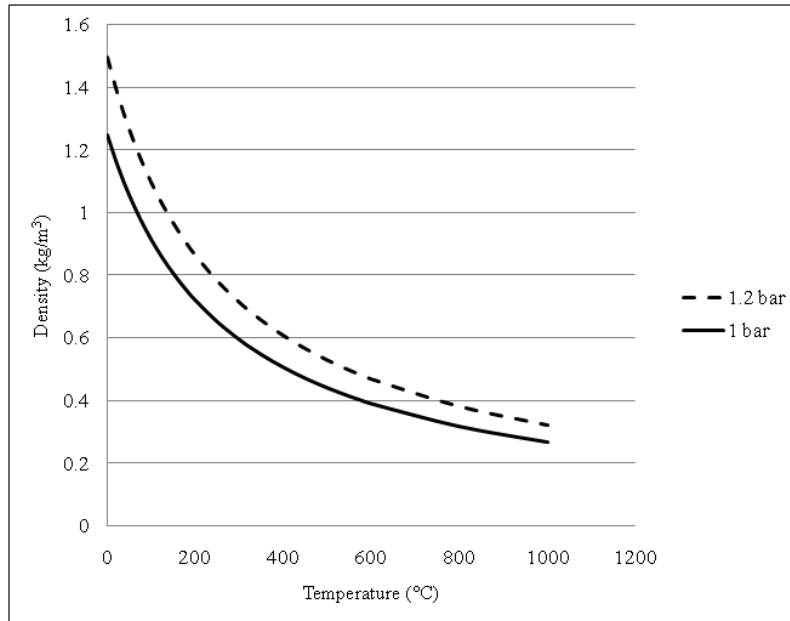
Figure 48: The density of nitrogen as a function of temperature.

11.2.3 Calculations of sphericity

Table 59: Calculation of sphericity (for two different cases)

D (mm)	L (mm)	Area (mm^2)	Volume (mm^3)	D_{sphere} (mm)	A_{sphere} (mm^2)	Sphericity
0.5	2	4.38	0.39	0.91	2.59	0.59
0.2	2	1.45	0.06	0.49	0.76	0.53

11.2.4 _Calculations for the fluidized bed reactor_

Table 60: Variables and properties for fluidization calculations

Variable/ property	Value	Unit	Reference
Reactor diameter	0.075	m	
Average gas flow rate	6	m^3/h	3 Nm^3/h with gas density 0.5 kg/m^3 at 500°C and 1.1 bar
	0.002	m^3/s	
Area	0.004	m^2	Calculated
Average velocity	0.377	m/s	
Density gas	0.5	kg/m^3	Cengel, 2003
Fluid viscosity	3.45E-05	kg/ms	
Sand density	2650	kg/m^3	Estimated from sand bulk density of 1700 (suppliers) with voidage of 0.35
Biomass density	200	kg/m^3	Cengel, 2003
Biomass shericity	0.55		Calculated
Bed voidage at incipient fluidization	0.45		Rhodes, 2005

Table 61: Calculation of minimum fluidization velocity: the RHS and LHS refer to the Right and Left Hand Side of Equation 7. Excel function 'Solver' was used to minimize the difference.

	x_p (mm)	x_{sv} (m)	RHS	LHS	Difference	Re_{mf}	U_{mf} (m/s)
	3.0	0.0017	3691	3691	0.001	3.775	0.158
Biomass	2.0	0.0011	1094	1094	0.001	1.179	0.074
	1.0	0.0006	137	137	0.001	0.151	0.019
	0.6	0.0006	2357	2357	0.001	2.474	0.285
Sand	0.5	0.0005	1364	1364	0.001	1.461	0.202
	0.4	0.0004	698	698	0.001	0.759	0.131

Table 62: Calculation of transport particle velocity: the RHS and LHS refer to the Right and Left Hand Side of Equation 11. Excel function 'Solver' was used to minimize the difference.

	Ar	U_t (m/s)	x_p (mm)	x_{sv} (m)	RHS	LHS	Difference	n	U_p (m/s)
	3691	8.58	3	0.00165	0.667	0.666	0.001	3.84	0.399
	1094	3.81	2	0.0011	0.539	0.538	0.001	3.96	0.161
Biomass	137	0.95	1	0.00055	0.258	0.257	0.001	4.31	0.031
	2357	15.06	0.6	0.0006	1.252	1.251	0.001	3.47	0.946
	1364	10.46	0.5	0.0005	0.999	0.998	0.001	3.6	0.59
Sand	698	6.69	0.4	0.0004	0.747	0.746	0.001	3.77	0.329
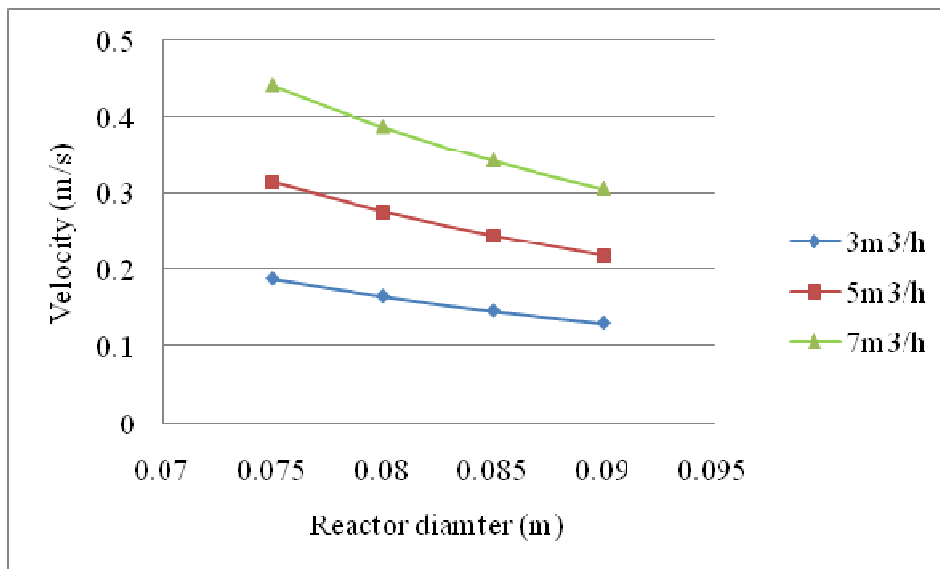
Figure 49: The reduction of velocity due diameter changes inside the reactor shown for different volumetric flow rates at 1bar.

11.2.5 *Calculations for the screw feeder*

Table 63: Variables for the design of the screw

Variable	Value
Biomass density SG (kg/m^3)	100 -200
Flow rate (kg/h)	1 to 2
Percentage filled tube	50 - 100%
Motor RPM	0 - 42
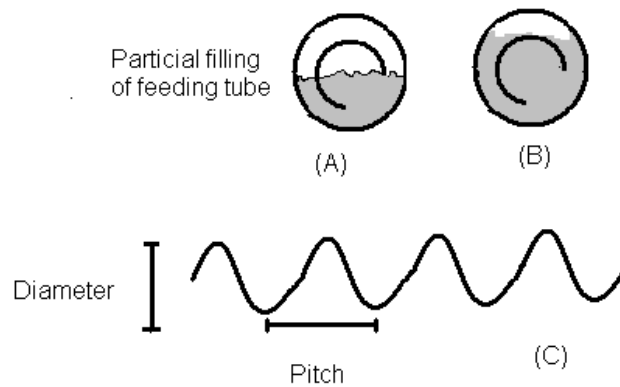
Figure 50: Front view of screw inside tube with different levels of particle filling (A, B) and side view (C) of feeder screw.

11.2.6 *Calculations for feeder heat exchanger*

A 200 mm long double pipe heat exchanger was constructed at the tip of the feeding unit. Baffles are inside to ensure that the water is dispersed throughout the entire pipe section. Water is fed through the bottom and exits at the top. Standard SS316 tube sizes were used for construction. The construction was scaled up from the design of the FZK FP feeding unit. By controlling the water flow rate the temperature of the exit water can be controlled. An energy balance, presented in Table 64, was done to estimate how much energy will be required from this short double pipe heat exchanger to heat the incoming water from 20°C to 40°C.

Table 64: Calculation of heat transfer rate inside pipe

Variable	Value	Units
M(water)	0.05	kg/s
Water Cp	4.18	kJ/kg
Tin	20	°C
Tout	40	°C
Energy per second to raise the temperature of the water from 20 to 40ºC	**4.18**	kW

It is complex to model the exact amount of heat that can be transferred from this short section of double pipe. The model will also be subject to many assumptions. Only the tip of the pipe will be exposed to

162

high temperatures, with a significant temperature decrease along the length of the double pipe. It is safe to say that this pipe will not generate as much heat as a household kettle (2kW). Apart from this, the tap water flow rate can be increased to about double the design value. Therefore the water will be able to provide sufficient cooling.

11.2.7 *Cooling liquid properties*

Table 65: Properties of isopar G (www.exxonmobil.com, 2010)

Properties	Values
Density	750 kg/m³
Flash Point	>40°C
Auto ignition temperature	365°C
Boiling Point / Range	155°C - 179°C
Vapor Pressure	0.195 kPa at 20°C
Solubility in Water	Negligible
Viscosity	1.21 cSt at 40°C
Cp (10°C)	2.013 (kJ/kg°C)
Heat of vaporization (1.2bar/10°C)	1942.2 (kJ/kg)

11.2.8 *Calculation of nozzle surface area*

Table 66: Cooling tower nozzle types

Model name	Spray angle	Spray characteristics	Droplet size (µm)	Flow rate at 3bar (L/min)	Droplet SA (m²) per second
TF6NN	60°	Fine atomization	500	5.5	1.1
PJ40	90°	Mist	50	1.11	2.2

The flow rate and mean droplet surface area is given on the supplier website (www.bete.com, 2010). Approximating the droplets as spheres, the volume and surface area of each droplet can be calculated (Equation 19). The number of particles per minute is calculated by dividing the total volumetric flow rate (L/min) by the volume of a single droplet. The total surface area is then obtained by multiplying the number of particles by the surface area of a single particle. Finally divide by 60 s to obtain the droplet surface area per second.

$$SA = Surface\_Area\_sphere = \pi D^2$$

$$V = Volume\_sphere = \frac{\pi D^3}{6}$$

$$N = number\_of\_particles = \frac{Q}{V}$$

$$Total\_SA = N \times SA$$

<div align="right">Equation 19</div>

11.2.9 *Calculation for the mean temperature difference in cooling tower*

The temperature correction factor *F* is a function of temperature and the number of tube and shell passes. It was assumed to be equal to 1 for a direct contact heat exchanger.

$$\Delta T_m = F \times \Delta T_{lm} = \left[\frac{\Delta T^{biogas} - \Delta T^{coolant}}{\ln \dfrac{\Delta T^{biogas}}{\Delta T^{coolant}}} \right]$$

where,

$$\Delta T^{biogas} = T_{gas,IN} - T_{coolant,OUT}$$

$$\Delta T^{coolant} = T_{gas,OUT} - T_{coolant,IN}$$

$$F = 1$$

Equation 20: (Coulson and Richardson, 2005).

<div align="center">Table 67: Calculation of mean temperature difference</div>

	IN (°C)	OUT (°C)	ΔT (°C)	ΔTₘ (°C)
Biogas	500	20	480	104
Coolant	5	10	5	

11.2.10 *Operation of chiller cycle*

A schematic drawing of chiller cycle is shown in Figure 51. Cooling water (serves as the heat 'reservoir') (1) enters the condenser side of the chiller (2). At the (evaporator) cooling side the water is circulated by a pump (3) into a water bath (4). Cooling liquid is pumped through a cupper pipe in the water bath allowing the liquid to be cooled and then sprayed into the cooling tower. With pure water as cooling medium the minimum water temperature is 7°C. If colder temperatures are desired the water bath should be filled with a 30% glycol solution. Anti rust and anti bacterial solutions were added to the water bath to maintain high

quality water. The volume of the water bath is 150L. This allows a buffer volume for the chiller so that the compressor does not switch on and off regularly. The tower, liquid vessel, and water bath was insulated with foam insulation.
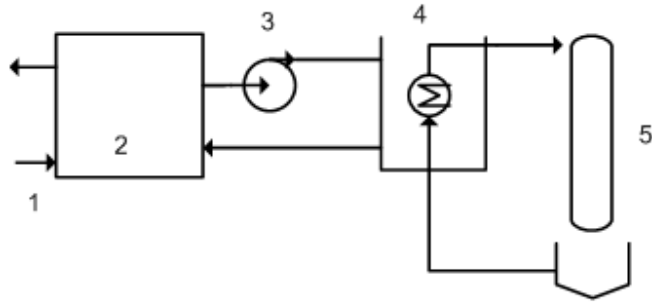
Figure 51: Chiller cycle: (1) Hot side (2) Chiller (3) Pump (4) Water bath (5) Cooling tower

11.2.11 _Component specifications_

Table 68: Specification sheet for biomass feeding (zone 1) and control

Component specification sheet Zone 1			
Control			
Pressure sensors	10 bar		
Thermocouples	Cold temperature	J type	
	Up to 700°C	K type	
Gas flow meter	0 - 15 m^3/h	Burkett	
Feeding system (F02)			
Hopper	Volume	MOC	SS 316
A (base)	12.5L		
B (enlargement section)	25L		
Motor			
Power	0.25kW		
rpm	0 - 42		
Feeding Screw		MOC	
L [mm]	550		SS 316, D=6mm round bar
Screw Coil OD [mm]	33		
Screw Pitch [mm]	33		
Heat Exchanger		MOC	SS 316
Outer pipe OD (ID) [mm]	52 (49)		
Inner pipe OD (ID)[mm]	37 (34)		
Total Size			
L [mm]	1000		
W [mm]	500		
H [mm]	1000		

Table 69 : Component specification sheet for heating section (Zone 2)

Component specification sheet Zone 2			
Oven			
OD (ID)	510 (350)	ments no (current)	
H1(Inner height)	770 (690)	6 @12A	top
H 2(Inner height)	230 (230)	2 @ 6A	middle (extended verstion)
H 3(Inner height)	360 (230)	3 @12A	bottom
H 1&3	1130		normal
H 1&2&3	1360		extended
Power	6.6 kW		
MOC	Refectory brick (1000°C), Fibreglass insulation, Mild steel casing		
Reactor (R04)			
OD	100	MOC	SS316
ID (gas inlet)	56		
ID (reactor)	75		
ID (top)	90		
ID (biomass inlet)	61		
H1	250	Concal top/ gas exit	
H2	230	Middle/ extention section	
H3	400	Conical bottom/ biomass&gas inlet	
Preheater (Q03)			
L	160	MOC	SS316 tube filled with SS316 shavings.
OD (ID)	52		
Cycones (C05&C06)			
L	130	MOC	SS 316
OD	34		
V	2L	Volume char container	
Gas Piping			
OD	19	MOC	SS 316
ID	16		

Table 70: Specification sheet for cooling section (zone 3)

Water chiller		
Brand	Daikin	EWWP104KAW1N
Nominal cooling capacity	13	kW
Nominal input	3.6	kW
Unit Dimensions	600	mm
Height	600	mm
Width	600	mm
Depth		
Minimum Volume in system	62	L
Evaporator: Cooling side flow	19-75	L/min
Condenser: Heating side flow rate	24-95	L/min
Chiller cycle		
Pump	55L/min	
Arcal filter	350 μm	
PVC tube	25mm	
Water bath volume	150L	
Cooling Units		
Tower		MOC
OD (ID)	100 (96)	SS 316
L_{top}	25	Cap with nozzle
L_{mid}	285	Gas inlet section
L_{bottom}	765	Main tower with nozzle points
L_{total}	1140	
Liquid vessel		
V_{liquid}	25L	
$V_{freeboard}$	5L	
$V_{at\ isopar\ take-off\ level}$	8L	
Pump		
Type	Air operated diaphragm pump, (explosion rated)	
Max pressure	5	bar
Flow rate	18	L/min
Electrostatic precipitator		
Voltage	25	kV
Current	0.2	mA
ESP 1		
ID	60	SS 316, teflon, glass
$L_{emitting\ electrode}$		MOC
$L_{collection\ electrode}$	675	
L_{total}	900	
ESP 2		
ID	48	
$L_{emitting\ electrode}$		
$L_{collection\ electrode}$	620	
L_{total}	900	

11.2.12 Component drawings
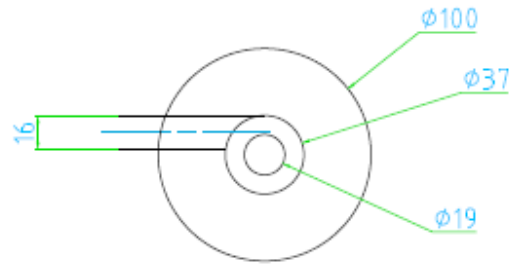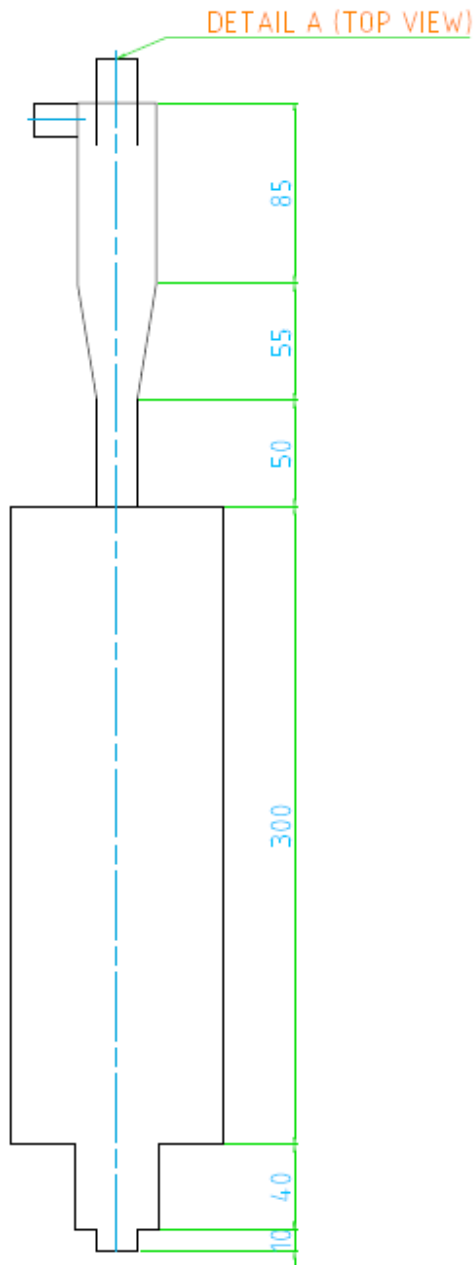
Figure 52: Cyclone and container (C05 and C06)
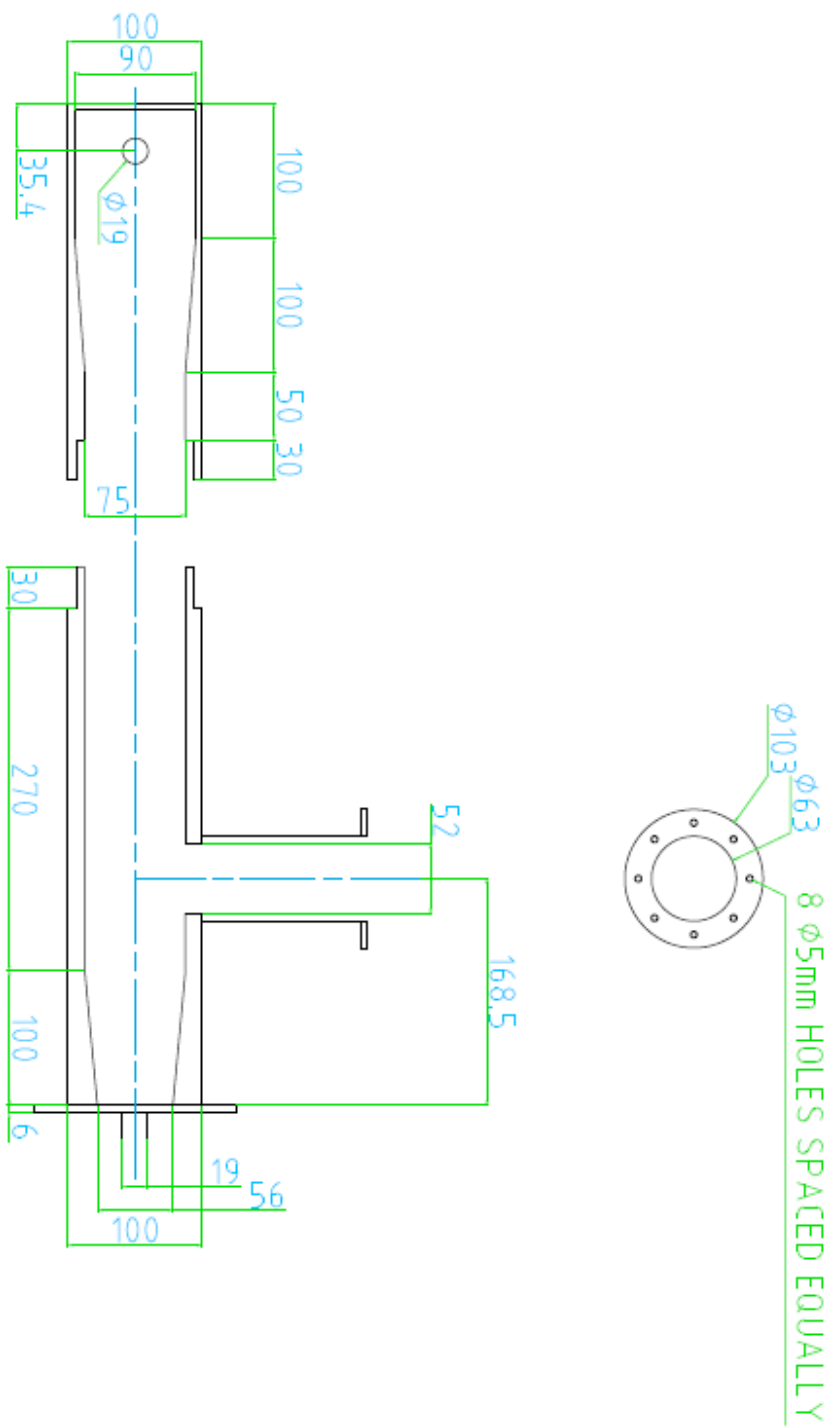
Figure 53: Reactor (R04)

170
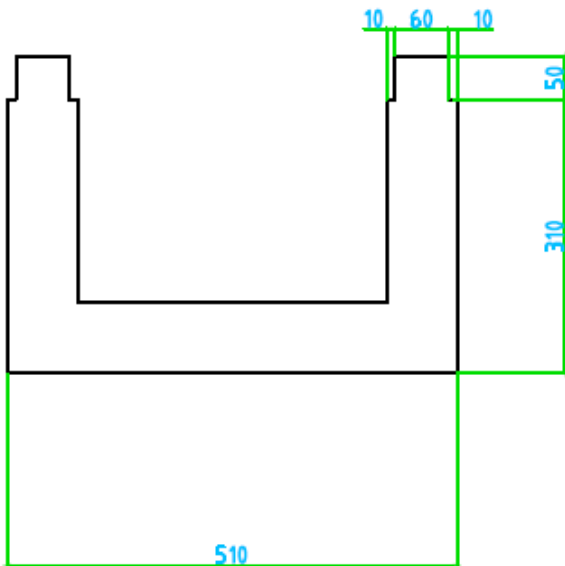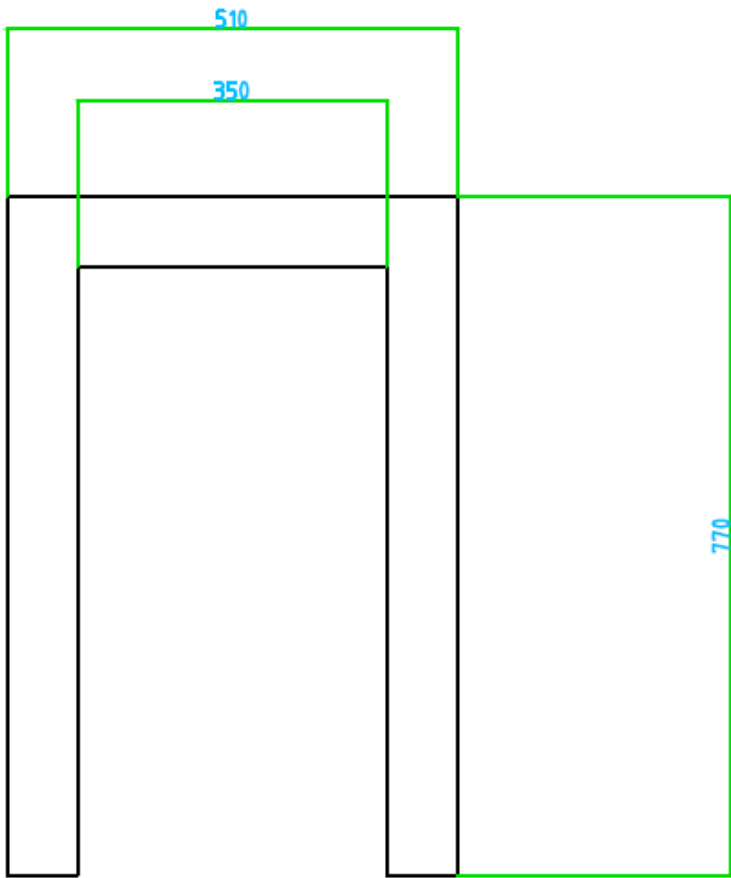
Figure 54: Oven
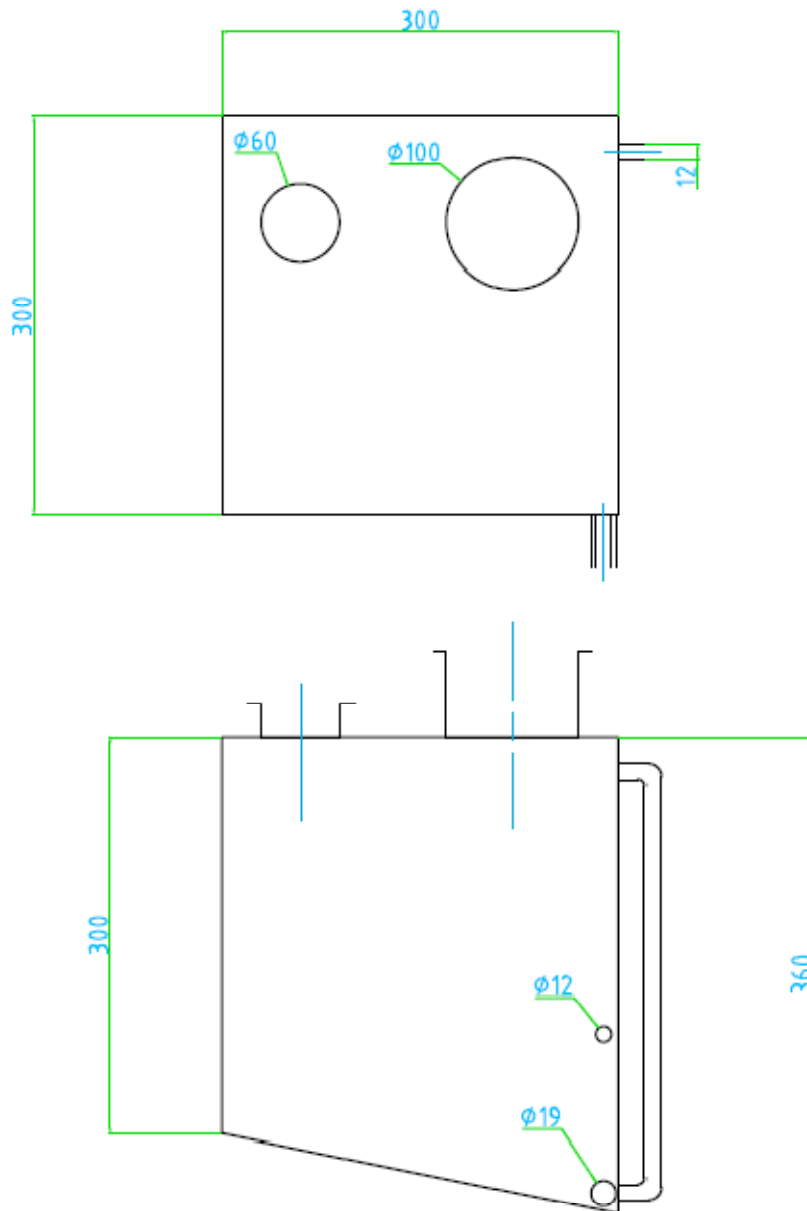
Figure 55: Liquid collection vessel (D08)
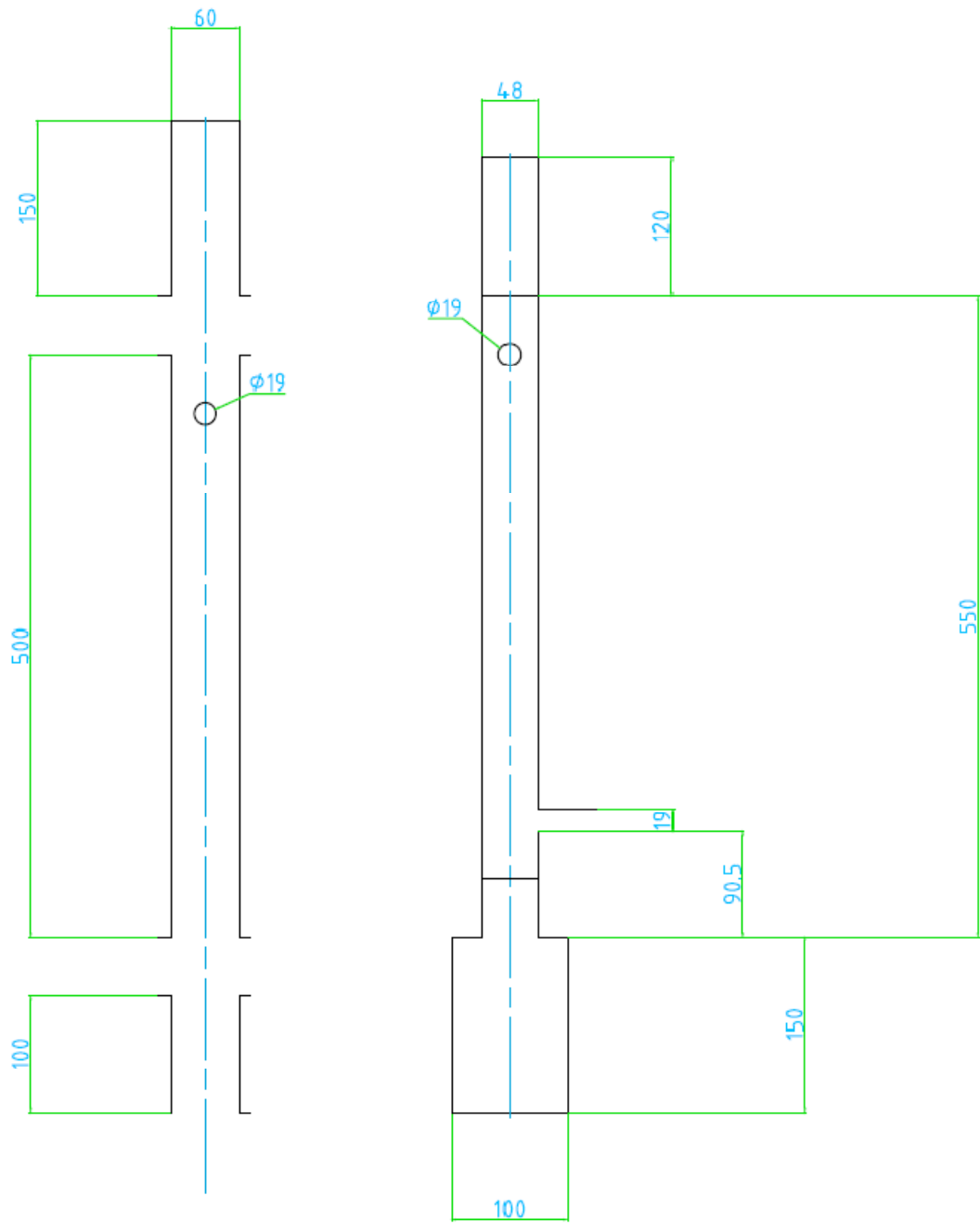
Figure 56: Electrostatic separators (EP 09) and (EP10)
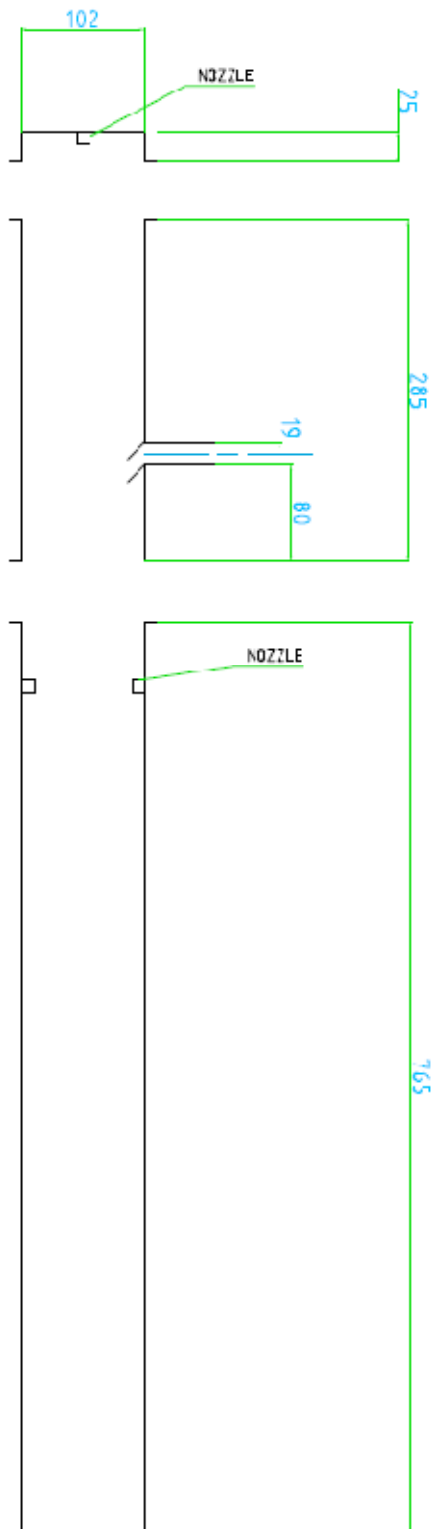
Figure 57: Cooling tower (T07)

300

200

200

215

Ø12

200

ᴴ5

SIDE VIEW

70 100 70

30

70

70

30

230

50

50

330

TOP VIEW

Ø40   Ø50

8 HOLES Ø5 SPACED EQUALLY

SECTION AA
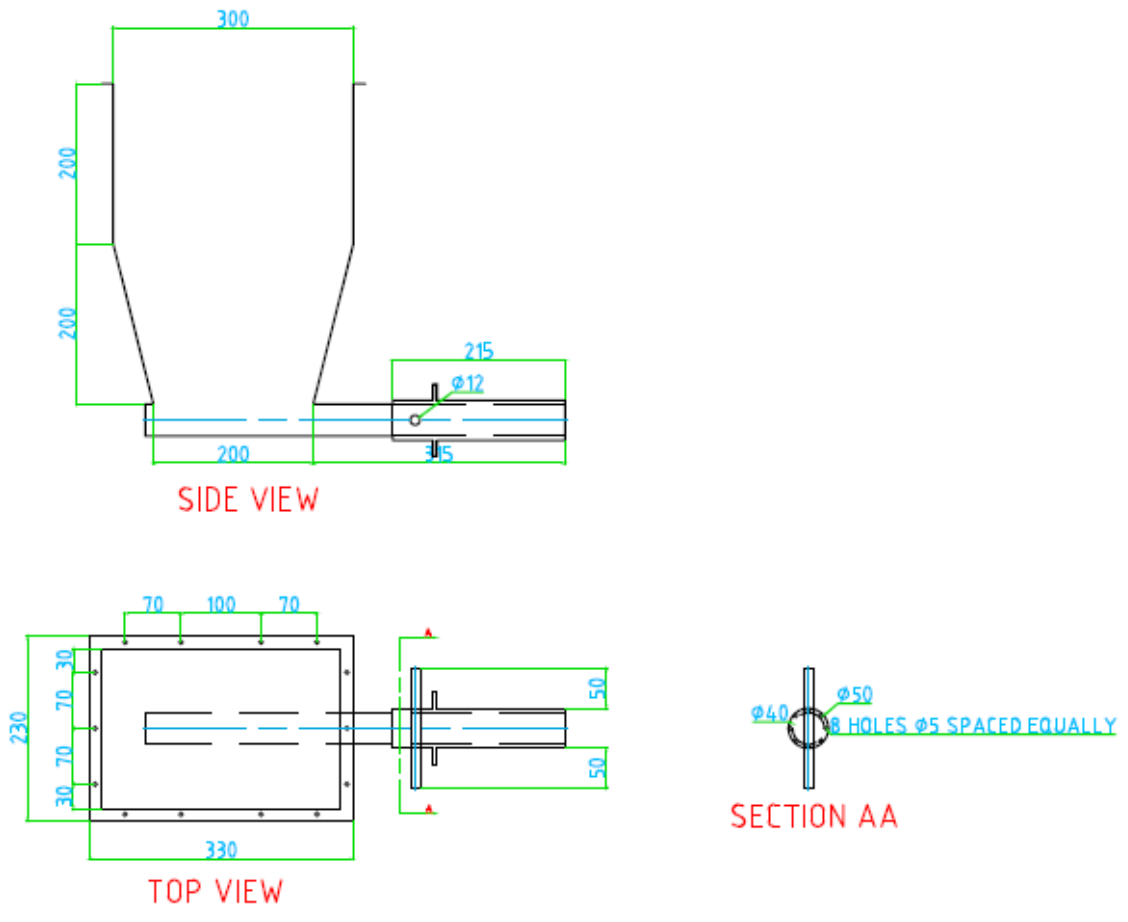
Figure 58: Feeder (F02)

Figure 59: Picture of cyclones (C05 & 06), reactor (R04) and feeding system (F02), (from left to right).
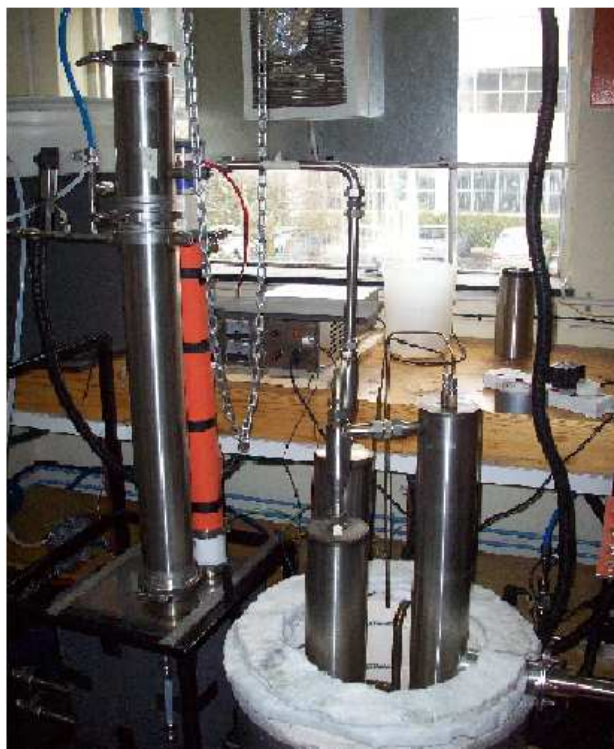
Figure 60: Picture of the cooling tower (T07), electrostatic precipitator (T09), cyclones (C05&06) and reactor (R04) (From left to right)

11.2.13Size reduction of biomass

The size reduction of biomass greatly affects the operation of the FPU. During commissioning the following biomass related problems were identified:

1. Feeding posed problems for larger particles and wetter particles.
2. Dust or bagasse fines entrained into the oil phase, and also caused vibration inside the feeder.
3. Milling was time consuming.

Before pyrolysis the biomass requires size reduction to about 2 mm. For the first experiments approximately 300 – 500 g will be used and therefore 5kg needed to be prepared. Size reduction of bagasse should ideally be done with a cutting mill. Such a mill was used at FZK to effortlessly produce the amount of product required. At the start of this project no funding was available for the purchase of milling equipment. The following options were investigated:

1. A shredder mill (Department of Forestry SU) is a large throughput mill that can handle approximately 5 kg/h of bagasse. A large percentage of the particles are approximately ~10mm in length. This mill is ideal for the first step of biomass size reduction.
2. The second mill at this department is a Retsch rotor mill (ZM- 200) which is not designed to mill fibrous bagasse particles. The mill does work for small amounts of bagasse. But original test showed that it was not optimal for use on bagasse, and it takes many hours of operation to prepare 5kg of bagasse.
3. Two hammer mills are in operation at the Department of Animal Feed Science (SU). The first a large throughput mill is designed to mill corn/ or maize like substances. This mill struggled to handle bagasse. The second mill at this department is a lab scale hammer mill. This mill produced a large amount of fines from bagasse because of its high rotational speed.

Many problems were experienced with the size reduction of sugarcane bagasse and therefore it was deemed essential to purchase a cutting mill capable of effortlessly proving a feedable sample of bagasse. The rule of thumb for sizing (personal communication: Grath Davy, Retsch product manager) is that the mill should be capable of producing 100 g of sample in 30 seconds; otherwise a larger mill is required. The smallest available cutting mill (SM-100, Retsch) was ordered for SU and is capable of biomass throughput of 50kg/h.

After testing the different options the final bagasse preparation procedure which allows easy operation of the unit included the following steps:

1. Air dry to 10% moisture;
2. use shredder mill to cut to 10mm particle size;
3. remove the dust by sieving and discarding < 250 μm; and
4. final size reduction to cut size 2mm

11.2.14 *Commissioning of the feeder*

Fibrous bagasse particles are difficult to feed due to its tendency to bunch together. Original tests revealed that the tendency of the feeder to fail increased with higher moisture content and larger the particles. Failure occurred when a large clog was formed inside the feeder tip. This was found to be due to mechanical pressure and the inability of the bagasse to flow if compressed. Fibre length makes particles clog together more easily, and moisture makes particles stick together. When the particle size < 2mm was used and moisture content was low enough feeding was linear, as shown in Figure 61.
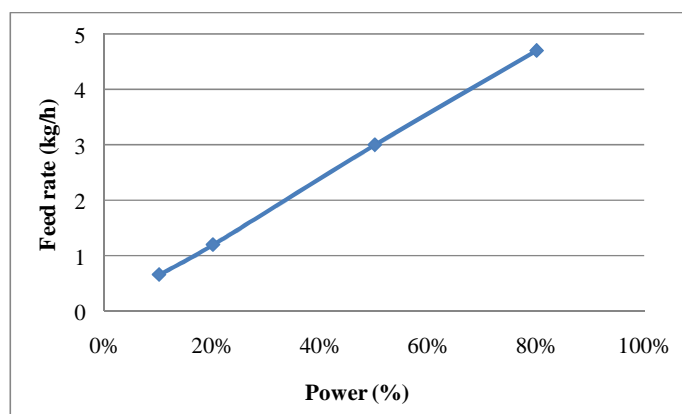
Figure 61: Feed rate of bagasse at 10% moisture and 2 mm sieve size.

Although the feeder functioned at the correct feed rate the some problems were identified. The hammer mill produced a large percentage of dust form the bagasse which entrained into liquid product from the FPU. Only small amounts of biomass could be produced from this mill. Bridging of biomass may occur sometimes, specifically with fibrous particles. Therefore a manual stirrer device was installed in the hopper to disrupt the bridging if it occurred. Tapping with a hammer also helped to avoid bridging. It is recommended that an automatic tapping or vibrating device is installed onto the hopper to disrupt bridging. Non fibrous biomass will feed mush easier. The feeder heat-exchanger was tested. Cooling inside the reactor creates a cold sport for secondary reactions to occur. Therefore the heat exchanger

should only be used for very slow linear feed rates. This will prevent pyrolysis from occurring inside the feeder pipe.

11.2.15 *Mass flow controller*

The mass flow controller (Type 8626) was calibrated by Bürkert technicians. Figure 62 shows the calibration of the nitrogen mass flow controller.
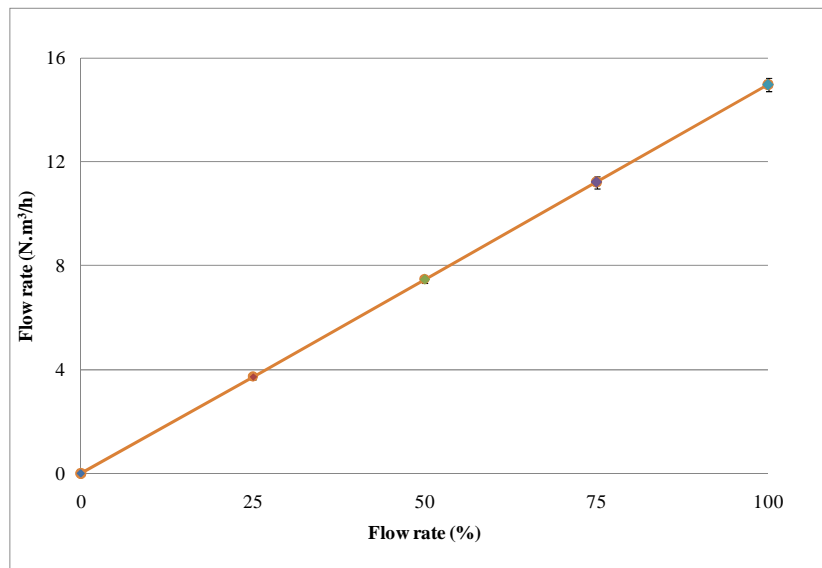
Figure 62: Calibration of flow controller.

11.2.16 Piping & fittings

Table 71: selection of pipe sizes

Stream (S)	S01	S02	S03	S04	S05	S06	S07	S08	S09	S10	S11&12	S13
Temperature (°C)	25	25	25	50	500	500	500	500	450	10	5	15
Pressure (bar)	3	1.2	1.2	1.15	1.15	1.15	1.1	1.1	1.05	1	3	1
Density N_2 (kg/m^3)	3.4	1.4	1.4	1.2	0.5	0.5	0.5	0.5	0.5	1.2	750	1.2
Q N_2 (m^3/h)	1.5	3.3	0.4	0.4	9.8	0	10.3	0	10.1	0	n.a.	4.2
Mass flow (g/s)	1.4	1.3	0.1	0.6	1.8	0.1	1.7	0	1.7	0.3	12.5	1.5
Recommended pipe size (mm)	5	7	2	5	13	2	13	1	12	3	2	8
Chosen pipe size (mm)	**10**	**10**	**10**	n.a.	**16**	**16**	**16**	n.a.	**16**	**16**	**10**	**16**
Material of construction (MOC)	Nylon	Nylon	Nylon	n.a.	SS 316	SS 316	SS 316	n.a.	SS 316	SS 316	Teflon	SS 316

To ensure that there are no leaks in the piping the entire system was slightly pressurized and leak detection spray was used at all fittings. The FPU runs very close to atmospheric conditions (0.01-0.04 bar) because of a low the downstream pressure drop. To protect the fittings against seizing a high temperature Ni-based spay was applied each time. The high temperature carbon gasket used to seal feeder-reactor flange. The clamp and ferrule system, used to join the tower sections, functioned perfectly (rated at 4 bar). The glass on steel connections of the ESPs required some petroleum gel (Vaseline) to seal the fittings.

11.2.17 *Calculations for cyclone*

Table 72: Sizing of the cyclone

Calculating the characteristic length (D)		
Inlet gas flow velocity	~7.5	m^3/h
	0.0021	m^3/s
Average inlet velocity	15	m/s
Inlet area	0.00014	m^2
D	0.0372678	m

11.2.18 *Commissioning of oven*

Initial testing of the oven revealed that a large temperature gradient was present inside the reactor. In light of the poor control that the oven demonstrated, an investigation revealed that controller thermocouples were switched. A fibreglass partition was also installed in the bottom section of the oven, because this section will need to be warmer than the top section to heat the cold nitrogen stream. Three thermocouples are located inside the reactor. T_4 is about 40 mm from the top of the reactor, therefore receiving significant amount of conduction from the reactor top, whereas T_3 is about 400 mm long and is heated mainly by convection. T_2 is close to the gas inlet into the oven. In some other FPUs only one temperature sensor was used inside the reactor (Yanik *et al.*, 2007). This is less accurate and does not consider the temperature gradient effect. The aim of oven calibration is to obtain a small temperature difference (10 °C) between temperature sensors T_3 and T_4.

To establish the correct top and bottom temperatures various temperatures were tested. Each time the conditions were changed to improve on the previous run. In Table 73 the different temperature set points for the calibration runs are shown.

Table 73: Oven calibration runs

Run number	T_{top} (°C)	T_{bottom} (°C)	ΔT (°C)
1	450	400	50
2	450	550	100
3	450	650	200

The data collected from run 1 revealed that T_2, and T_4 closely resembled T_{bottom} and T_{top} respectively. The temperature difference between T_3 and T_4 during heating of the oven is shown Figure 63. The gas is passed through the bottom section of the reactor and should then acquire enough heat to heat the top part to the desired temperature. Therefore the temperature difference was increased to 100°C for run 2. After approximately 65 minutes N_2 was introduced into the system at a flow rate of 2 m³/h. The variation was decreased because the hot gas heated the colder sections of the oven. The gas required slightly more heat and therefore the bottom of the oven was 200°C higher than the top in run 3. The improved design is discussed in paragraph 3.8.1.
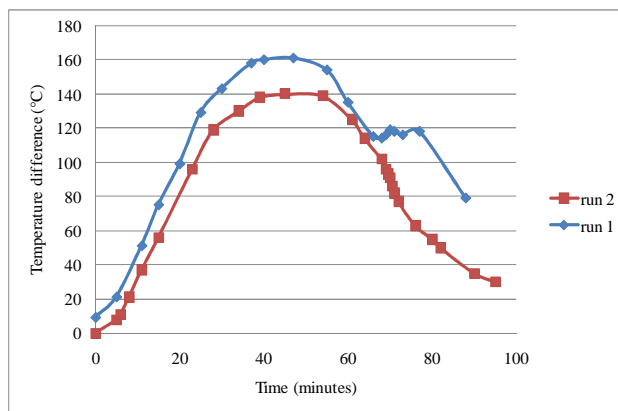
Figure 63: Temperature difference between top and bottom of the reactor

11.2.19 *Instrumentation*

The control system was functional but was not calibrated after installation. All the pressure sensors were calibrated correctly, and were tested with gauges to ensure that they read the correct pressure. The temperature sensors were calibrated with ice water and boiling water to confirm that a linear reading was produced. The data for each run is automatically logged into an Excel spreadsheet during a run.

Table 74: Summary of instrumentation

Summary of Instrumentation				
	Nitrogen			
ZONE1	Temperature	T1	°C	
	Pressure	P1	Bar(g)	Pressure gauge
	Flow rate	Q1	m3/h	Set point control value
	Feeding			
	Flow rate	Q2		Rothameter
	Feeder pressure	P3	Bar(g)	Electronic sensor
ZONE 2	**Reactor**			
	Reactor inlet pressure	P2	Bar(g)	Electronic sensor
	Inlet	T2	°C	Electronic sensor
	Middle	T3	°C	Electronic sensor
	Top	T4	°C	Electronic sensor
	Outlet	T5	°C	Electronic sensor
ZONE 3	**Cooling Liquid**			
	Temperature	T6	°C	Electronic sensor/Barrier
	Pressure	P3	Bar(g)	Electronic sensor/Barrier
	Chiller Bath temperature	T9	°C	Electronic sensor
	Cooling Tower			
	Cooling tower temperature	T7	°C	Electronic sensor/Barrier
	Exit temperature	T8	°C	Electronic sensor
	Exit pressure	P4	Bar(g)	Electronic sensor

11.2.20 *Cooling system*

The first test runs on the cooling system were performed with water as coolant and 2 mm milled bagasse (fine and fibres particles). The water acted as a solvent for bio-oil. Some fines collected on the surface of the water-oil mixture which indicated that the fines presented problems for the system. Very fine mist producing nozzles were used, and due to the particle contamination they became clogged. The system required some modifications to ensure that reproducible data could be generated. To obtain pure bio-oil as product, water could not be used as coolant. Water also presented problems for accurate mass balances because of the dilution factor (20 L coolant is used in a typical test would yield 0.5 kg of oil). Therefore water was dismissed as coolant an instead an immiscible hydrocarbon will be used. To solve the problem of entrained fines in the system a slightly larger nozzle, designed to deal with small particles in the spray liquid, was purchased. This nozzle allows larger flow rates at the expense of a slightly larger mist particle size. This will increase the robustness of the cooling system and allow for the comparison of different nozzles on the cooling system. The bagasse fines will be removed before further experiments, to significantly reduce entrainment in the condensed phase. An elemental analysis was done on isopar which indicated that the liquid composition did not change significantly. The clear liquid became slightly coloured after consecutive experiments. Previous researchers that used a similar type of liquid also did not report changes in composition (Bridgwater *et al.* 1999; Gerdes *et al.*, 2002).

11.2.21 *Operation manual*

Table 75: Operation manual

Day before run		
Steps	**Check**	**NB!**
Calibrate feeder for biomass/ particle size/ moisture content	Run continuously for 5 min (in duplicate) : Take average as flow rate	avoid bridging
Sand 400 - 600 µm	400-500g	
N_2	Pressure should be high enough to complete a run	If pressure is too low connect new gas cylinder.
Weigh condenser units: (ESP1, ESP2, Tower top, Teflon section)	Note how many fittings are used per unit	
Assemble unit + sensors	Fittings lubricated (Ni- spray)! Reactor lubricated (Ni- spray). ESP sealed with Vaseline	Ni-Spray!
Add sand to the reactor		
Connect feeder	Gasket in place	
Test for leaks at high N_2 flow rate (8 m^3/h)	Check for leaks in piping and at fittings	No leaks in system
Assemble oven	Check that oven is sealed with fiber-glass insulation	Take precaution with the outlet section

Table 75: Continued:

During the run		
Steps	Check	NB!
Start Oven	Wait to reach equilibrium at set temperature (1-2h)	
Add biomass to feeder	Seal feeder top	Take biomass sample
Flush system with N_2	3 minutes at 0.5 m³/h	
When oven is close to set temperature:		
Open chiller water	Chiller hose should be in the sink	
Switch on chiller	Values and leaks	4°C lowest temperature for water. Glycol solution required for lower temperatures
Once oven is at set temperature start N_2 flow	Set flow rate (2.4 - 4m³/h)	
Start Isopar pump	line pressure (1.8-3 kPa)	
Attach pipe heater for oven exit gas	set point 400°C	Take precaution not to damage equipment
Monitor T_3 and T_4	Temperature difference (10°C)	
Start Electrostatic separators	Voltage 15 and 12 kV respectively for ESP1, and ESP2	Earth wire is connected
Check for any problem in system, leaks, low/high pressure		
Insert flash disc for data capture		
Start feeder at calibrated feeding rate	Continuously check for bridging and flow obstruction	Ensure that feeder pressure is higher than reactor pressure
Monitor process during experiment		
Once all biomass has been fed, continue feeding for two more minutes	No gas in ESP	
Reduce N_2 flow	0.5 m³/hr	maintain inert atmosphere
Stop chiller	close chiller water tap	
Switch off ESP		
Redirect gas flow to vent		maintain N_2 flow rate
Remove flash disc		
Remove oven top when temperature is lower than 300°C		maintain N_2 flow rate
Leave unit until cool enough to handle		maintain N_2 flow rate

Table 75: Continued:

After the run		
Steps	Check	NB!
Collect oil from condenser		Sample
Weigh dirty condenser components		
Remove isopar and clean collection vessel with acetone		Take precaution to collect all oil and acetone from washing the collection vessel
Weigh sand and char		sample
Order items required	N_2, Cooling liquid, sand, gaskets, Ni-spray, acetone	

11.2.22 Risk assessment

Table 76: Risk assessment: The Risk (R) is quantified by the Probability of an incident (P) multiplied by Severity (S) of an incident.

Hazard	Example of hazard	Example of activities	Cause	Preventative action	P	S	R
Fire							
Inside lab	caused by oven	biomass spillage in oven	CO_2 release & damage to equipment	Clean oven before each run. Do not leave cleaning towels inside oven	1	2	2
Uncontrolled substance release							
Inside lab	Reactor gas release	Loose connection /leakage	Burn; asphyxiation	Check for leakages before each run is started	1	2	2
	Cooling liquid release	Loose connection /leakage	Flammable substance release	Check for leakages before each run is started. Shut down if leakage is detected.	1	4	4
Outside lab	N_2, low temperature exposure	pipe leakage	cold burns	monitor pressure on pipeline	1	2	2
Hazardous chemicals							
Gasses	CO_2, CO, Me, H_2, higher molecular organic molecules (low concentration inside nitrogen atmosphere)	leakage // exit gas	asphyxiation, odor	Test lines before operating unit, monitor for leakages, vent off gas	1	2	2
	O_2 into furnace causes combustion	O_2 inside cooling tower	Fire// explosion	Purge system with N_2 before heating// O_2 monitor	1	5	5
Dust	Biomass// char	leakage	inhaling of small particles	Use face mask for biomass handling	1	4	4
Liquids	Isopar G	leakage	Flammable substance release	Check for leakages before each run is started. Shut down if leakage is detected.	1	2	2
High temperature surfaces							
Machinery	Furnace, units inside furnace	Disassembly after run	Burns	PPE, Oven gloves, allow sufficient cooling time	2	2	4

Table 76: continued

Hazard	Example of hazard	Example of activities	Cause	Preventative action	P	S	R
Electricity							
Machinery	Touching High voltage equipment	accidental	Electrocution	insulation of electrostatic separator // PPE	1	3	3
	Water spillage near electrical equipment	spillage from heat exchangers/ tower	Electrocution/ fire	Check equipment before each run.	1	3	3
Physical hazards							
Obstacles	Top section of oven is lifted with pulley system	accidental release	Equipment damage/ cause injury	securely fixed at all times	1	3	3
Heights	standing on ladder		fall	be careful	1	2	2
heavy equipment	falling of heavy equipment		injury, equipment damage	be careful, large equipment must be securely fixed	1	2	2
Heat exposure	Warmer ambient temperature		heat exhaustion	Take fluid in stainless flask	1	2	2

11.3 Appendix for chapter 6

11.3.1 *Mass balance table*

Table 77: Specific Mass Balance for FPU$_1$ ('rel wt%' refers to the 'wt%' above it)

Specific Mass Balance											
Temperature	°C	500	500	500	500	495	495	495	428	526	500	500
Name	-	R 1	R 2	R 3	R 4	R 5	R 6	R 9	R 7	R 8	FZK 05	FZK 06
Biomass	g	208.8	162.5	92.1	141.2	294.9	283.6	279.6	323.6	309.2	31900	36200
Moisture content	wt%	3.3	2.8	6.4	4.3	6.0	6.2	7.8	8.1	7.6	9.0	10.1
Ash content	wt%	3.4	3.7	2.5	3.3	2.1	2.1	1.7	1.1	1.2	4.2	4.2
Biomass Organics (maf)	wt%	93.2	93.5	91.1	92.5	91.9	91.7	90.5	90.8	91.2	86.8	85.7
Residual solids	wt%	11.2	10.9	10.9	10.7	10.1	9.6	8.2	11.2	11.2	16.8	16.8
Ash	rel wt%	34.9	46.6	26.8	29.6	19.1	25.8	20.3	14.1	19.9	22.6	22.5
Chars	rel wt%	65.1	53.5	73.2	70.4	80.9	74.2	79.7	85.9	80.1	77.4	77.5
Liquid condensate (oil)	wt%	34.0	52.6	35.3	54.7	63.5	64.6	67.7	59.5	59.4	59.2	67.8
Organic condensate	rel wt%	74.4	75.8	71.7	85.5	79.2	80.5	78.9	78.2	78.8	77.2	76.4
Moisture content	rel wt%	25.6	24.2	28.3	14.5	20.7	19.3	21.0	21.8	21.2	17.6	18.8
Ash	rel wt%					0.1	0.1	0.1	0.0	0.0	5.2	4.8
Pyrolitic gas (by difference)	wt%	54.8	36.6	53.9	34.6	26.4	25.8	24.0	29.3	29.4	24.0	15.4
Biomass organics IN	wt%	100.0	100.0	100.0	100.0	100.0	100.0	100.0	100.0	100.0	100.0	100.0
Char organics	wt%	7.8	6.2	8.7	8.1	8.9	7.8	7.3	10.6	9.9	15.0	15.2
Oil organics	wt%	27.1	42.6	27.8	50.6	54.8	56.7	59.1	51.2	51.3	52.7	60.5
Gas organics (by difference)	wt%	65.1	51.2	63.5	41.3	36.3	35.5	33.7	38.2	38.8	32.3	24.3
Biomass water IN	wt%	3.34	2.84	6.36	4.25	6.02	6.17	7.82	7.57	10.10	9.04	10.10
Liquid water OUT	wt%	8.70	12.73	9.98	7.96	13.12	12.49	14.22	12.56	12.76	10.42	12.76
Pyrolitic Water	wt%	5.37	9.89	3.61	3.71	7.10	6.32	6.40	4.99	2.66	1.38	2.66
Biomass ash IN	wt%	100.0	100.0	100.0	100.0	100.0	100.0	100.0	100.0	100.0	100.0	100.0
Char & oil ash OUT	wt%	114.0	136.3	115.0	96.9	93.3	119.9	101.3	142.2	179.2	163.9	167.4

ar: arrive/original

mf: moisture free

maf: moisture and ash free
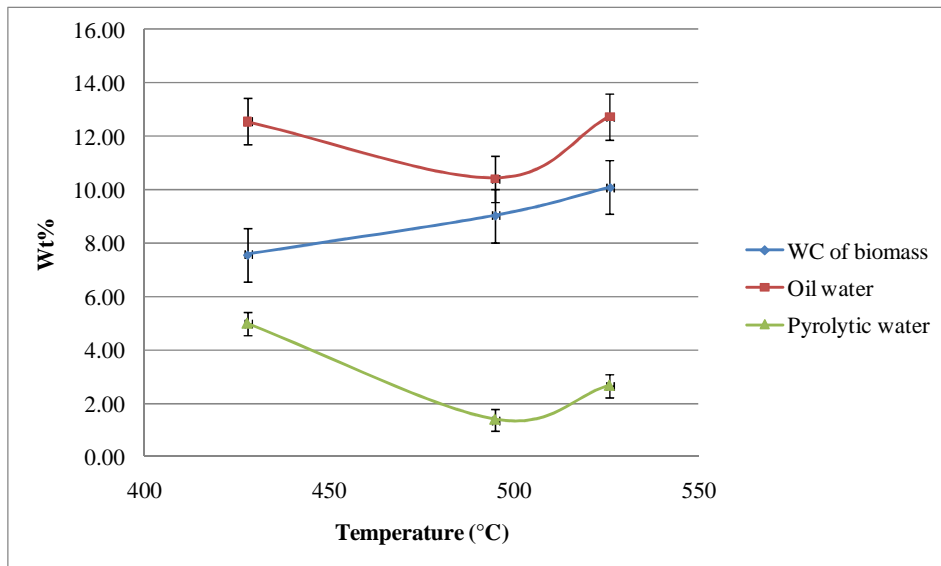
11.3.2 *Additional figures*

Figure 64: Pyrolytic water plotted as a function of temperature for runs on FPU at SU. (All weight %'s are relative to the original biomass weight). For this figure 'pyrolytic water' refers to water produced by pyrolysis reactions.
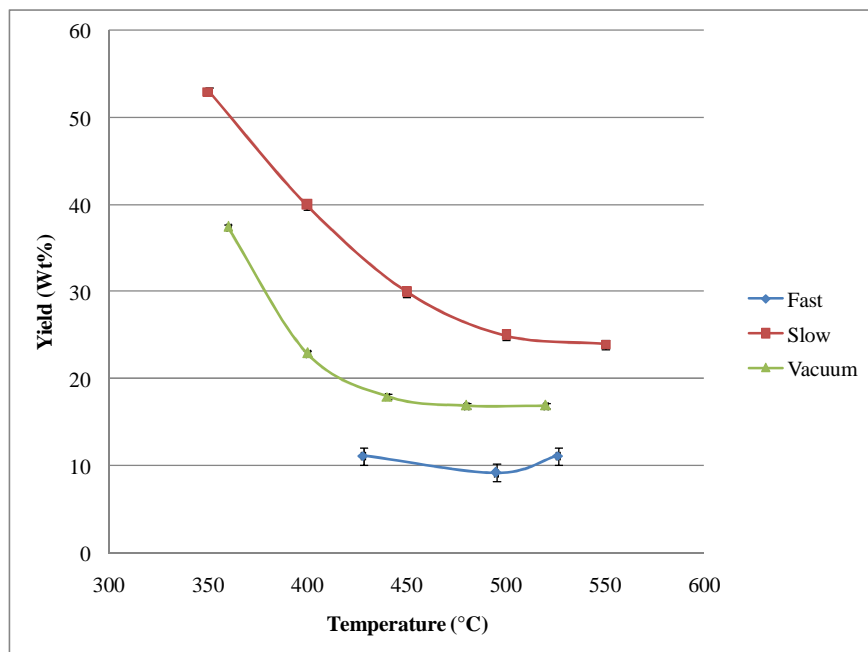

Figure 65: An illustration of char product yield from Slow, Vacuum, and Fast pyrolysis at optimal liquid producing heating rates

11.3.3 *ANOVA*

Table 78: An example of ANOVA calculation in excel.

SUMMARY						
Groups	*Count*	*Sum*	*Average*	*Variance*		
SU	3	65.18	21.73	12.731		
FZK	2	45.1	22.55	0.005		
ANOVA						
Source of Variation	*SS*	*df*	*MS*	*F*	*P-value*	*F crit*
Between Groups	0.813	1	0.813	0.096	0.778	10.128
Within Groups	25.468	3	8.489			
Total	26.282	4				

Table 79: Single factor ANOVA for comparison of FZK and SU data

	F	Allowable variation in mean	Different mean values
F_{crit}	**10.13**		
Char			
Char yield	111.40		**X**
Char ash %	0.10	**X**	
HHV char	16.22		**X**
O%	259.47		**X**
H%	53.65		**X**
C%	20.41		**X**
Bio-oil			
Bio-oil yield	0.23	**X**	
Moisture content	7.26	**X**	
HHV Liquid	0.00	**X**	
Carbon%	0.41	**X**	

11.3.4 *Energy balance*

Table 80: (Complete version) Product energy distribution for SU and FZK FP experiments

Energy balance of products from US and FZK				
	HHV	x	h	Energy cont.
	MJ/kg	kg/kg (mf)	MJ/kg biomass	[e%]
Bagasse	18.96	1	18.96	100
FP_{10} run 05				
Oil	18.83	0.59	11.15	58.78
Char	20.95	0.17	3.53	18.6
Gas	8.9	0.16	1.41	7.44
FP_{10} run 06				
Oil	17.99	0.68	12.2	64.35
Char	20.59	0.17	3.45	18.21
Gas	9.56	0.12	1.17	6.17
FP_1 run 05				
Oil	18.02	0.63	11.44	60.32
Char	25.9	0.1	2.61	13.77
FP_1 run 06				
Oil	18.07	0.65	11.67	61.54
Char	23.33	0.1	2.24	11.79
FP_1 run 09				
Oil	19.26	0.68	13.04	68.77
Char	24.81	0.08	2.05	10.79
FP_1 Average (three experiments at 495°C)				
Oil	18 ± 1	0.65 ± 0.03	12.1 ± 0.9	64 ± 5
Char	25 ± 2	0.09 ± 0.01	2.3 ± 0.3	12 ± 2
FP_{10} Average (two experiments at 500°C)				
Oil	18 ± 1	0.64 ± 0.06	11.7 ± 0.8	60 ± 4
Char	21 ± 1	0.17 ± 0.00	3.49 ± 0.05	18.4 ± 0.3
Gas	9.3 ± 0.4	0.14 ± 0.03	1.3 ± 0.5	7 ± 1

11.3.5 *Error analysis*

Typical experimental data has experimental error and measurement error (e.g. inaccuracy of scale). The combination of these two error values results in the final error of the data point (Equation 21). In most cases either the experimental error or measurement error is significantly larger than the other, and can therefore be omitted.

$$E_{total} = \sqrt{\left(E_{measurement}^2 + E_{experimental}^2 \right)}$$

<div align="right">Equation 21</div>

Experimental error is easy to calculate once three data points have been generated the standard deviation can be calculated in excel. When two or more measurement errors are combined an arithmetic operation is required. For example when the weight of a sample is calculated, the scale is used at least three times: to zero the scale, to measure sample and container weight; and measure container weight. Each time the scale portrays some error value.

Adding errors

$$A = a \pm \Delta a$$
$$B = b \pm \Delta b$$
$$A + B = (a \pm \Delta a) + (b \pm \Delta b)$$
$$A + B = (a + b) + (\pm \Delta a \pm \Delta b)$$
$$A + B = (a + b) \pm (\Delta a + \Delta b)$$
$$E_{relative} = \frac{E}{Value} = \frac{\Delta a + \Delta b}{a + b} \approx \frac{\Delta a}{a} \approx \frac{\Delta b}{b}$$
$$(if - \Delta a \approx \Delta b)$$

Similarly multiplication of errors is calculated as follows:

$$E_{relative} = \frac{E}{Value} = \frac{b\Delta a + a\Delta b}{ab} = \frac{\Delta a}{a} + \frac{\Delta b}{b}$$

The laboratory scale was assumed to have an error of ±0.1g, which is 10 times larger than a typical new scale. Therefore to calculate the error on the char yield from a typical experiment with 300g of biomass, the following calculations are required:

$$E_{relative} = zero \pm 0.1(g) + (char + container) \pm 0.1(g) + container \pm 0.1(g)$$

$$E_{relative} = 0 \pm 0.1(g) + (30 + 10) \pm 0.1(g) + 10 \pm 0.1(g)$$

$$E_{relative} = \frac{3 \times \pm 0.1(g)}{30 + 10(g)} = \frac{\pm 0.3}{40}$$

$$E_{Char} = 30 \frac{\pm 0.3}{40}$$

$$Yield_{char} = 30 \pm 0.2$$

11.4 Appendix for chapter 7

11.4.1 *Statistical test of data*

Because of the overlap within the confidence intervals (Figure 46), the data can be interpreted with more confidence once it has been proven that the 3 curves are not from the same distribution. The null hypothesis is therefore that the three curves are from the same distribution. This analysis is based on the assumption that the data, as well as the model parameters, follow a normal distribution. For this analysis many values are required for each data point. Therefore the 'random number generator' function in Excel was used to generate 100 numbers (normally distributed) with the known mean and standard deviation. A second order regression model (Equation 22) was the fitted to this data. A 95% confidence interval for upper and lower model parameters was generated. If the model parameters all overlap, the null hypothesis cannot be rejected. Based on the results of the regression analysis (Table 81) it can be seen that only one overlap occurs with parameter 'a' from VP and SP. The null hypothesis can therefore be rejected. All three curves are different. In order to calculate the standard deviation from data, it was assumed that the measurement error from VP and SP (Carrier *et al.* 2010) resembled two standard deviations (95% confidence interval).

$$Wt\% = aT^2 + bT + c$$

Equation 22

Table 81: Upper and lower model coefficients for liquid yield from FP, VP, SP.

Model coefficients	Slow		Vacuum		Fast		Comments
	Lower 95%	Upper 95%	Lower 95%	Upper 95%	Lower 95%	Upper 95%	
c	-125.8	-121.2	-165.6	-138.9	-668.6	-542.2	No overlap
b	0.658	0.682	0.817	0.940	2.555	3.091	No overlap
a	-0.001	-0.001	-0.001	-0.001	-0.003	-0.003	Slow and vacuum overlap